AD-A152 801 FUEL FREEZE POINT INVESTIGATIONS(U) BOEING MILITARY AIRPLANE CO SEATTLE WA L A DESMARAIS ET AL. JUL 84 D180-28285-1 AFWAL-TR-84-2049 F33615-82-C-2262 1/3

UNCLASSIFIED F/G 21/4 NL

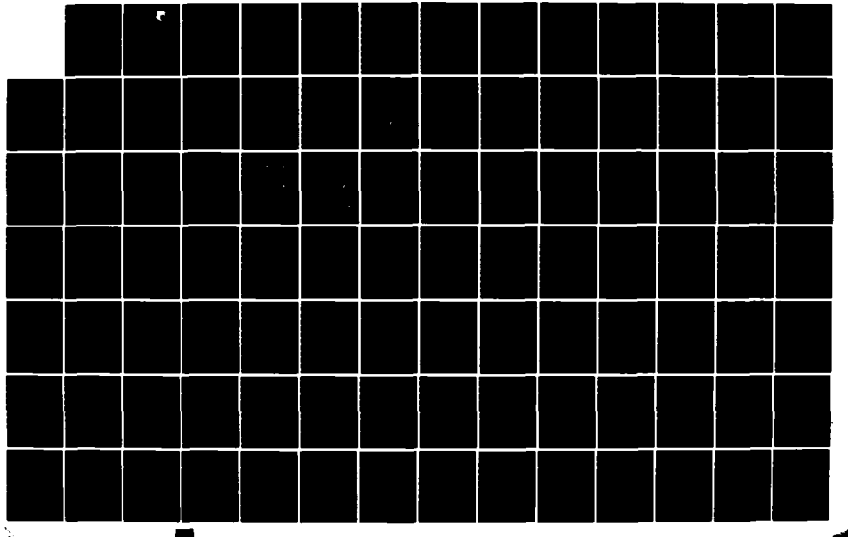

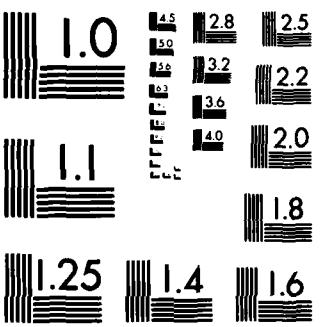

AFWAL-TR-84-2049

FUEL FREEZE POINT INVESTIGATIONS

L. A. Desmarais, F. F. Tolle
Boeing Military Airplane Company
P.O. Box 3707
Seattle, WA 98124

July 1984

FINAL REPORT FOR PERIOD September 1982 - March 1984

AERO PROPULSION LABORATORY
AIR FORCE WRIGHT AERONAUTICAL LABORATORIES
AIR FORCE SYSTEMS COMMAND
WRIGHT-PATTERSON AIR FORCE BASE, OHIO 45433-6563

NOTICE

When Government drawings, specifications, or other data are used for any purpose other than in connection with a definitely related Government procurement operation, the United States Government thereby incurs no responsibility nor any obligation whatsoever, and the fact that the Government may have formulated, furnished, or in any way supplied the said drawings, specifications, or other data, is not to be regarded by implication or otherwise as in any manner licensing the holder or any other person or corporation, or conveying any rights or permission to manufacture, use, or sell any patented invention that may in any way be related thereto.

This report has been reviewed by the Office of Public Affairs (ASD/PA) and is releasable to the National Technical Information Service (NTIS). At NTIS, it will be available to the general public, including foreign nations.

This technical report has been reviewed and is approved for publication.

Eva M. Conley
Project Engineer
Fuels Branch
Fuels and Lubrication Division
Aero Propulsion Laboratory

Arthur V. Churchill
Chief, Fuels Branch
Fuels and Lubrication Division
Aero Propulsion Laboratory

FOR THE COMMANDER

R. D. SHERRILL
Chief, Fuels and Lubrication Division
Aero Propulsion Laboratory

"If your address has changed, if you wish to be removed from our mailing list or if the addressee is no longer employed by your organization, please notify AFWAL/POSF, WPAFB, OH 45433-6563 to help us maintain a current mailing list."

Copies of this report should not be returned unless return is required by security considerations, contractual obligations, or notice on a specific document.

Unclassified
SECURITY CLASSIFICATION OF THIS PAGE

REPORT DOCUMENTATION PAGE

1a. REPORT SECURITY CLASSIFICATION: Unclassified	1b. RESTRICTIVE MARKINGS: N/A
2a. SECURITY CLASSIFICATION AUTHORITY	3. DISTRIBUTION/AVAILABILITY OF REPORT: Approved for public release; distribution unlimited.
2b. DECLASSIFICATION/DOWNGRADING SCHEDULE: N/A	
4. PERFORMING ORGANIZATION REPORT NUMBER(S): D180-28285-1	5. MONITORING ORGANIZATION REPORT NUMBER(S): AFWAL-TR-84-2049
6a. NAME OF PERFORMING ORGANIZATION: Boeing Military Airplane Company; 6b. OFFICE SYMBOL (If applicable):	7a. NAME OF MONITORING ORGANIZATION: Fuels Branch, Aero Propulsion Laboratory
6c. ADDRESS (City, State and ZIP Code): P.O. Box 3707, M/S 41-52, Seattle, WA 98124	7b. ADDRESS (City, State and ZIP Code): AFWAL/POSF, Air Force Wright Aeronautical Laboratories, Wright-Patterson AFB, Ohio 45433-6563
8a. NAME OF FUNDING/SPONSORING ORGANIZATION: Fuels/Lubrication Division Aero Propulsion Lab.; 8b. OFFICE SYMBOL (If applicable): AFWAL/POS	9. PROCUREMENT INSTRUMENT IDENTIFICATION NUMBER: F33615-82-C-2262
8c. ADDRESS (City, State and ZIP Code): Air Force Wright Aeronautical Laboratories, Wright-Patterson AFB, OH 45433-6563	10. SOURCE OF FUNDING NOS.

PROGRAM ELEMENT NO.	PROJECT NO.	TASK NO.	WORK UNIT NO.
63215F	2480	04	01

11. TITLE (Include Security Classification): Fuel Freeze Point Investigations (U)	
12. PERSONAL AUTHOR(S): Desmarais, Lynn A.; Tolle, Frederick F.	
13a. TYPE OF REPORT: FINAL; 13b. TIME COVERED: FROM Sept 82 TO Mar 84	14. DATE OF REPORT (Yr., Mo., Day): July 1984; 15. PAGE COUNT: xiii + 273
16. SUPPLEMENTARY NOTATION	

17. COSATI CODES		
FIELD	GROUP	SUB. GR.
07	01	03
21	04	09

18. SUBJECT TERMS (Continue on reverse if necessary and identify by block number): freeze point, fuel tanks, holdup

19. ABSTRACT (Continue on reverse if necessary and identify by block number)

The objective of this program was to conduct a detailed assessment of the low temperature environment to which USAF aircraft are exposed for the purpose of defining a maximum acceptable fuel freeze point and also to define any operational changes required with the use of a high freeze point fuel. A previous study of B-52, C-141, and KC-135 operational missions indicated that the -58°C freeze point specification was too conservative. Based on recommendations resulting from the previous program, several improvements in the method of analysis were made, such as: expansion of the atmospheric temperature data base, the addition of ground temperature analysis, the addition of fuel freezing analysis to the one-dimensional fuel temperature computer program, and the examination of heat transfer in external fuel tanks, such as pylon or tip tanks. The B-52, C-141, and KC-135 mission were analyzed again, along with the operational missions of two tactical airplanes, the A-10 and F-15; -50°C was determined to be the maximum allowable freeze point for a general purpose USAF aviation turbine fuel. Higher freeze points can be tolerated if the

20. DISTRIBUTION/AVAILABILITY OF ABSTRACT: UNCLASSIFIED/UNLIMITED ☐ SAME AS RPT. ☒ DTIC USERS ☐	21. ABSTRACT SECURITY CLASSIFICATION: Unclassified

22a. NAME OF RESPONSIBLE INDIVIDUAL	22b. TELEPHONE NUMBER (Include Area Code)	22c. OFFICE SYMBOL
Eva M. Conley	(513)255-7211	AFWAL/POSF

DD FORM 1473, 83 APR EDITION OF 1 JAN 73 IS OBSOLETE.

Unclassified
SECURITY CLASSIFICATION OF THIS PAGE

Number 19. Abstract (Continued)

probability of operational interference is acceptably low or if operational changes can be made. Study of atmospheric temperatures encountered for the missions of the five study aircraft indicates that a maximum freeze point of -48°C would not likely create any operational difficulties in Northern Europe.

PREFACE

This final report of work conducted under F33615-82-C-2262 is submitted by the Boeing Military Airplane Company, Seattle, Washington. Dates of research were 20 September 1982 through 19 March 1984. Program sponsorship and guidance were provided by the Fuels Branch of the Aero Propulsion Laboratory (AFWAL/POSF), Air Force Wright Aeronautical Laboratories, Air Force Systems Command, Wright-Patterson Air Force Base, Ohio, under Project 2480, Task 04, and Work Unit 01. Eva M. Conley was the Government project engineer and Charles L. Delaney was the Government program manager.

Boeing wishes to acknowledge the contributions of the following to this program: Mr. Gerry Speck of the Naval Air Propulsion Center (NAPC) for fuel samples and characterization data, Mr. Dennis Joseph of the National Center for Atmospheric Research (NCAR) for the atmospheric temperature data, Mr. Mac Fountain of the USAF Environmental Technical Applications Center (ETAC) for the ground temperature data, Lt. Col. Copler and Majors Keeney and Roulston of Headquarters TAC for the A-10 and F-15 mission data, Mr. Robert Friedman of NASA-Lewis for inflight fuel temperature data, and Prof. C. T. Moynihan of Rensselaer Polytechnic Institute for fuel specific heat data. The cooperation of these individuals and organizations is appreciated.

Key Boeing contributors to the program were: F. F. Tolle, program manager, A. F. Grenich, technical guidance, L. A. Desmarais, principal investigator, C. K. Forester, computational fluid dynamics, P. M. McConnell, thermal analysis, M. S. McKenzie, programming support, S. J. Kihara, test engineer, and D. R. Christmann, fuel property measurements.

TABLE OF CONTENTS

TABLE OF CONTENTS (Continued)

TABLE OF CONTENTS (continued)

LIST OF ILLUSTRATIONS

LIST OF ILLUSTRATIONS (Continued)

LIST OF ILLUSTRATIONS (Continued)

LIST OF ILLUSTRATIONS (Continued)

LIST OF TABLES

SECTION I
INTRODUCTION

This report represents a continuation of work performed by Boeing for the Air Force to study the operational effects of increasing the freeze point of jet fuel. Previous work, conducted under F33615-78-C-2001, is reported in References 1 and 2, and provides the rationale for the approach used in the study.

In the initial Boeing investigation (Reference 1) performed for the Air Force, a method for establishing the fuel freeze point requirement based on operational factors was established. The results of the study indicated that the freeze point specification for JP-4 could be increased from the current $-58^{o}C$ to approximately $-46^{o}C$ without risk of inflight operational interference. Recommendations for further work were made, and became the basis for the study reported here.

1. BACKGROUND

Problems experienced by the Air Force in obtaining fuel supplies and continuing price escalation, coupled with the increased use of heavy, more difficult to process petroleum crudes and the projected use of syncrudes have motivated the Air Force to re-examine the technical requirements of aviation turbine fuel. Accordingly, a Government survey of US refiners (summarized in References 3 and 4)was taken to determine what, if any, changes could be made to the current fuel specification to aid in the production of fuel or to motivate refiners to produce the fuel; freeze point was cited as being one of the technical requirements which restricts the production of jet fuel.

In general, studies are being pursued which consider the effects of changing the specifications to allow increased aromatic content, higher boiling and freezing points, reduced flashpoint and lessening of thermal stability. These were selected because of the sensitivity of refinery jet fuel yield to the particular property, or in response to anticipated changes in crude quality. The goals of these studies included determination of the impact of fuel property changes on fuel system design, investigation of the changes in other

interrelated fuel properties as well as changes in the effectiveness of fuel additives and, as in the case of this study, investigation of the effect on airplane operations of fuel property changes. In terms of the impact of freeze point in particular, conclusions of the jet fuel availability study (Reference 4) were that, for each $3^{o}C$ increase in freeze point an increase in production yield of 5 to 10 percent could be achieved for kerosene type fuels, and an increase of 5 to 20 percent for JP-4 fuels.

2. OBJECTIVE

The objective of this program was to conduct a further detailed assessment of the low temperature environment to which USAF airplanes are exposed, make recommendations as to the maximum acceptable freeze point, and deduce any operational changes required with the use of higher freeze point fuel.

3. APPROACH

Five USAF airplanes were to be studied including three from the previous studies, the B-52, C-141, and KC-135. The A-10 and F-15 were also studied to determine the usability of high freeze point fuels in tactical aircraft. The routes studied were those which had a high probability of encountering extreme low temperature conditions.

This work was performed in a sequence of interdependent tasks with the exception of the multi-dimensional heat transfer model development which continued throughout the length of the program due to its complexity. The steps were as follows:

Computer Program Development

- Extension of the existing one-dimensional (rectangular fuel tank) heat transfer model to include the latent heat of fusion in fuel freezing calculation

- Development of a model to perform calculations of fuel temperature in cylindrical geometries, as for pylon or tip tanks

- Development of fuel property data on specific heat, viscosity, density, and thermal conductivity in the vicinity of the freeze point

- o Improvement of ROUTEMP to perform statistical analysis of routes

Calculation of Thermal Exposure Extremes

- o Identification of routes, in particular the northernmost routes, which each airplane type is required to fly

- o Identification of the most critical tank for each airplane from a low temperature standpoint

- o Determination of fuel usage for the critical tank as a function of time of flight for each aircraft

- o Expansion of an atmospheric thermal exposure data base, and definition of ambient temperature versus time of flight along each route

- o Development of a ground thermal exposure data base, and definition of ambient temperature versus time prior to each mission

- o Calculation of the fuel thermal profile development (fuel temperature versus fuel tank height) in the critical tank as a result of the time varying thermal environment

- o Calculation of the amount of fuel expected to be frozen at different times during the worst case missions

Experimental Verification

- o Measurement of the fuel freezing (holdup) characteristics of each of the selected test fuels

- o Simulation of route temperatures in the cold fuel simulator tank to verify the predictions of thermal profile development computer program and to evaluate fuel freezing predictions

Analysis of the Effect of Increasing Fuel Freeze Point

- o Determination of the probability of operational interference, i.e. instances in which frozen fuel would impact airplane performance, with increasing fuel freeze point

- o Evaluation of current operating procedures and recommendation of changes that would allow the Air Force to use higher freeze point fuels

- o Assessment of abnormal operating conditions or failure modes which could affect the fuel freeze point requirement

Based on the results of these steps, a maximum fuel freeze point recommendation was made to the Air Force for a general purpose turbine engine fuel.

4. SUMMARY

The results of this study indicate that -50°C is the maximum fuel freeze point that can be used if all of the operational requirements of the fire study airplane are to be met. The limiting case was the ground temperature exposure at Eielson AFB, Alaska, where the A-10 and KC-135 are based, and where extreme temperatures as low as -50°C are known to have occurred for periods as long as 24 hours. If the extreme Eielson AFB case is neglected, the next highest freeze point which would satisfy operational requirements is -48°C, assuming that a remote, but finite, possibility of fuel freezing is acceptable.

A related question of the acceptability of Jet A-1, which has a freeze point of -47°C, for use in northern Europe arose during the conduct of this study. Review of surface temperature data for northern Europe showed not only that -47°C is an acceptable specification, but that a maximum as high as -43° would not be likely to create any operational difficulties. Again, this conclusion is based on examination of surface temperatures. A final conclusion should include examination of the fuel systems of the airplanes in question, as well as their missions; route, altitude, and airspeed. Experience with atmospheric temperatures encountered for the missions of the five study airplanes indicates a freeze point of -48°C would be satisfactory for European operations. It is therefore concluded that -47°C would also be acceptable, with an estimated probability of operational interference of less than 1.0% during the winter months.

SECTION II
THERMAL EXPOSURE CALCULATIONS

Given specific fuel system information, tank geometry, fuel management procedures, and details of the missions for each study airplane, an analytical model was used to predict fuel temperatures as a function of mission time, and in turn, the quantity of frozen fuel as a function of time.

1. ROUTE STRUCTURE

Two classes of routes were considered, one for long range airplanes, and a second for smaller airplanes.

a. Long Range Airplanes

Routes were selected for each airplane which emphasized Arctic and long endurance/high altitude flights. Ten operational routes per airplane had been studied earlier for the B-52, C-141, and KC-135. Three of these ten routes were selected for re-evaluation using the same airplanes with the new capabilities developed during this study which included:

- o a larger atmospheric data base
- o a ground temperature data base using actual data from the takeoff bases
- o an improved heat transfer model which included more accurate hold up predictions

The mission routes, also called tracks, are shown plotted for each airplane on a polar projection of the northern hemisphere in Figures 1, 2, and 3. The severity of both ground and atmospheric thermal exposures was considered in the selection of the study routes. Data characterizing ground temperatures during the winter months at each of the B-52, C-141, and KC-135 takeoff bases were obtained and are plotted in Figures 4 and 5. The routes selected which had the most severe temperature exposure both on the ground prior to flight and inflight, are listed in Table 1.

The mission chosen for the KC-135 was that of inflight refueling of the B-52 airplanes. Accordingly, the KC-135 tracks coincide with the initial portions of the B-52 tracks; the KC-135s then turn around after aerial refueling (usually just prior to B-52 penetration) and return to the takeoff base. The

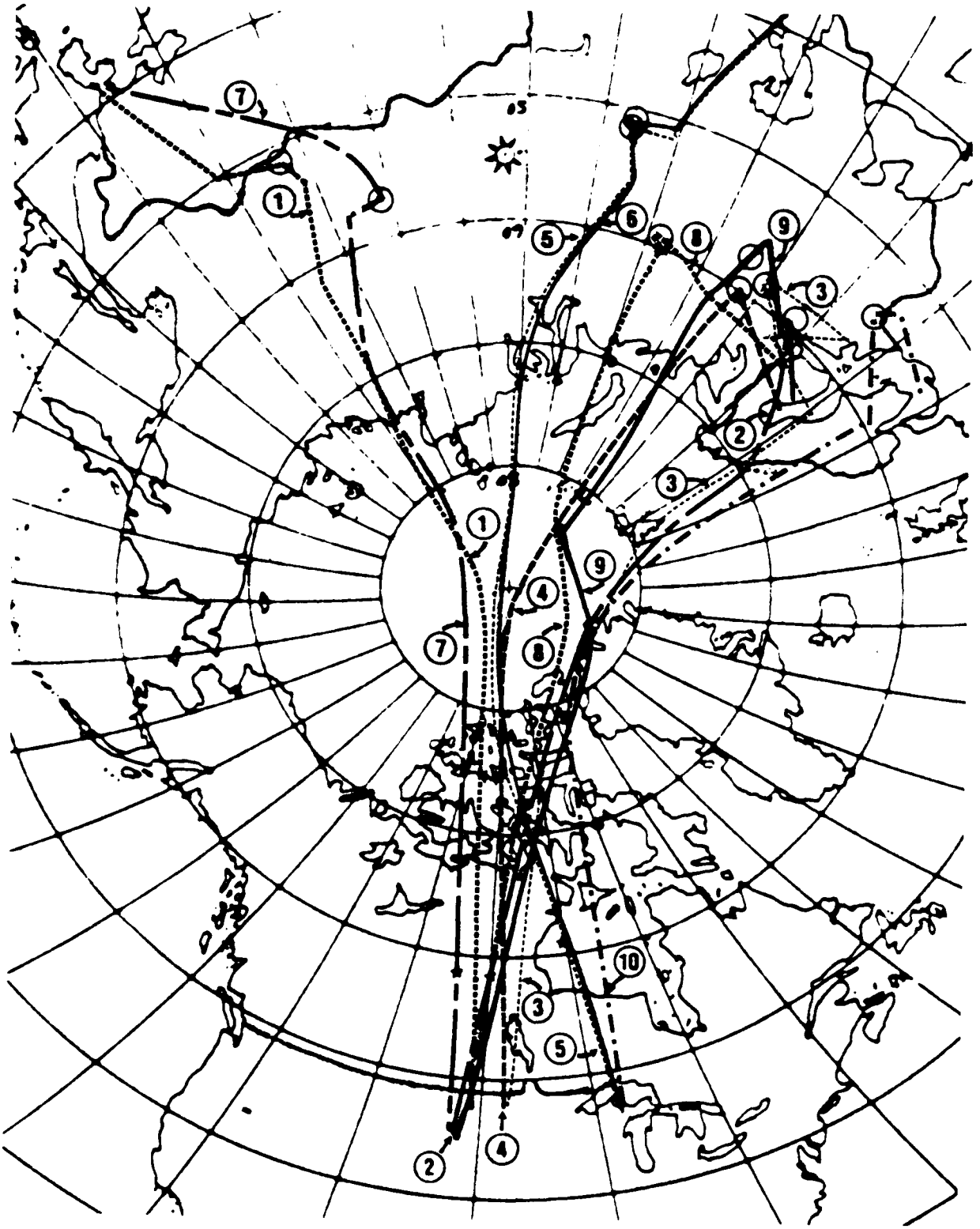

Figure 1. B-52 Routes

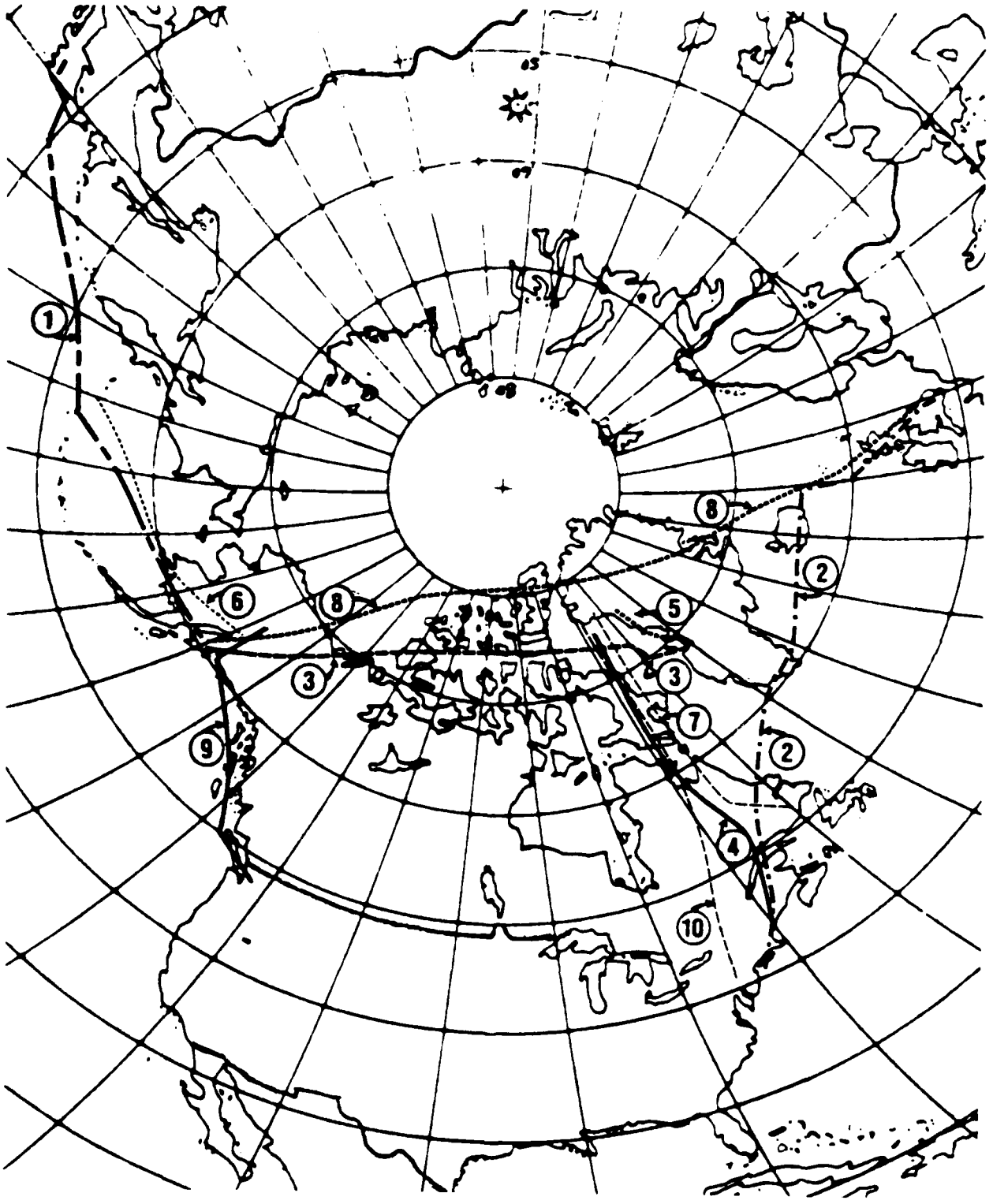

Figure 2. C-141 Routes

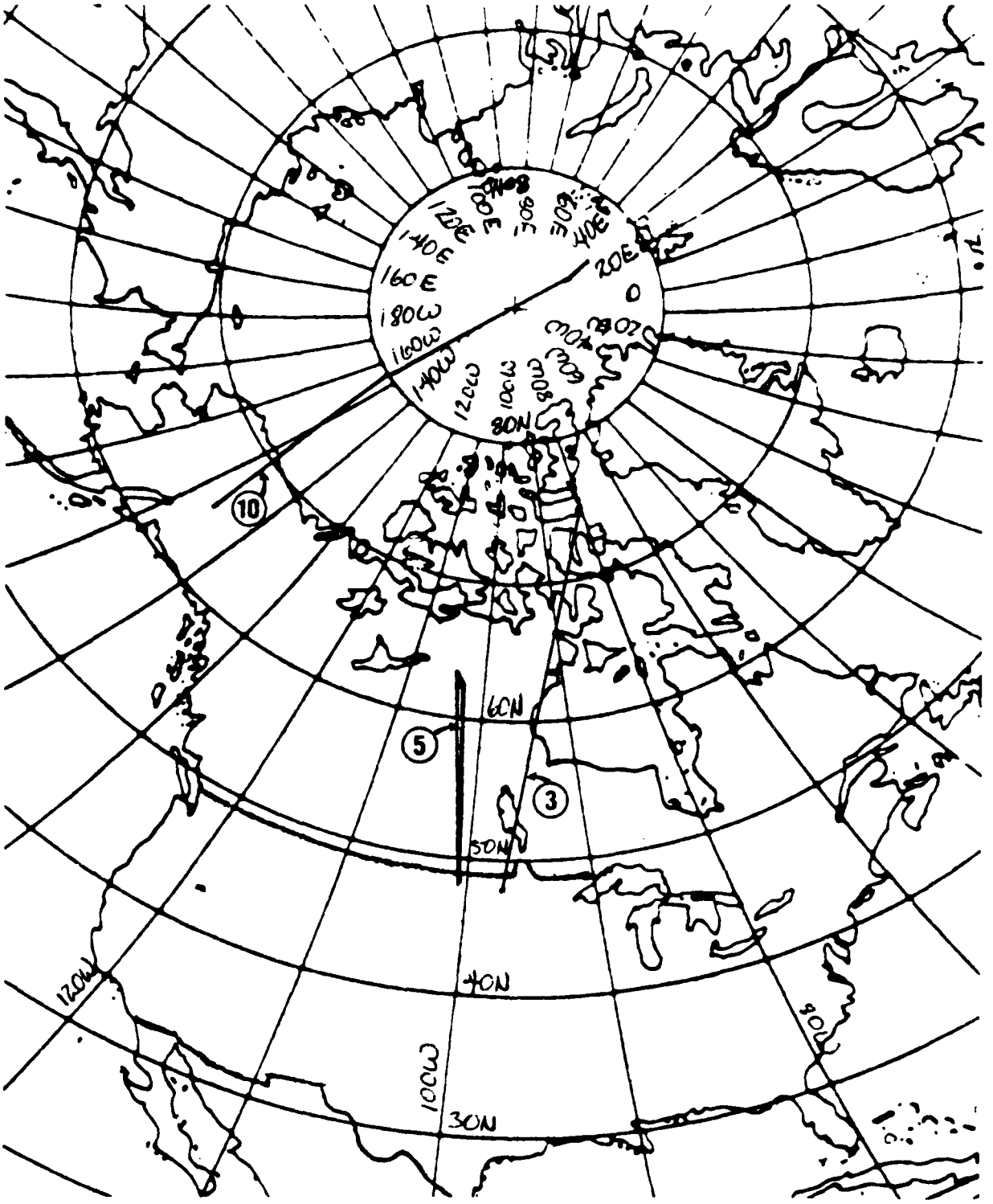

Figure 3. KC-135 Routes

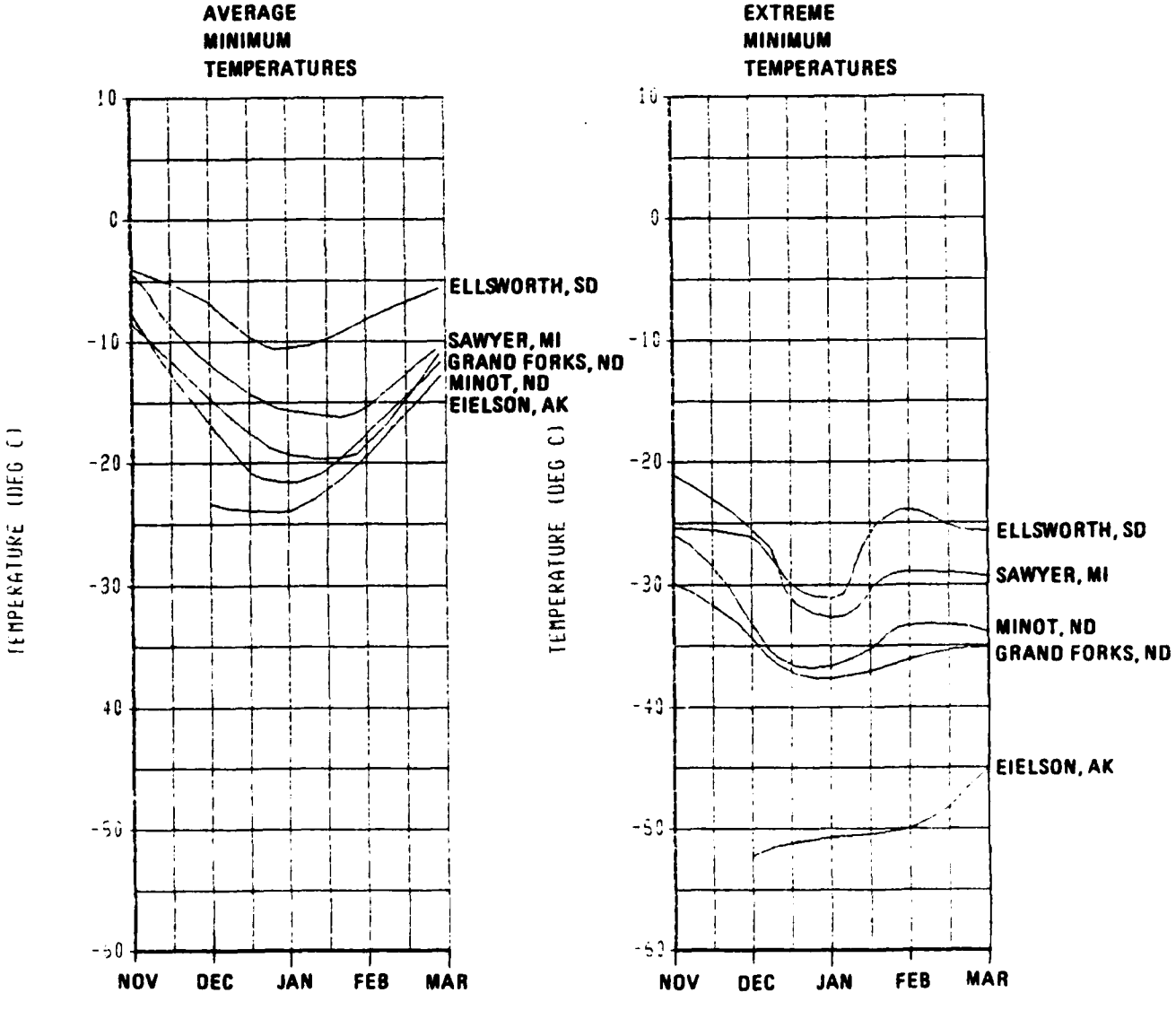

Figure 4. Winter Surface Air Temperatures at B-52 and KC-135 Takeoff Bases

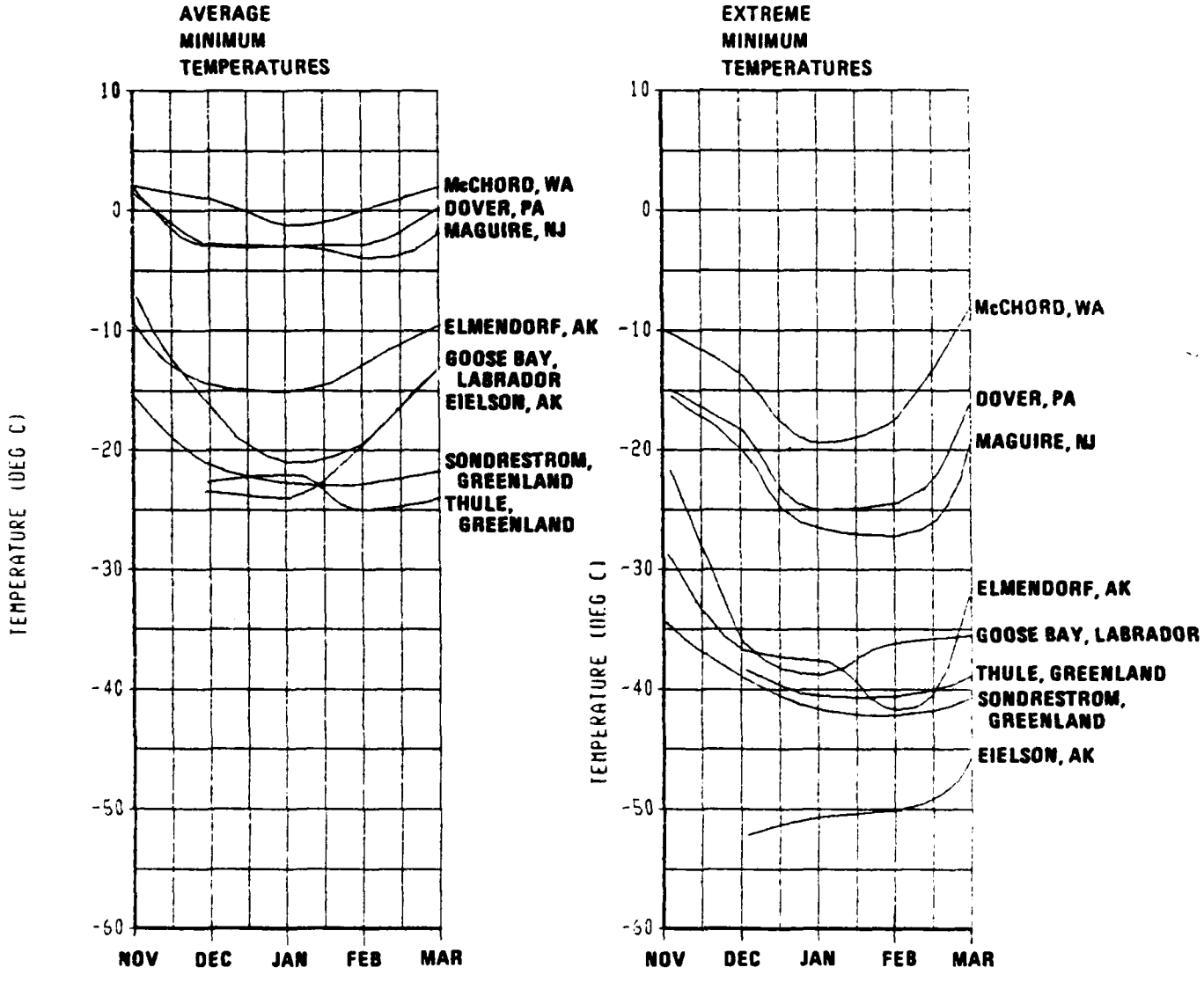

Figure 5. Winter Surface Temperatures at C-141 Takeoff Bases

Table 1. B-52, C-141, and KC-135 Selected Tracks and Takeoff Bases

Airplane	Track	Takeoff Base
B-52	1	Minot, ND
	3	Grand Forks, ND
	4	Grand Forks, ND
C-141	1	Elmendorf, AK
	8	Elmendorf, AK
	10	Thule, Gl
KC-135	3	Grand Forks, ND
	5	Minot, ND
	10	Eielson, AK

B-52 and KC-135 tracks are representative of wartime missions and the need to fly these or similar tracks during wartime is estimated to have a probability of 80%. Peacetime missions for these airplanes were determined to take place in warmer climates, and were thus less severe. The C-141 missions examined were expected to be flown in peacetime or wartime. The need for flying the selected routes was estimated to be 2% based on C-141 fleet operating experience.

b. Tactical Airplanes

Two tactical airplanes were also selected for study, the A-10 and F-15. Low speed, long duration winter flights in northerly latitudes were sought, and resulted in the identification of a relatively few ferry and combat missions. The use of northern routes for ferry missions with these airplanes is limited by the lack of suitable abort bases, therefore, most of the ferry missions (peacetime and wartime contingency) are flown considerably south of the routes (Figure 6).

Operational F-15 and A-10 missions of interest to this study were more difficult to identify, and a multiple step process was required. Four flight profiles (Figures 7 and 8) were established for both the A-10 and F-15, and the operating bases identified which have very cold winter environments. Ground temperature data for the winter months were tabulated for each of these bases (Figures 9 and 10) to determine the most severe. Routes were then defined which departed from the selected worst case bases (Grissom AFB and Eielson AFB for the A-10, and Minot AFB and Elmendorf AFB for the F-15) in the direction of the coldest average inflight temperature (Figures 11 and 12).

c. Track Conversions

The mission tracks for all five airplanes were converted into latitude, longitude, altitude and airspeed (Appendix A).

2. FUEL MANAGEMENT

The low temperature critical fuel tank for each study is the one in which the fuel becomes the coldest due to thermal exposure and fuel management. In airplanes with several integral wing tanks, the outboard wing tank is normally

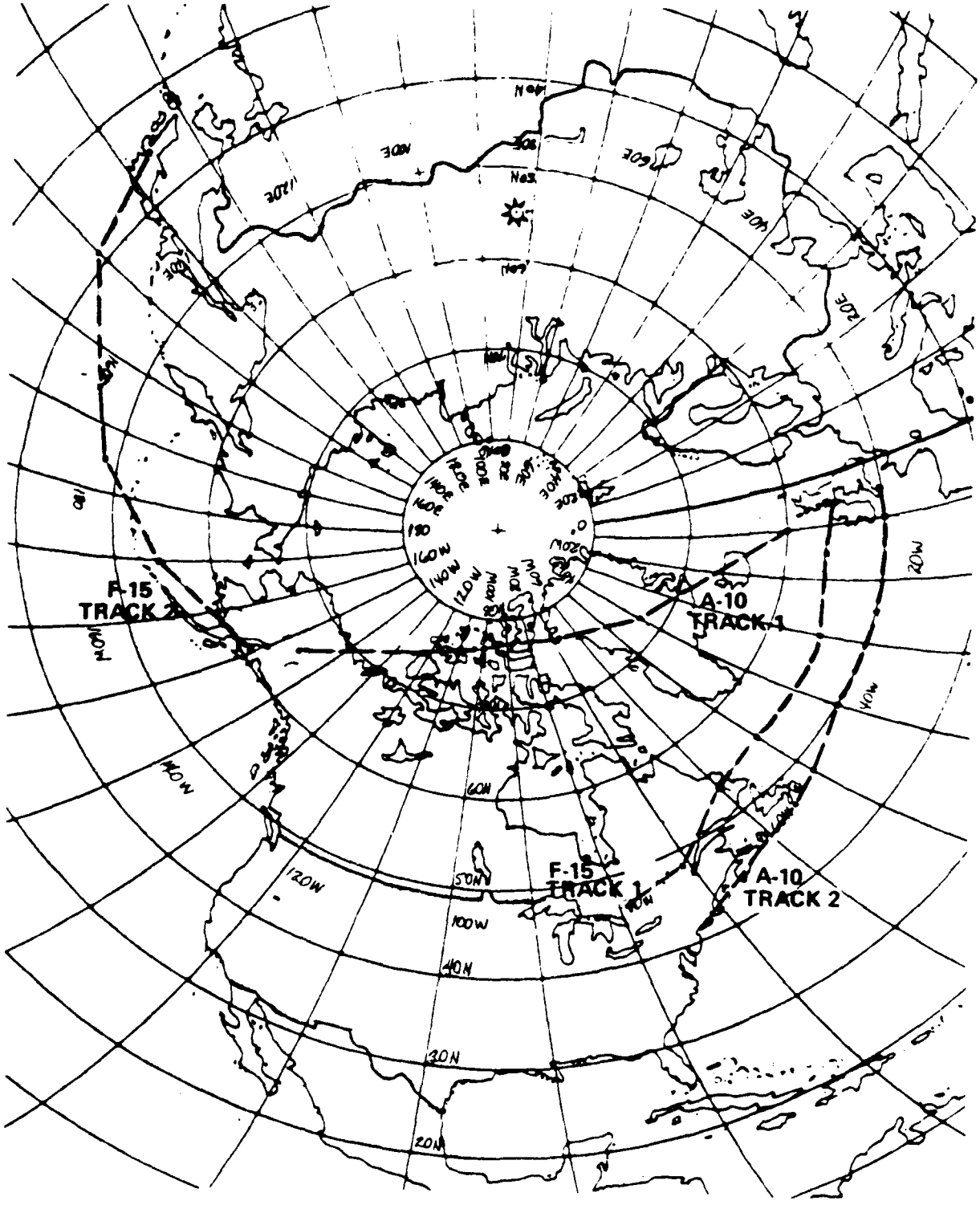

Figure 6. A-10 and F-15 Ferry Missions

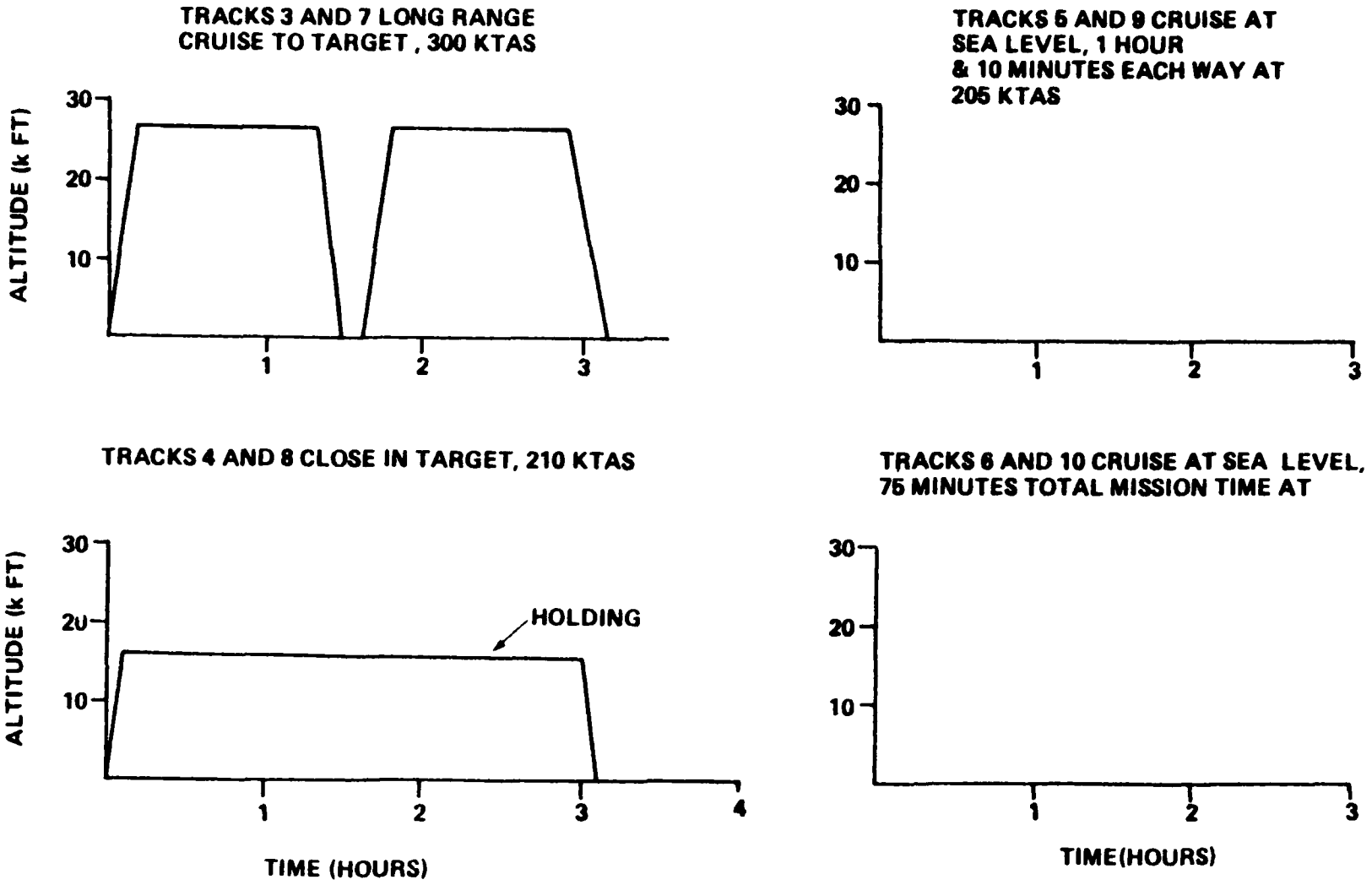

Figure 7. A-10 Short Range Missions

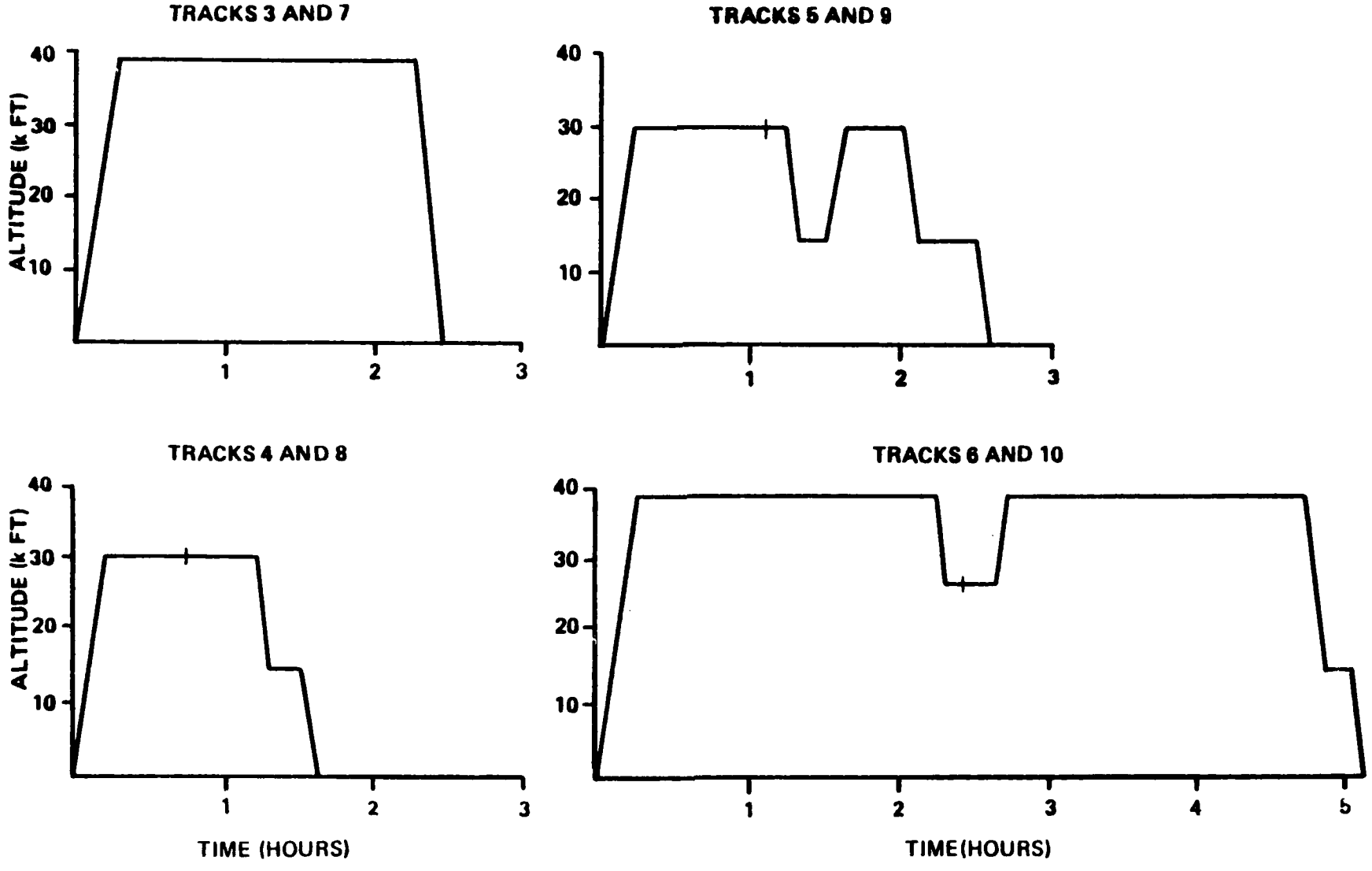

Figure 8. F-15 Short Range Missions

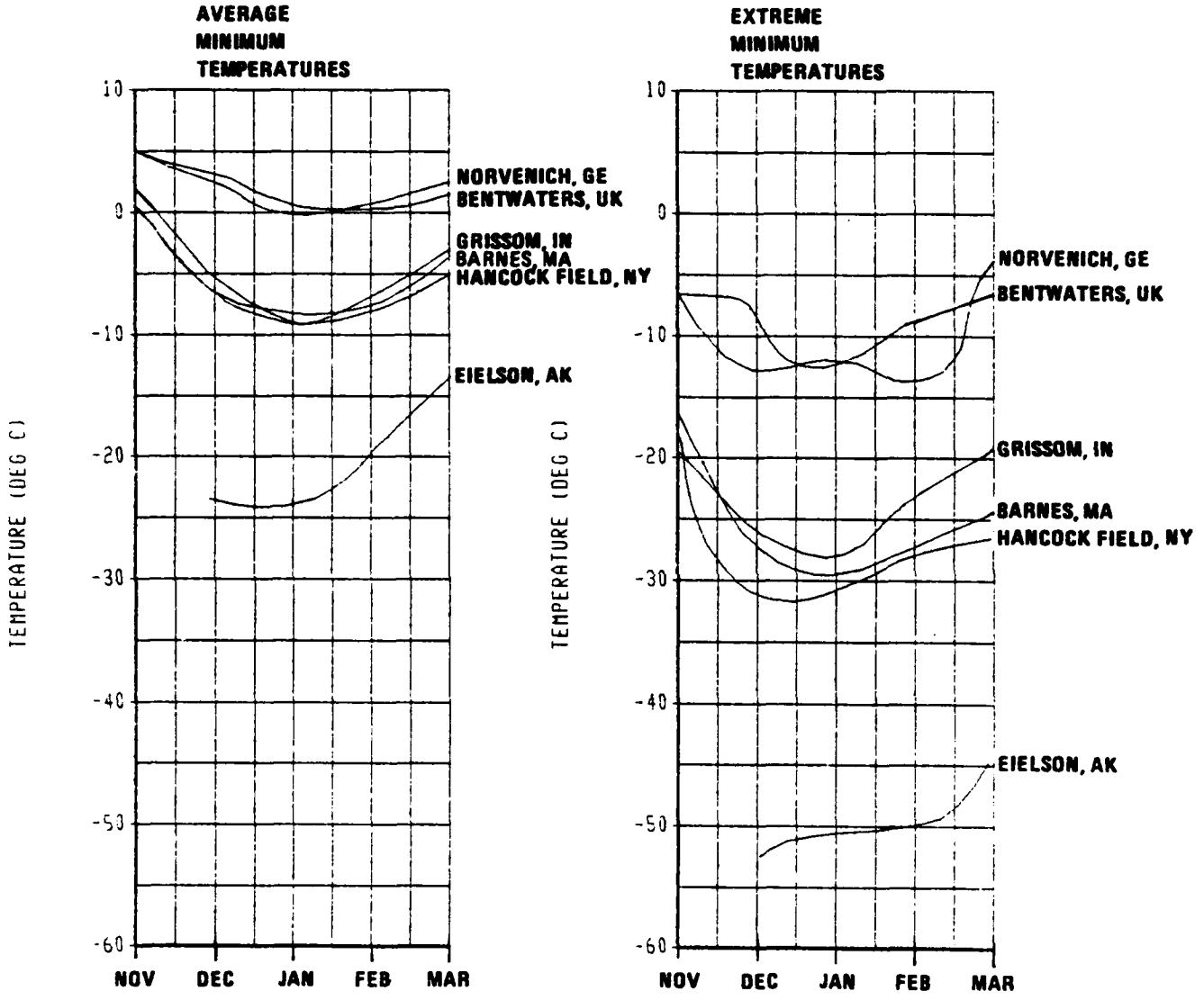

Figure 9. Winter Surface Air Temperatures at A-10 Takeoff Bases

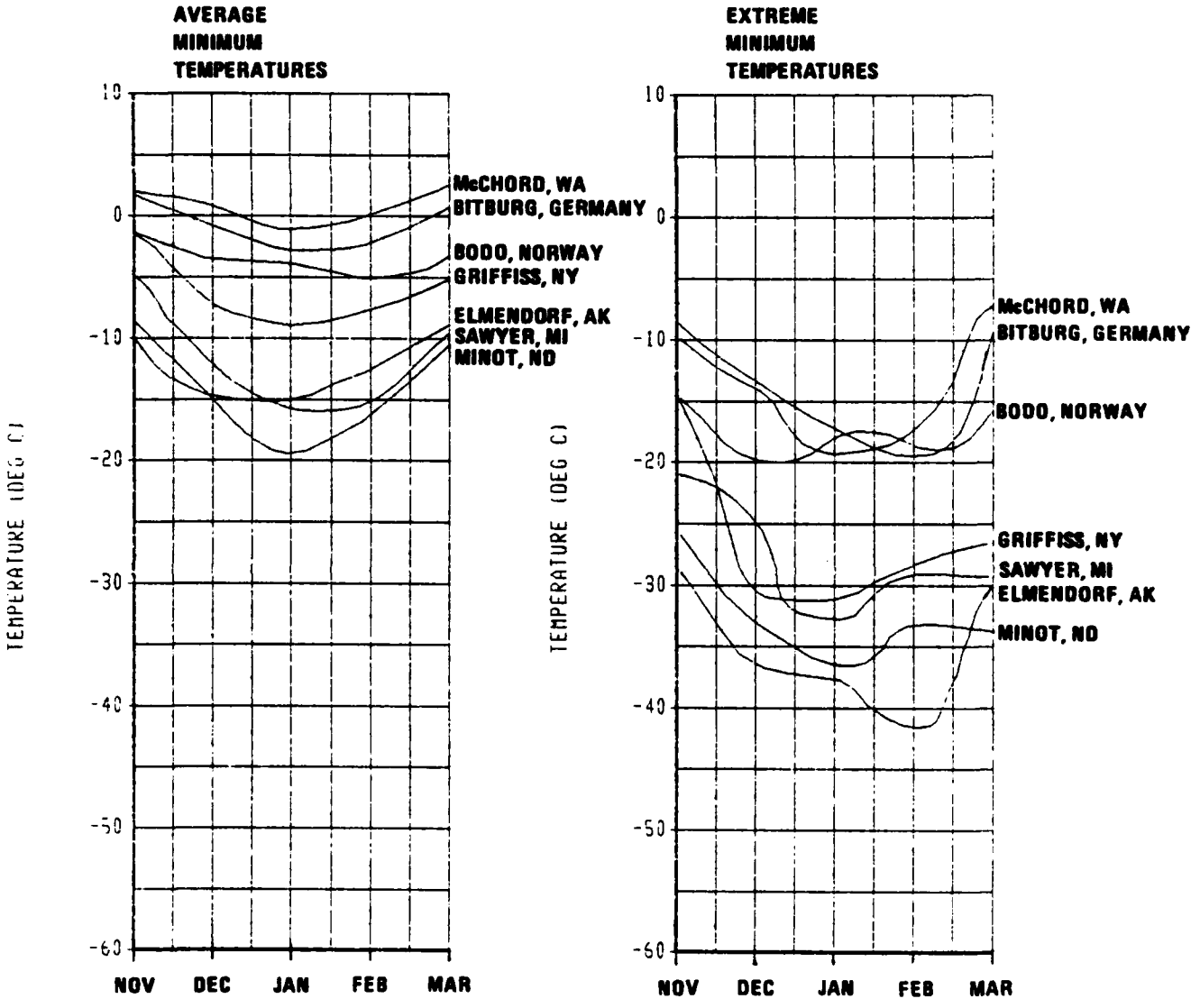

Figure 10. Winter Surface Air Temperatures at F-15 Takeoff Bases

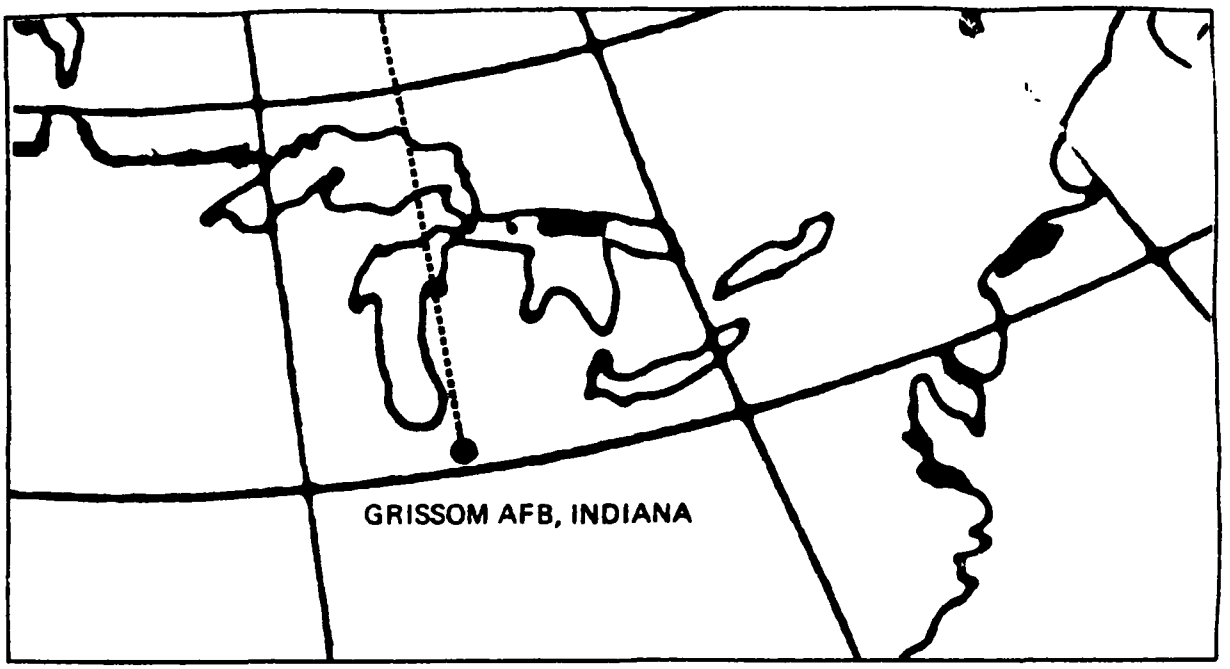

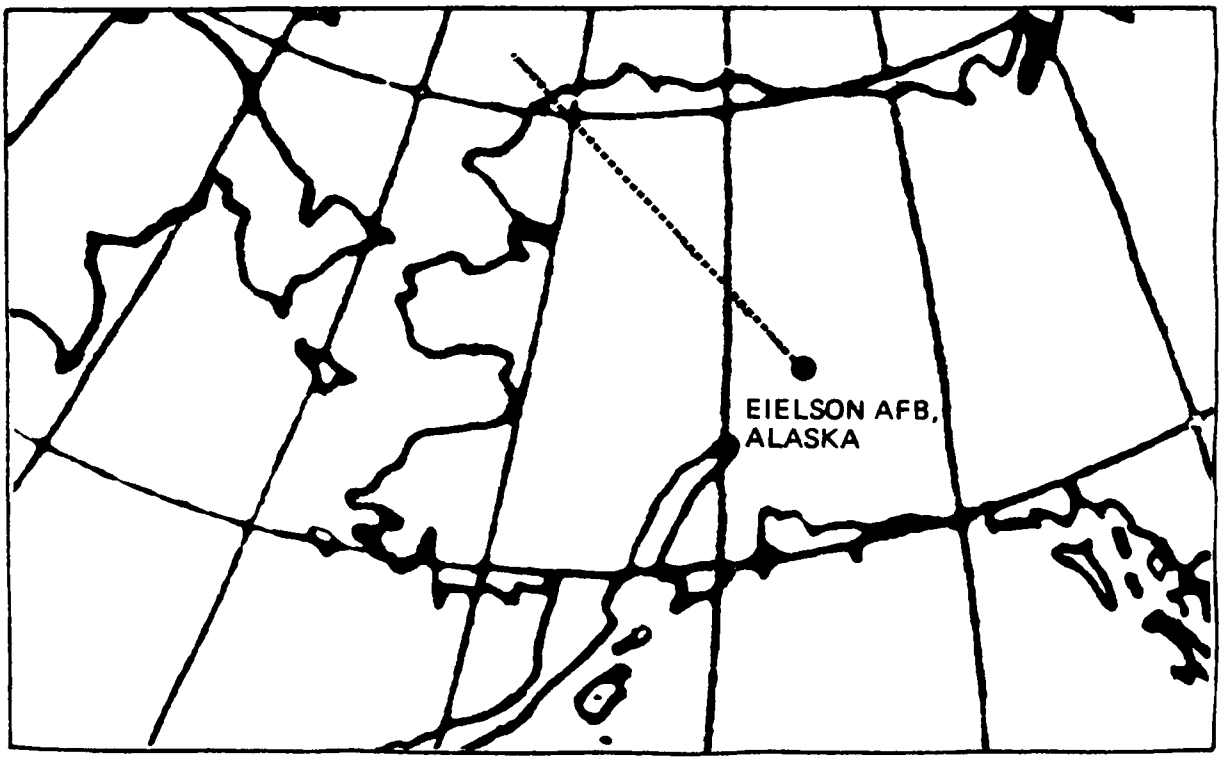

Figure 11. A-10 Short Range Mission Routes

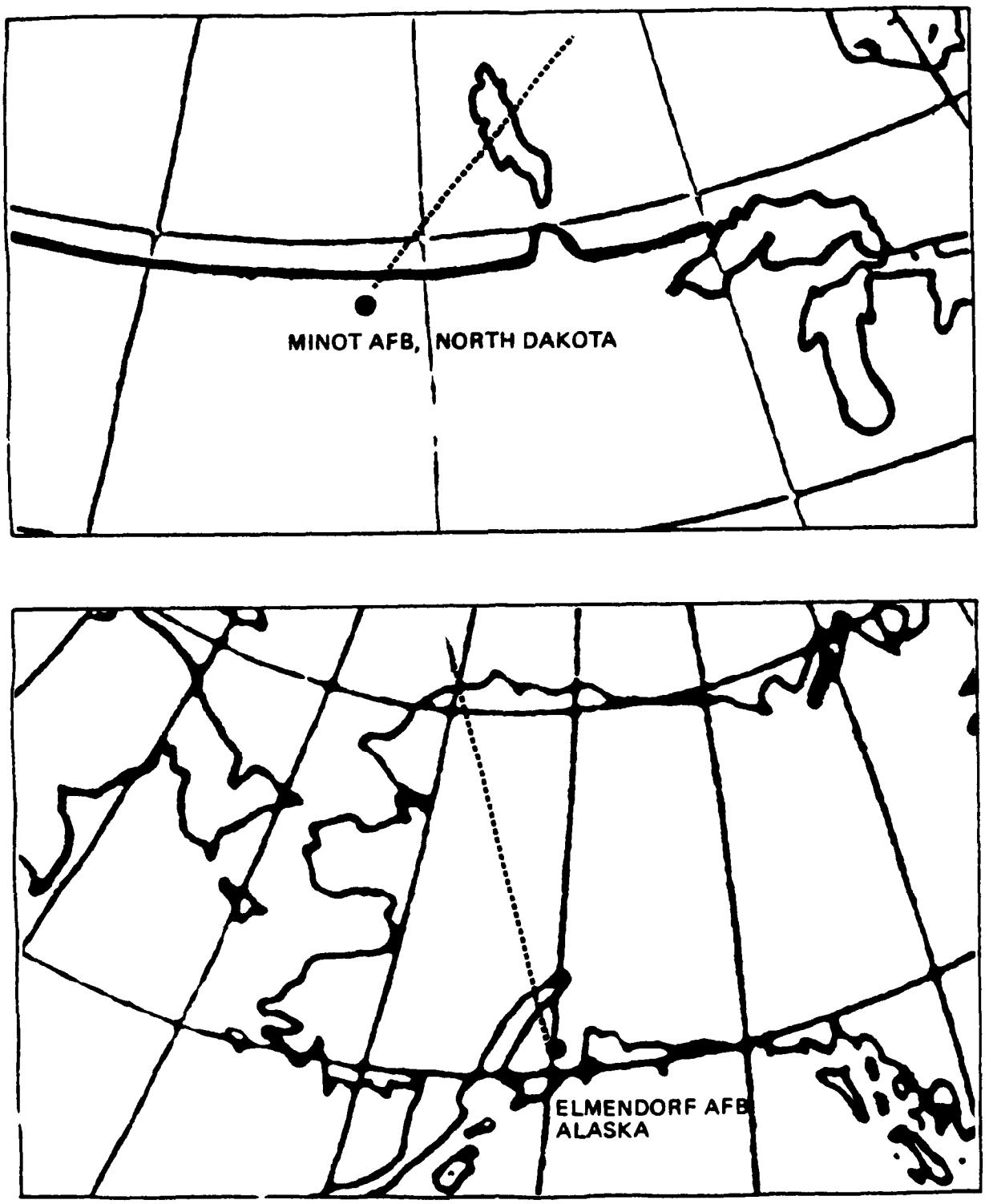

Figure 12. F-15 Short Range Mission Routes

the one from which the fuel is used last. (Retaining outboard wing fuel until late in the mission reduces wing bending moments and extends the airplane's structural life). Fuel tank location of the three study airplanes of this type (B-52, C-141, and KC-135) are shown in Figures 13, 14 and 15, and fuel usage sequences are given in Appendix B. Fuel management in fighter/attack airplanes with only one fuel tank per wing is considerably different; wing fuel is commonly consumed early in the mission for vulnerability reduction. In these airplanes, fuel is often carried in external cylindrical-shaped tanks. The A-10 and F-15 both have a single internal fuel tank per wing and have two or more external tanks; the configurations are shown in Figures 16 and 17 and the fuel management sequences given in Appendix B. All fuel management and fuel tank geometry data were obtained from the airplane technical orders (References 5 through 14).

3. ATMOSPHERIC THERMAL EXPOSURE

The purpose of this portion of the study was to determine the magnitude and extent of cold regions along the desired routes. In addition, the likelihood of encountering the extreme low temperature conditions was evaluated.

The basis for these calculations was a library of magnetic tapes which were acquired from the National Center for Atmospheric Research (NCAR) from which was extracted the atmospheric data base. The fifteen year data base covers the period from 1966 through 1982 (excluding 1971 and 1972) and contains twice-daily records of temperature at various altitudes to 53,000 feet at each of 1,977 grid points covering most of the Northern Hemisphere (Figure 18). Only winter data (15 December through 14 March) were examined in the present study since the most severe low temperature problems occur during the winter months.

a. Thermal Exposure

The thermal exposures were extracted from the data base by specifying the latitude, longitude, altitude, and airspeed that define each airplane trajectory, with the thermal exposure of the airplane between the established grid points (Figure 18) determined by interpolation. The time averaged temperature along each route was used to identify the 15 worst case cold days

TANK	USABLE FUEL (GAL)	FUEL SERVICED (GAL)
MAINS 1 & 4	9,798	9,810
MAINS 2 & 3	13,618	13,668
C. WING	3,228	3,240
FWD. BODY	2,049	2,053
MID BODY	7,140	7,154
AFT BODY	8,491	8,498
OUTBD (BOTH)	2,306	2,320
EXT. (BOTH)	1,400	1,410
TOTAL	48,030	48,153

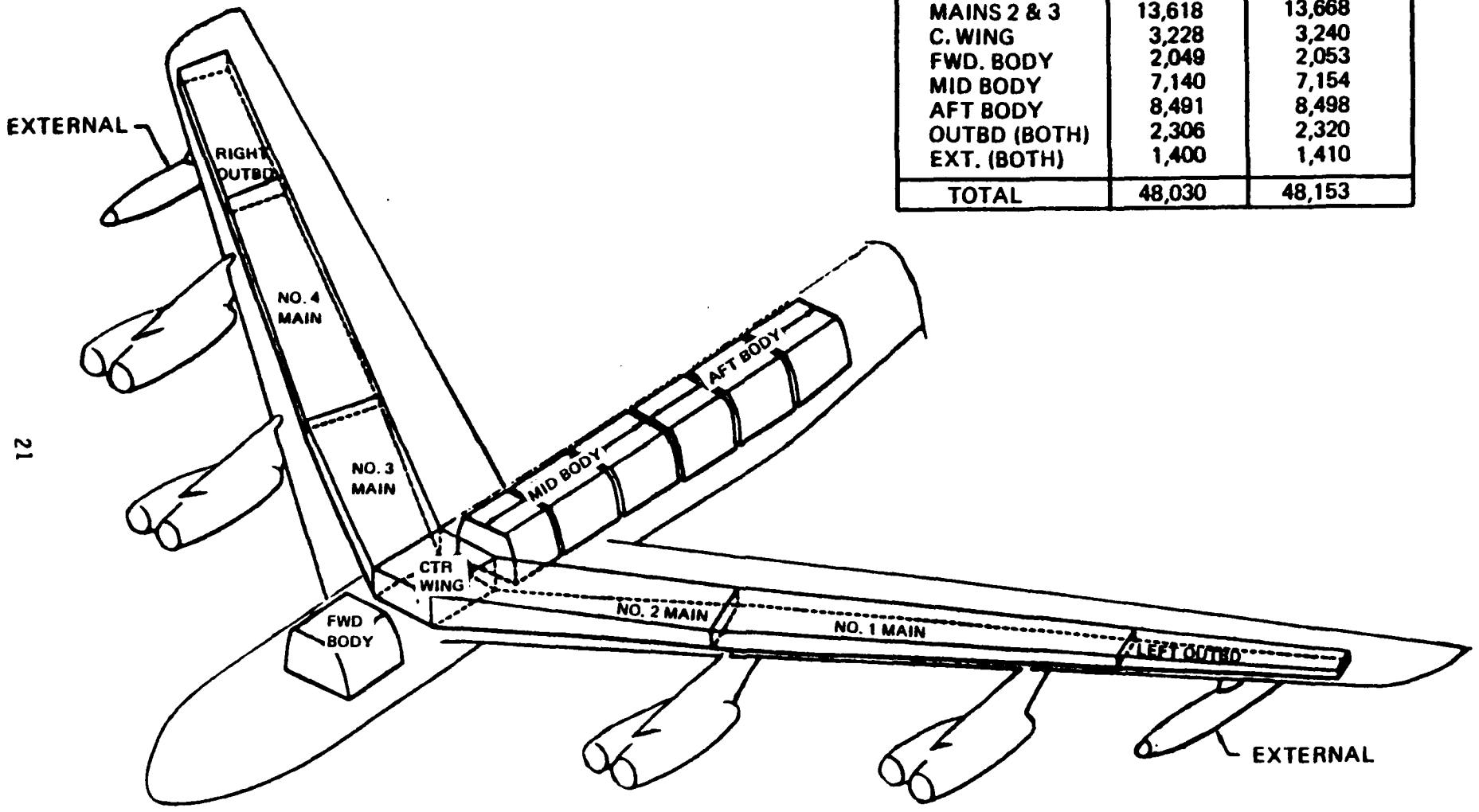

Figure 13. B-52 Fuel Tank Locations

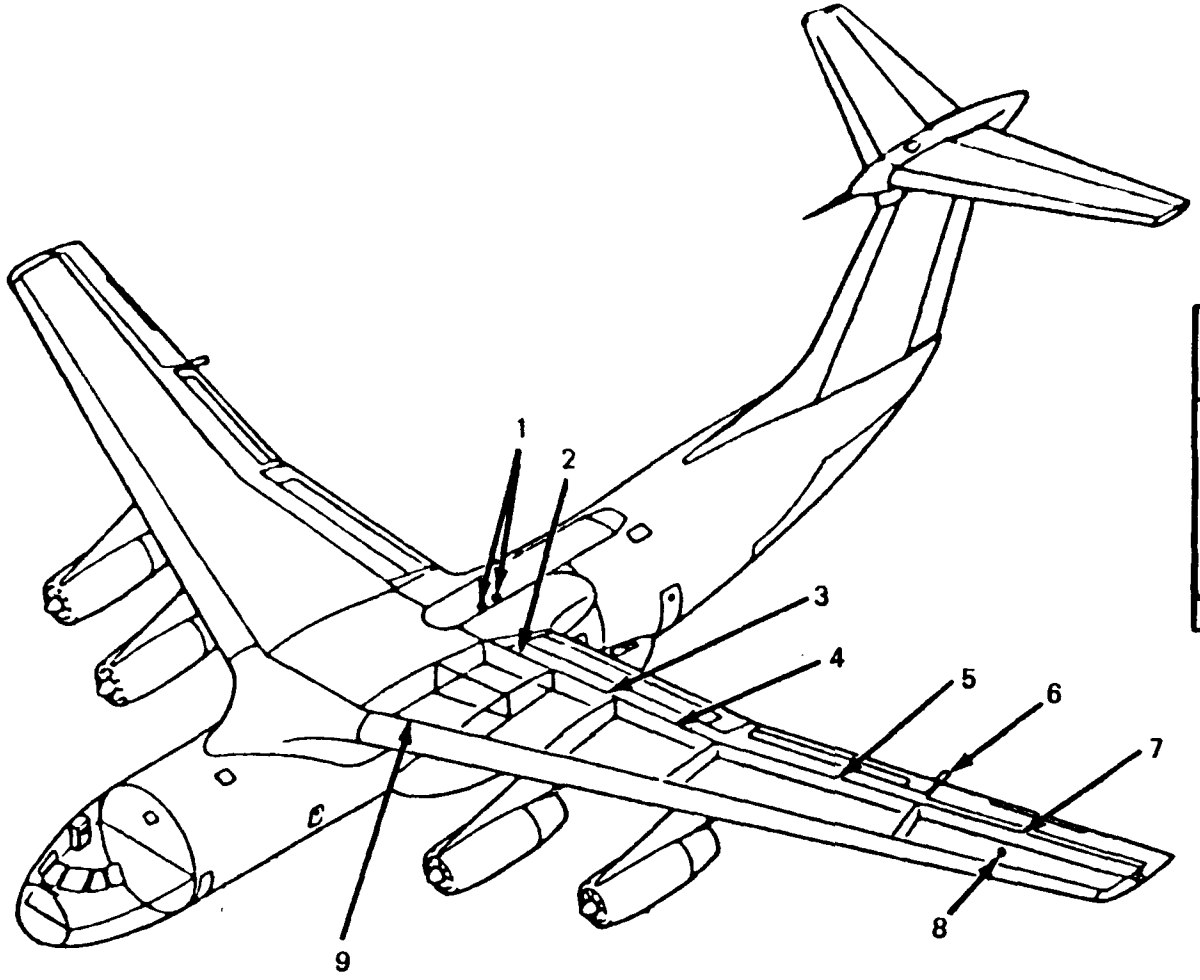

TANK	USABLE FUEL (GAL.)	FULLY SERVICED (GALLONS)
MAINS 1 & 4	2,466	2,530
MAINS 2 & 3	4,338	4,356
AUX'S 1 & 4	5,140	5,144
AUX'S 2 & 3	3,392	3,402
EXT RANGE L & R	8,256	8,280
PLUMBING	—	64
TOTAL	23,592	23,776

1. SINGLE POINT REFUELING AND DEFUELING ADAPTERS (NEAR AFT END OF RIGHT WHEEL WELL POD)
2. NO. 2 AUXILIARY TANK (NO. 3 AUX TANK SYMMETRIC)
3. INBOARD COMPARTMENT OF LEFT HAND EXTENDED RANGE TANK (RIGHT HAND TANK SYMMETRIC)
4. OUTBOARD COMPARTMENT OF LEFT HAND EXTENDED RANGE TANK (RIGHT HAND TANK SYMMETRIC)
5. NO. 1 AUXILIARY TANK (NO. 4 AUX TANK SYMMETRIC)
6. LEFT JETTISON MAST
7. NO. 1 MAIN TANK (NO. 4 MAIN TANK SYMMETRIC)
8. VENT OUTLET (IN LOWER SURFACE OF WING)
9. NO. 2 MAIN TANK (NO. 3 MAIN TANK SYMMETRIC)

Figure 14. C-141 Fuel Tank Locations

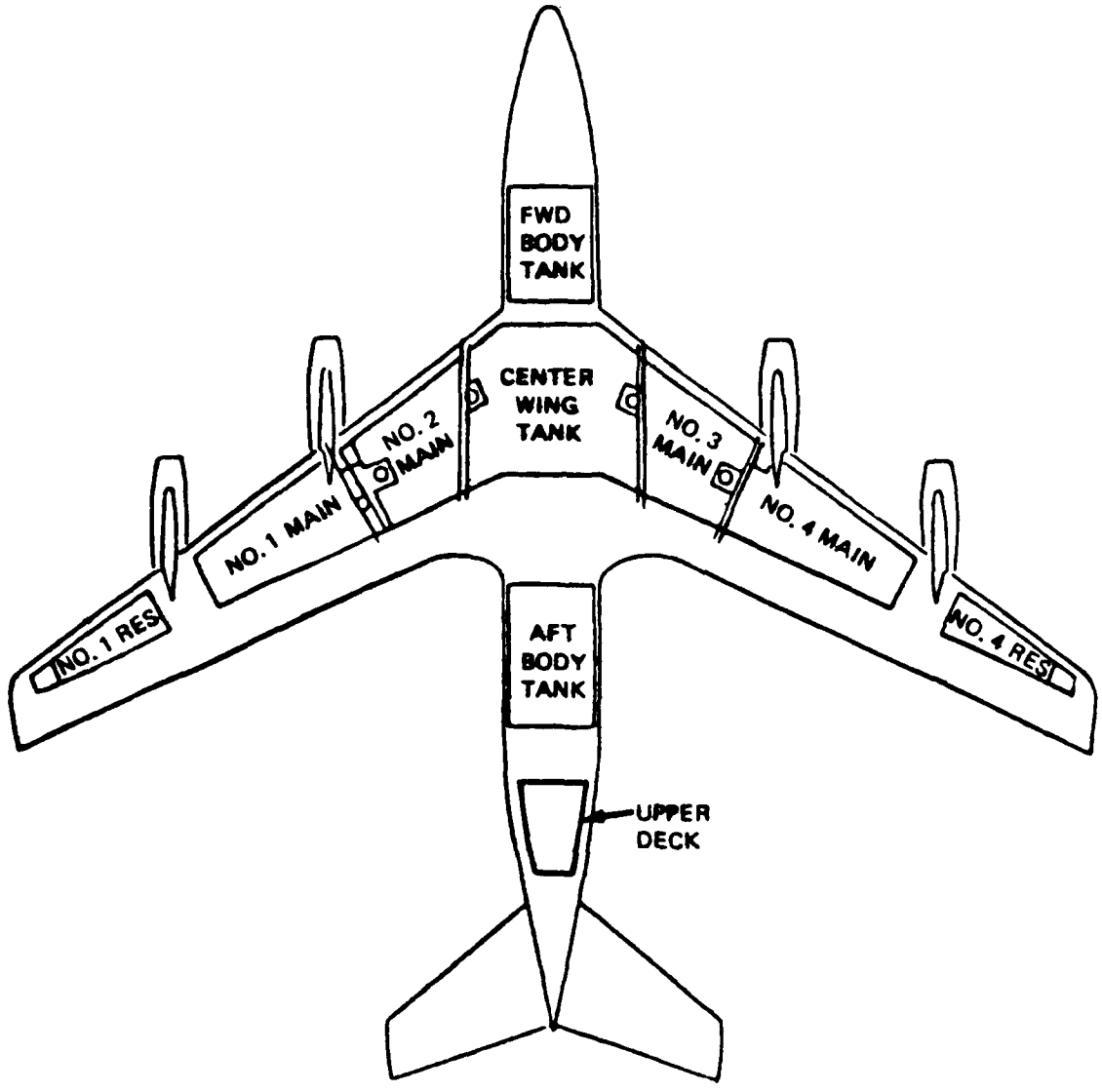

TANK	USABLE FUEL (GAL)	FULLY SERVICED (GAL)
MAINS 1 & 4	4,124	4,144
MAINS 2 & 3	4,550	4,588
RESERVES 1 & 4	868	870
FWD BODY	5,800	5,811
CNTR WING	7,306	7,339
AFT BODY	6,378	6,418
UPPER DECK	2,174	2,184
TOTAL	31,200	31,354

Figure 15. KC-135 Fuel Tank Locations

TANK	USABLE FUEL (GAL)
WING L & R	622
BODY L & R	1,022
EXTERNAL L, R, & C	1,800
TOTAL	3,444

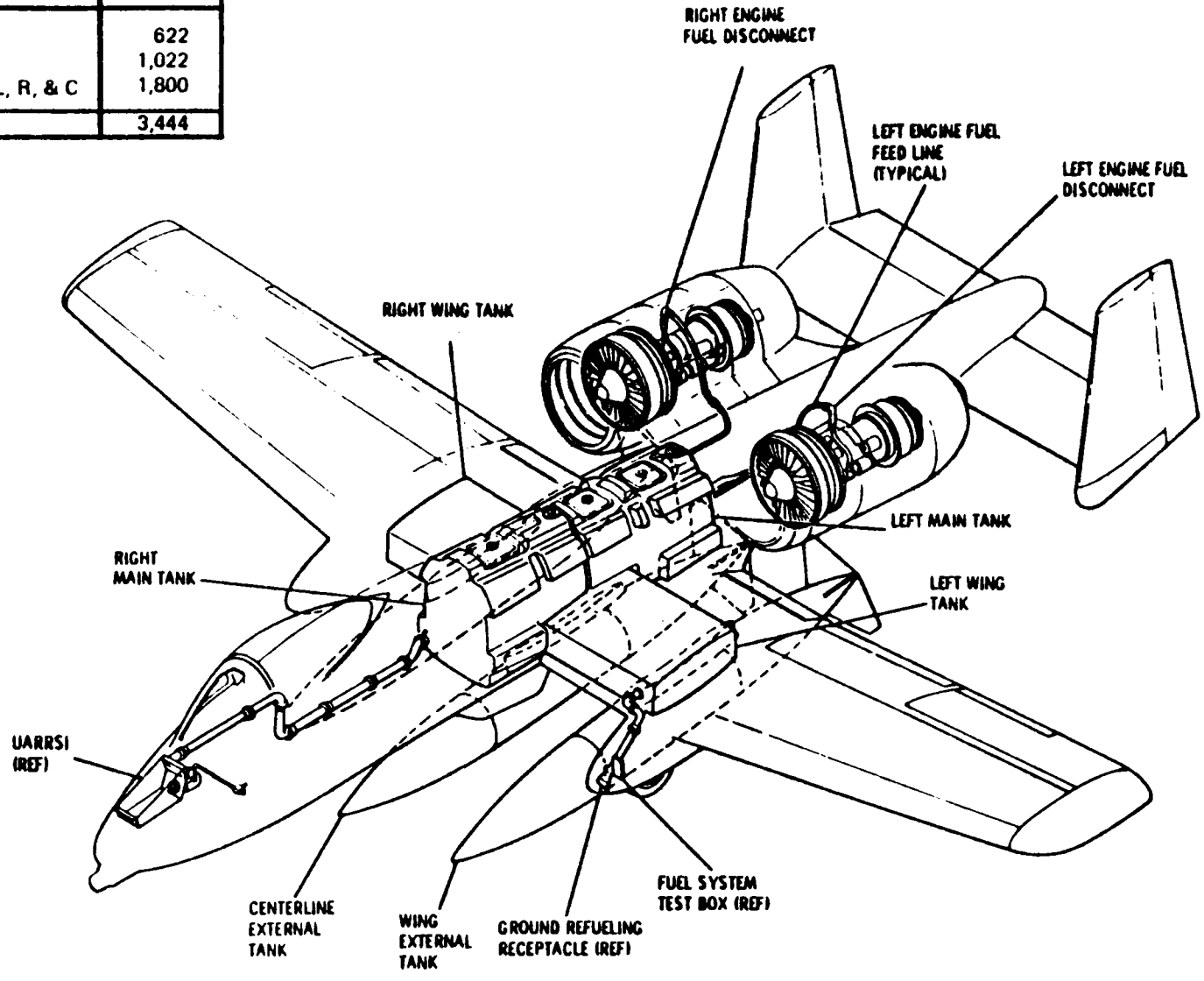

Figure 16. A-10 Fuel Tank Locations

TANK	USABLE FUEL (GAL)	FULLY SERVICED (GAL)
WING L & R	844	848
TANK 1	508	517
TANK 2	234	253
TANK 3A & 3B	184	202
EXTERNAL L, R, & C	1,830	1,839
TOTAL	3,600	3,659

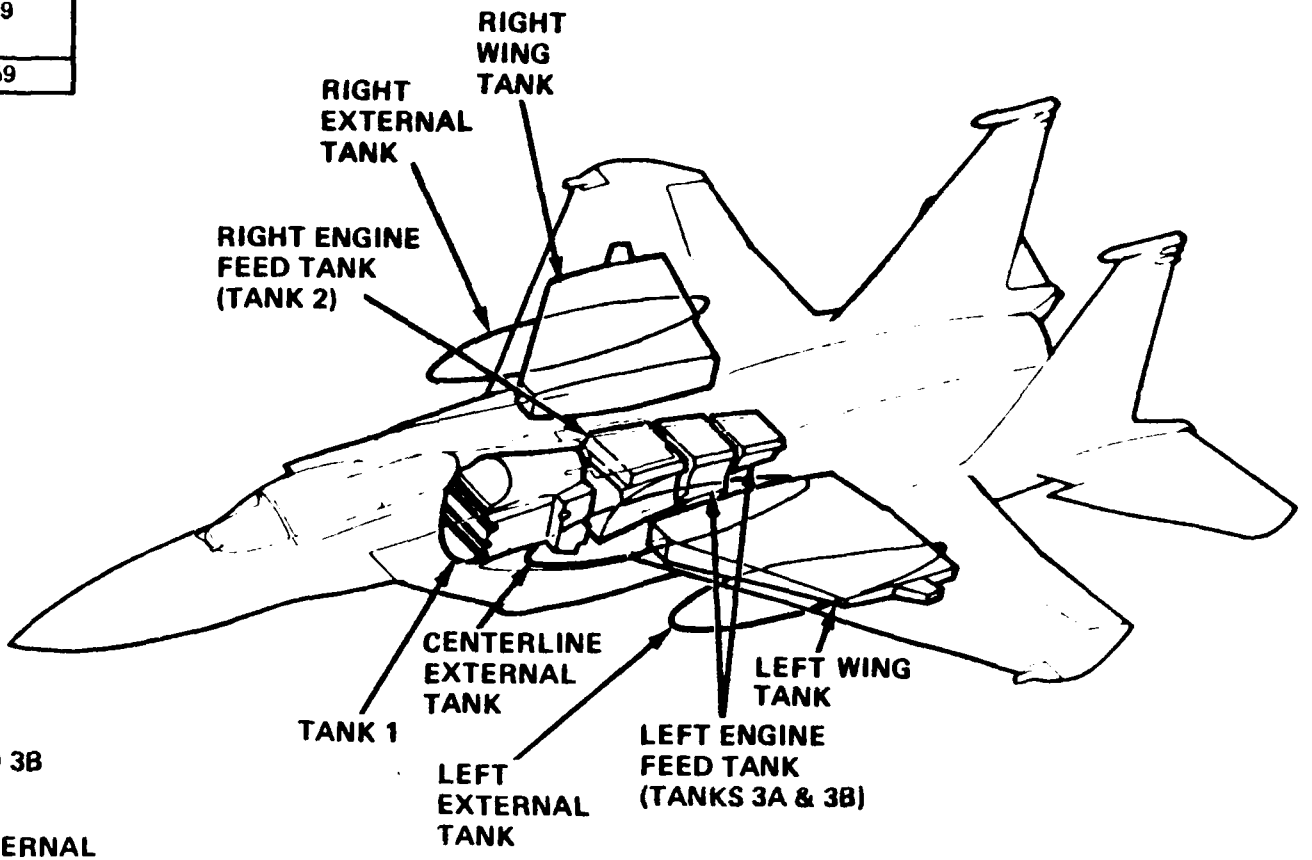

- FUEL TRANSFERRED FROM TANK 1 TO TANKS 2, 3A, AND 3B (FEED TANKS)
- BEGIN TRANSFER FROM EXTERNAL TANKS WHEN TANK 1 IS APPROXIMATELY ½ EMPTY

Figure 17. F-15 Fuel Tank Locations

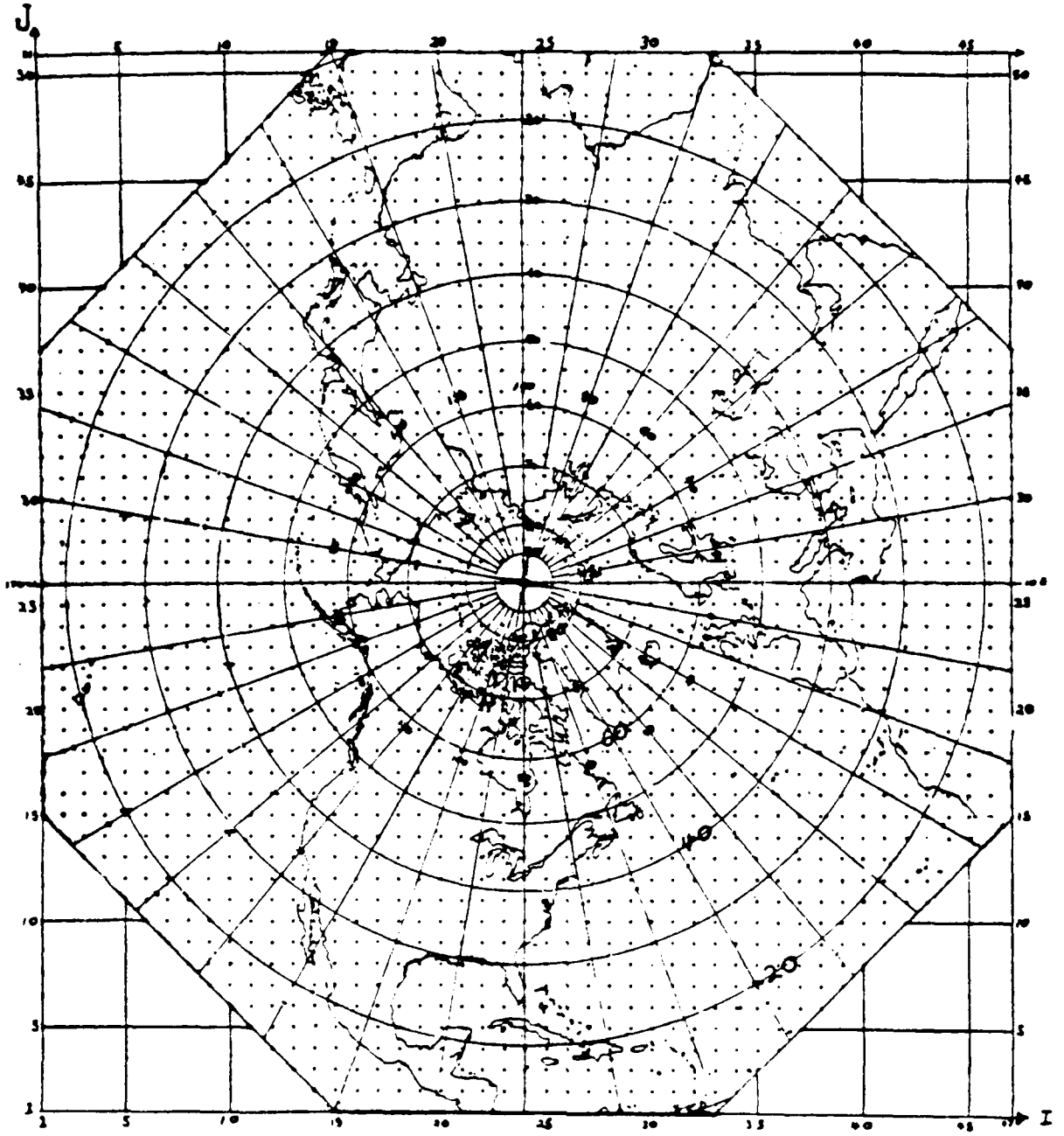

Figure 18. NCAR Meteorological Grid

are reported in Appendix C, Figures C-1a through C-29a, and the single worst case cold day ambient and recovery temperatures, in Figures C-1b through C-29b. The recovery temperature, Tr, (Reference 15) forms the time varying thermal boundary condition for the temperature calculations, and is defined as

$$T_r = T_\infty \left[1 + r\left(\frac{\gamma-1}{2}\right)M_\infty^2\right] \quad (1)$$

where T_∞ = free stream temperature
r = recovery factor ($\simeq$0.9)
$\gamma = C_p/C_v$ ($\simeq$ 1.4 for air)
M_∞ = free stream Mach number

The recovery factor r is taken to be the cube root of the Prandtl number (P_r) for turbulent flow and since P_r is independent of any characteristic dimension, it is essentially constant over all airplane surfaces (Reference 16).

b. Verification of Atmospheric Temperature Data Base

Data were made available during this study which provided the first opportunity to check the Boeing atmospheric data base and computer program which predicts enroute temperatures. Flight test data were obtained for two flights from the NASA Global Air Sampling Program (GASP). The data were provided by Mr. Robert Friedman of the NASA-Lewis Research Center, and was qualified at the time as preliminary data (Reference 17). The route information (latitude, altitude, and airspeed) was input to ROUTEMP (computer program described in paragraph c) to extract predicted enroute temperatures for the days on which the flights occurred, and the results compared to the flight test measurements (Figures 19a and 19b). The flight test data included static temperature, inferred from the measured total temperature. The route input data is reported in Appendix A. The data base temperatures were interpolated from data which were recorded at twelve-hour intervals bounding the period during which the flight actually occurred. The data for 1 December 1978 agree very well except for a 60-70 minute period during the middle of the flight. Agreement for the 25 November 1978 flight is not as close, especially after the 450 minute point. However, considering the relatively low frequency

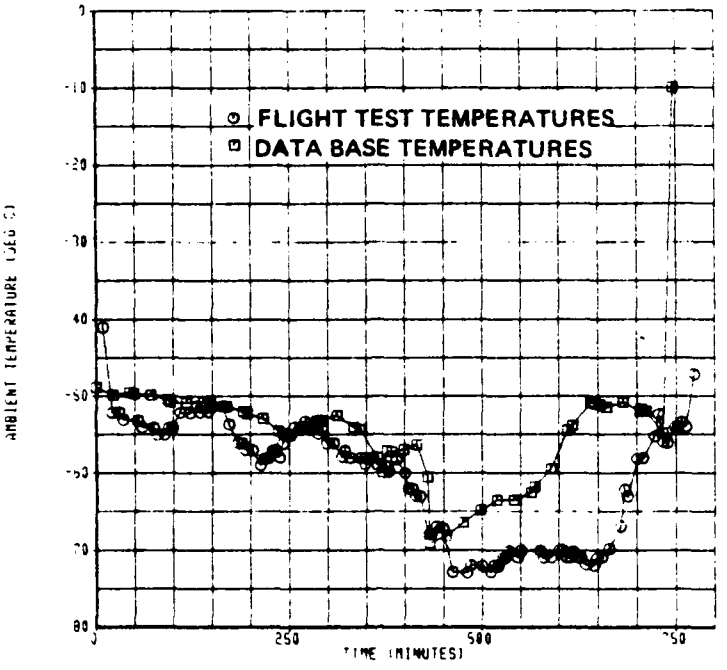

a. 25 November 1978

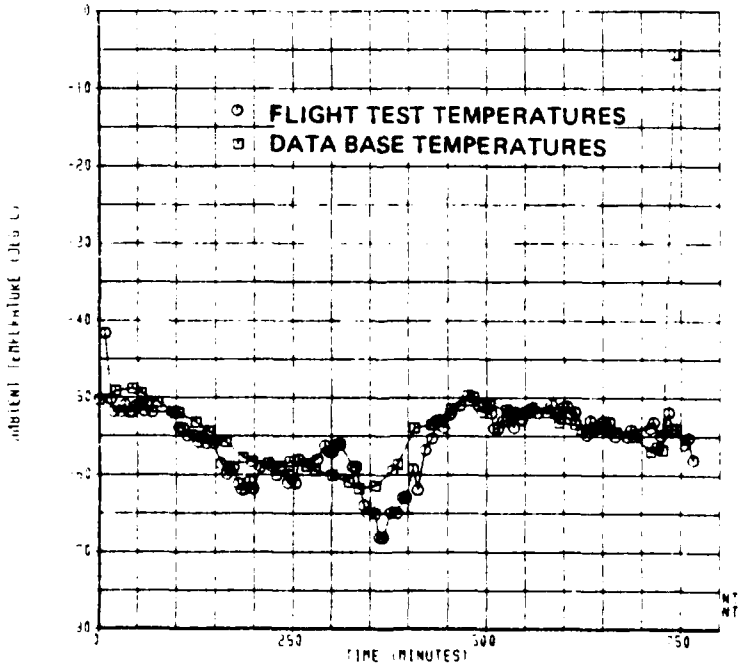

b. 1 December 1978

Figure 19. Comparison of L-1011 Flight Test Data and ROUTEMP Results

at which the weather services record data, and the fact that atmospheric data is drawn from isotherm and isobar maps which are based on comparatively few points, the overall agreement is quite good. Note that the lowest temperatures encountered correspond within 3 to 5°C, and that the periods in which temperatures increase and decrease correlate well.

In order to accomplish the extraction of data for the two flights referenced above, it was necessary to further modify the ROUTEMP computer program to select the date and time specified (rather than the 15 worst case days as described earlier). Note also that the 2 days of interest are outside the 90-day period covered by the atmospheric data base (Section II.4). A version of the program was created which will now search any NCAR magnetic tape and extract temperatures along designated route. Should more route-temperature data become available in the future, this version can be used to further check the validity of the data base search technique.

c. Statistical Analysis of Atmospheric Thermal Exposure

A statistical analysis was performed to evaluate the probability of a severe low temperature encounter. It was performed by modifying the computer program (ROUTEMP) which extracts the thermal exposure data to further process the temperature data, generating useful information relative to the duration and frequency of low temperature exposures. The analysis also ensured that the cases selected for study included a representative number of extreme low temperature exposures as well as extremes of time averaged temperature.

(1) Duration of Low Temperature Encounters

The first modification was to quantify the magnitude and duration of low temperature exposure on a given route. A sample of the output of ROUTEMP portraying ambient temperature encountered versus flight time is shown in Figure 20a. Five-degree temperature increments were defined, as indicated by the dashed lines in the figure. As the route is "flown", the length of time spent below each temperature is accumulated for each flight along a specified route. For example, on the day depicted in Figure 20a:

- -60°C or less is encountered for 330 minutes
- -65°C or less is encountered for 290 minutes

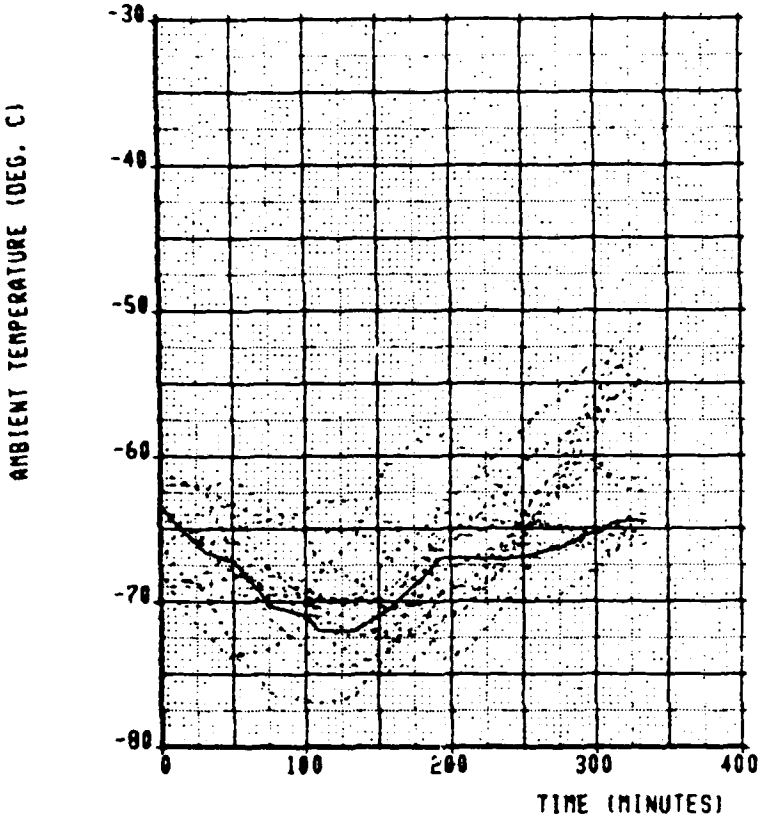

Figure 20a. Sample Output of ROUTEMP Program, C-141 Track 10

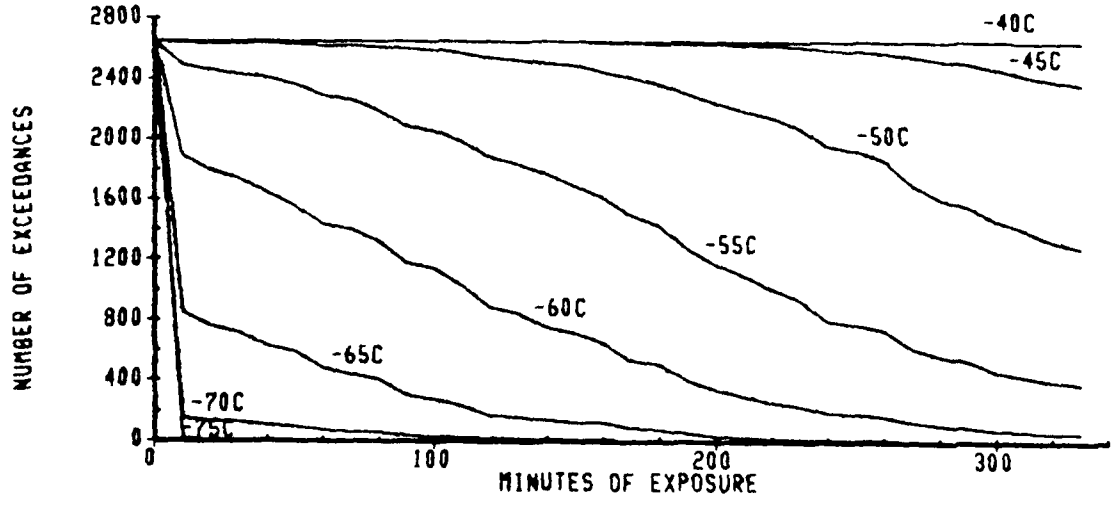

Figure 20b. Number of Exceedances vs. Duration of Exposure, C-141 Track 10

- o $-70^{o}C$ or less is encountered for 90 minutes
- o $-75^{o}C$ was never encountered

These data were accumulated on tape for each day, and used to generate a plot of the type represented in Figure 20b which shows:

- o no exposures at or below $-80^{0}C$, and relatively few of short duration below $-75^{o}C$ and $-70^{o}C$
- o approximately 300 exposures to $-65^{o}C$ for 100 minutes

These "duration of exceedance" plots for all the study routes are contained in Appendix C, Figures C-1c through C-29c.

(2) Frequency of Encounters

A frequency distribution was also created for each route based on the time-averaged (ambient) temperature of the route for each sample. It was hypothesized that either of two types of distribution might result. The first (Figure 21a) represents a nearly normal distribution of average temperatures. In this case, a large number of days (samples) may appear in the low temperature "tail" of the distribution where the fifteen worst cases are located. This would indicate that a large number of days are nearly as severe, on average, as the nominal 15 cases selected in previous studies and that a fuel unacceptable on these few days would be a major operational problem. If, on the other hand, a skewed distribution was found (Figure 21b), it would indicate that a relatively few days are included in or near the low temperature tail, and that a fuel which could not meet the requirements of the low temperature extreme might still be satisfactory in operational use, that is, carry small risk of operational interference.

The distribution constructed for C-141 Track 10 is shown in Figure 21c. This indicates an essentially normal distribution, as do the majority of the other resulting distributions which are included in Appendix C, Figures C-1d through C-29d. Due to the large number of samples contained in the data base, approximately 2,700, the fifteen worst cases used in this study comprise only the tip of the low temperature tail. They are, however, within only a few degrees of a significant number of other near-worst cases.

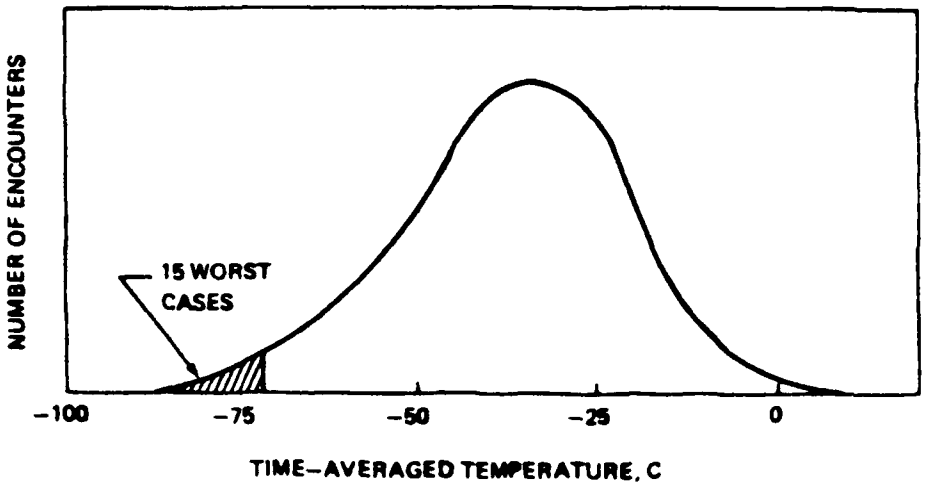

Figure 21a. Quasi-Normal Frequency Distribution

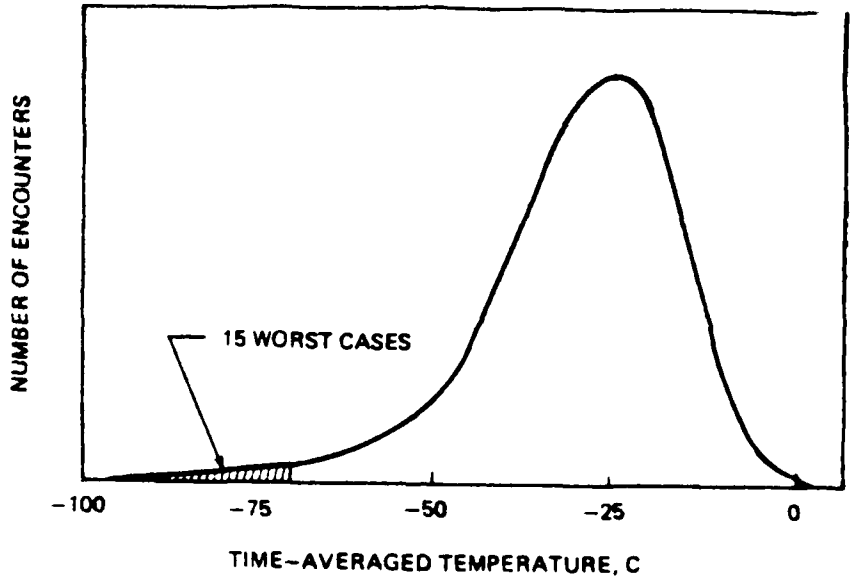

Figure 21b. Skewed Distribution

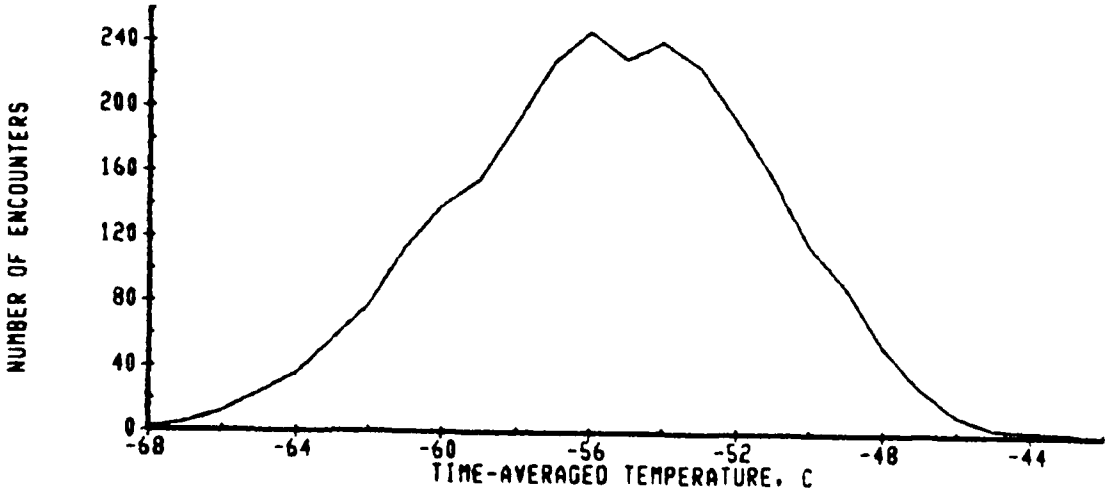

Figure 21c. Frequency Distribution of Time-Averaged Ambient Temperature, C-141 Track 10

4. GROUND TEMPERATURE EXPOSURE

In military operations, most airplanes are refueled shortly after landing but may not be flown again for many hours. Exposure to extremely low temperatures during this waiting period could produce fuel freezing problems, depending on the type of fuel and loading temperature. To study this cold soak phenomenon, ground temperature and surface wind data were obtained at selected stations and thermal analyses performed.

Ground temperature data, termed surface data, were obtained from the USAF Environmental Technical Applications Center (ETAC), which is co-located with the National Climatic Center (NCC) in Asheville, North Carolina. Surface data for U.S. Air Force Bases is available from ETAC, and for civilian airports from NCC. The takeoff bases of the study routes are indicated in Table 2 for reference.

Data tapes for each of these bases were obtained from USAFETAC, and a computer program written to extract the temperature data. The program searches the multi-year data, which contains temperatures recorded at 1-hour intervals, and identifies the ten lowest temperature 24-hour periods on a time-averaged basis; a frequency distribution of the 24-hour averages similar to that generated for the atmospheric data is simultaneously generated. The time period covered by the available data varied from one base to another (Table 3), but generally includes either 14 or 15 years. Data were not readily available for the years 1971 and 1972.

An example of the computer search product is given in Figures 22a and 22b, with the remainder of the data included as Appendix D. Figure 22a indicates, for example, that the worst case 24-hour period at Grand Forks AFB was about $-32.5^{o}C$ for the period of time surveyed; Figure 22b indicates that the probability of encountering temperature below $-10^{o}C$ for the time surveyed is about 65%. Data received for Hancock Field, NY and Sondrestrom, GL are also included in Appendix D for reference, but were not used in this study. The single lowest temperature 24-hour period is represented in the figure by a solid line, and the next lowest nine periods by dotted lines. The date and time of each case is given in the legend; for example, 12866.00 indicates the day of 28 January 1966, beginning at 0000 hours GMT (Greenwich Mean Time).

Table 2. Takeoff Bases for Study Routes

	Eielson Alaska	Elmendorf Alaska	Grand Forks North Dakota	Grissom Indiana	Langley Virginia	Minot ND	Sawyer Michigan	Thule Greenland
B-52								
1						X		
3			X					
4			X					
C-141								
1		X						
8		X						
10								X
KC-135								
3			X					
5						X		
10	X						X	
A-10 *								
1	X							
2					X			
3	X							
4	X							
5	X							
6	X							
7				X				
8				X				
9				X				
10				X				
F-15 *								
1							X	
2		X						
3		X						
4		X						
5		X						
6		X						
7						X		
8						X		
9						X		
10						X		

* assumed takeoff bases

Table 3. Time Period Covered by Available Surface Temperature Data

Base	Period of Record
Eielson AK	Jan 65-Dec 70 and Jan 73-Dec 82
Elmendorf AK	Jan 65-Dec 70 and Jan 73-Dec 81
Grand Forks ND	Jan 65-Dec 70 and Jan 73-Dec 82
Grissom IN	Jan 65-Dec 70 and Jan 73-Dec 82
Hancock Field NY	Jan 60-Dec 64 and Jan 73-Dec 82
Minot ND	Jan 65-Dec 70 and Jan 73-Dec 82
Sondrestrom GL	Jan 65-Dec 70 and Jan 73-Dec 82
Thule GL	Jan 65-Dec 70 and Jan 73-Dec 81

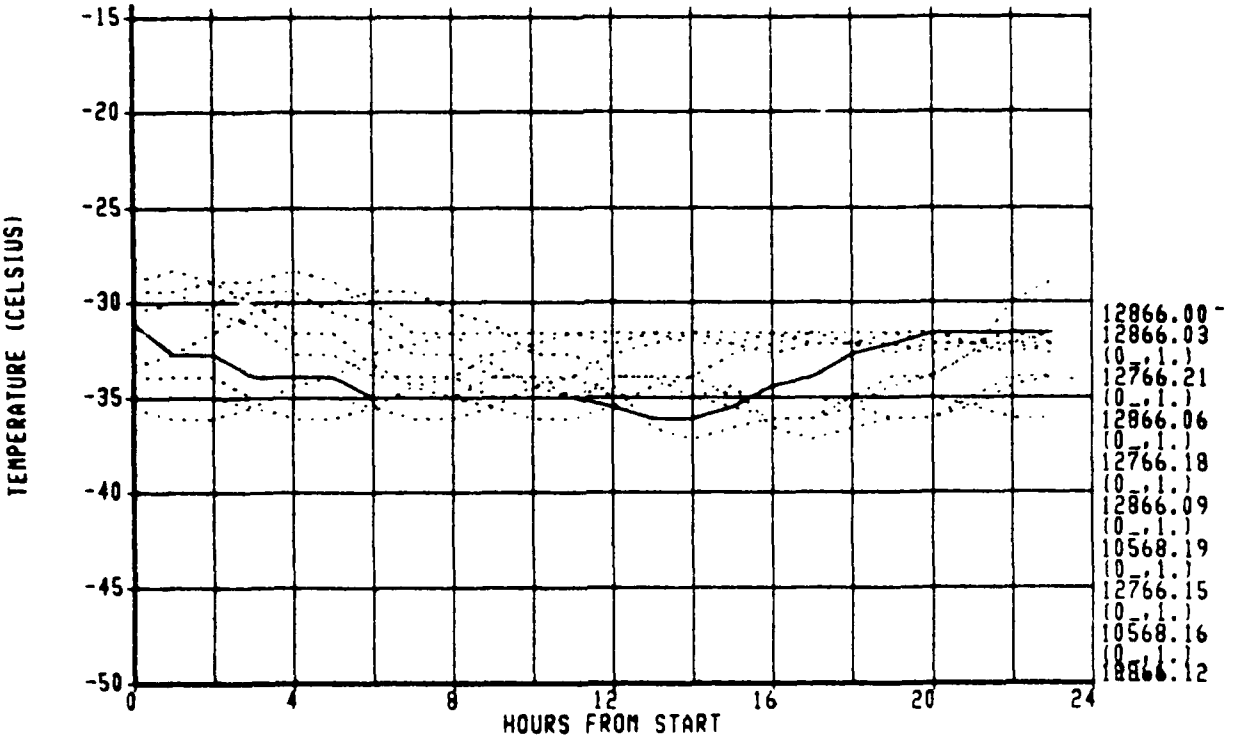

a. Grand Forks ND; 10 Worst Case 24-Hour Periods

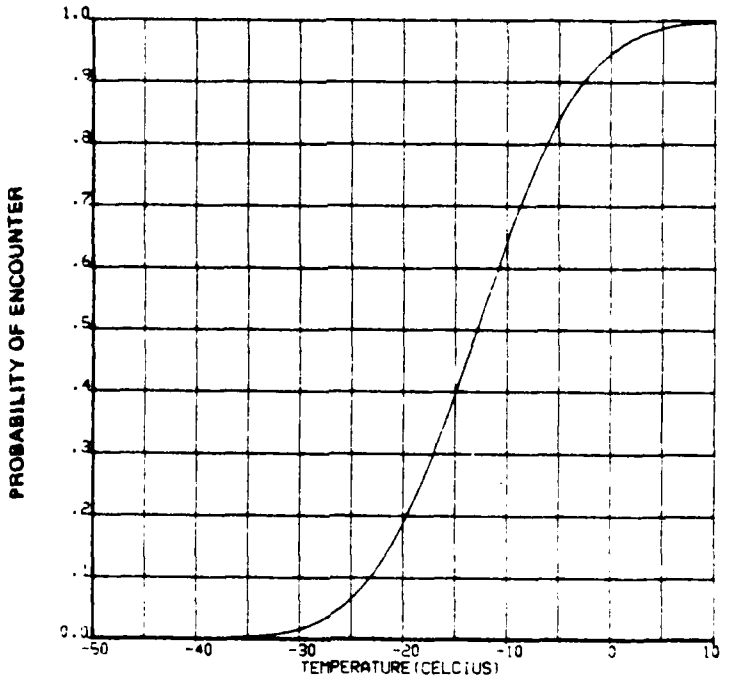

b. Time - Averaged Temperature Frequency Distribution

Figure 22. Grand Forks AFB Ground Temperature Data

Based on a limited investigation of military and commercial operating bases, no records are kept of the temperatures at which fuel is loaded into airplane tanks. However, previous studies have shown that the tank temperatures achieved after 24-hour cold soaks are essentially independent of loading temperature. An arbitrary loading temperature of $10^{o}C$ was, therefore, assumed for this study.

5. THERMAL MODEL DEVELOPMENT

Two models are used to calculate temperature versus time in airplane fuel tanks. Wing tank computations are done in a one-dimensional model, while cylindrical tank computations are done in a two-dimensional model. Both models use fuel properties as next described, after which the computer programs are discussed.

An earlier developed one-dimensional (1-D) heat transfer program was improved to accurately predict the thermal behavior of fuel when significant amounts of frozen fuel are present on the upper and lower surfaces. Previous analytic efforts were hindered by a lack of knowledge of fuel properties below $-40^{o}C$; *for example, the most recent* Coordinating Research Council fuel property handbook (Reference 18) presents no fuel properties below $-40^{o}C$ and it is tempting to assume that property variations at lower temperatures can be linearly extrapolated. This assumption must be in error for specific heat, since the latent heat of solidification will cause an apparent non-linear change at and below the freeze point. Work was done to develop specific heat, thermal conductivity, density and viscosity for low temperatures, and to integrate it into the 1-D computer program.

The geometry of a rectangular tank permits the use of a one-dimensional model to solve the energy equations without solving the other conservation equations. Cylindrical geometries, however, do not permit these simplifications and the solution must be carried out in two dimensions and involves simultaneous solution of the mass, momentum and energy conservation equations.

a. Fuel Properties at Low Temperature

Without full knowledge of the thermodynamic properties of fuel in the low temperature range, any mathematical solution for temperature will be substantially in error when compared to experiment. Specifically, no method can be created to accurately locate the liquid-solid interface in fuel tanks without knowing or assuming values for the thermodynamic properties of fuel (specific heat, viscosity, density, and thermal conductivity) which undergo major changes during and after the freezing process.

To develop the needed data, fuel samples of various types were obtained from the Navy and the Air Force, and fuel property measurements were performed by the Boeing Materials Technology laboratory. This fuel property data was generated for the temperature range from $0^{o}C$ to $-60^{o}C$. The fuel types are listed in Table 4; the identification numbers given in the table are used throughout this section to refer to individual samples. Composition data supplied with each sample is listed in Table 4, and routine fuel analysis data in Appendix E, Fuel Characterization Data. Data spread within a particular fuel type can be attributed to differing P-N-A (paraffin-naphthene-aromatic) ratios.

(1) Density

Gas turbine fuel density variation with temperature is a critical requirement in calculations involving free convection heat transfer. Figures 23a through 23c show low temperature density characteristics of various aircraft fuels obtained from laboratory experimentation. For the various blends of JP-4 shown in Figure 23a variations in density are small. Data from the Coordinating Research Council (Reference 18) and Schmidt/Momenthy (Reference 19) are shown with the Boeing laboratory measurements for comparison, denoted CR and SM, respectively. It can be seen that JP-5 and JP-8 (Figures 23b and 23c) are higher density fuels and there is a wider variation density between blends.

The low temperature density characteristics of JP-4 fuel were used in the one and two dimensional heat transfer models. Fuel density was selected from a straight line fit of the Schmidt/Momenthy data shown in Figure 23d.

Table 4. Fuel Sample Identification

IDENTIFICATION	FUEL TYPE	FREEZE POINT	DESCRIPTION	SOURCE
81-POSF-114	JP-4	-63°C	Shale-derived	Suntech
81-POSF-117	JP-5	-51°C	Shale-derived	Suntech
82-POSF-125	JP-4	-60°C	Petroleum, spec	Friendswood
82-POSF-159	JP-4	<-80°C	Petroleum, spec	Exxon
82-POSF-168	JP-8	-69°C	Petroleum	
82-POSF-445	JP-8	-44°C	Petroleum	Tyndall
82-POSF-447	JP-4	-64°C	Petroleum	
83-POSF-562	JP-8	-52°C	Shale-derived	Sohio
83-POSF-709	Jet A	-47°C		Shell
NAPC-1	JP-5	-32°C	Modified (out-of-spec)	Suntech
NAPC-2	JP-5	-27°C	Modified (out-of-spec)	Suntech
NAPC-3	JP-5	-36°C	Modified (out-of-spec)	Suntech
NAPC-4	JP-5	-35°C	Modified (out-of-spec)	Suntech
NAPC-5	JP-5	-56°C	Low aromatic	Suntech
NAPC-6	JP-5	-56°C	High aromatic	Suntech

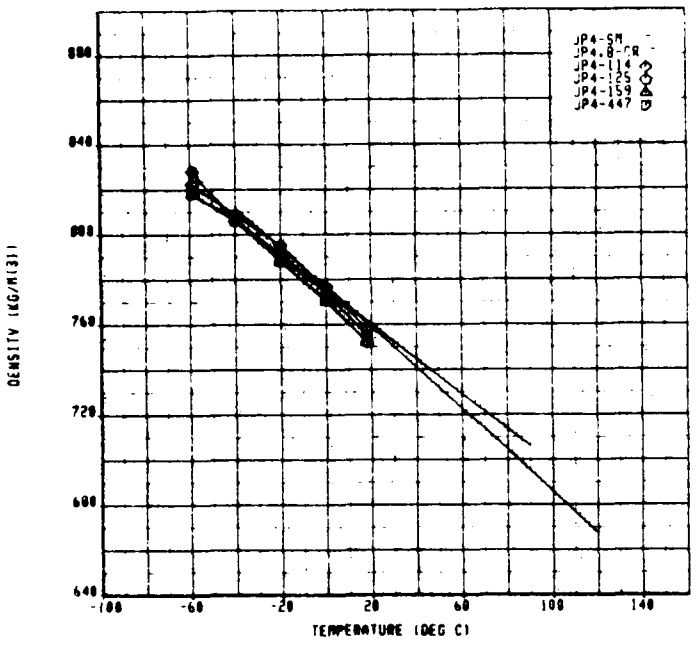

a. JP-4

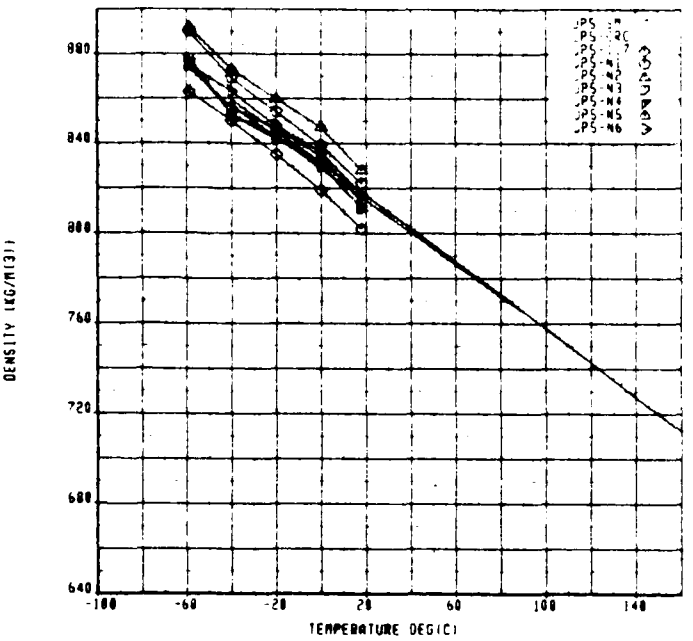

b. JP-5

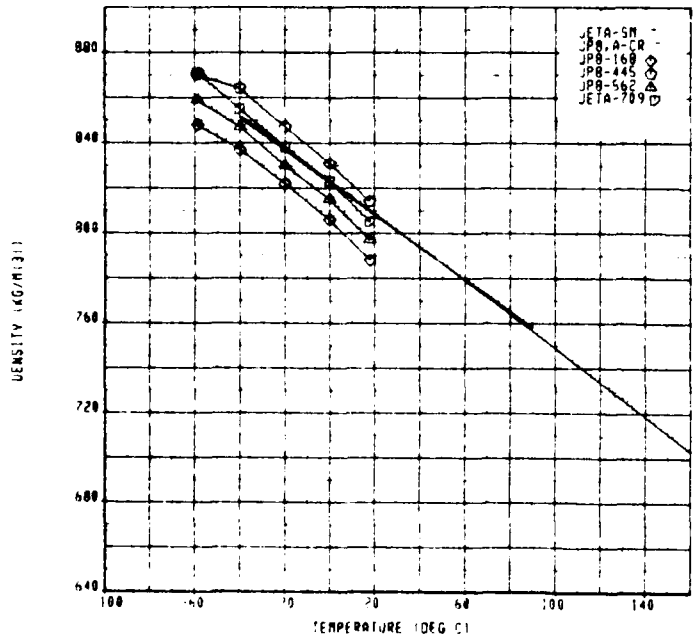

c. JP-8

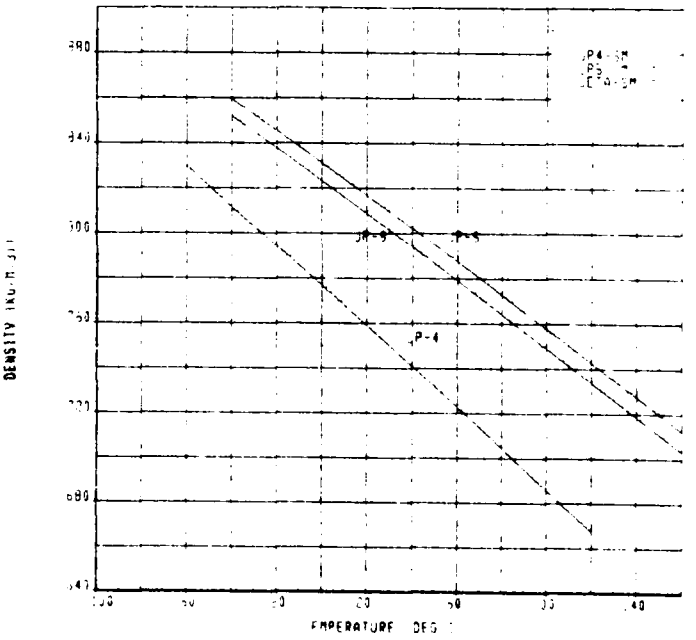

d. Data Used in One-Dimensional Thermal Model

Figure 23. Density Measurements

(2) Viscosity

The viscosity of an aircraft fuel is a measure of the internal resistance to flow due to molecular motion. Lowering the temperature of the fuel increases its viscosity.

Recent measurements of viscosity at low temperatures for various blends of JP-4, JP-5, and JP-8 are shown in Figures 24a through 24b. The figures also show data obtained by Schmidt/Momenthy, Coordinating Research Council and Exxon (EXX, Reference 20). Variation in the laboratory measured viscosity data is small between the various blends and fuel types. The laboratory data agree with published data, particularly at low temperatures. As with the density data, the viscosity data used in the 1-D and 2-D heat transfer models are shown in Figure 24d.

(3) Specific Heat

When the temperature of a unit mass of fuel is changed, the amount of heat energy transferred per degree of temperature change is called the specific heat. Fuel specific heat varies with temperature, particularly near the freeze point. Boeing Laboratory measured values of specific heat for various blends of JP-4, JP-5 and JP-8 are shown in Figures 25a through 25c. The specific heat data used in the 1-D and 2-D heat transfer models was a combination of lab data (at and below freezing) and the values obtained from Schmidt/Momenthy (Figure 25d) above freezing.

The specific heat of fuel at low temperature is also being studied by Moynihan (References 21, 22, and 23). A comparison of Moynihan's data and the Boeing lab measurements for the same fuels is shown in Figure 26. The Jet A measurements agree fairly well, however, a reason for the difference in JP-5 measurements has not been investigated. Unlike the density and viscosity measurements which were tightly grouped, there is a large variation in the value of specific heat within and between fuel types which is likely to be due to varying compositions. Also, each of the fuel blends has a different freeze point and the curves indicate there might be a correlation between fuel specific heat and freeze point.

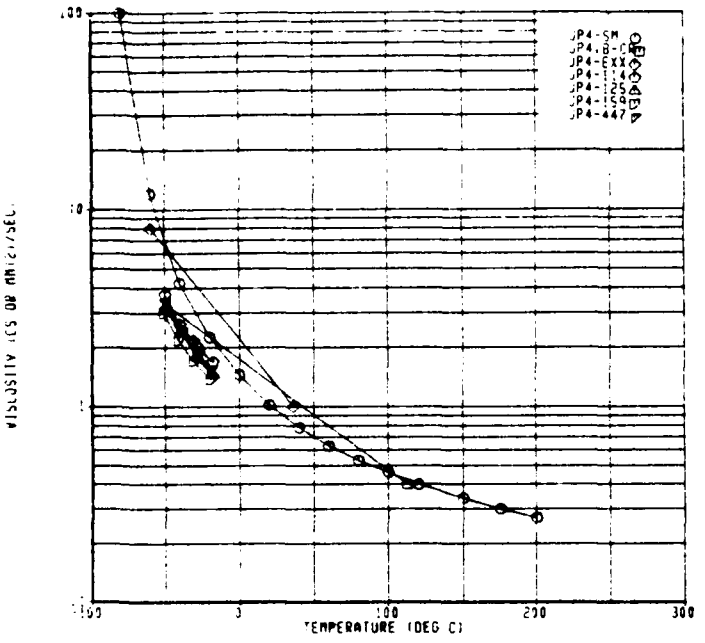

a. JP-4

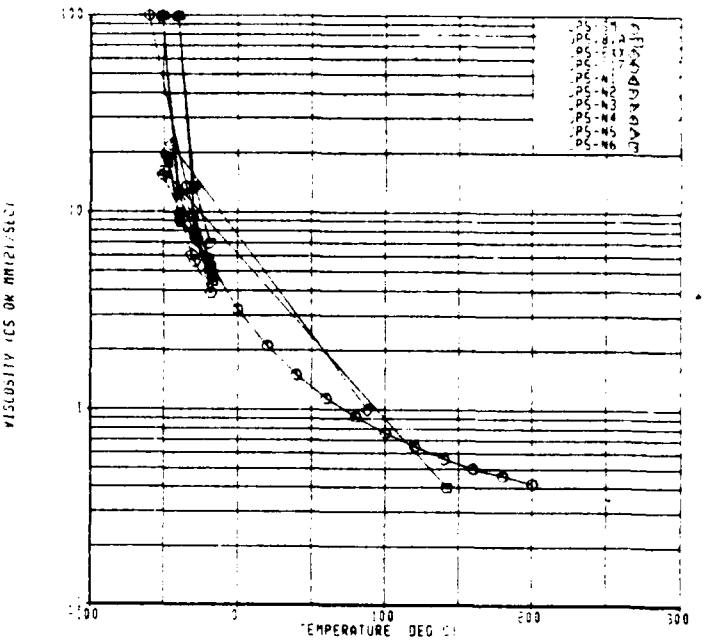

b. JP-5

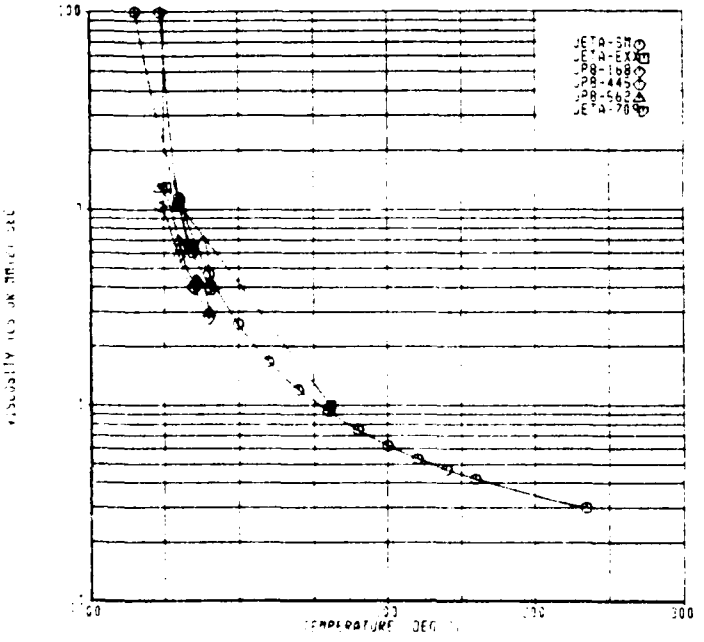

c. JP-8

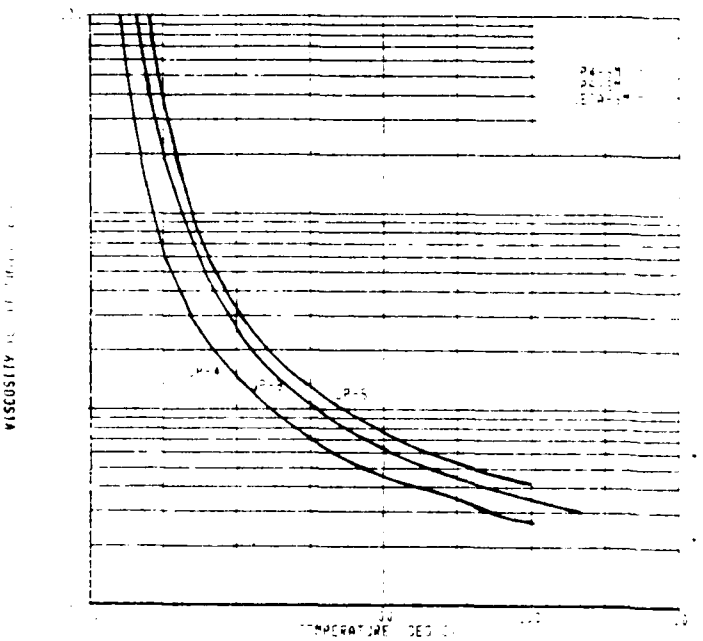

d. Data Used in One-Dimensional Thermal Model

Figure 24. Viscosity Measurements

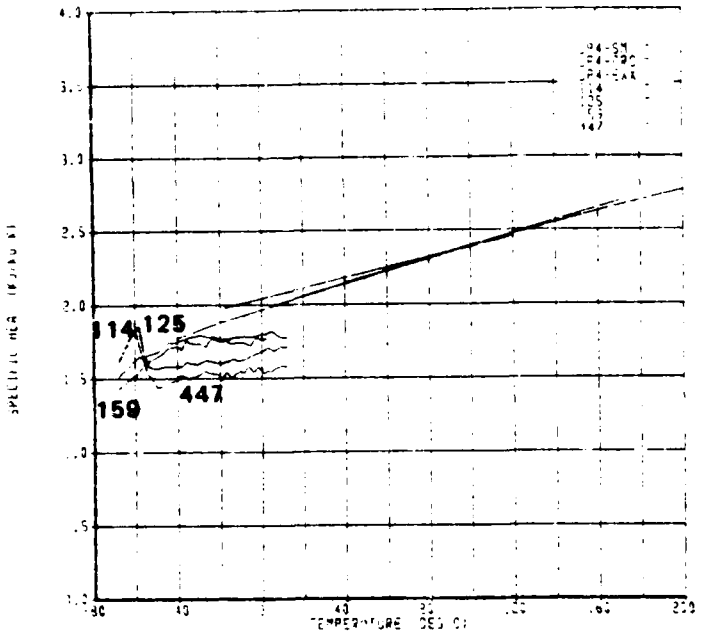

a. JP-4

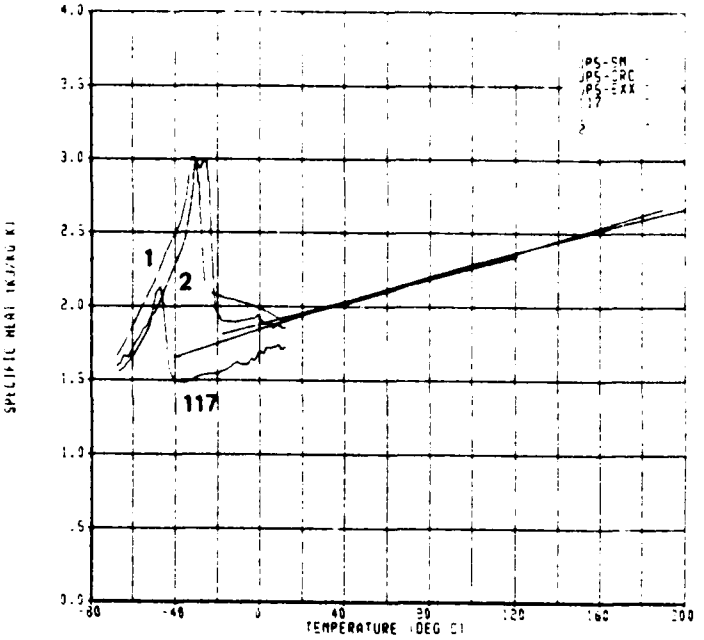

b. JP-5

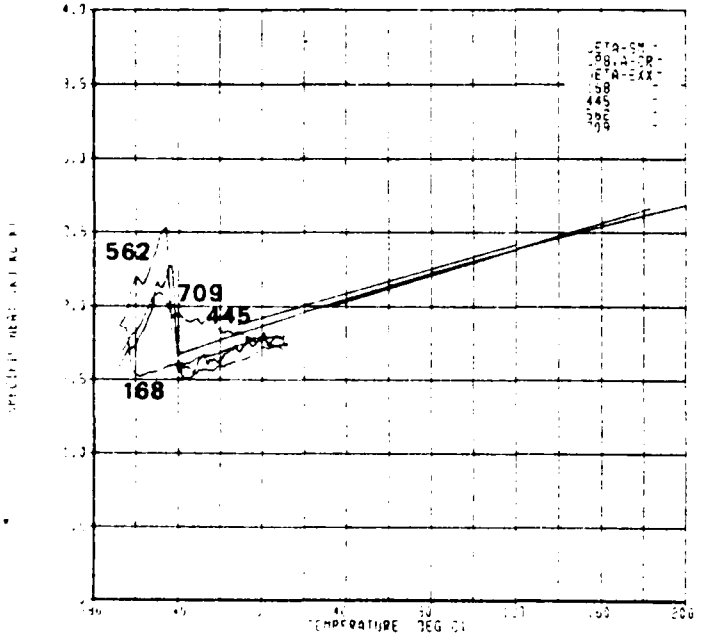

c. JP-8

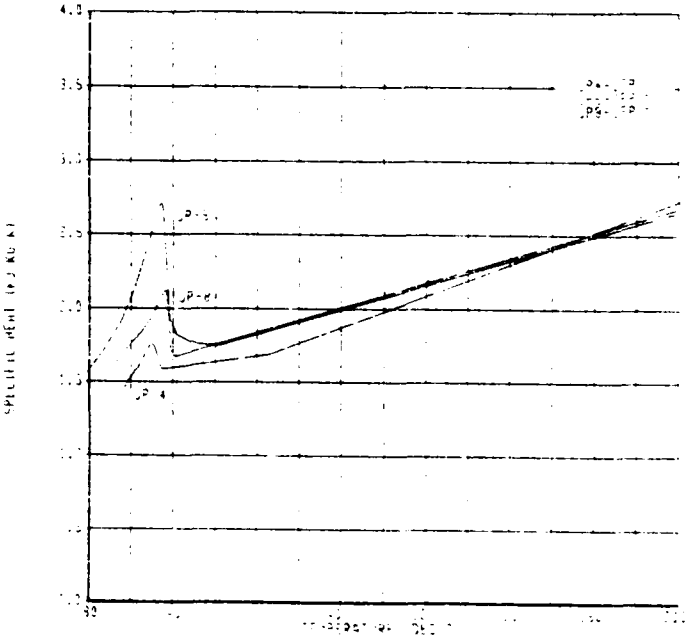

d. Data Used In One-Dimensional Thermal Model

Figure 25. Specific Heat Measurements

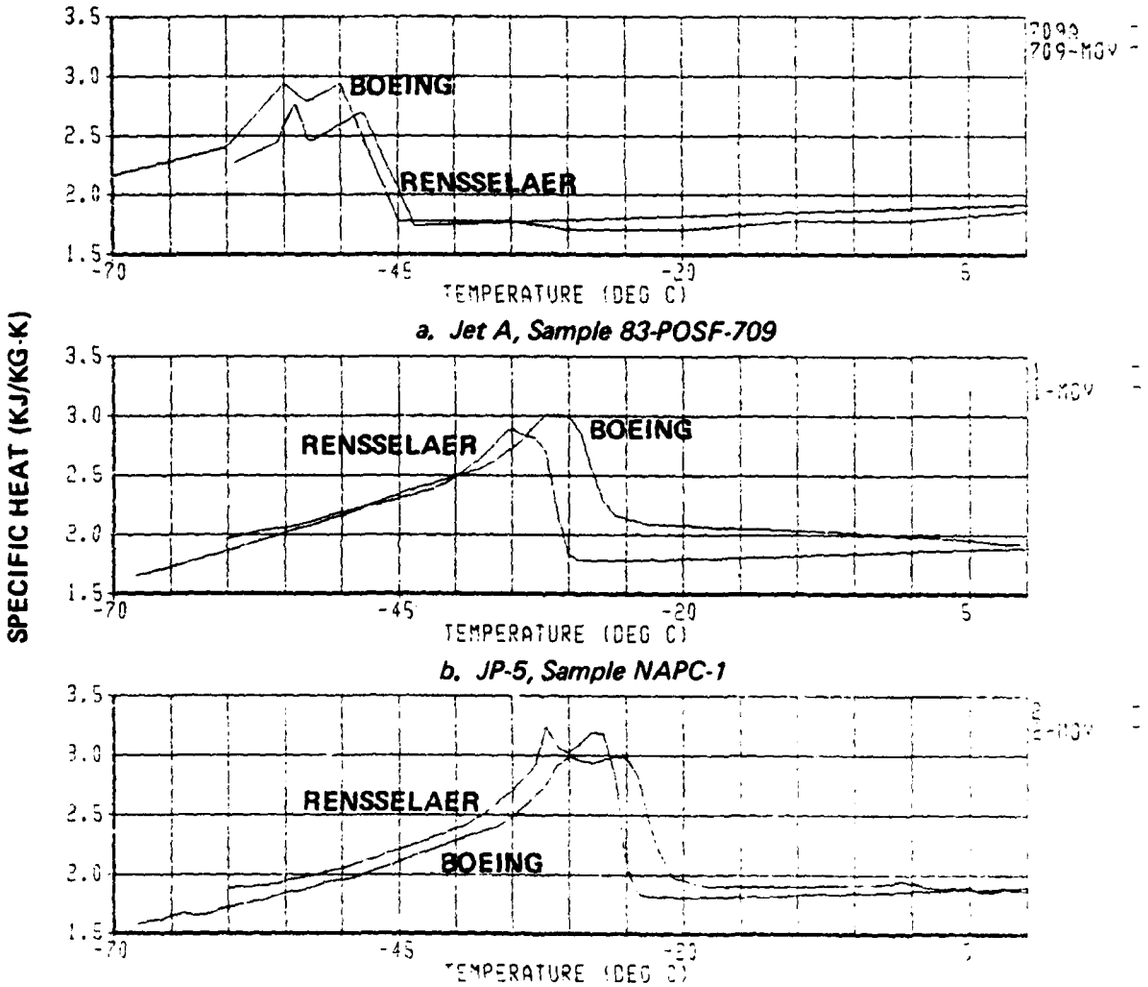

a. Jet A, Sample 83-POSF-709

b. JP-5, Sample NAPC-1

c. JP-5, Sample NAPC-2

Figure 26. Specific Heat Test Data Comparison

(4) Thermal Conductivity

The thermal property that regulates the rate at which heat can flow through the fuel by conduction is called thermal conductivity. For purposes of this study, thermal conductivity for all fuel types was assumed to be the same, no experimental data was obtained for this property because of the difficulty of measurement. Values for thermal conductivity were obtained from the Boeing Design Manual (Reference 24) and the CRC fuel properties manual shown in Figure 27. There appears to be a strong disagreement between the Boeing and CRC data and no new data are available at or below most fuel freeze points.

b. Wing Fuel Tank Heat Transfer Model

In the development of the analytical method to calculate fuel temperatures it was necessary to account for the following factors which contribute to the heat transfer:

- o initial fuel temperature resulting from pre-flight ambient exposure
- o periodic transitions from cooling to heating to cooling of the fuel tanks caused by flying into and out of warmer air masses
- o changing wetted area of the fuel tank as fuel is consumed
- o influence of increasing fuel tank ullage on heat transfer
- o influence of fuel freezing on heat transfer

A flow diagram of the computational procedure is shown in Figure 28.

The problem of calculating fuel temperatures in an airplane wing tank can be reduced to a one-dimensional transient heat transfer problem $T=T(x,\tau)$, where the temperature (T) is a function of tank height (x) and time (τ), assuming that temperature variations in the span-wise and fore-and-aft directions are negligible compared to top and bottom variations. This assumption is based on order of magnitude arguments which consider tank depth to tank lateral dimensional ratios. Because tank depth varies in the spanwise direction, the region modeled was chosen to be the inboard portion of the fuel tank. The dominant low temperature effects were anticipated to occur in this location since the fuel in that zone of the tank is usually used last.

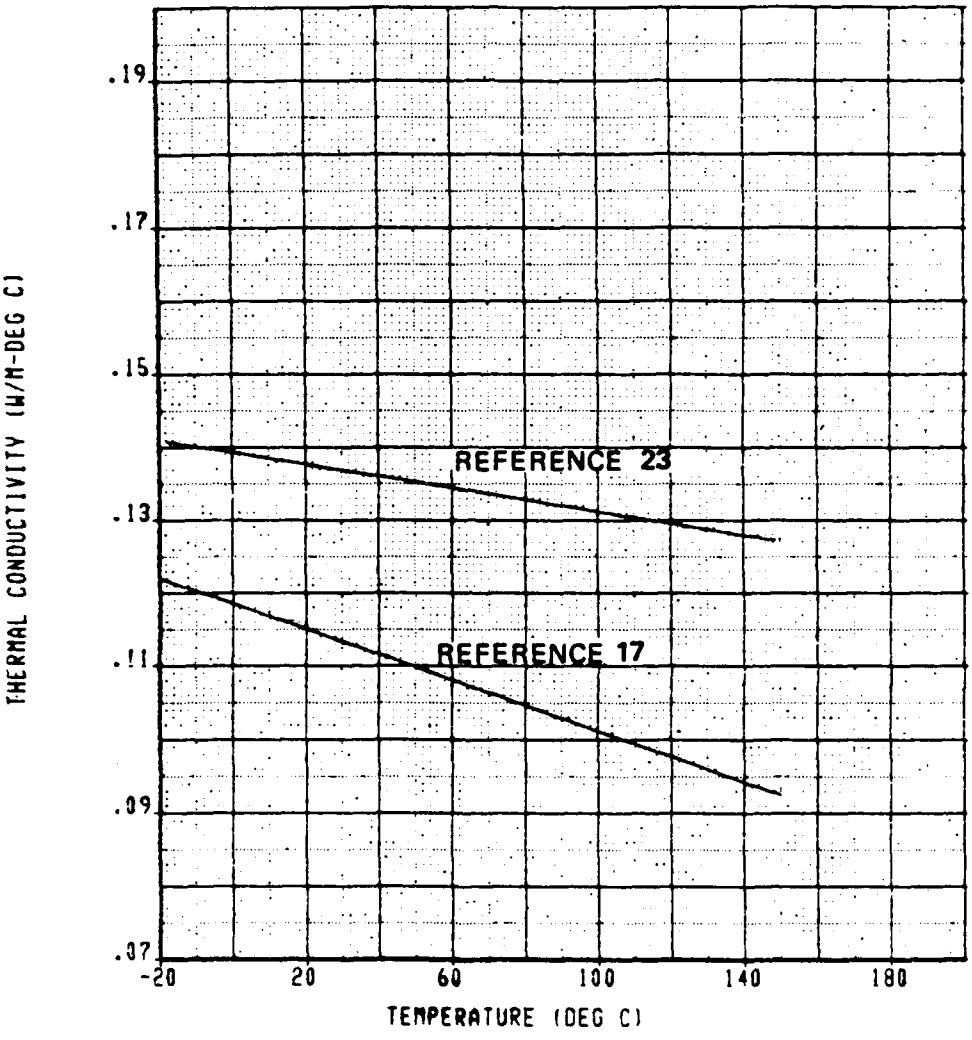

Figure 27. Published Thermal Conductivity Data

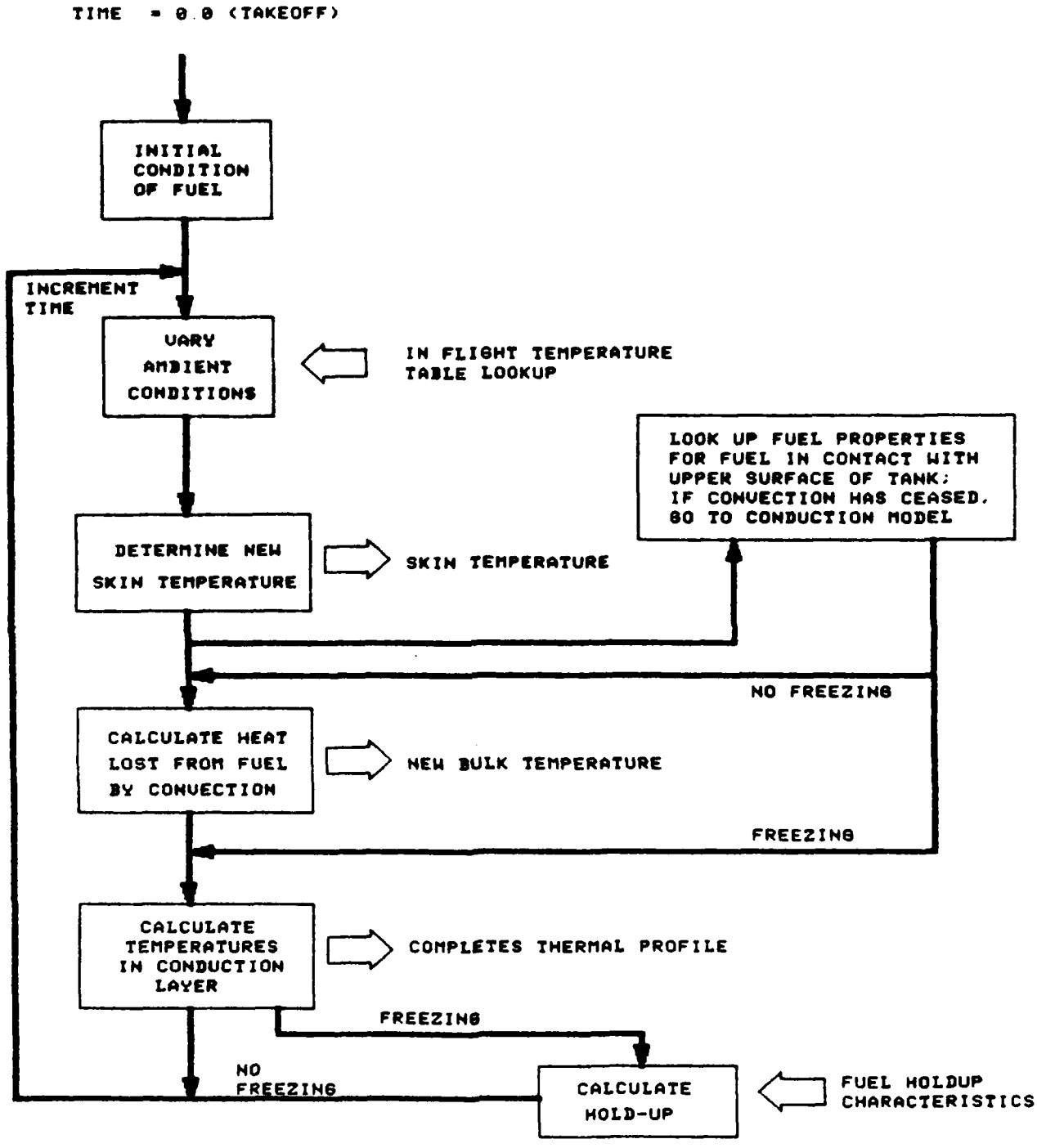

Figure 28. Flow Diagram for the One-Dimensional Heat Transfer Model

During cooling the denser layers of cooled fuel at the top of the tank will tend to settle, creating a free convective zone in the upper portion of the tank (Figure 29). The cold layer of fuel along the skin at the bottom of the tank tends to be stagnant, and too dense to be penetrated by the low velocity fuel descending from the top of the tank. Thus heat transfer at the bottom of the tank is primarily a conductive process. At the beginning of the cooling process when the tank is full, the majority of fuel is involved in the convection process; because of convectively driven mixing, the convective zone is characterized by a nearly constant (bulk) temperature. Over time, as the temperature of the fuel decreases and approaches that of the tank skins, the driving force for convection is reduced, and the convection zone decreases in depth while the conduction zone grows.

During heating of the fuel, the heat transfer processes described in the preceding paragraph are reversed, with a convection zone forming at the bottom and a conduction zone at the top of the tank.

As fuel is withdrawn from the tank, the liquid contact is broken, an air space develops at the top of the tank, and there is a reduction in heat transfer through the upper skin which is also accounted for by the program. The position of the air space depends on the wing dihedral angle. In a cooling situation, a convective zone forms in the air space, which in turn drives convection in the upper portion of the remaining fuel. The convection heat transfer which predominates in the wetted condition loses most of its driving force once an air space develops, and the heat transfer rate at the upper skin is greatly reduced. The predicted effect of a completely nonwetted upper skin is shown in Figure 30 for a KC-135 flight.

The computer solution logic was designed to evaluate internal conditions in the tank by:

- reference to the Grashof number in the convective zone
- solving the unsteady thermal diffusion equation in the conduction zone
- matching temperatures at the convective/conductive zone interface

(1) Convective Heat Transfer Relations

When the temperature differences between the tank skin and the bulk fuel are large, the resultant free convection flows are likely to be turbulent. For smaller differences, the flow tends to be laminar. The criterion used is the Grashof number (Gr). Accordingly, the free convective heat transfer correlation used in the thermal analysis have the form given in Equation (2); the value of C_1 is slightly dependent on tank depth, and C_2 is associated with the Grashof number (Table 5).

$$h_f = C_1 \, (Gr.Pr)C_2 \frac{K}{l_c} \tag{2}$$

where,

h_f = fuel side heat transfer coefficient

l_c = characteristic length

The characteristic length used in the correlations is defined as

$$l_c = \frac{l_h . l_v}{l_h + l_v} \tag{3}$$

where,

l_h = maximum lateral dimension

l_v = height of tank

(2) Conductive Heat Transfer Relations

During the cooling of liquid fuel, heat is transferred from the tank by conduction through the bottom wall. Within the conductive region, the thermal diffusion equation applies

$$\frac{\partial^2 T}{\partial x^2} = \frac{1}{\alpha} \frac{\partial T}{\partial t} \tag{4}$$

where,

α = thermal diffusivity of fuel, $k/(\rho C_p)$

As long as the fuel remains a liquid, the thermal properties (k, ρ, and C_p) can be evaluated at the average of the skin and bulk temperatures. As the fuel begins to freeze, the large changes in the value of the specific heat and of the viscosity make it necessary to evaluate the properties as a function of temperature in the conduction zone. The sudden change in specific heat is, of course, due to the latent heat of solidification which is released as the fuel begins to freeze.

However, acceptable (if conservative) analytical results have been obtained without considering this term as long as the other thermal properties in the freezing region are accurately evaluated, and it has therefore been neglected in the current analysis.

(2) Boundary Conditions for the One-Dimensional Model

Boundary conditions which describe the interface conditions at the tank skins have been previously reported, (Reference 1), but will be described briefly for completeness. Correlations found in the literature were used to define exterior (air side) heat transfer coefficients in terms of flight conditions, the reference temperature, and the reference Reynolds number (Reference 25). All the necessary values can be obtained from airplane altitude, speed (V_∞), and ambient temperature (T_∞), defined by the flight profile. Boundary conditions then have the form

Bottom Skin:

$$h_a (T_s - T_r) = -k_f \frac{dT}{dx} \Big|_{\text{lower skin}} \tag{5}$$

Top Skin:

$$h_a (T_s - T_r) = \int \rho C_p \, dT_b \, dx \Big|_{\text{convection zone}} \tag{6}$$

where,

x = vertical distance
h_a = air side convective heat transfer coefficent
k_f = thermal conductivity of fuel
T_s = skin temperature
T_r = recovery temperature
T_b = convection zone (bulk) temperature

As the computer simulation proceeds through a given mission, the boundary conditions are updated according to the changing thermal environment.

(4) Initial Conditions

The initial conditions for the solution are the temperature distribution in the fuel tank at the start of the calculation. Commonly, the temperature is considered uniform, and equal to the temperature at which fuel is loaded into the tanks. The calculation usually begins 24 hours prior to takeoff, during which time the boundary conditions are the soaking temperatures of the ground environment. This procedure ensures that the fuel temperature at takeoff properly reflects the thermal environment at the takeoff base.

(5) Estimation of Holdup Due To Fuel Freezing

The estimation of the quantity of frozen fuel (holdup) based on fuel temperature is an integral part of the one-dimensional thermal model (Figure 28). The first formation of frozen fuel will be along the wetted tank skins. In a full tank, if low temperatures are sustained, the entire upper and lower surfaces will be covered with a layer of frozen fuel which will thicken with increasing time and inhibit the loss of heat by convection as described earlier.

In addition to the thermal profile of the fuel in the tank, the hold-up calculations require information on the percentage of non-flowable (holdup) fuel as a function of temperature in an isothermal fuel sample. The test device used to generate these data is known as a Shell-Thornton tester (Reference 26). In this test, a 100 ml sample of fuel in a metal container is

immersed into a constant low temperature bath long enough to reach thermal equilibrium. A valve is then opened from the top chamber to a lower chamber, allowing fuel to flow. Any remaining liquid fuel is drained and its volume measured, and the percent non-flowable fuel is calculated. The test is repeated at several different bath temperatures for the construction of a holdup curve; a typical Shell-Thornton test curve is shown in Figure 31a. The extent of the "tails" (the approach to zero percent holdup) of the curve is strongly dependent on the fuel chemistry.

To calculate the amount of fuel hold-up in a fuel tank, the in-tank temperature profile is subdivided into N equal increments (Figure 31b) and the average temperature, $T_{AVG} = 1/2(T_1+T_2)$, in each ΔX increment is calculated. Each ΔX layer is treated as isothermal to compute the percent hold-up from the Shell-Thornton curve. The mass of fuel hold-up in each layer is $\rho A \Delta X$, where A is the tank area. The mass percent of fuel hold-up in the tank is found by summing the hold-up mass (m_i) in each layer and dividing by the total mass in the tank.

$$\text{mass hold-up (\%)} = \frac{100}{m_t} \sum_{i=1}^{N} m_i \qquad (7)$$

It is important to note that an accurate holdup estimate depends entirely on an accurate temperature profile (temperature vs. depth), that is, an accurate model of the freezing phenomenon. This is illustrated clearly in Figure 32. The layers of frozen fuel will interfere with convective processes, reducing heat transfer, and resulting in less predicted holdup. If the inhibition of the convective heat transfer is not taken into account, the apparent temperature will continue to decrease and more holdup will be predicted.

c. External Fuel Tank Heat Transfer

Based on a recommendation from the previous study (Reference 1), heat transfer in cylindrical tanks, representative of pylon and tip tanks, has been examined. The fuel in these tanks is susceptible to freezing due to extremely low ground temperatures or fuel management during flight, as are internal fuel tanks, however, the existing model does not account for the two dimensional effects expected because of wall curvature.

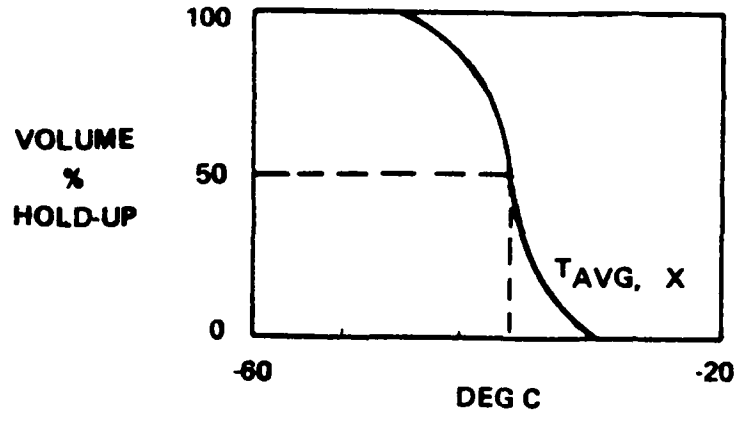

a. Typical Shell-Thornton Curve

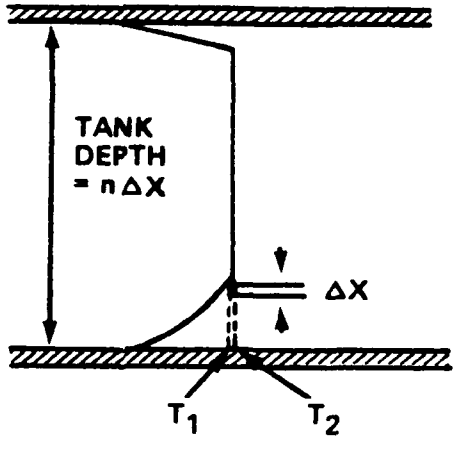

b. Diagram of Holdup Calculation

Figure 31. Holdup Estimation Procedure

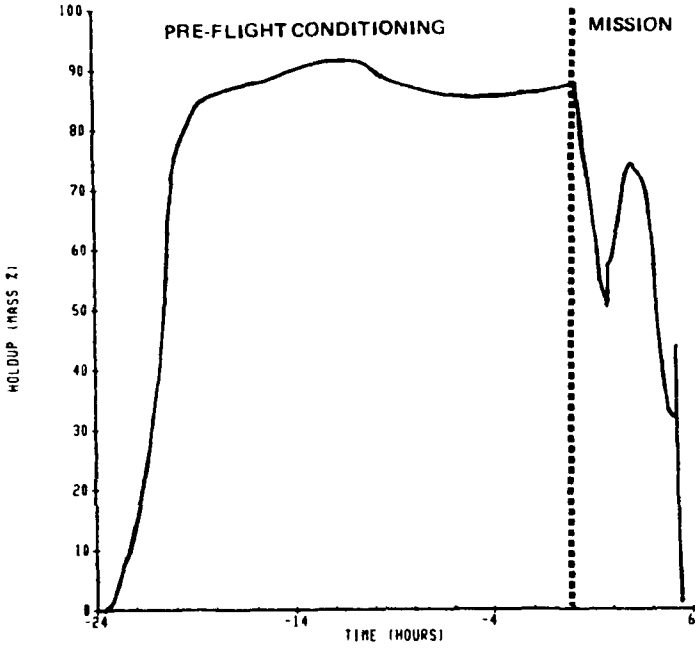

a. Neglecting Effect of Frozen Layer

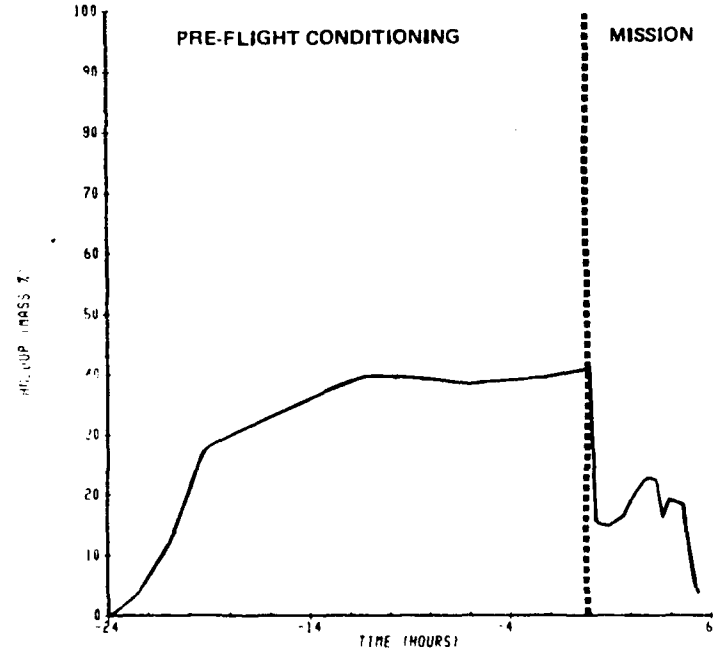

b. Including Effect of Frozen Layer

Figure 32. Holdup Predictions

During the course of this study, the Navy awarded Boeing a contract to perform multi-dimensional thermal modeling of airplane fuel tanks. Because the goals of the Air Force and Navy programs were closely related, an arrangement was developed to avoid duplication of effort. Background work and problem definition were accomplished under the Air Force contract and analysis proceeded under the Navy program. As each phase of the analysis was completed, the analytical techniques were applied to the computation of fuel temperatures in Air Force airplanes. At the time of the preparation of this report the two-dimensional analysis of a cylindrical fuel tank with time varying boundary conditions had been completed, with the effects of fuel removal and of fuel freezing to be next examined.

The mathematical model employed in the analysis is PHOENICS, an existing general purpose computer program. PHOENICS solves the time-averaged conservation equations for a finite number of small control volumes (cells) which artificially subdivide the tank volume (References 27 and 28). The elements of the solution procedure used by PHOENICS are described in the following paragraphs.

When heat is transferred to the fuel in more than one direction, as would be the case for an external fuel tank, a multi-dimensional transient heat transfer analysis is required. This class of heat transfer problem, generally referred to in the literature as buoyantly driven flow, is characterized by complex flow phenomena such as

- o attached wall boundary layer flow over the near vertical portions of the tank
- o separated wall boundary layers with buoyant plumes from horizontal walls
- o different flow regimes (e.g., laminar, transition, and turbulent)
- o vortical cells, and complex unsteady circulation patterns
- o inherent coupling between the boundary regions and the core regions (exterior to the boundary layer); the two regions cannot be treated independently in the analysis.

Other factors which complicate the heat transfer process during flight are:

- o the tank dynamics (slosh and vibration)
- o the angle of attack (tank inclined with respect to the gravity vector)

- o free surface (partially full tank)
- o nonuniform tank wall temperatures
- o internal structure (ribs and baffles)

(1) Rayleigh Number

The dimensionless group which characterizes the heat transfer process for natural convection in enclosures is the Rayleigh number, Ra, defined as

$$Ra = Pr \cdot Gr = \beta g \Delta T L^3 / \nu\alpha \qquad (8)$$

where, P_r = Prandtl number
G_r = Grashof number
β = volumetric expansion coefficient
ΔT = temperature difference
L = characteristic length
ν = kinematic viscosity
α = thermal diffusivity
g = local acceleration of gravity

Physically, Ra represents the ratio of buoyant and inertial effects to viscous and thermal diffusion effects. During the early portion of a low temperature flight (when the bulk fuel temperature is relatively high) the ΔT between the tank skin and bulk fuel can reach $50^{o}C$ causing the Ra to reach a maximum; values of the order of 10^{12} (based on L=20 inches) are typical. Later in the flight, as the bulk temperature decreases, the Rayleigh number will decrease by several orders of magnitude and the flow regime will change from turbulent to laminar. The flow tends to be turbulent when $Ra>10^{9}$ and in the transition regime when $10^{6}<Ra<10^{9}$.

(2) Conservation Equations

The conservation equations for transient multi-dimensional buoyant flow in vector notation are:

Mass

$$\nabla \cdot \vec{V} = 0 \tag{9}$$

Momentum (Navier-Stokes)

$$(\frac{\partial}{\partial t} + \vec{V} \cdot \nabla)\vec{V} = -\nabla(\frac{p}{\rho_o}) + \frac{Ra}{Pr} \Delta T \hat{n} + \Delta \cdot \nu\nabla\vec{V} \tag{10}$$

Energy

$$(\frac{\partial}{\partial t} + \vec{V} \quad \nabla)c_p T = \nabla \cdot \frac{k}{\rho_o} \nabla T \tag{11}$$

where,

ρ_o = mean fluid density
c_p = specific heat
k = thermal conductivity
α = thermal diffusivity
ν = kinematic viscosity
β = coefficient of thermal expansion

ΔT = local temperature differences
p = local static pressure
$\vec{V}$ = velocity vector

$\frac{\partial}{\partial t}$ = time derivative
∇ = space vector operator
$\hat{n}$ = unit vector in buoyant force direction
D = tank diameter
$Pr = \frac{\nu}{\alpha}$

The above equations have been simplified using the approximation that all the fluid properties are constant except the density in the buoyancy term of the momentum equation (Boussinesq approximation). This assumption is valid when large density variations are not encountered in the fluid. For the fuels in question, such as JP-4, JP-5, JP-8, and Diesel #1, the environmental

temperature variations are such that the use of these assumptions is appropriate. Since the properties c_p, k, ν and β are all temperature dependent, they cannot be taken through the vector or time differential operators which may be done when they are constant. This is particularly critical in the freezing regime, where c_p may increase by a factor of two, and where the apparent viscosity becomes very large.

The significance of the Rayleigh number was discussed earlier; the Prandtl number (Pr) expresses the ratio of momentum and thermal diffusivities and physically represents the ratio of the thermal and velocity boundary layer thicknesses. For the fuels of interest to this investigation, the Prandtl number is on the order of twenty at ambient temperature, and approaches values of the order of 100 as temperature decreases. This implies that the velocity boundary layer is thicker than the thermal boundary layer at room temperatures and becomes increasingly thick at low temperatures.

Generally turbulence will increase the rate of heat transfer between fluid and the tank surface and will alter the velocity and temperature distributions and therefore should be considered in the development of the model. In turbulent flows the preceeding equations (9) to (11) must hold at any instant but also on the average. Solving for the instantaneous quantities for a turbulent flow situation would require an extremely fine mesh accompanied with small time steps, making this approach prohibitively expensive for most problems. The alternative is to use the time averaged conservation equations which contain additional terms (e.g. the turbulent shear stress and turbulent heat flux) which result from averaging the turbulent fluctuations. A turbulence model is needed accordingly to express these turbulent time averaged quantities in terms of mean flow variables. The most widely used model is the k-ε model, proposed first by Launder and Spalding (Reference 29) which has often been applied to calculate forced and boundary layer flows. This model has also recently been applied to simulate buoyancy driven recirculating flow in a square enclosure at high Grashof number. However, the k-ε model cannot be expected to accurately model localized turbulence such as buoyant plumes. For such phenomena a new model whose development is based on experiment would be needed.

(3) Solution Procedure

The PHOENICS program embodies a "finite-domain" formulation of the differential equations of conservation. Finite-domain equations are derived by integration of equations 9 through 11 over finite control volumes (called "cells" or "sub-domains") which taken together, wholly fill the domain under study. The fluid property values, e.g. temperature, viscosity, specific heat, etc. are computed at the centroid of each cell (called a "grid node") and are regarded as representative of the whole cell. Integration leads to "finite-domain equations" having the forms:

$$a_P\varphi_P = a_N\varphi_N + a_S\varphi_S + a_E\varphi_E + a_W\varphi_W + a_H\varphi_H + a_L\varphi_L + a_T\varphi_T + b \qquad (12)$$

where, subscripts

P = nodal point in question
N = north neighbor node
S = south neighbor node
E = east neighbor node
W = west neighbor node
H = high neighbor node
L = low neighbor node
T = grid node at earlier time

and

a_P, a_N, etc. = coefficients (these coefficients contain convection and diffusion contributions added together)

b = source term

the above equation can be written as

$$\varphi_P = \frac{\sum_i a_i\varphi_i + b}{a_P} \qquad (13)$$

These finite domain equations differ from both the usual finite-difference and finite-element equations and are inherently non-linear, since the a's themselves are dependent on the φ's. Because of this non-linearity, an

iteration procedure (as distinct from direct matrix inversion) is essential. A more detailed discussion of the solution procedure is given in References 29-30.

(4) Cylindrical Tank Simulation

It was assumed for the purpose of computer modeling of cylindrical fuel tanks that because of the high length/diameter ratios typical of these tanks that the end effects would be small and the physical situation could be approximated with the 2-D model with features shown in Figure 33. Because of the circular cross section, the numerical solution was assumed to be symmetric about the vertical centerline. A typical solution grid for this case is shown in Figure 34. As with the wing tank analysis, the recovery temperature, T_r, is assumed to apply uniformly over the external boundary layer of the tank. The skin temperature, T_s, which is higher than T_r during cooling, is determined from the solution of the boundary conditions

$$K_{cell}\ (T_{cell} - T_s)/o = \bar{h}_o(T_s - T_r) \qquad (14)$$

where, $\bar{h}_o$ = average external heat transfer coefficient

K_{cell} = thermal conductivity of the cell adjacent to the tank wall

T_{cell} = temperature of the cell

o = distance from wall to cell center

The temperature dependence of the fuel properties is incorporated into the program and the properties for each cell are updated at the end of each time step. This is an extremely important feature of the model since changes in one of the physical properties (e.g. viscosity) could be used to predict the on-set of freezing and the total accumulation of frozen fuel. However, at this writing, modeling of the freezing phenomenon is in the development phase.

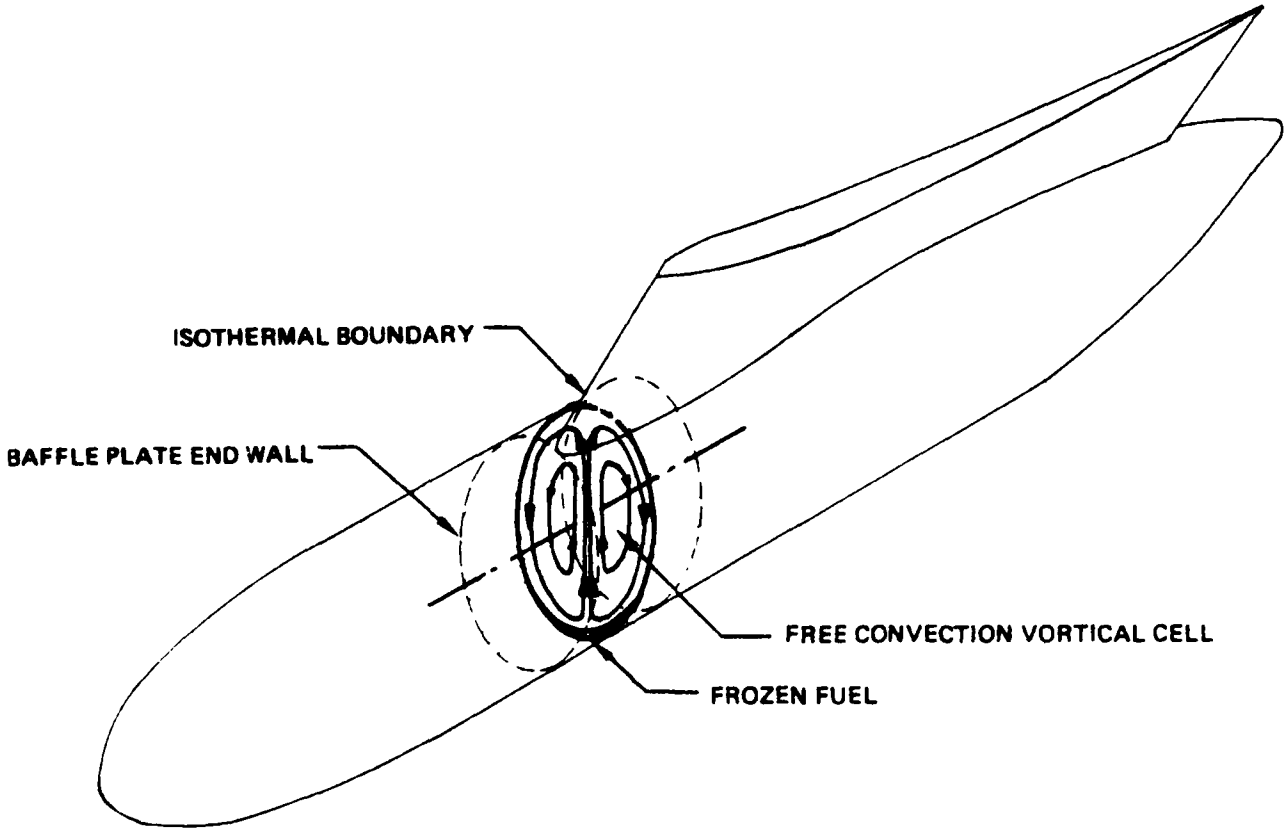

Figure 33. Free Convection Circulation Cells in a Full External Tank During Cooling

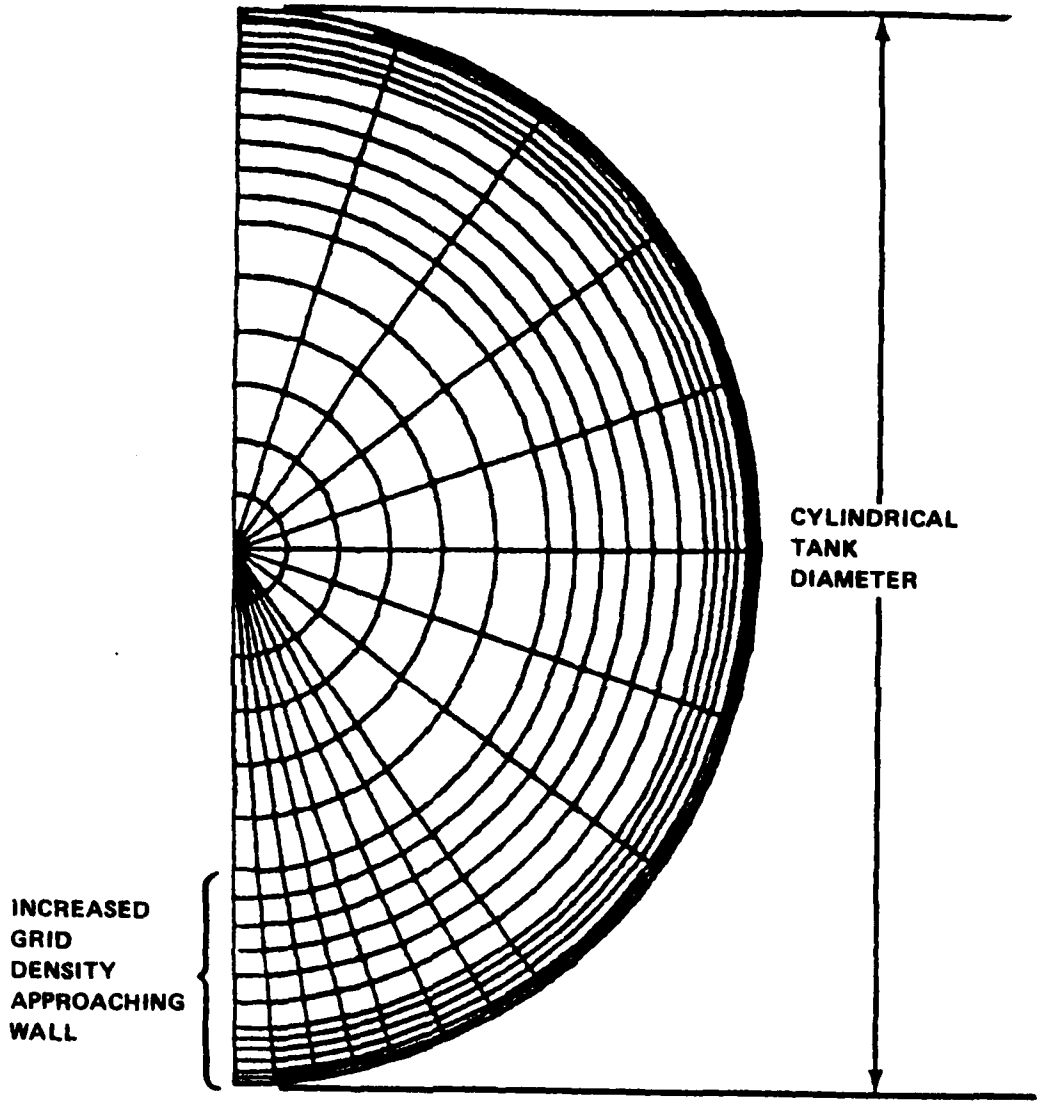

Figure 34. Solution Grid Used for 2-D Cylindrical Tank Analysis

6. RESULTS OF FUEL TEMPERATURE CALCULATIONS

The fuel temperatures calculated for each mission depend both on the thermal exposure of the airplane on the ground prior to flight and on the atmospheric exposure.

a. Wing Tank Calculations

Ground temperatures were first considered; in Figure 35 the predicted one-dimensional result of exposure to the worst case 24-hour periods for each ground base is shown, using the data presented in Section 2.4 and assuming specification JP-4 properties. Initial ambient and bulk fuel temperatures were arbitrarily chosen to be $10^{o}C$. The average bulk temperature for the thick wing airplanes is shown because the critical tanks have various, but similar vertical dimensions.

Also considered was the combined effect of preflight and inflight thermal exposures from the results of the ground and atmospheric temperature analyses. The worst case 24 hour ground temperature exposure and the worst case atmospheric exposure for a given mission were first combined to produce the absolute worst case thermal exposure for the fuel. The ground and atmospheric data base search programs were then modified to allow extraction of

- o any 24-hour ground temperature scan given the date and initial hour
- o the atmospheric exposure along a selected track, on any selected day

With this information, the following thermal exposures were also examined

- o the worst case ground exposure and actual atmospheric temperatures that occurred subsequently, and conversely
- o the actual ground temperatures that occurred 24 hours prior to the worst case atmospheric exposure

Each of these 3 ground/atmospheric temperature combinations was then input to the one-dimensional computer program. The results of these calculations for the inflight portion of the simulation are shown in Figures 36 through 40 for the apparent worst case mission for each airplane. (The results for all 29 missions are too extensive to be included in this report, and would not add

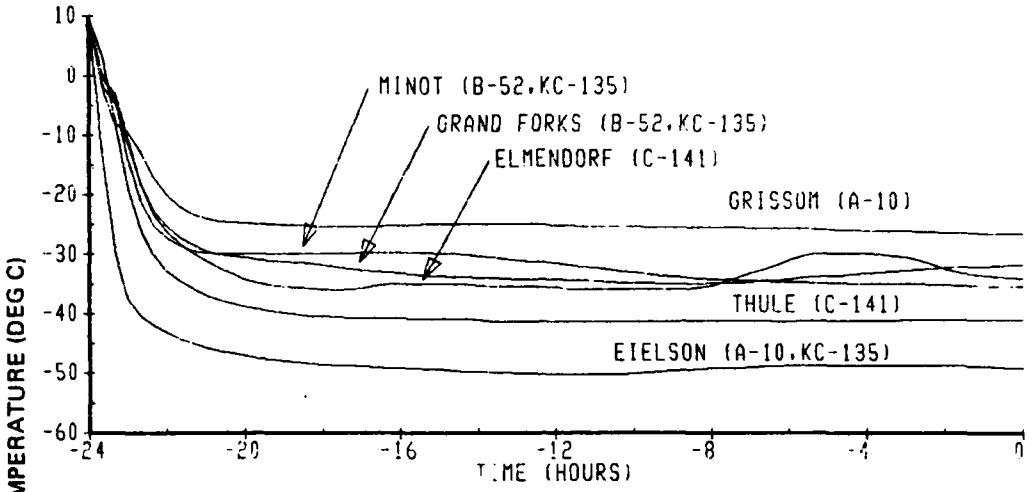

a. Thick Wing Airplanes

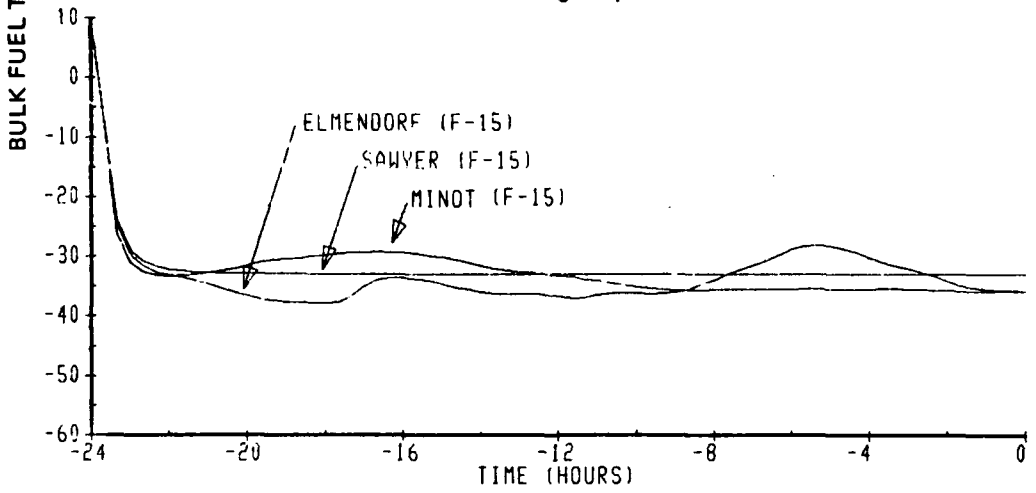

b. Thin Wing Airplanes

Figure 35. Effect of Worst Case Ground Temperatures on Bulk Fuel Temperature

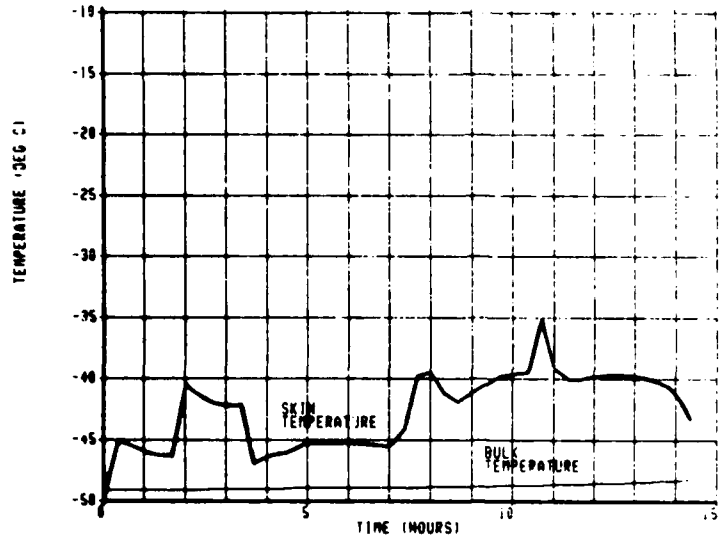

a. *Worst Case Ground Temperatures and Worst Case Atmospheric Temperatures*

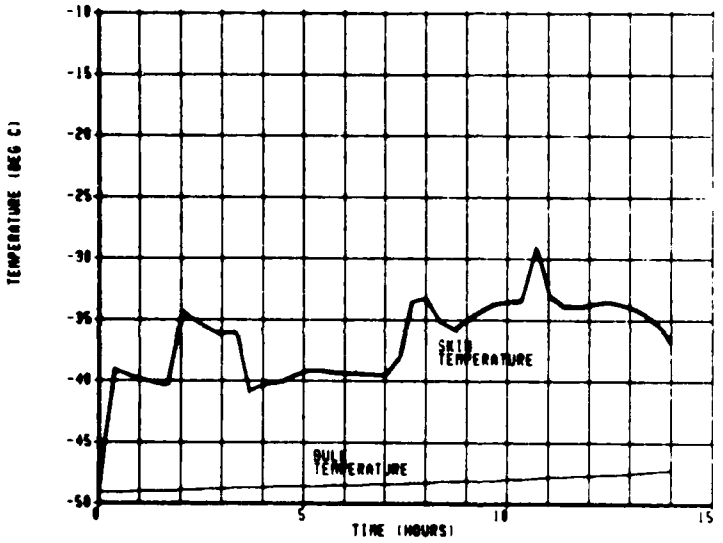

b. *Worst Case Ground Temperatures and Actual Atmospheric Temperatures*

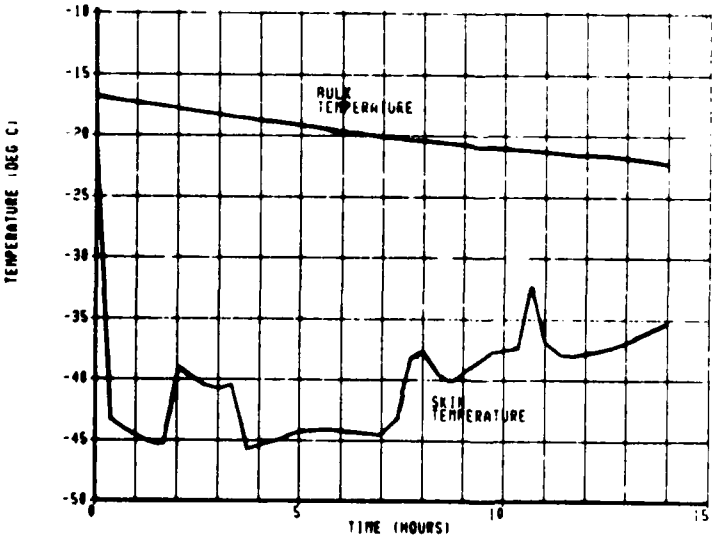

c. *Actual Ground Temperatures and Worst Case Atmospheric Temperatures*

Figure 36. Worst Case Thermal Exposures For A-10 Track 1

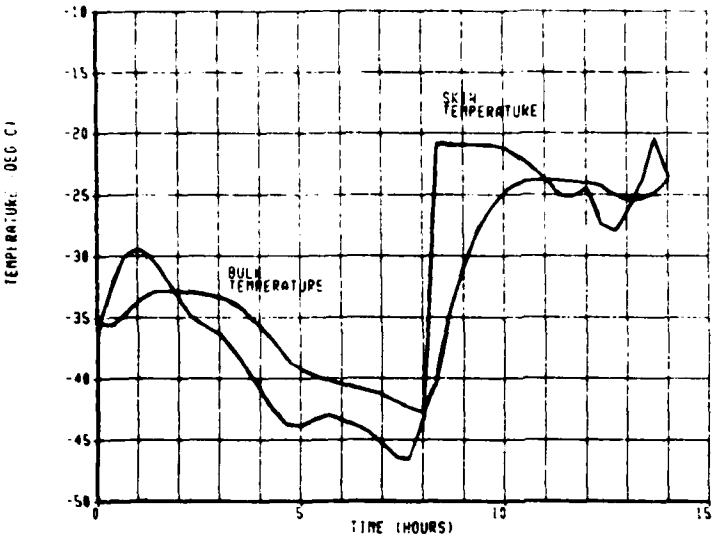

a. Worst Case Ground Temperatures and Worst Case Atmospheric Temperatures

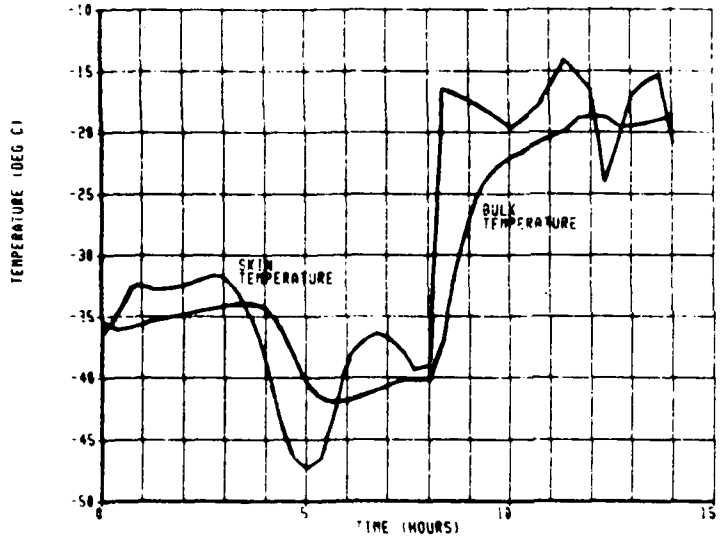

b. Worst Case Ground Temperatures and Actual Atmospheric Temperatures

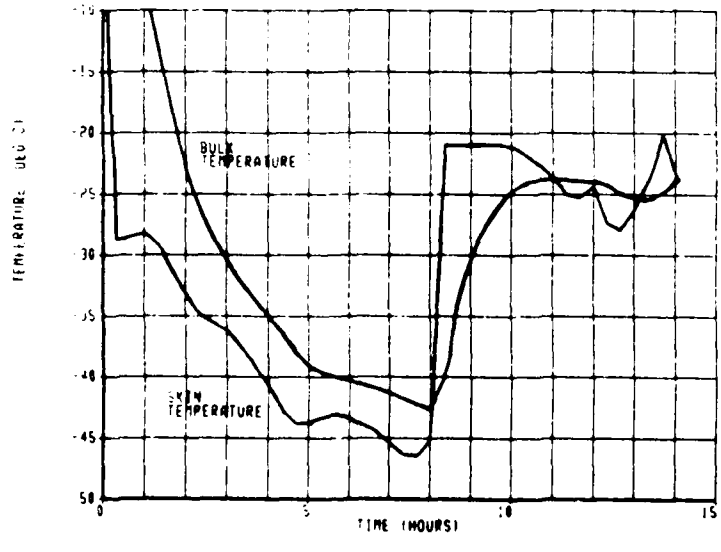

c. Actual Ground Temperatures and Worst Case Atmospheric Temperatures

Figure 37. Worst Case Thermal Exposures for B-52 Track 1

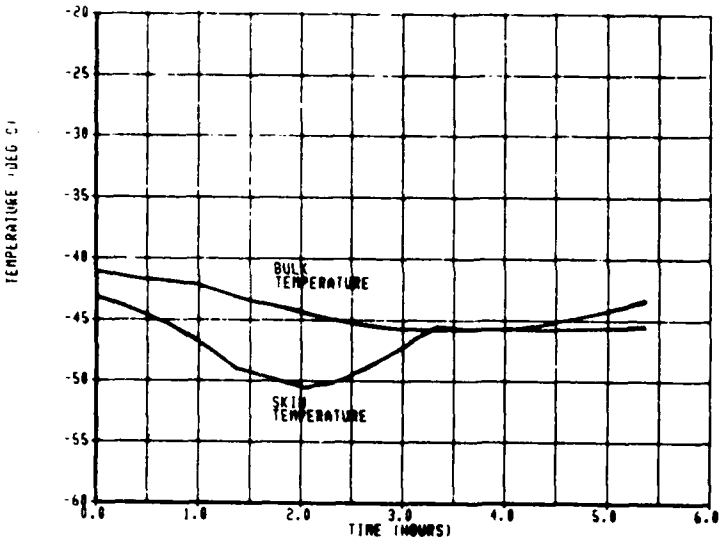

a. *Worst Case Ground Temperatures and Worst Case Atmospheric Temperatures*

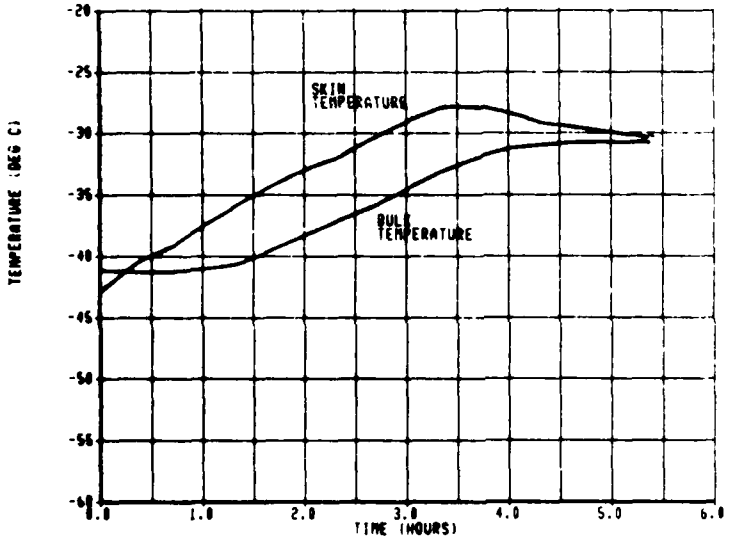

b. *Worst Case Ground Temperatures and Actual Atmospheric Temperatures*

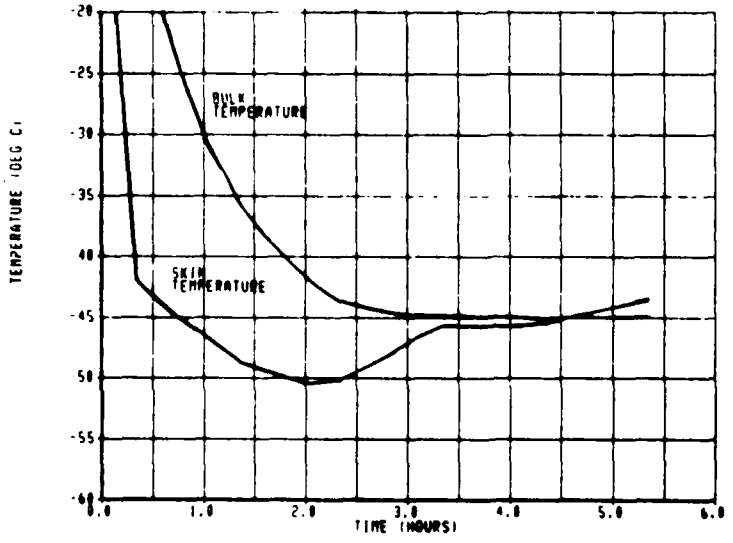

c. *Actual Ground Temperatures and Worst Case Atmospheric Temperatures*

Figure 38. Worst Case Thermal Exposures For C-141 Track 10

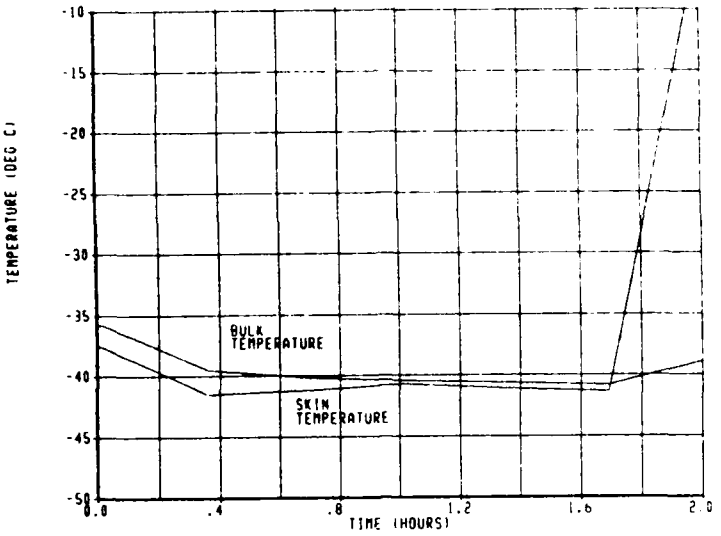

a. *Worst Case Ground Temperatures and Worst Case Atmospheric Temperatures*

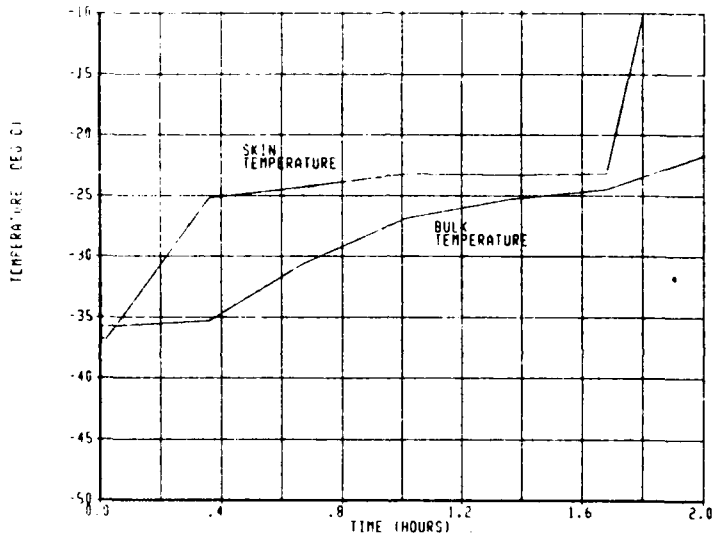

b. *Worst Case Ground Temperatures and Actual Atmospheric Temperatures*

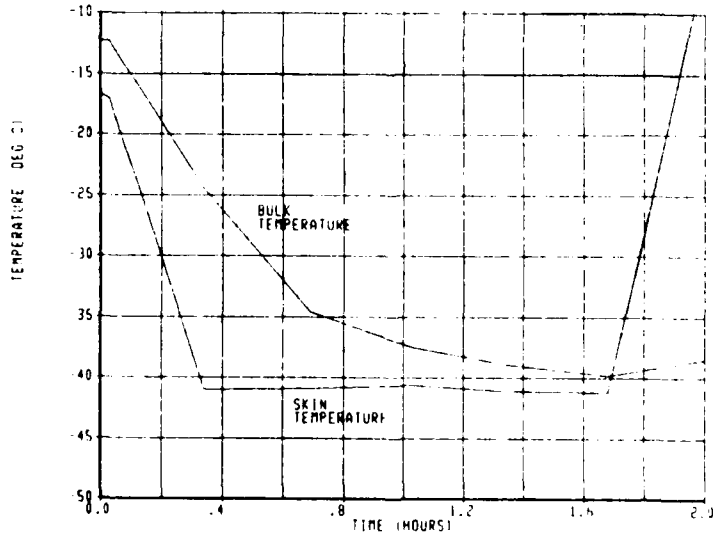

c. *Actual Ground Temperatures and Worst Case Atmospheric Temperatures*

Figure 39. Worst Case Thermal Exposures for F-15 Track 3

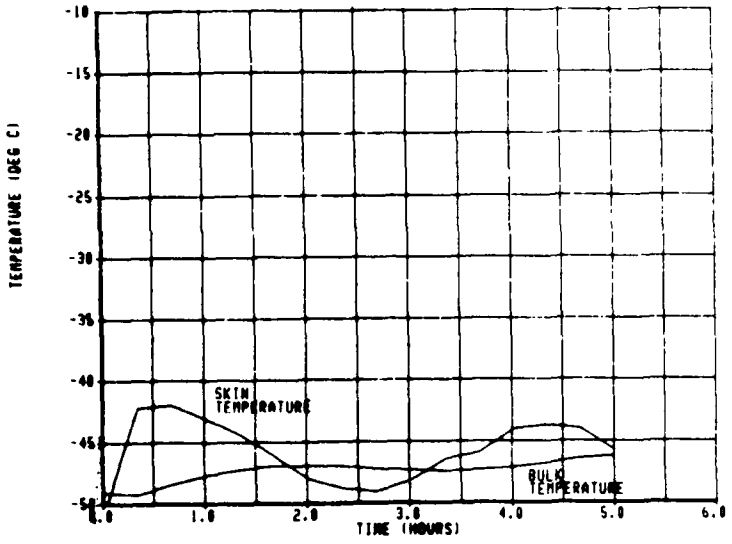

a. *Worst Case Ground Temperatures and Worst Case Atmospheric Temperatures*

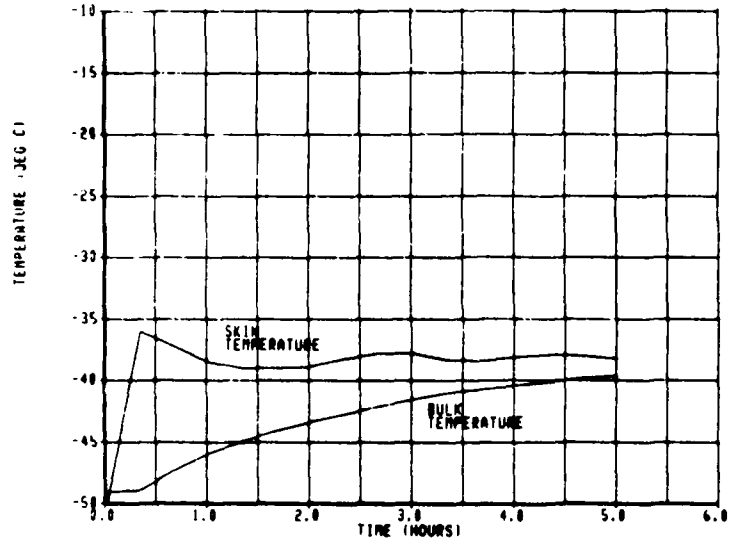

b. *Worst Case Ground Temperatures and Actual Atmospheric Temperatures*

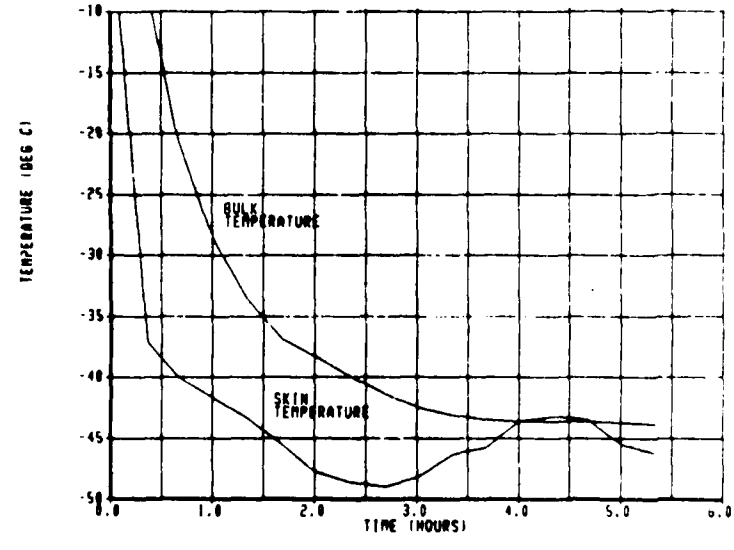

c. *Actual Ground Temperatures and Worst Case Atmospheric Temperatures*

Figure 40. Worst Case Thermal Exposures for KC-135 Track 10

significantly to the discussion.) The thermal properties of JP-4 were used in this calculation; with a freeze point of $-58^{o}C$, no fuel freezing is predicted in any instance.

As an illustration of the effect of fuel freezing, however, a fuel freeze point of $-46^{o}C$ (same as JP-5) was selected, and the calculation repeated for KC-135 Track 10, which appears to experience the lowest preflight and inflight temperatures of the thick wing missions. Comparable low temperatures are encountered inflight by C-141 Track 10, but for a much shorter period of time. A much higher freeze point, $-36^{o}C$, was used for F-15 Track 3, the most severe thin wing mission. A comparison of the predicted bulk temperatures is shown in Figure 41; the predicted thermal profiles (higher freeze point cases) in Figures 42 and 43. The estimated quantity of holdup as a function of time is shown in Figure 44. Several plots describe different phases of each mission, defined below; the time interval covered by each plot is identified in the right margin.

- The effect of pre-conditioning the fuel because of thermal exposure prior to takeoff (Figures 42 and 43) is shown in the form of thermal profiles at four-hour intervals beginning twenty-four hours prior to the flight and ending at takeoff time (-24 to 0 hrs).

- The effect of in-flight thermal exposure is shown in the form of thermal profiles at hourly intervals throughout the flight (Figures 42b and c, and 43b and c). In most cases more than one plot is required for clarity, since alternating cooling and warming cycles tend to cause overlapping in the profiles

- The coldest fuel temperatures calculated occurred at the tank bottom; temperature profiles in this region are shown at twenty minute intervals in Figures 42d and 43d, which exhibit details of the lowest skin and bulk temperatures.

A review of the analytically derived profiles produced the following observations:

- the practice of having fully fueled airplanes parked on the runway for operational readiness greatly increases the possibility of fuel freezing due to ground temperature exposures

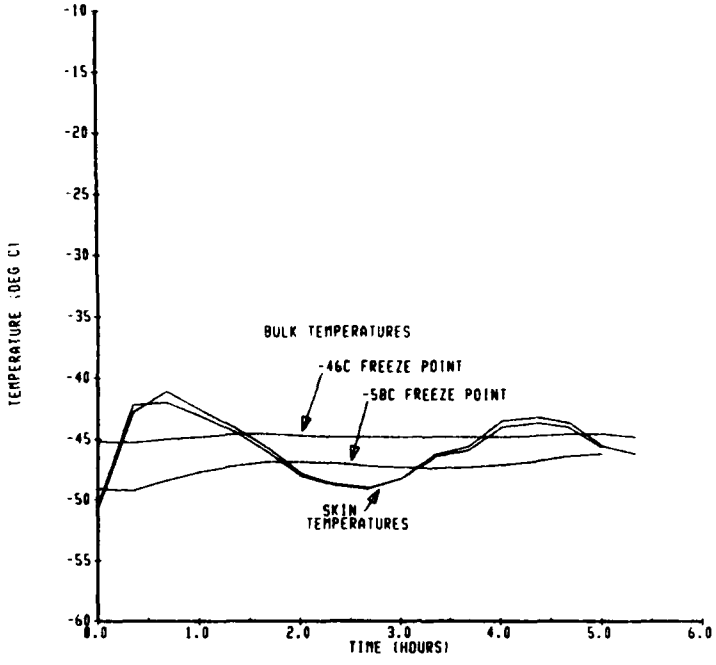

a. KC-135 Track 10

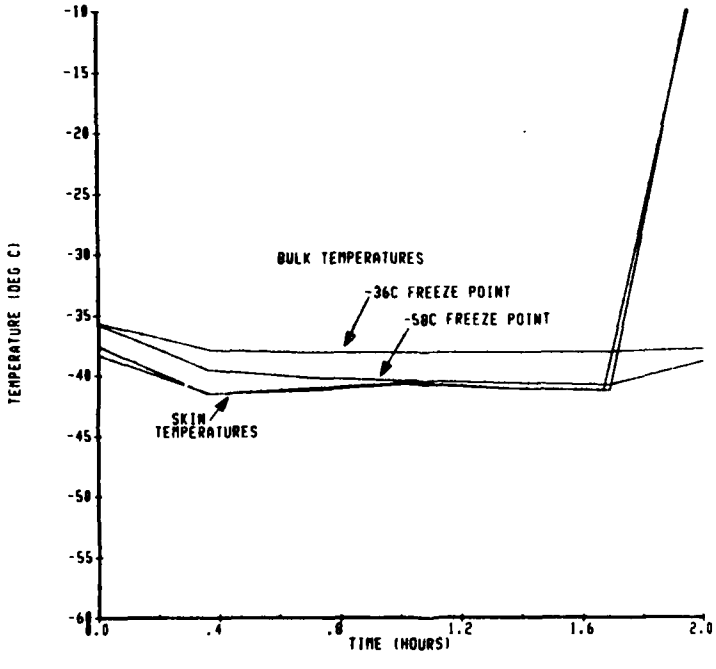

b. F-15 Track 3

Figure 41. Predicted Bulk Fuel Temperatures

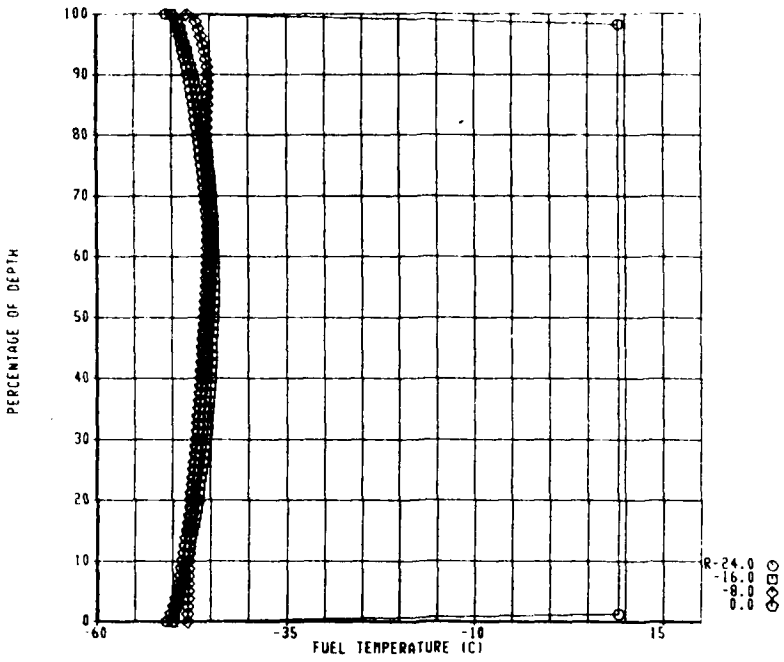

a. Preflight Phase

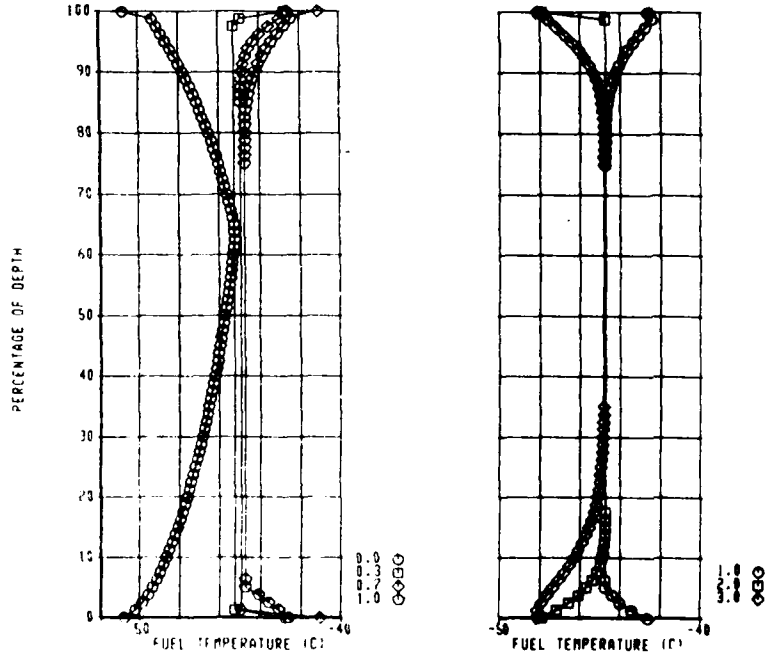

b. Mission Phase (Warming and Cooling)

Figure 42. KC-135 Track 10; Thermal Profiles

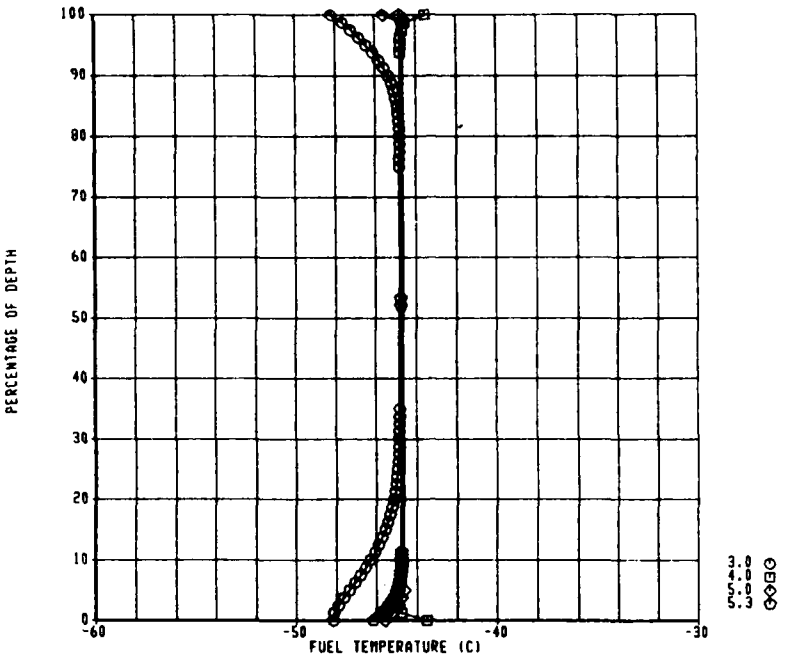

c. Warming and Fuel Withdrawal Phase

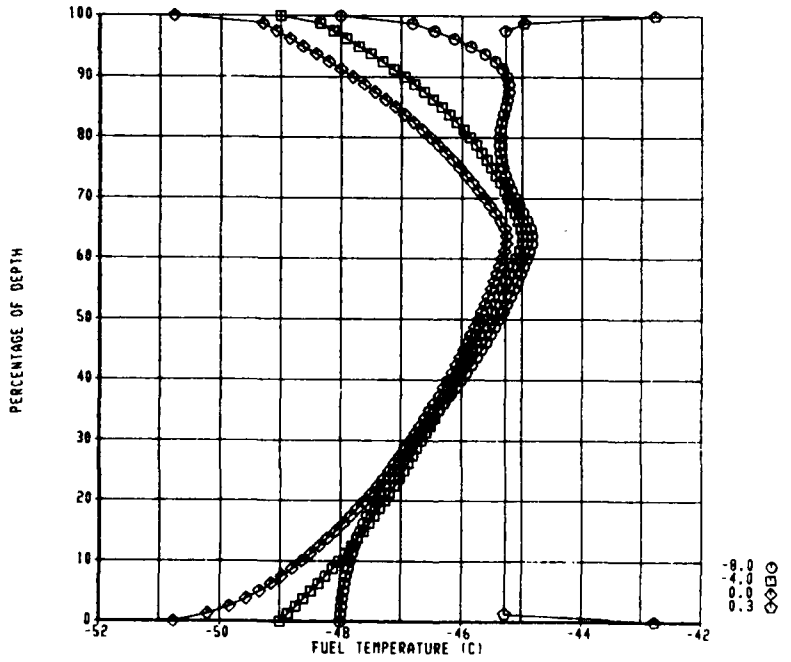

d. Detail of Coldest Phase

Figure 42. KC-135 Track 10; Thermal Profiles (Continued)

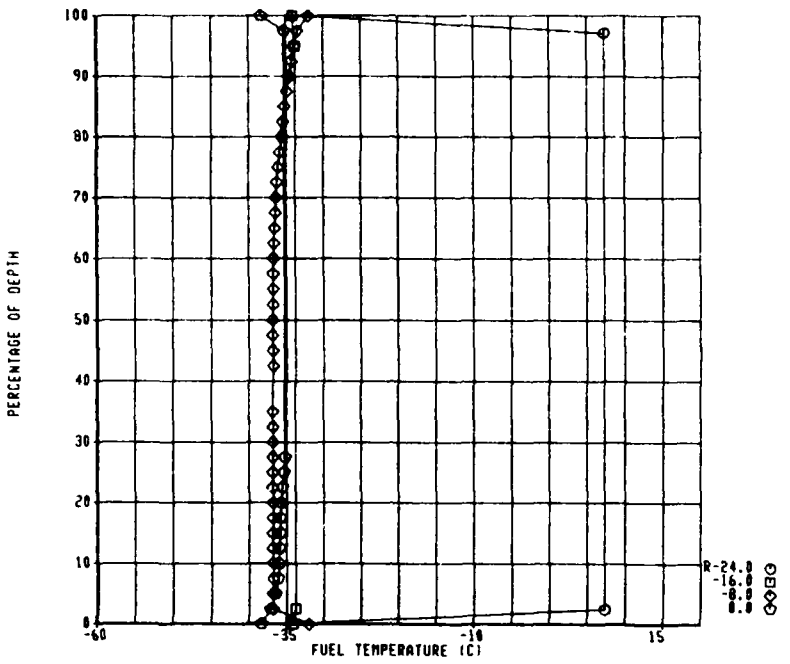

a. Preflight Phase

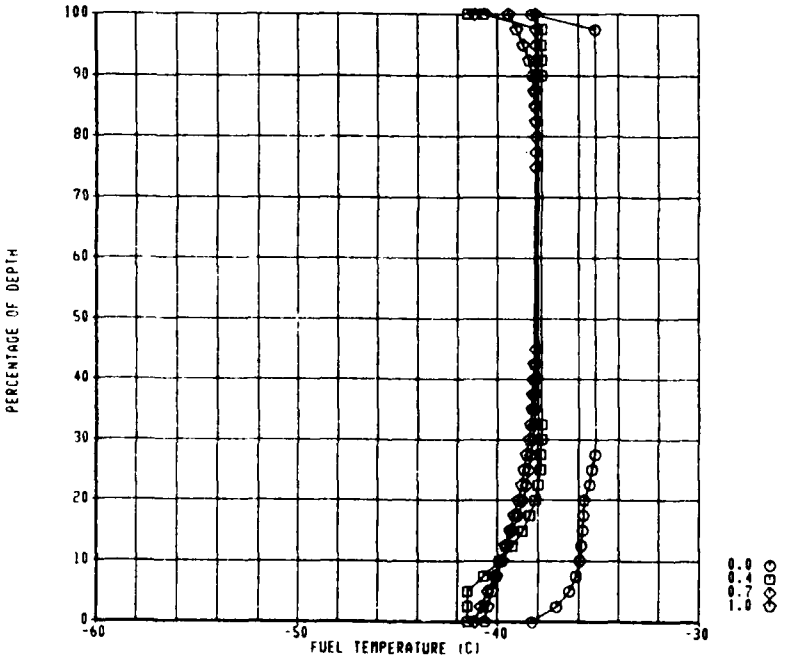

b. Cooling Phase

Figure 43. F-15 Track 3, Thermal Profiles

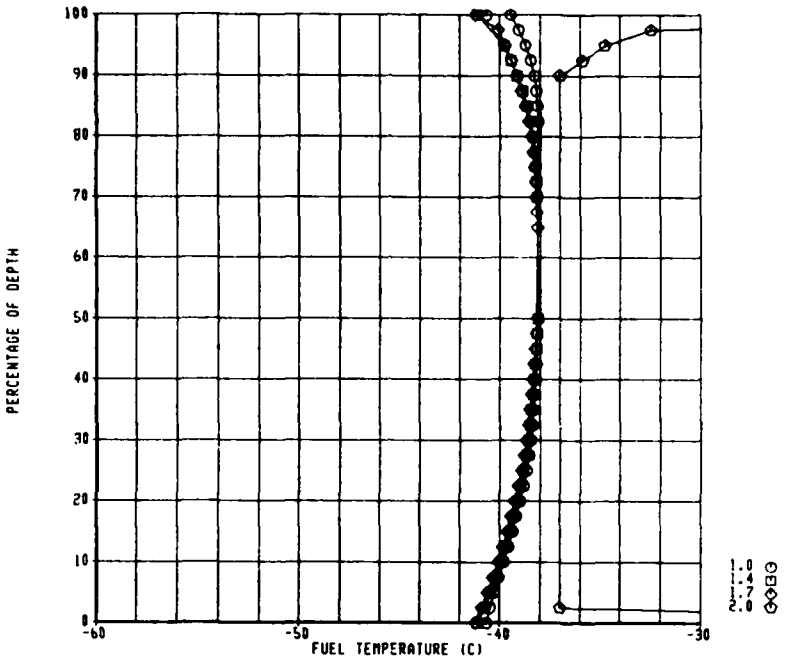

c. Warming and Fuel Withdrawal Phase

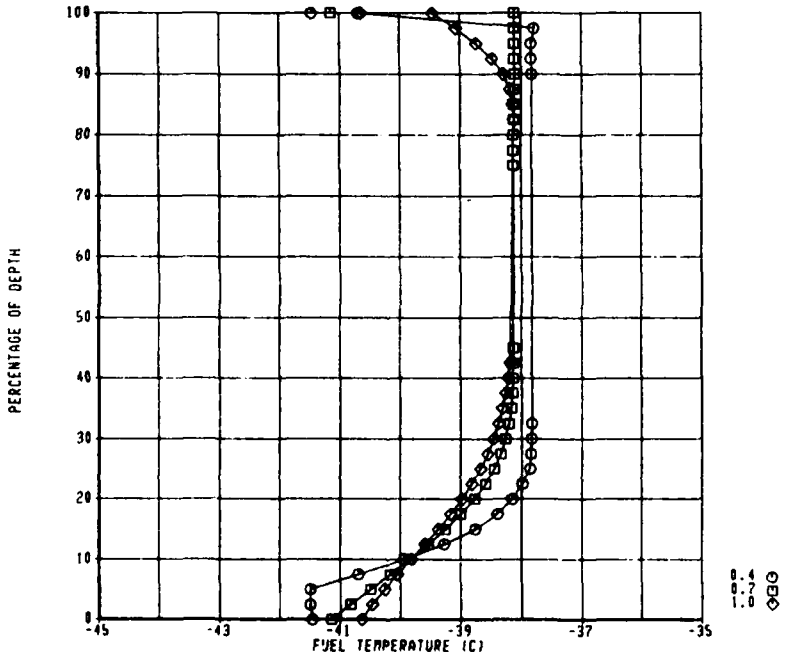

d. Detail of Coldest Phase

Figure 43. F-15 Track 3, Thermal Profiles (Continued)

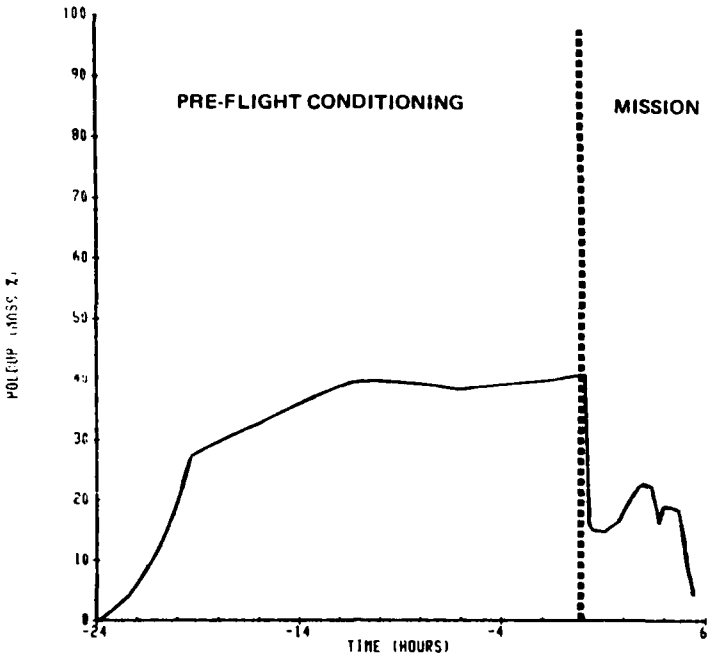

a. KC-135 Track 10

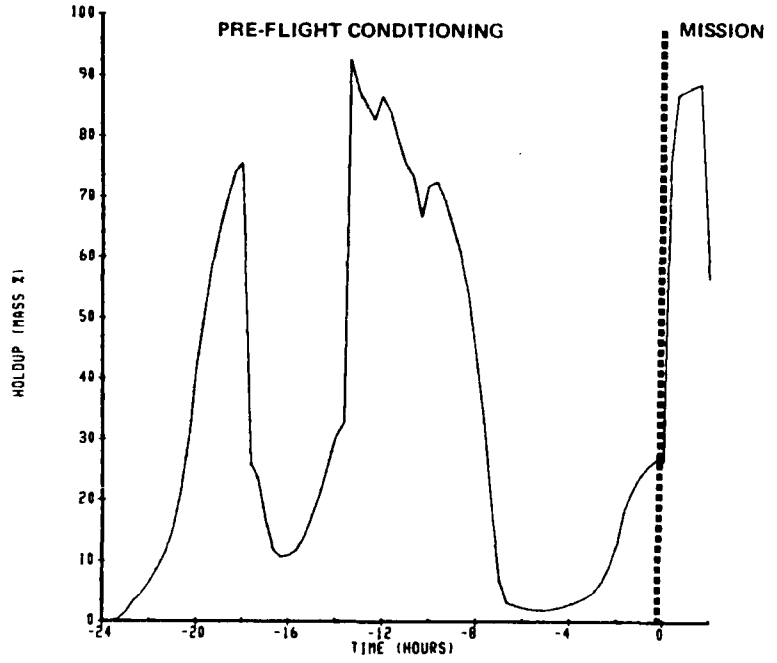

b. F-15 Track 3

Figure 44. Estimated Holdup versus Mission Time

- o the practice of retaining fuel in relatively small outboard wing tanks until the end of the mission significantly increases the potential for fuel freezing in these tanks
- o temperatures are lower at the bottom of the tank where conduction dominates than at the top which is convection dominated; the presence of an ullage space greatly alters heat transfer at the top of the tank

A test plan was formulated based on the results of the preceding analysis to verify the fuel temperature calculations. Following this confirmation, further analysis was performed to examine the effect of frozen fuel.

b. External Tank Calculations

As described earlier, the three study airplanes designed to carry external fuel tanks are the A-10, B-52, and F-15. Considering the preflight and inflight thermal exposures of each, the single most severe experienced is the preflight exposure of A-10 airplanes based at Eielson AFB, AK. (Tracks 1, 3, 4, 5, and 6). In effect, this exposure was simulated analytically by applying a constant, uniform temperature of -50^{o} to the tank skin (Figure 45). Because fuel freezing could not yet be accounted for in the calculation, standard JP-4 fuel properties and a specification freeze point of $-58^{o}C$ were assumed. Several important conclusions based on the analytic model are:

- o the low outside wall temperatures create boundary layers of cold fuel which descend down the walls until they are deflected by colder layers of fuel below
- o the top half of the cylindrical tank is dominated by convection heat transfer whereas the bottom half is dominated by conduction heat transfer
- o even with initially warm fuel temperatures, fuel near the bottom of the tank begins to approach the skin temperature in less than one hour which may result in freezing during extremely low temperature flights
- o for the reason just described and pending re-calculation of the problem with fuel freezing effects included, the freeze point limitation for cylindrical tanks is conservatively estimated to be $-50^{o}C$ for the worst case thermal exposure

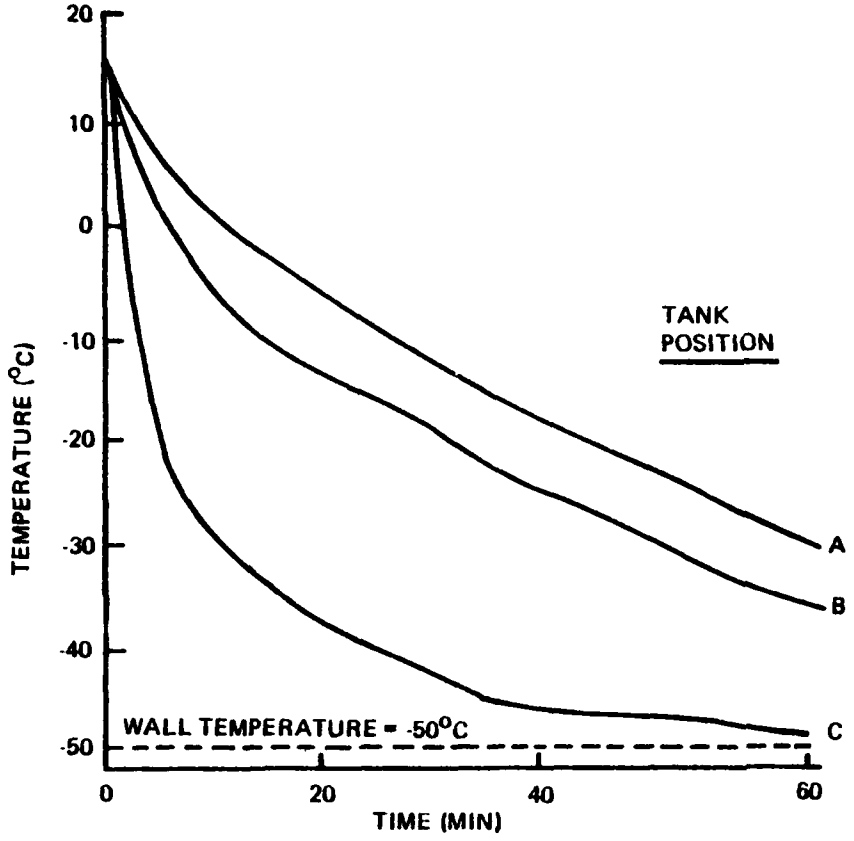

a. Temperature Histories of Selected Points

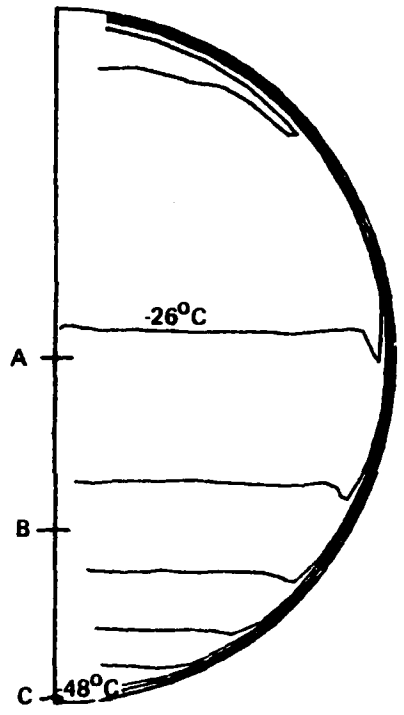

b. Temperature Contour Plot 1-Hour After Start of Cooling

Figure 45. Results of Cylindrical Tank Calculation

In order to develop confidence in the results predicted by the computer program, a cylindrical tank simulator was built and test data obtained for comparison with the calculation. The data which serves to validate the analytical simulation of the cylindrical tank heat transfer problem is reported in Section III.

SECTION III
EXPERIMENTAL VERIFICATION

The basic experimental apparatus for measuring the behavior of low temperature fuels was a rectangular integral wing fuel tank simulator, and most tests were conducted in this essentially one dimensional (1-D) heat transfer apparatus. The primary purpose of the test program was to verify the mathematical technique used to predict inflight temperature profiles in airplane wing tanks. Four fundamental goals were to:

- o confirm temperature profiles and fuel holdup estimates
- o determine the effect of fuel chemical composition on holdup for two fuels with the same measured freeze point
- o determine the effect of a fuel tank boost pump on the drainability of partially frozen fuel
- o compare actual in-flight test fuel temperature measurements with results from the fuel tank simulator to verify the ground simulator

During the course of this study, a cylindrical tank thermal simulator was also constructed by Boeing. While not capable of performing mission simulations with fuel, the cylindrical tank was used to obtain thermal data to help validate predictions of a two-dimensional computer model under development for the Navy.

1. TEST PLAN

The test plan to accomplish the goals listed above is given in Table 6. The tests simulated the extremes in low temperature exposures for the airplanes included in this study to provide estimates of maximum fuel hold-up due to freezing during fleet operations.

2. TEST FUELS

Five test fuels were selected for use in the one-dimensional simulator because of their freeze points; specific reasons for selection of the fuels will be discussed in the following section. Fuel characterization data for these fuels is summarized in Table 7, and Shell-Thornton holdup measurements are given in Figure 46.

Table 6. Summary of Tests Performed

Test Number	Fuel Freeze Point	Fuel Type	Configuration	Description
	Mission Simulation			
(1)	-46C	Jet A	Thick Wing	Conditioning for 24 hours with worst case ground temperatures from Eielson AFB, followed by simulation of KC-135 Track 10
(2)	-51C	JP5/JP8	Thick Wing	Repeat of Test Number 1 with lower freeze point fuel
(3)	-40C	Jet A/ JP5 (10%DFM)	Thin Wing	Conditioning for 4 hours with worst case ground temperatures from Elmendorf AFB, followed by simulation of F-15 Track 3
(4)	-42C	Jet A	Thin Wing	Repeat of Test Number 3 with lower freeze point fuel
(5)	-46C	Jet A	Thin Wing	Conditioning with Eielson AFB ground temperatures
(6)	-51C	JP5/JP8	Thin Wing	Repeat of Test Number 5 with lower freeze point fuel
	Flight Test Data Comparison			
(7)	-46C	Jet A	Thick Wing	Simulation of L-1011 flight test using NASA data
	Drainability and Pumpability			
(8)	-46C	Jet A	Thick Wing	
a				Cold soak at -50C, drain line not insulated, gravity drain
b				Repeat of test number 8a, boost pump drain
c				Cold soak at -50°C, drain line insulated, gravity drain
d				Repeat of Test Number 8c, boost pump drain

Table 6. Summary of Tests Performed (Continued)

Test Number	Fuel Freeze Point	Fuel Type	Configuration	Description
	Effect of Composition			
(9)	-50C	JP8	Thick Wing	
a				Cold soak at -60°C with paraffinic fuel, gravity drain
b				Repeat of Test Number 9a, boost pump drain
(10)	-51C	Jet A	Thick Wing	
a				Cold soak at -60°C with naphthenic fuel, gravity drain
b				Repeat of Test Number 10a, boost pump drain

Table 7. Fuel Characterization Data

Fuel Number		1	2	3	4	5	6
Fuel Type	ASTM	Jet A/ JP5 (10%DFM)	Jet A	Jet A	JP 8	Jet A	JP5/JP8
Freeze Point (^{o}C)	D2386	-40.0	-42.0	-46.0	-50.0	-51.1	-51.1
Pour Point (^{o}C)	D97	NA	-50.0	-48.3	-53.9	-52	-57.2
Viscosity at 15^{o}C (cst)	D445	NA	NA	2.27	NA	NA	NA
Specific Gravity (15/15C)	D1298	0.7985	0.8017	0.8169	NA	0.8265	0.8035
Water Content (ppm)	D1744	49.0	53.0	34.0	NA	NA	NA
Reid Vapor Pressure at 38^{o}C (psi)	D323	NA	NA	0.38	NA	NA	NA
AKA		NA	LFP1	NA	82-POSF-562	LFP8	NA
Composition					paraffinic	naphthenic	

NA- not available

AD-A152 801 FUEL FREEZE POINT INVESTIGATIONS(U) BOEING MILITARY AIRPLANE CO SEATTLE WA L A DESMARAIS ET AL. JUL 84 D180-28285-1 AFWAL-TR-84-2049 F33615-82-C-2262 2/3

UNCLASSIFIED F/G 21/4 NL

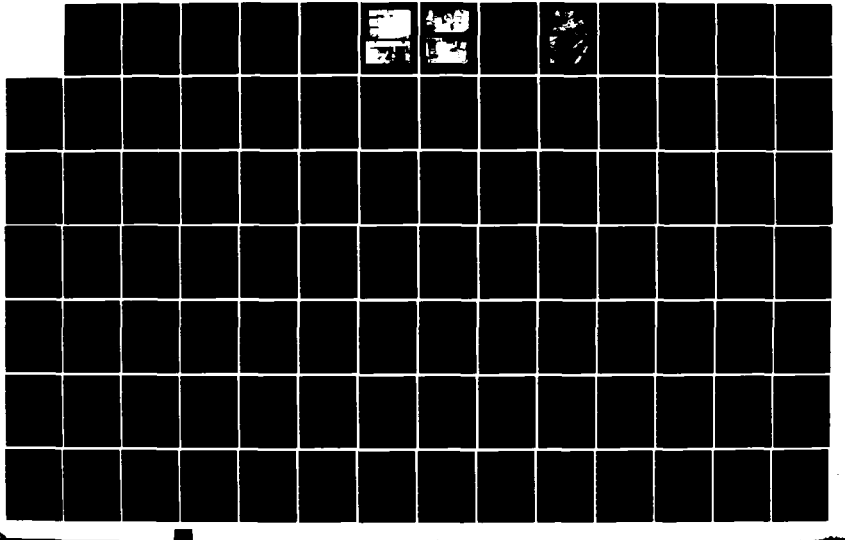

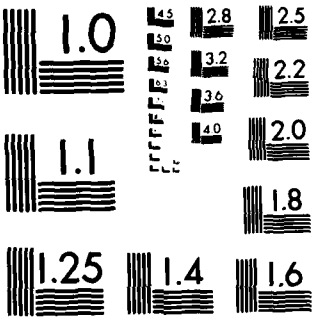

MICROCOPY RESOLUTION TEST CHART
NATIONAL BUREAU OF STANDARDS-1963-A

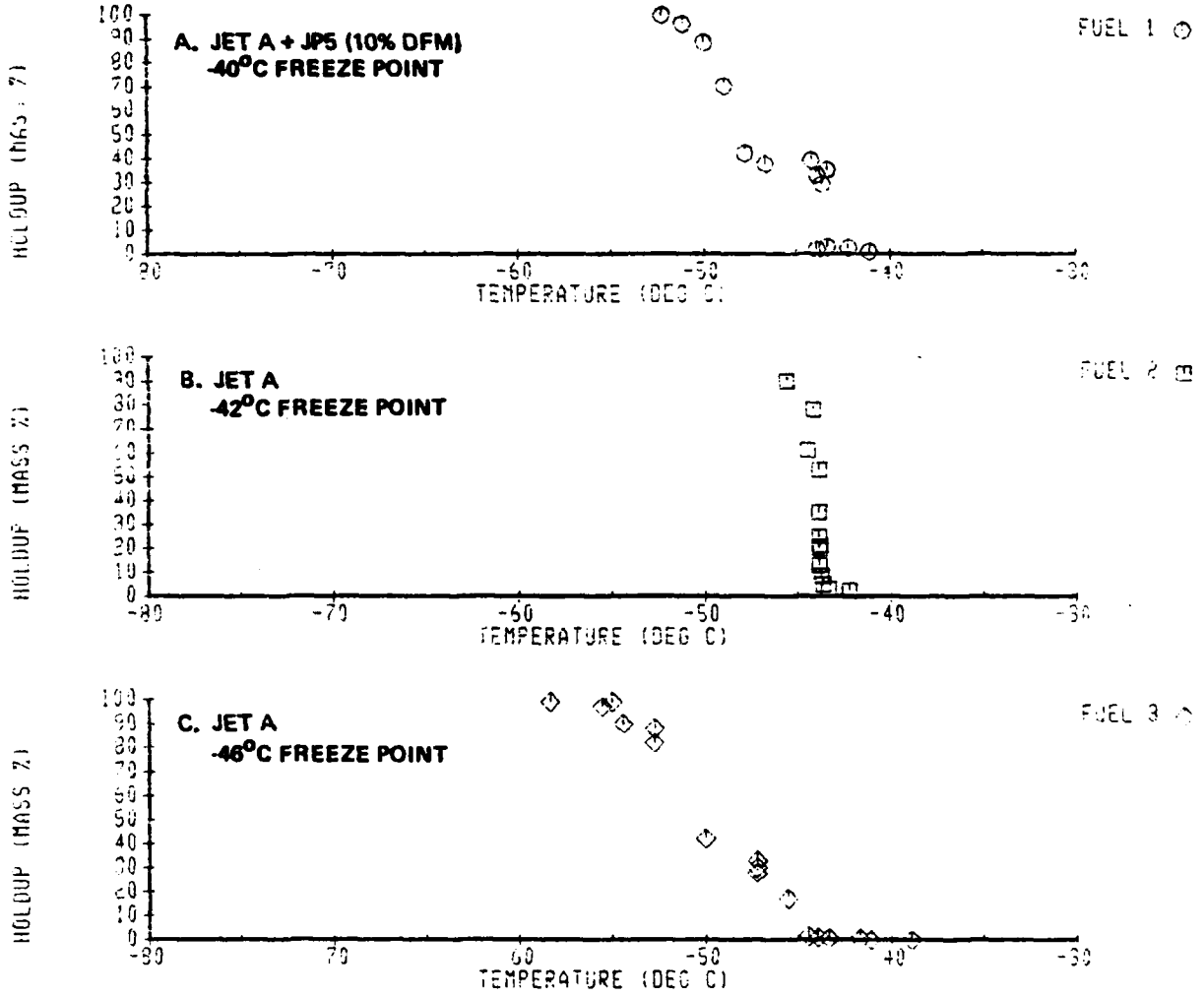

CHKD.		13AUG84	REVISED	DATE	*Figure 46.* SHELL-THORNTON TEST DATA
CHECK					
APPD.					
APPD.					THE BOEING COMPANY

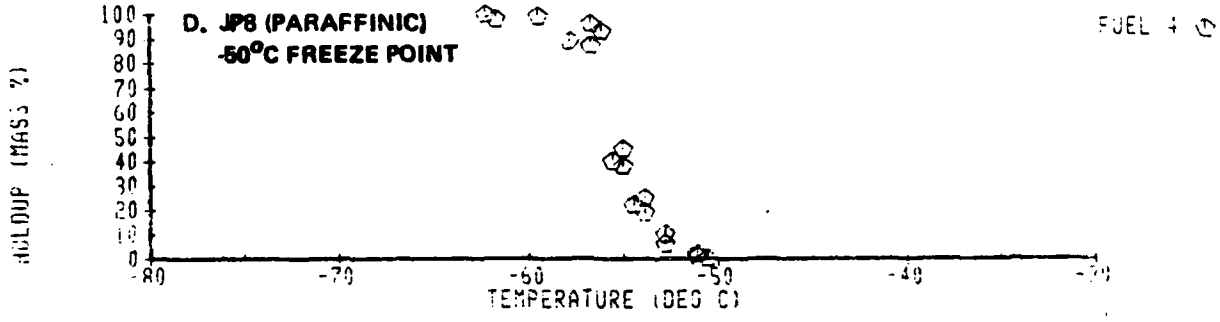

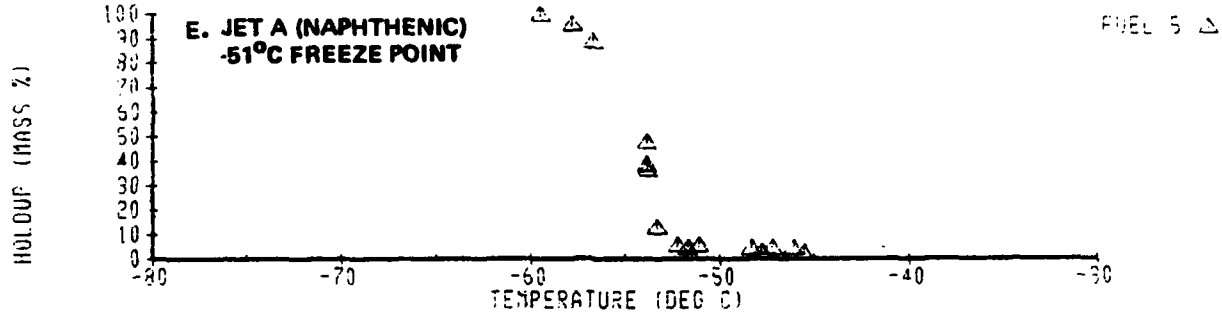

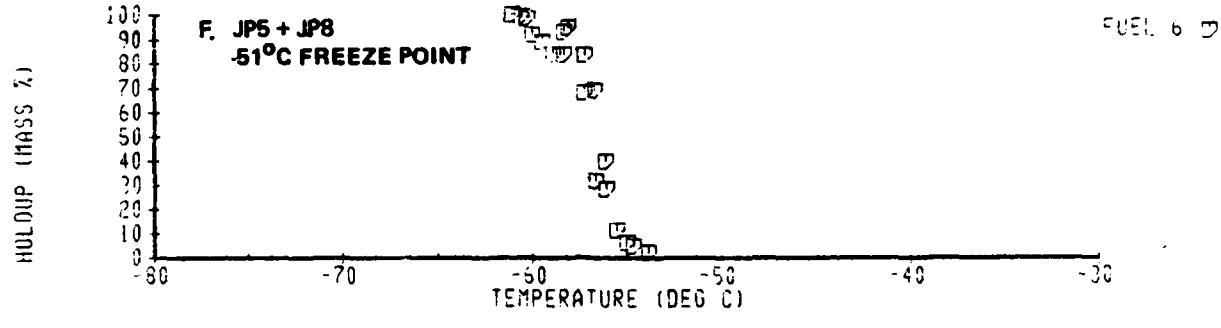

CALC		13AUG84	REVISED	DATE	*Figure 46.* SHELL-THORNTON TEST DATA *(Continued)*	
CHECK						
APPD.						
APPD.					THE BOEING COMPANY	PAGE 87

Two of the fuels used in this test program, and in previous work (Reference 1), were mixtures of fuels of differing freeze points, combined to obtain an intermediate freeze point. The proportions of each base fuel to blend for a desired freeze point was predicted by using a blending index (Reference 31). The desired freeze points of the mixtures are compared with measured freeze points in Figure 47.

3. TEST FACILITIES

The wing fuel tank simulator can be configured to model either a thick (transport) wing or a thin (fighter) wing (Figure 48). The cylindrical tank simulator (Figures 49) was used to obtain data to help validate the two-dimensional analytical code.

a. Integral Wing Fuel Tank Simulator

The 1-D simulator is shown schematically in Figure 50. The internal contents of the tank in its thick wing configuration are shown in Figure 51a; the contents of the tank in its thin wing configuration are shown in Figure 51b. The internal dimensions of the thick wing tank are 76 cm (l) x 51 cm (w) x 51 cm (h), and the thin wing, 76 cm (l) x 51 cm (w) x 20 cm (h). All features of the two configurations are common, except that internal baffles and the boost pump were not included in the thin wing version. Additional details of the fuel tank simulator and its support equipment are given in Reference 32.

Simulation of the upper and lower skin surface temperature is achieved by pumping refrigerant (chilled methanol) through the upper and lower skin cooling chambers. Flow control valves (A6 and A7 of Figure 50) are automatically controlled to provide the desired (mission) skin temperature which is programmed on the temperature data track. The automated control system is capable of producing equal upper and lower skin temperatures within about $\pm 1^{o}C$; results reveal excellent agreement between programmed and actual temperatures. Additional instrumentation was installed to measure test control parameters. An eleven (11) liter auxiliary tank was located on top of the simulator to compensate for fuel contraction during cooling and thus prevent an ullage space from forming during cool down.

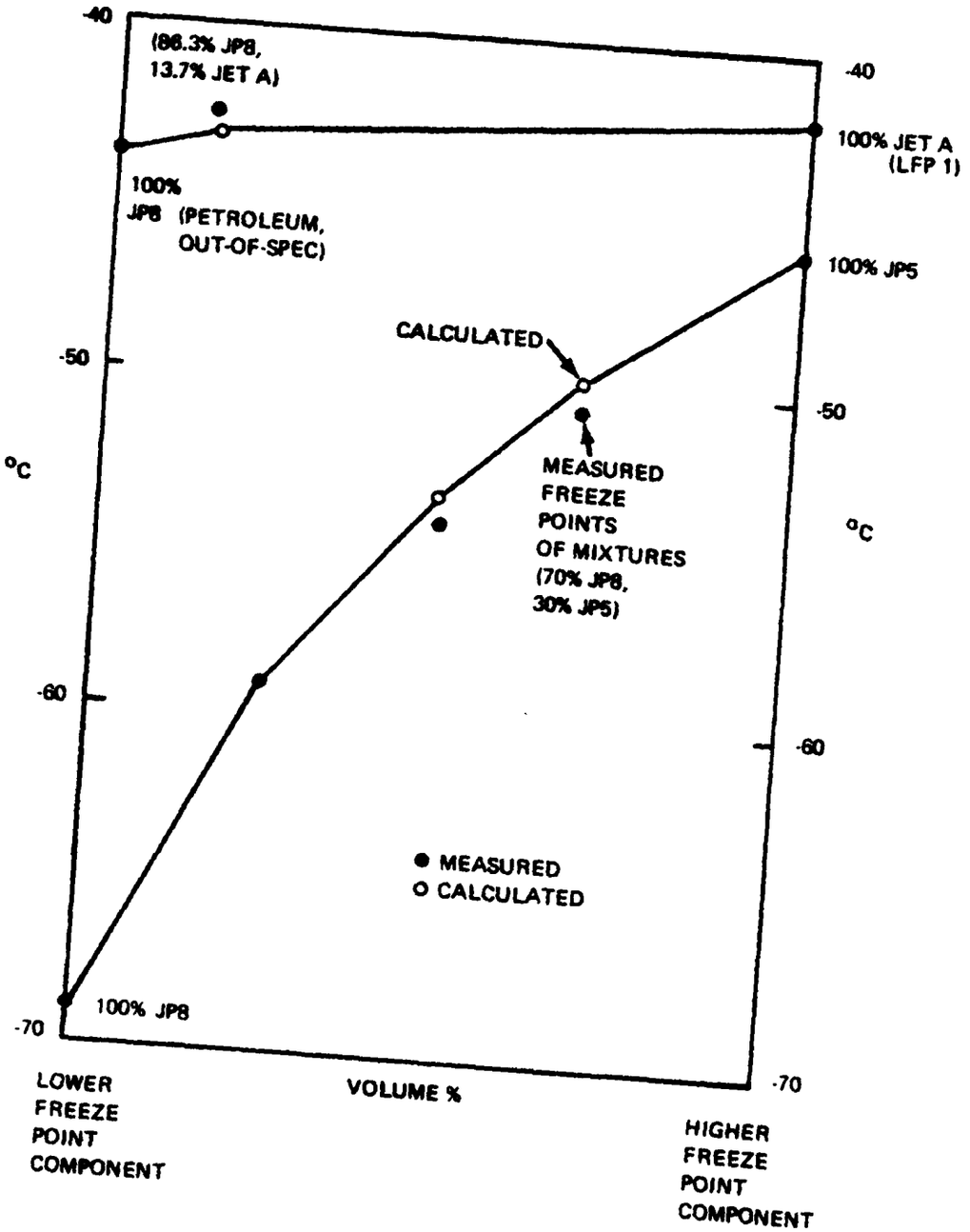

Figure 47. Freeze Points of Mixed Fuels

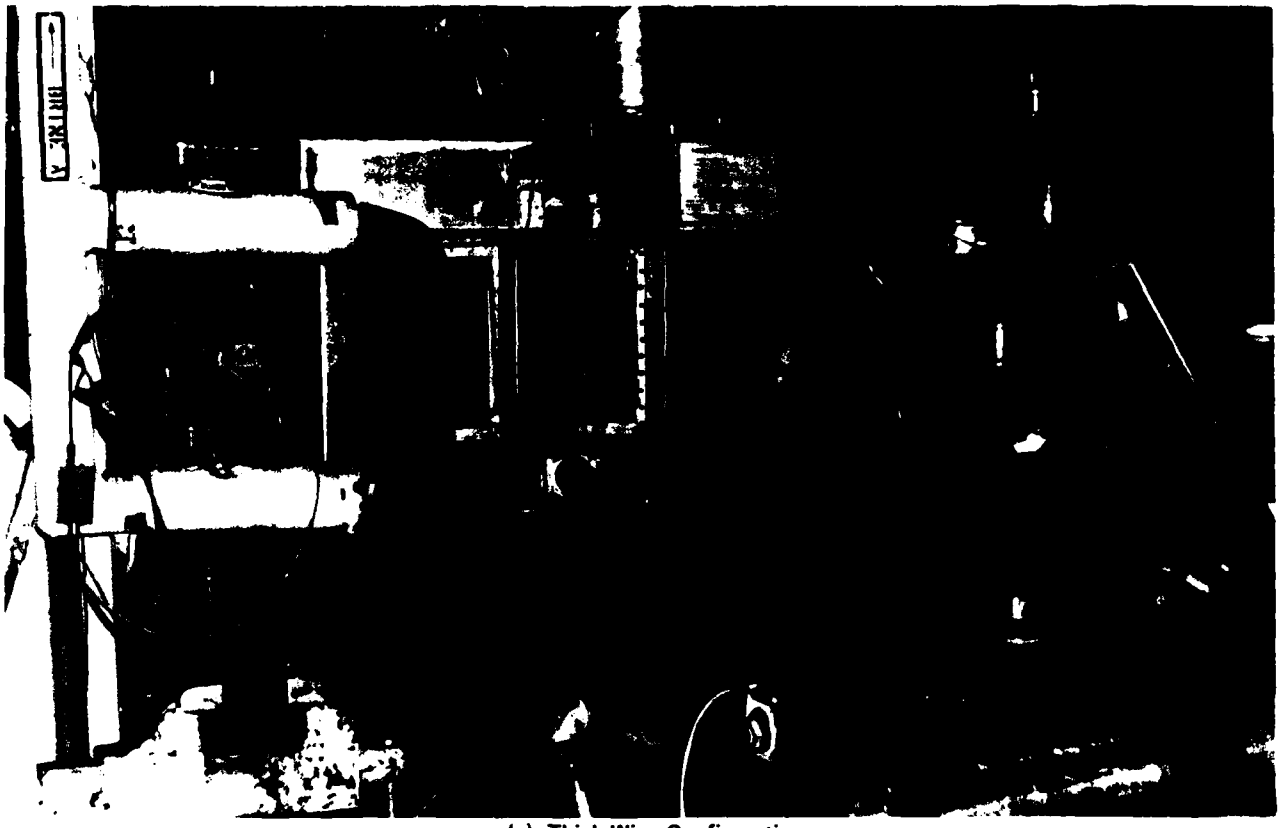

(a) Thick Wing Configuration

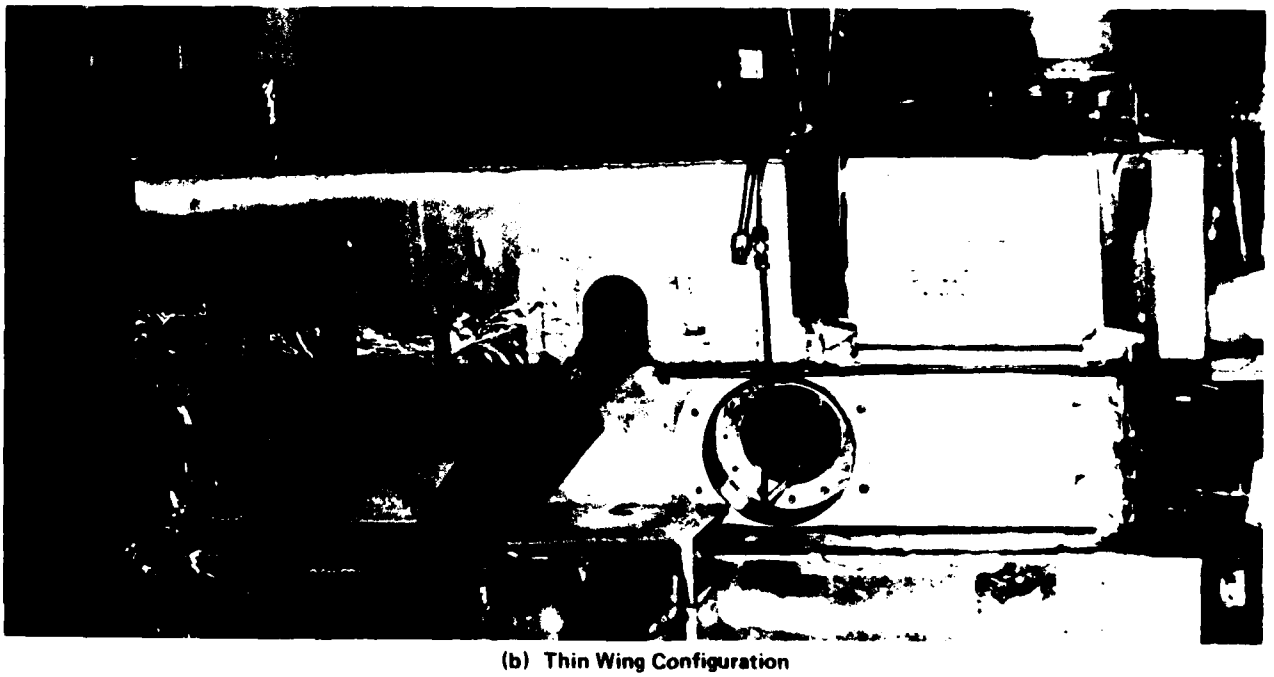

(b) Thin Wing Configuration

Figure 48. Integral Wing Fuel Tank Simulator

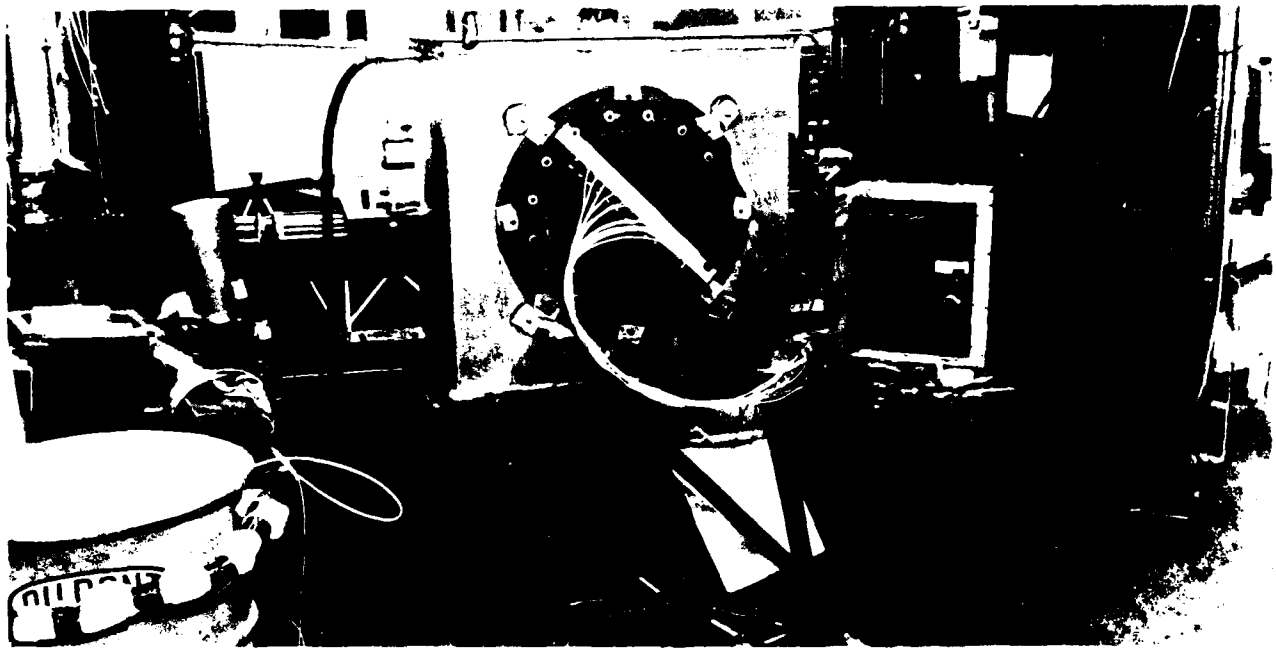

(a) Thermocouple End

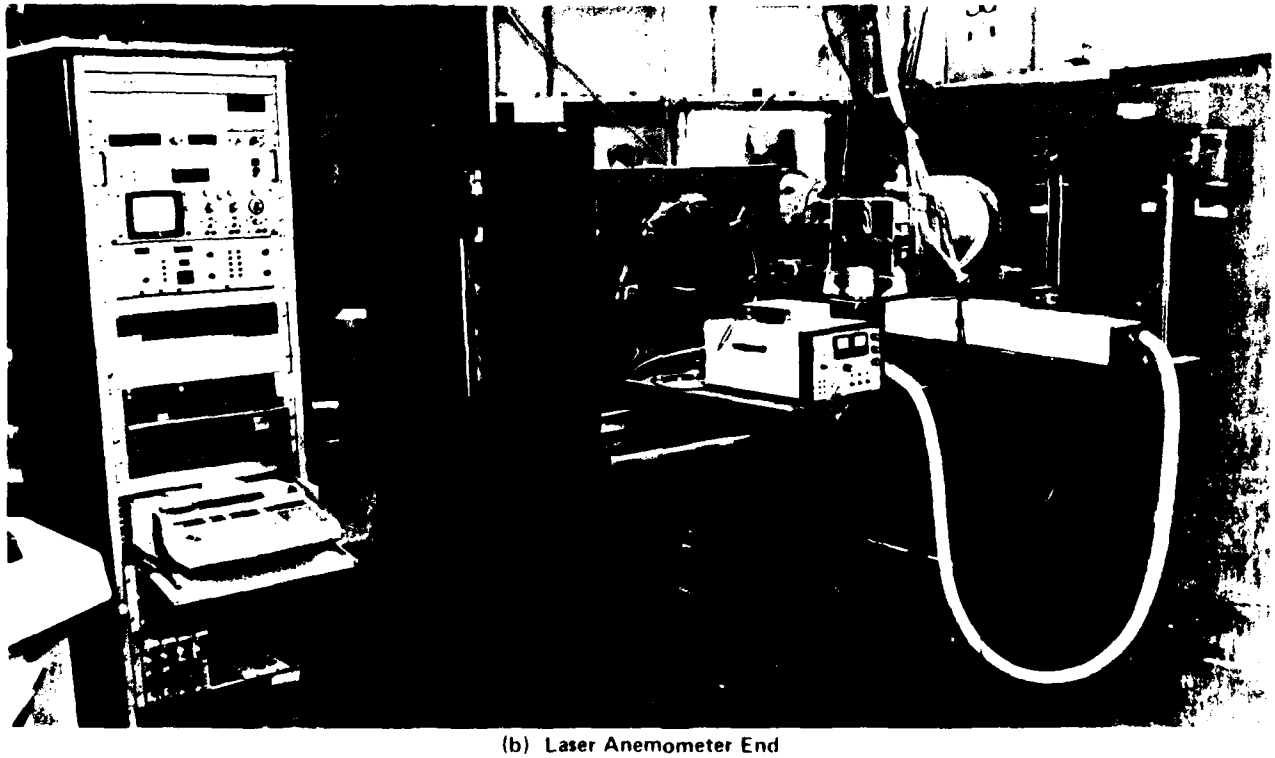

(b) Laser Anemometer End

Figure 49. External (Cylindrical) Fuel Tank Simulator

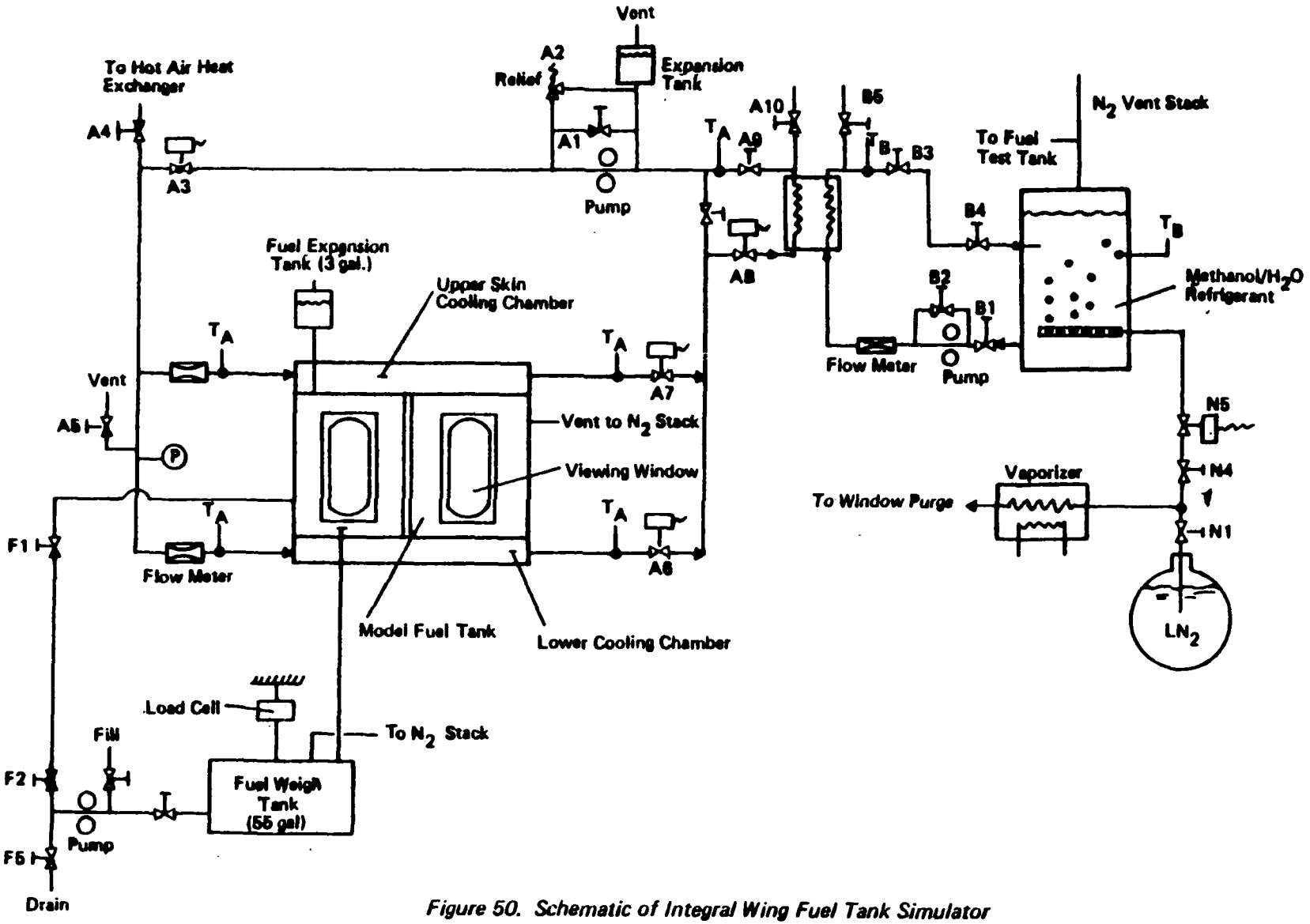

Figure 50. Schematic of Integral Wing Fuel Tank Simulator

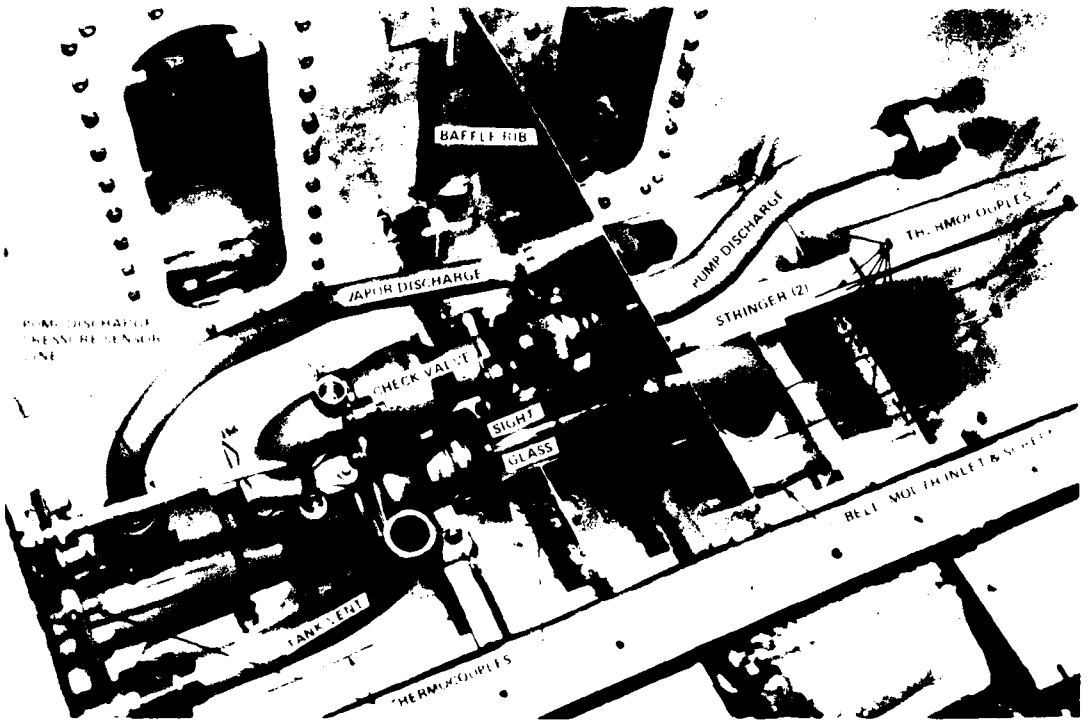

(a) Thick Wing Configuration

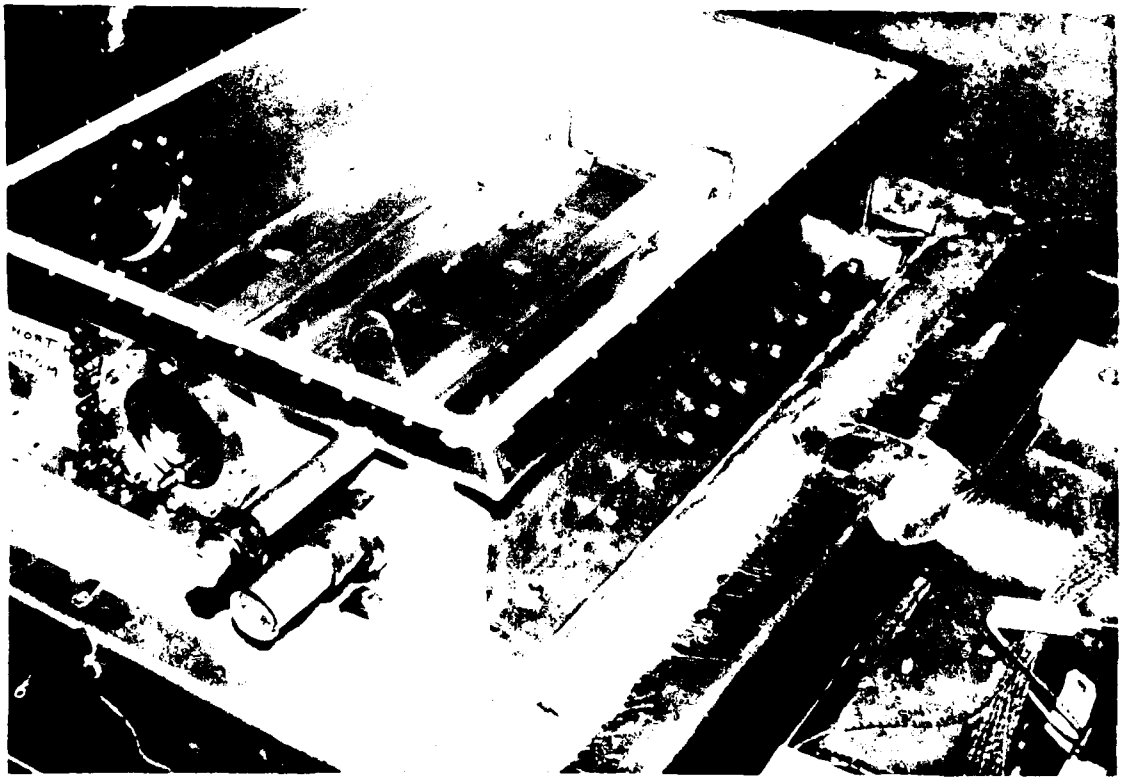

(b) Thin Wing Configuration

Figure 51 Interior of Integral Wing Fuel Tank Simulator

(1) Instrumentation

Temperature profiles were measured inside the simulator tank with chromel/alumel thermocouples distributed in the thick wing tank as shown in Figure 52a and in the thin wing tank, as shown in Figure 52b. Over the range of test temperatures, the uncertainty of the temperature measurements was $\pm 1.1^{o}C$. When fuel was drained from the thin wing simulator, it flowed into a catch tank suspended from a 300 pound load cell, which provided fuel depletion versus mission time data. Load cell accuracy was $\pm 0.25\%$ of full scale (± 0.75 lb.). The HP3052A data acquisition system (Figure 53) recorded time, thermocouple output, and load cell readings. The data system provided printed paper output for "quick look" and a cassette tape for subsequent data analysis and plotting.

(2) Procedures

The skin temperature-time histories from the analysis of route temperature for each mission were transcribed to a temperature data tape for automatic skin temperature control purposes. Each test run was started when the skin temperature and bulk liquid temperature were both within $\pm 2.8^{o}C$ ($\pm 5^{o}F$) of the required pre-takeoff values. Data were recorded at fifteen (15) minute intervals during the mission, except during the relatively short drain period preceding hold-up measurements when data were recorded every one or two minutes.

Holdup is the fuel remaining in the tank after draining, and includes both solid fuel and liquid fuel trapped within the solid. The procedure for fuel withdrawal and holdup measurement at the end of a typical mission simulation is:

- first, a level gravity drain followed by a tilted tank gravity drain to insure that all liquids are drained
- second, warming of the tank to melt all frozen material, followed by a further tilted gravity drain

Holdup was deduced at the completion of the first step by subtracting the weight of the drained fuel (stored in the weigh tank) from the total quantity of fuel known to have been loaded into the simulator. Variations on the drain

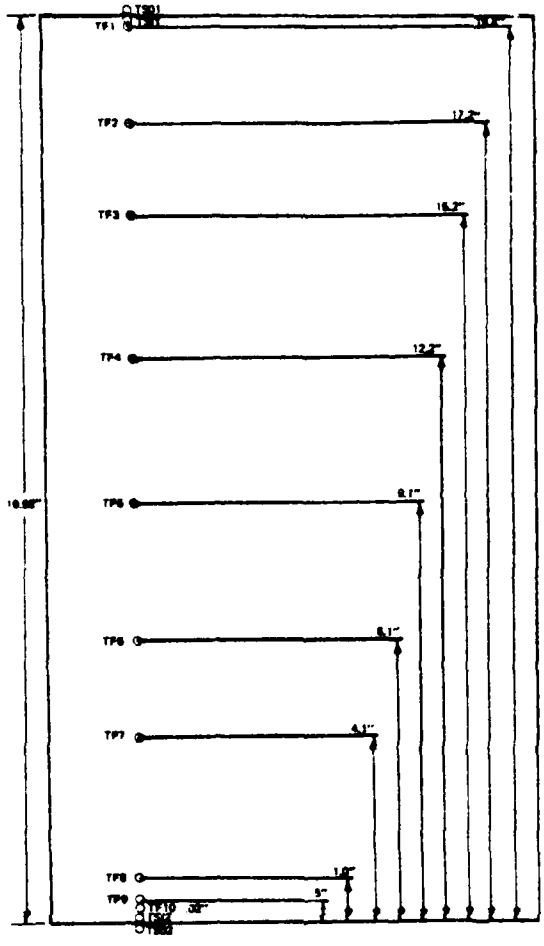

a. Thick Wing Configuration

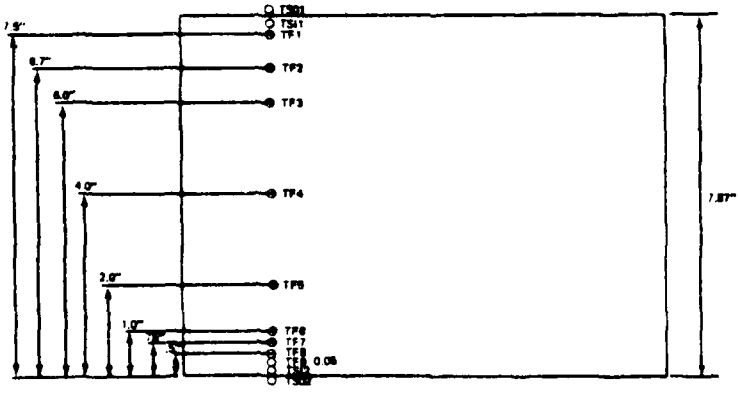

b. Thin Wing Configuration

Figure 52. Thermocouple Locations in Integral Wing Fuel Tank Simulator

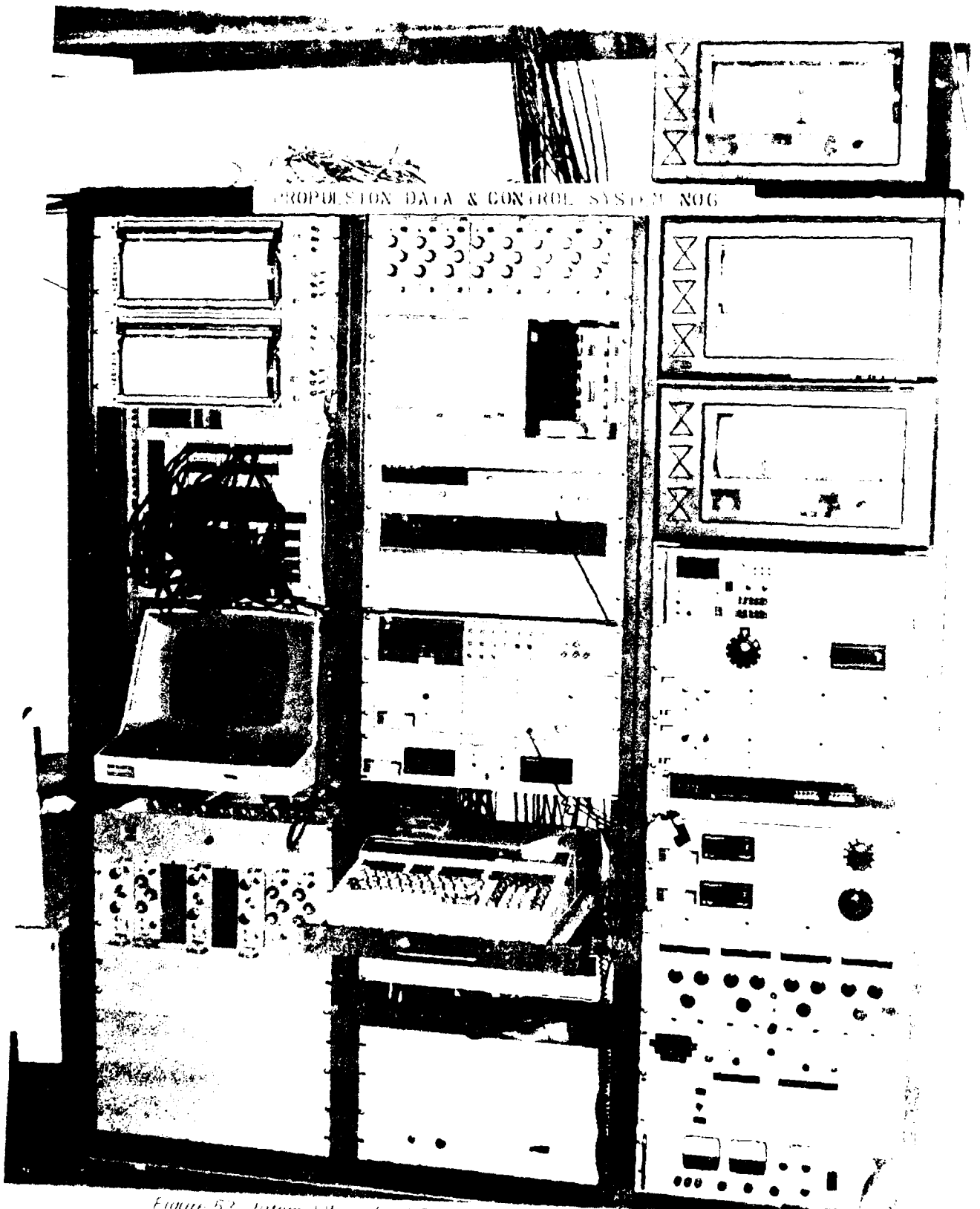

Figure 5.2 Integral Wing Fuel Tank Simulator Data Acquisition System

and holdup measurement procedure, for example, boost pumping of the fuel in lieu of the level gravity drain, were used in several tests to investigate the pumpability of the holdup and are pointed out in the section on results.

Even with liquid fuel in the tank, the visibility in the tank became progressively poorer as the temperature dropped, and photographs were not feasible at temperatures of interest. (Additional tank lighting and attempts to remove water from the fuel by bubbling dry nitrogen through the fuel prior to loading the simulator do not improve the visibility at low temperature.) At the lower temperatures, the fuel took on a very "waxy" dark yellow color. It is believed that microscopic wax or ice crystals form as the fuel temperature drops imparting the color, and eventually making the fuel opaque. After draining the tank, photographs were taken of the solid holdup fuel as viewed through the windows in the simulator.

b. External Fuel Tank Simulator

The two and three dimensional convective processes involved during fuel cooling in external tanks pose an extremely difficult mathematical modeling problem. Therefore, experimental verification of the mathematical model is required prior to its acceptance as a tool for predicting in-tank temperatures and holdup due to freezing. A literature review showed that experimental data for the cylindrical geometry (pylon tank) and boundary conditions of interest were either inadequate or nonexistent. Therefore, Boeing constructed a cylindrical fuel tank simulator and conducted fluid cooling experiments to provide velocity and temperature measurements for comparison to those predicted from the mathematical model. The test results were used to help validate the mathematical model.

Since the inflight external temperature field is nearly uniform over the tank surface, the Boeing cylindrical tank simulator utilized a "tank within a tank" scheme for experimental modeling (Figure 54a). The outer tank was rectangular, 0.94 m on a side by 76.7 cm long. This tank provided a water bath environment for the inner tank which was constructed from an aluminum cylinder (45.7 cm in diameter by 76.2 cm long) to match the length of the outer tank. The end caps of the inner tank were made of transparent plastic to permit flow visualization and velocity measurements with a laser

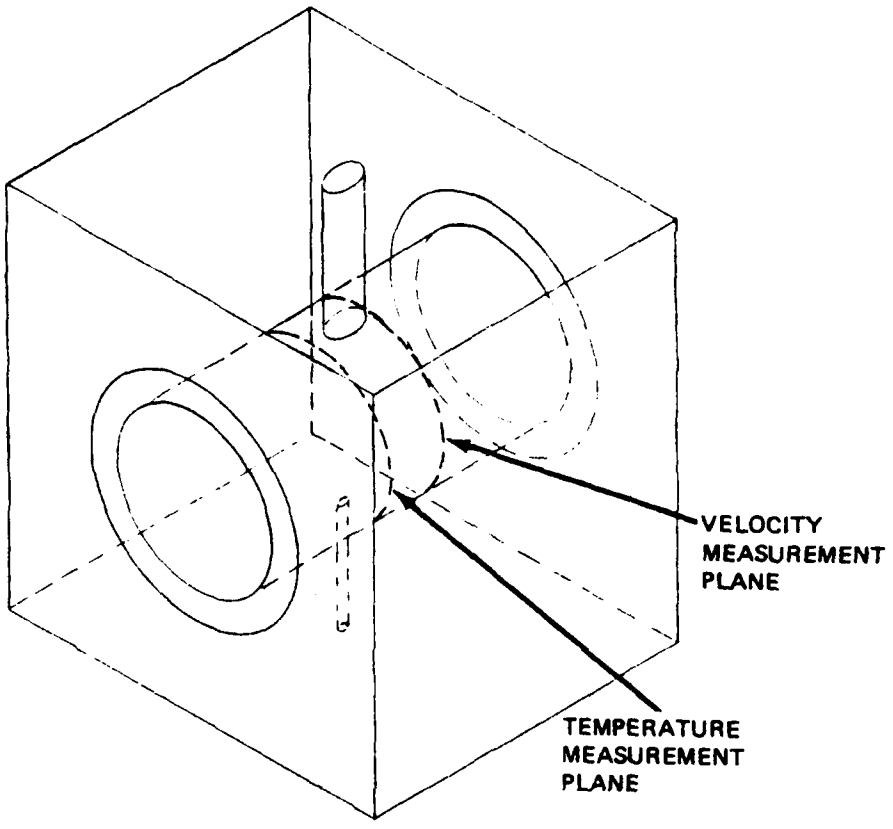

a. "Tank in Tank" Design

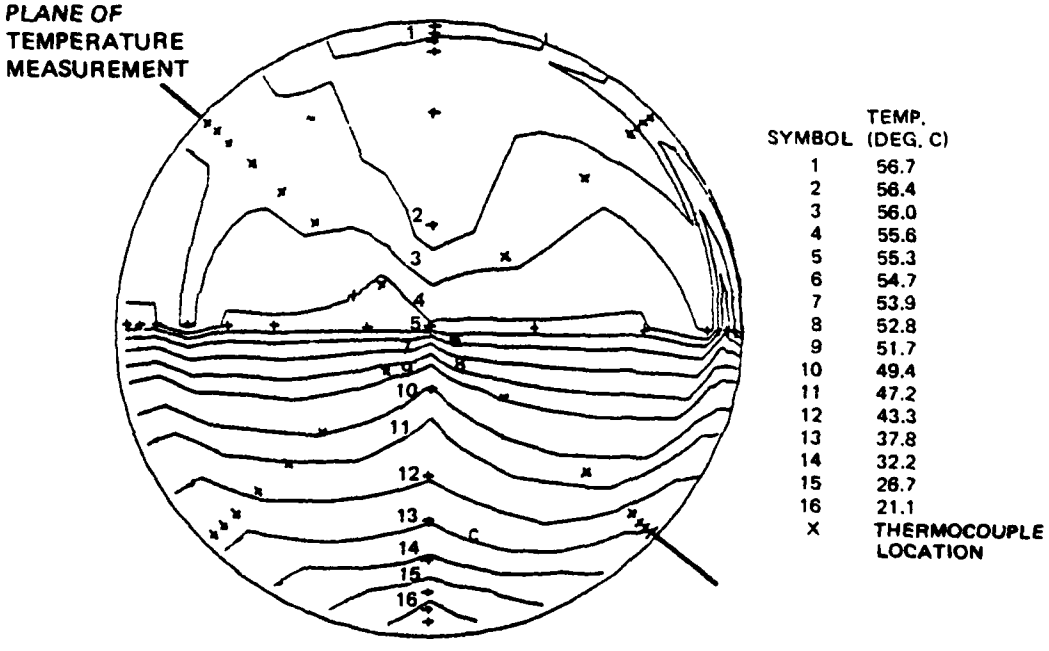

b. Sample Temperature Measurements

54. Cylindrical Fuel Tank Simulator

velocimeter. The tank diameter was approximately the same as that of a typical pylon tank and the desired fuel Rayleigh number range could be modeled with an appropriate mixture of glycerine and water. (Because of safety considerations and because of poor optical qualities, fuel was not used in these experiments.) All tests were performed with a full tank and measurements were made in vertical planes near the middle of the cylinder (about 12 inches from one end) where the end effects would be minimized. Velocity measurements were taken in a plane an equal distance from the opposite end of the tank. Assuming a symmetrical flow field, this procedure provided velocity and temperature data at the same plane.

(1) Instrumentation

Temperature measurements were made using thirteen thermocouples cantilevered from one of the end plates of the cylindrical tank and aligned in a plane which bisected the tank longitudinally. The response time of these thermocouples was on the order of 0.1 second which was sufficient to detect the average temperature changes of the liquid during the most severe transients. The thermocouple probes could be bent as desired, allowing closer probe spacing near the wall of the tank where temperature gradients were expected to be much larger. To obtain a complete temperature map, repetitive runs of the same experiment were performed with the probe rake "clocked" at 45^{o} intervals between each run. Sample temperature results are shown in Figure 54b.

Preliminary velocity measurements were made with a laser velocimeter mounted outside the end plate opposite to that of the thermocouples. The fluid was seeded with a small number of aluminum particles (mean diameter approximately 1 mil). As seed particles passed through a moving fringe pattern, produced by the intersection of two laser beams, the incident light was reflected to a detector. A Bragg cell modulated the wavelength of one of the laser beams to create the fringe pattern at the spot where the beams crossed. A discrimination process was established to ensure that only a single particle was observed per velocity measurement. After fifty such measurements, the mean velocity and standard deviation were recorded and the beam center moved to a new location. Since this technique yielded only one velocity component, the beams were rotated 90^{o} and the process repeated to obtain the resultant

velocity vector. The results revealed that improvement in the velocity measuring technique was required before the data could be used for code validation purposes.

(2) Procedures

The test fluid was commercial grade glycerine (96% pure) heated to an initial nominal temperature of 66°C and pumped into the inner cylindrical test tank. Flowing tap water (nominally 10°C) was then circulated through a baffle arrangement around the exterior of the test tank and discharged from the bottom of the outer tank. In conducting the initial test program, difficulties were experienced in maintaining desired external temperatures and in eliminating thermal gradients in the glycerine at time zero. Both of these effects complicated checking the numerical simulation. (The test fixture was subsequently modified to minimize these effects, but results were not available at the time of this report.).

4. COMPARISON OF CALCULATION AND EXPERIMENT

This section deals with:

- o comparison of calculated and experimentally obtained thermal profiles
- o the results of the improved holdup calculation method
- o investigations into the behavior of freezing and frozen fuels

a. Route Simulations and Holdup Predictions

The missions which indicated the most severe cases (Section II.1) of thermal exposure were selected for experimental verification; one mission each for the thick wing and thin wing airplanes.

(1) Thick Wing Tests

Tests 1 and 2 were simulations of a KC-135, and began with the worst case ground temperature exposure at Eielson AFB Alaska, followed by KC-135 Track 10, the worst case atmospheric exposure; different fuels (of -46°C and -51°C freeze points) were used in the tests. Results in the form of thermal

profiles are shown in Figures 55 and 56. The thermal profiles predicted by calculation were presented in Section II, while comparisons of predicted and experimental temperatures are shown in Figure 57. In this and all the other comparisons to follow, the calculations were repeated using the initial fuel temperature in the test tank; this procedure ensured that the same initial conditions would apply in the two cases. This was necessary since the initial temperature in the test tank was very difficult to regulate, while the analysis readily accepts any initial condition. Holdup measurements were taken at the end of the 24-hour preflight conditioning test phase and again at the specified point in the mission; the results are given in Table 8.

(2) Thin Wing Tests

Tests 3 and 4 were simulations of the worst case F-15 ("thin" wing) mission, which began with the ground temperature exposure at Elmendorf AFB Alaska, followed by F-15 Track 3. In order to reduce test time, the 24-hour temperature conditioning period was shortened to approximately 4 hours, since the skin and bulk fuel temperatures were predicted to be essentially identical at the end of 4 hour and at the end of 24 hours (Figure D-2a) and hence no additional meaningful data would have been gained by extending the ground conditioning period. Results of these tests (thermal profiles) are shown in Figures 58 and 59 with calculated and experimental results compared in Figure 60 and holdup measurements in Table 8. Unfortunately, no fuel with a measured freeze point higher than $-40^{o}C$ was available for use in this test to check the holdup predictions, but useful information was gained from the temperature comparisons.

Because the $-50^{o}C$ cold soak (Eielson AFB) was the worst case of all the ground thermal exposures considered, Tests 5 and 6 were conducted with the boundary conditions of the Eielson AFB ground temperature exposure to observe the thermal response of F-15 wing tanks. Results are presented in the same format as above in Figure 61 and 62, and Table 8.

(3) Cylindrical Tank Tests

As discussed previously, assumptions of uniform initial temperature and constant uniform wall temperature were not totally valid for the numerical

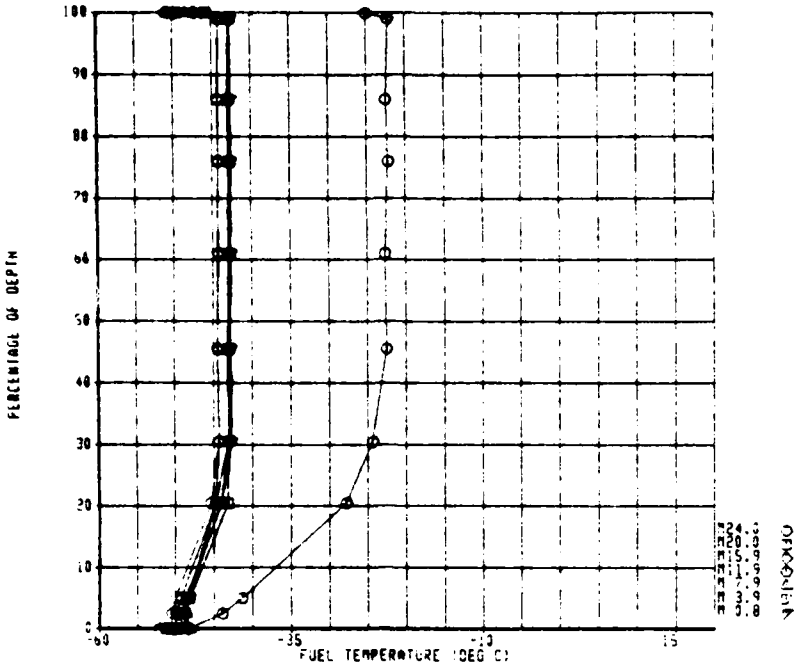

a. Test 1, Fuel 3

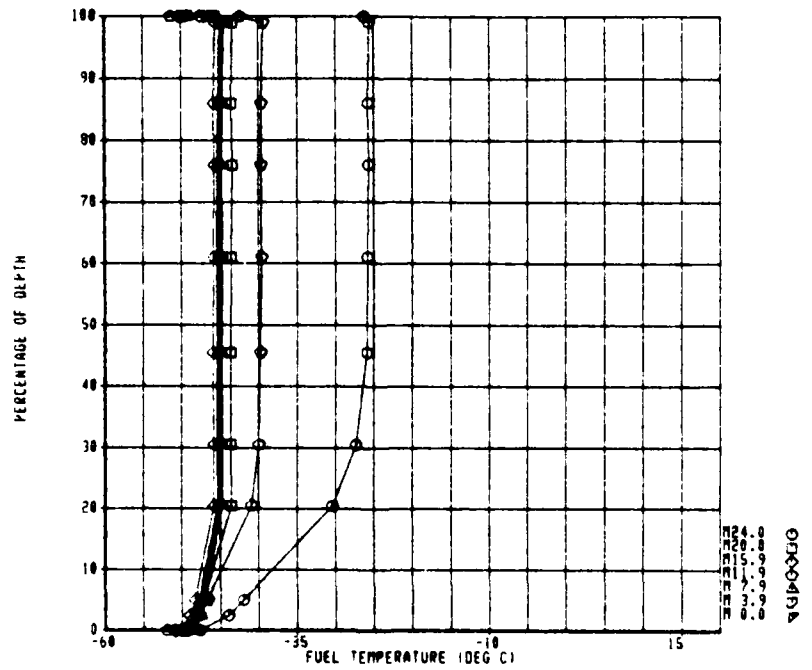

b. Test 2, Fuel 6

Figure 55. Thermal Profiles During Preflight Temperature Conditioning

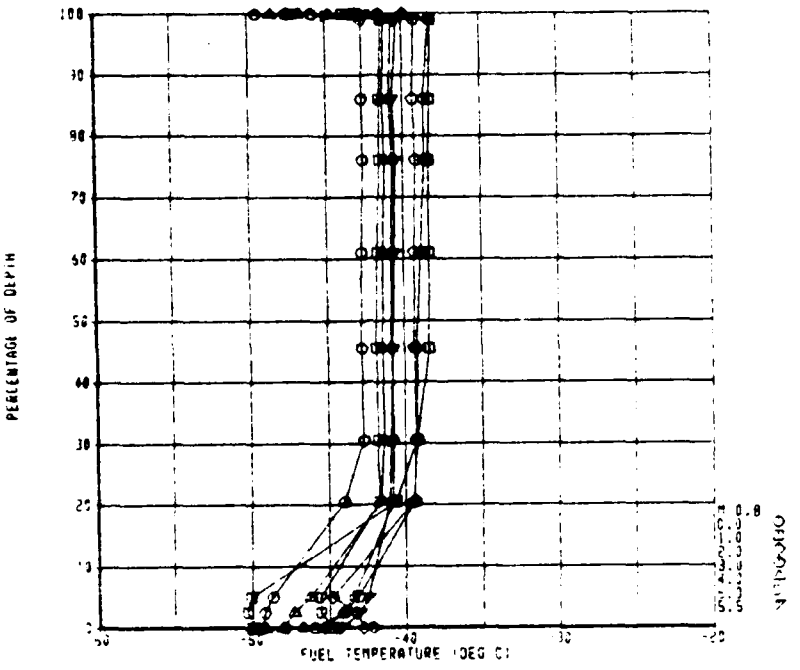

a. Test 1, Fuel 3

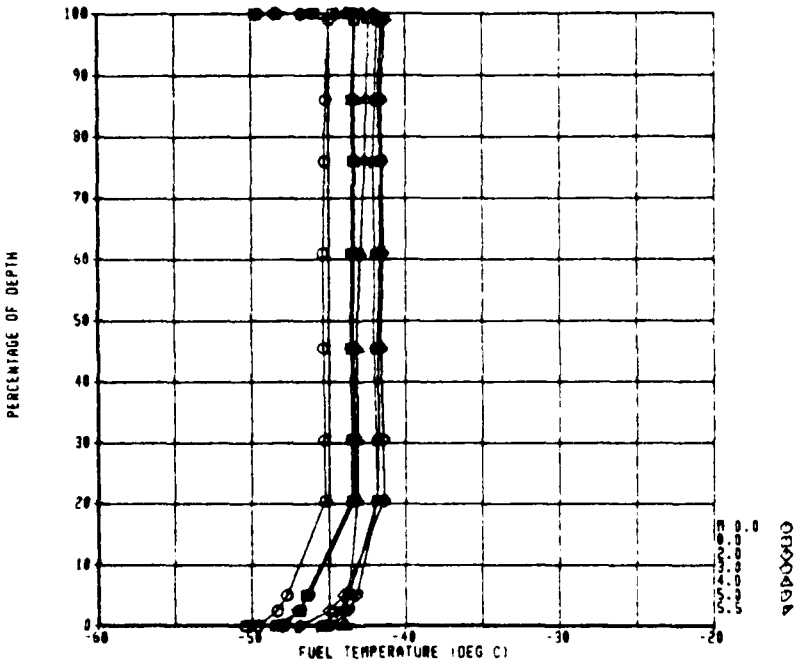

b. Test 2, Fuel 6

Figure 56. Thermal Profiles During Mission

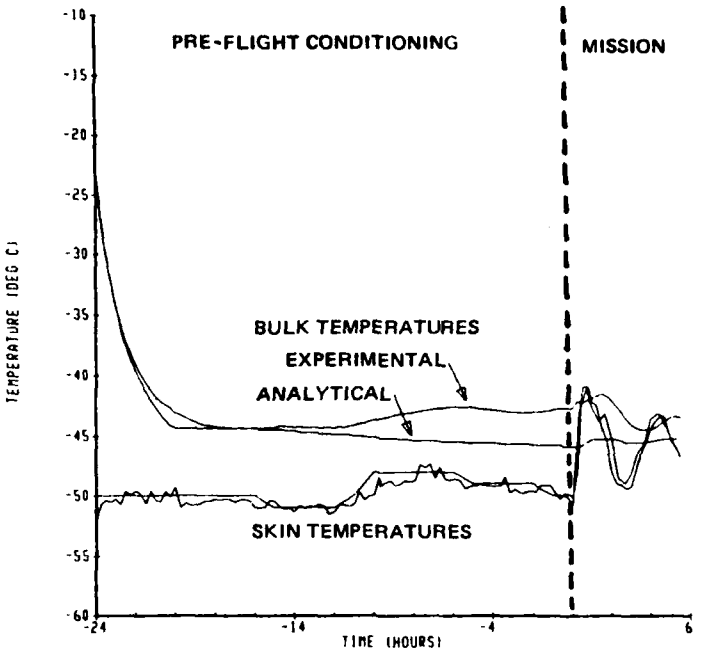

a. Test 1; -46C Freeze Point (Jet A)

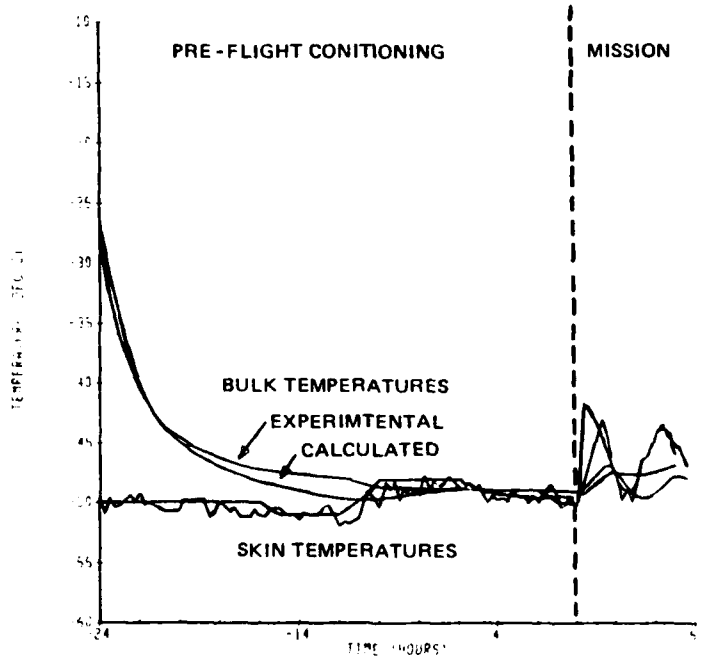

b. Test 2; -51C Freeze Point Fuel (JP5 + JP8)

Figure 57. Comparison of Experimental and Analytical Results

Table 8. Holdup Measurement Results

Test No.	Purpose	Time of Holdup Meas'ment	Required Fuel Withdrawal Time	T_{skin} (°C)	T_{bulk} (°C)	Hold up Measured (mass %)
	Mission Simulation					
(1)	Eielson AFB	end of 24 hrs	N/A	-50.0	-43.0	17.6 (horizontal) 16.9 (tilt drain)
	KC-135 Track 10	5.5 hrs	5.5 hrs	-45.5	-41.0	0.0
(2)	Eielson AFB	end of 24 hrs	N/A	-49.0	-45.5	0.0 (horizontal) 0.0 (tilt)
	KC-135 Track 10	5.5 hrs	5.5 hrs	45.5	-42.0	0.0
(3)	Elmendorf AFB	end of 4 hrs	N/A	-38.0	-36.0	13.9 (horizontal) 0.3 (tilt)
	F-15 Track 3	2.0 hrs	[1]	-39.0	-39.5	0.0
(4)	Elmendorf AFB	end of 4 hrs	N/A	-37.5	-35.0	8.2 (horizontal) 0.0 (tilt)
	F-15 Track 3	2.0 hrs	[1]	-35.7	-39.0	0.0
(5)	Eielson AFB (Thin Wing)	4.83 hrs	N/A	-50.0	-47.5	73.5 (horizontal) 65.9 (tilt)
(6)	Eielson AFB (Thin Wing)	5.55 hrs	N/A	-50.0	-50.0	11.2 (horizontal) 0.0 (tilt)
	Flight Test Data Comparison					
(7)	NASA FT1653	N/A	6.2 hrs	N/A	N/A	N/A
	Drainability & Pumpability					
(8)a	Gravity drain	N/A	N/A	-49.5	-44.5	10.0 (horizontal) 10.0 (tilt)
b	Boost Pump Drain	N/A	N/A	-49.5	-44.3	10.0
c	Gravity Drain	N/A	N/A	-48.0	38.0	8.5 (horizontal) 7.3 (tilt)
d	Boost Pump Drain	N/A	N/A	-48.5	-38.0	7.6

[1] In actual flight, fuel withdrawal begins at takeoff. Fuel withdrawal was not simulated during test in order to model worst case.

Table 8. Holdup Measurement Results (Continued)

Test No.	Purpose	Time of Holdup Meas'ment	Required Fuel Withdrawal Time	T_{skin} (°C)	T_{bulk} (°C)	Hold up Measured (mass %)
	Effect of Composition					
9a	Paraffinic/ Gravity Drain	N/A	N/A	-59.0	-51.0	25.9 (horizontal) 15.0 (tilt)
b	Paraffinic/ Boost Pump Drain	N/A	N/A	-58.0	-51.0	13.9
c	Naphthenic/ Gravity Drain	N/A	N/A	-58.0	-49.0	16.3 (horizontal) 9.7 (tilt)
d	Naphthenic/ Boost Pump Drain	N/A	N/A	-58.0	-48.0	10.5

N/A - Not Applicable

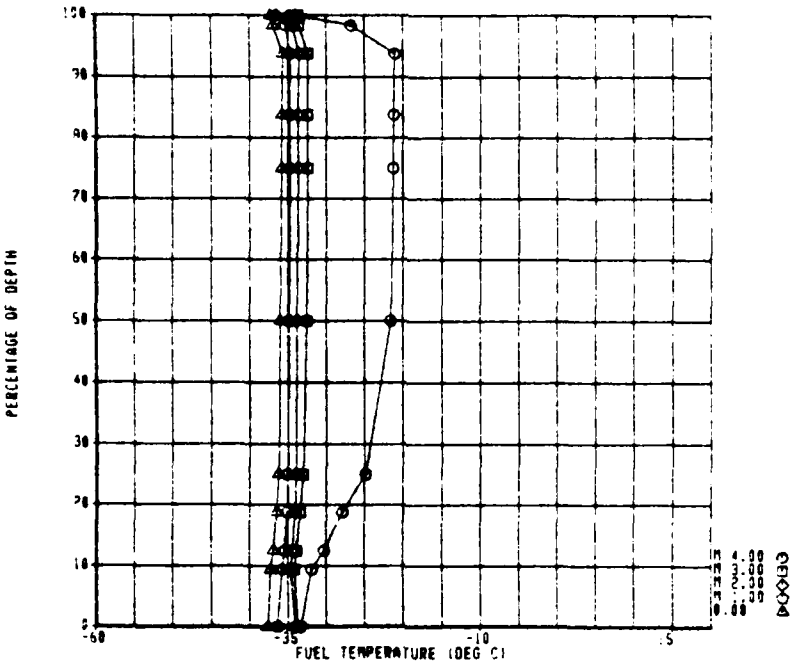

a. Test 3, Fuel 1

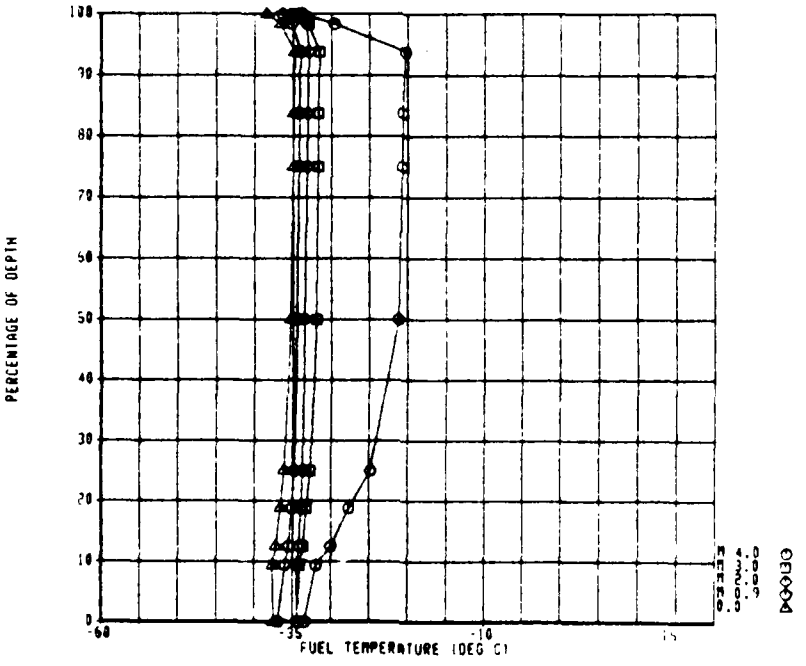

b. Test 4, Fuel 2

Figure 58. Thermal Profiles During Preflight Temperature Conditioning

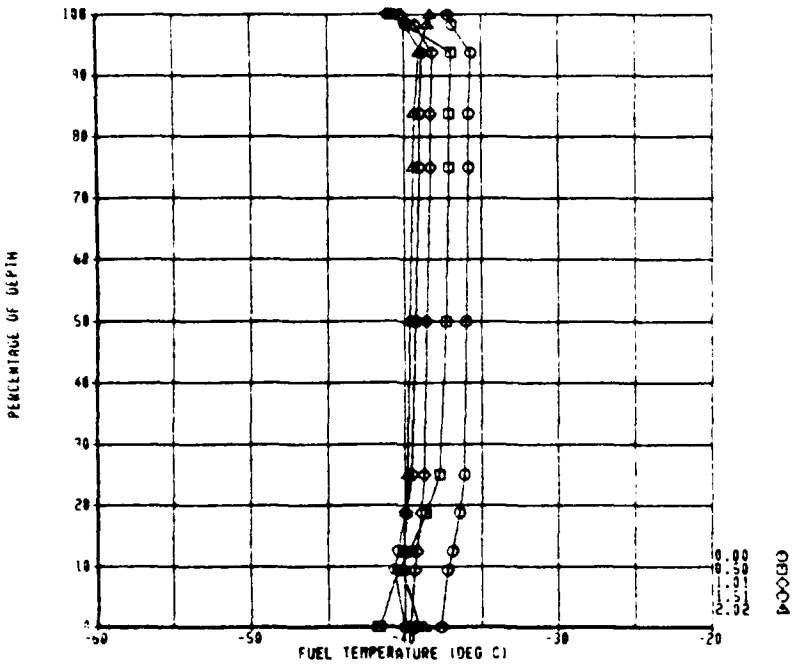

a. Test 3, Fuel 1

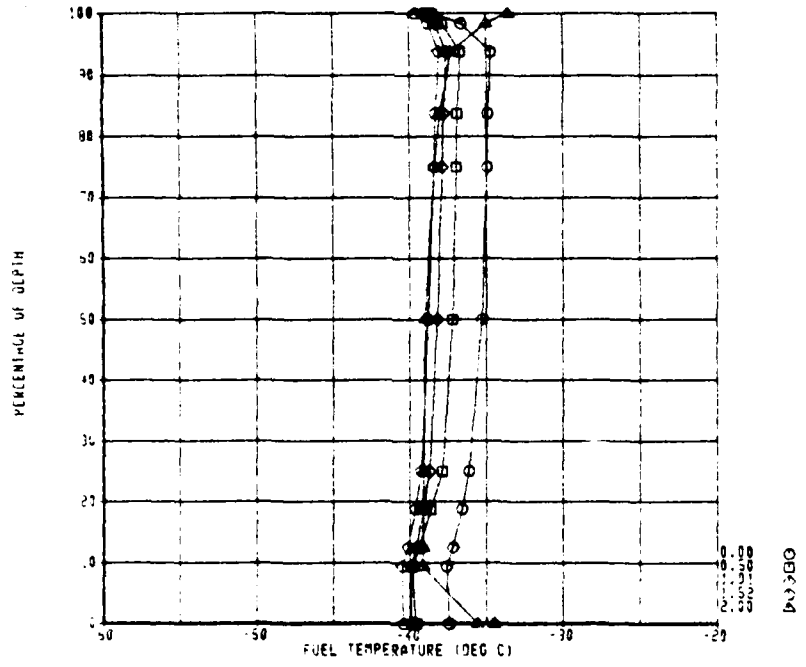

b. Test 4, Fuel 2

Figure 59. Thermal Profiles During Mission

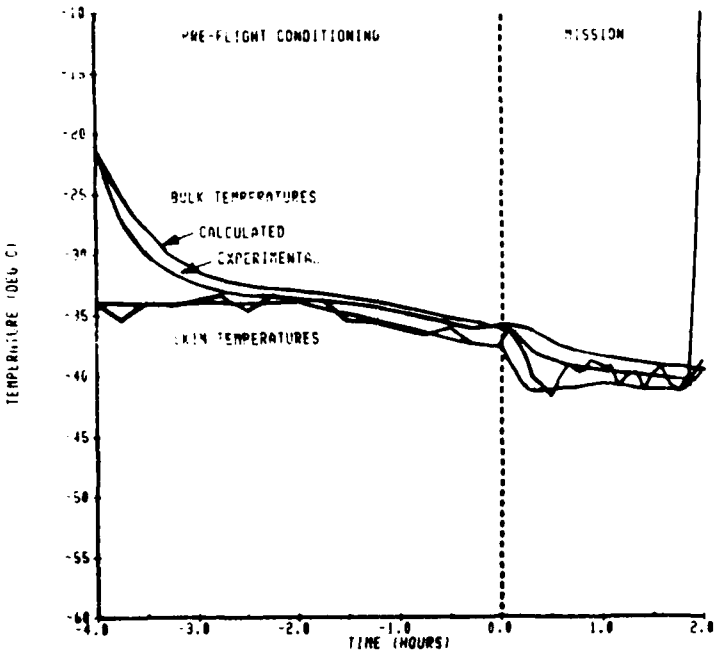

a. Test 3; -40 C Freeze Point (Jet A + JP5)

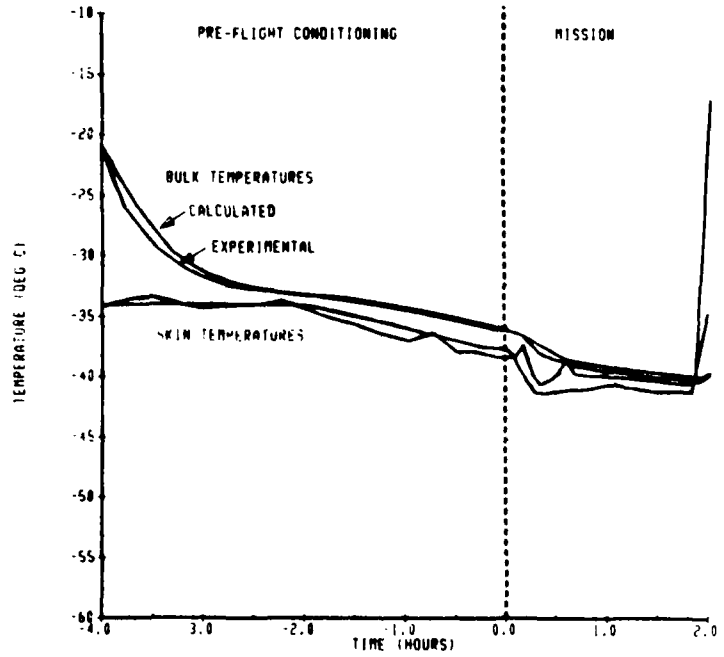

b. Test 4; -42C Freeze Point (Jet A)

Figure 60. Comparison of Experimental and Analytical Results

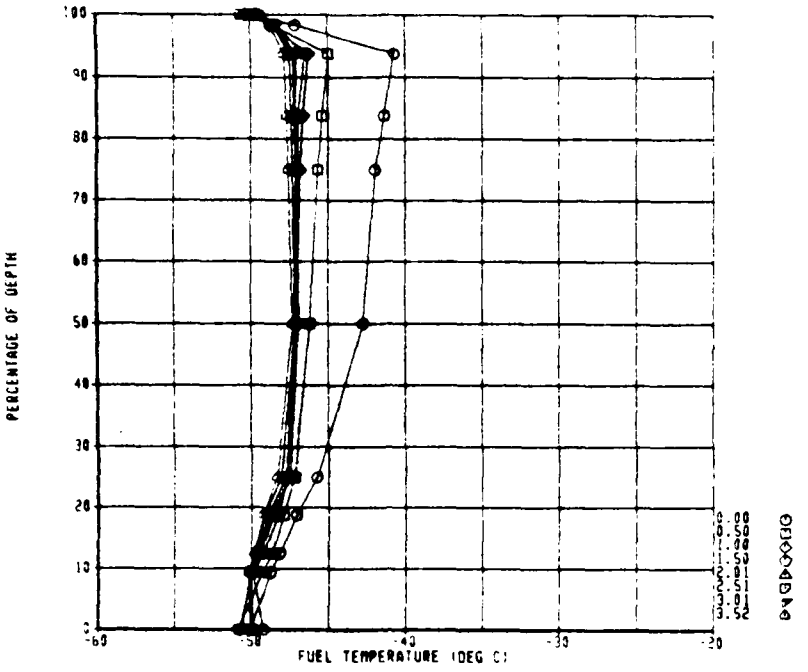

a. Test 5, Fuel 3

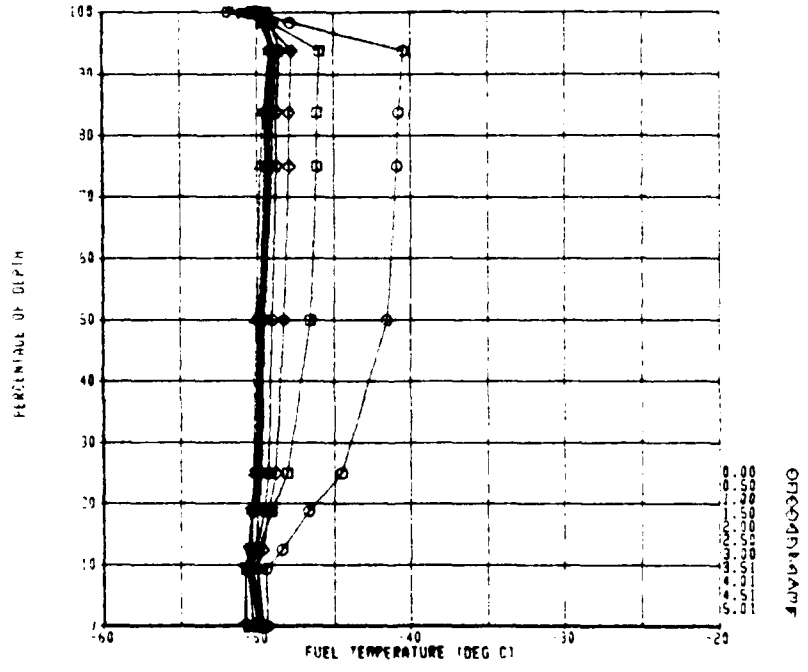

b. Test 6, Fuel 6

Figure 61. Thermal Profiles During Simulation of Eielson AFB Ground Temperature Exposure

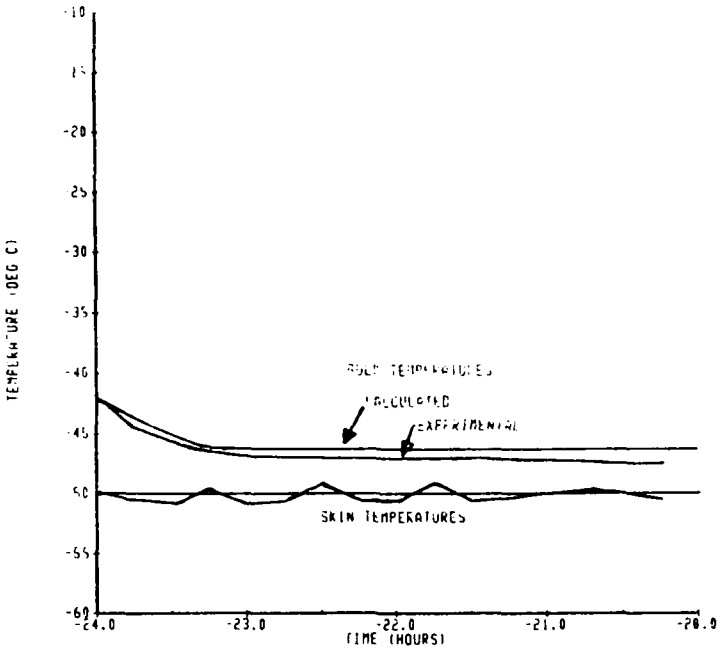

a. Test 5; -46C Freeze Point (Jet A)

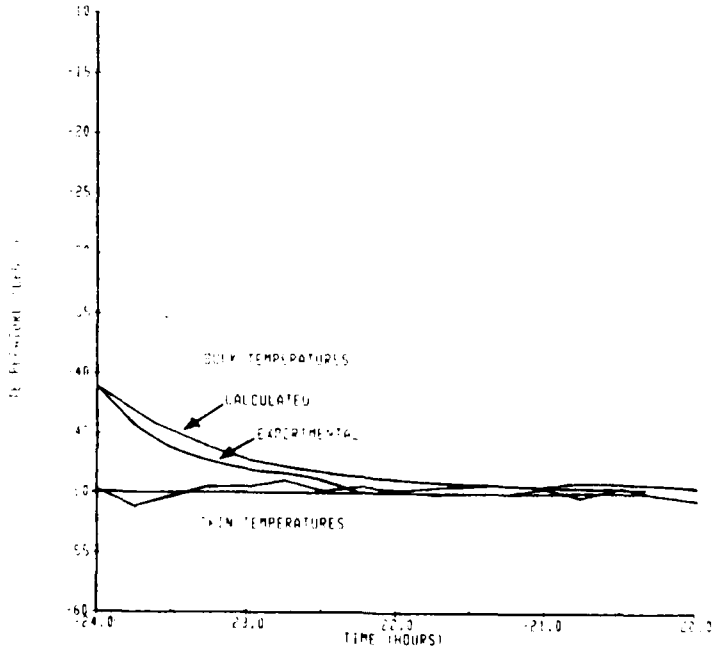

b. Test 6; -51C Freeze Point (JP5 + JP8)

Figure 62. Comparison of Experimental and Analytical Results

simulation of the glycerine cooling problem. Therefore, for a realistic numerical simulation, the initial measured temperature field and measured wall temperature distribution were used as the initial and boundary conditions, respectively. The results of the analytical simulation, Table 9, show that the predicted temperatures agree with experiment within less than $1^{o}C$ at the top half of the tank. However, in the lower region along the vertical centerline the discrepancy between predicted values and those measured range from 4 to $8^{o}C$, with the predicted temperatures being higher. Temperature contour plots approximately 22 minutes after the start of cooling are presented in Figure 63, with the thermocouple locations denoted by asterisks. The measured temperature profiles at the tank bottom have higher slopes (lower dT/dy) than those calculated, indicating a higher effective thermal conductivity than used for the simulation. The analysis predicts very small velocities in the bottom region which produces temperature profiles dominated by conduction. However, as discussed above, velocity test data were not of sufficient quality to be useful in evaluating the analysis.

The temperature fields predicted for the glycerine cooling tests are qualitatively similar to those predicted for the fuel cooling simulation (Section II 6.b.) although the Rayleigh numbers for fuel and glycerine differed by three orders of magnitude. Additional data is required with glycerine-water mixtures to produce Rayleigh numbers which more closely simulate those of low temperature fuel.

b. Flight Test Data Comparison

As a further verification of the one-dimensional thermal analytic model and of the fuel tank simulator, actual flight test temperature data were obtained for comparison. Two sets of data were provided by R. Friedman of NASA Lewis for this purpose. The data are of a preliminary, unchecked nature and are records of NASA tests conducted in a Lockheed L-1011 airplane. The NASA flight test data sets used carried NASA identification numbers 1653 (Reference 33) and 1755 (Reference 34).

The measured ambient temperature, recovery temperature, and the upper and lower (internal) skin temperatures from the inflight records are shown in Figure 64. A temperature difference between the upper and lower skins was

Table 9. Comparison of Predicted and Measured Temperatures, Cylindrical Tank, 96% Glycerine

	Thermocouple Number	0.0	6.0	10.0	13.0	14.0	17.0	19.0	24.0
	1 (top)	60.6	59.4	58.9	58.3	58.2	57.2	57.2	56.1
	2	60.6	60.1	59.7	59.2	59.1	58.5	58.1	57.0
	3	60.6	60.1	59.6	59.2	59.0	58.4	58.1	56.9
	4	60.6	60.0	59.5	59.0	58.8	58.3	57.8	56.7
Calculated	5	60.6	59.8	59.2	58.6	58.4	57.7	57.2	55.9
Tempera-	6	60.6	59.5	57.8	56.9	56.6	55.6	54.5	53.3
tures	7 (center)	60.6	58.3	56.5	55.6	55.0	53.8	53.1	51.4
(^{o}C)	8	60.0	55.6	53.3	51.8	51.4	50.1	49.3	47.4
	9	58.9	52.2	49.8	48.2	47.7	46.3	45.4	43.4
	10	58.9	48.2	45.5	43.8	43.3	41.8	40.9	38.9
	11	57.2	42.2	39.4	38.1	37.6	33.4	35.3	33.4
	12	42.8	35.6	33.6	32.2	31.8	30.6	29.8	28.2
	13 (bottom)	27.8	23.8	23.0	22.3	22.1	21.3	20.8	19.7

	Thermocouple Number	0.0	5.5	9.9	13.0	14.1	16.6	19.2	23.8
	1 (top)	60.6	60.0	58.9	58.3	58.3	57.8	57.2	56.1
	2	60.6	60.0	58.9	58.3	58.3	57.8	57.2	56.1
	3	60.6	60.0	58.9	58.3	58.3	57.8	57.2	56.1
	4	60.6	59.4	58.9	58.3	58.3	57.8	56.7	56.1
	5	60.6	59.4	58.9	58.3	57.8	57.2	56.7	55.6
Measured	6	60.6	59.4	58.3	57.8	57.8	57.2	56.7	55.6
Tempera-	7 (center)	60.6	59.4	58.3	57.8	57.8	57.2	56.7	55.6
tures	8	60.0	57.8	55.6	53.3	52.8	50.6	49.4	46.7
(^{o}C)	9	60.0	55.0	51.1	48.3	47.2	45.6	43.9	41.1
	10	58.9	50.0	44.4	41.7	40.6	38.6	37.2	35.0
	11	57.2	42.2	37.2	34.4	33.9	32.2	30.6	28.3
	12	42.8	30.0	26.7	24.4	24.4	22.8	22.2	20.6
	13 (bottom)	27.8	22.8	20.6	19.4	18.9	18.3	17.2	16.1

TC NO.	CALC (°C)	MEAS (°C)
1	56.5	56.1
2	57.4	56.2
3	57.4	56.1
4	57.2	56.2
5	56.4	56.3
6	54.0	56.6
7	52.1	55.6
8	48.2	48.9
9	44.2	43.3
10	39.7	37.8
11	34.2	32.2
12	28.8	26.7
13	20.2	21.2

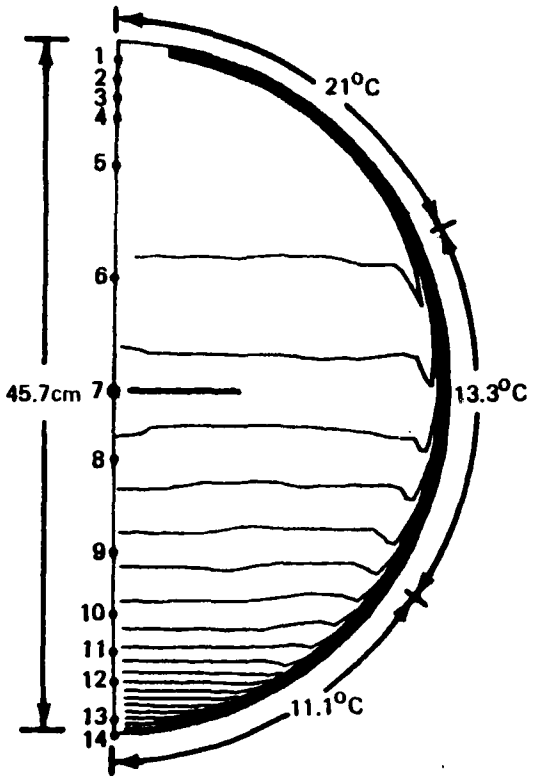

a. *Calculated Glycerine Temperature Contours 22 Minutes After Start of Cooling (Values Given in Table)*

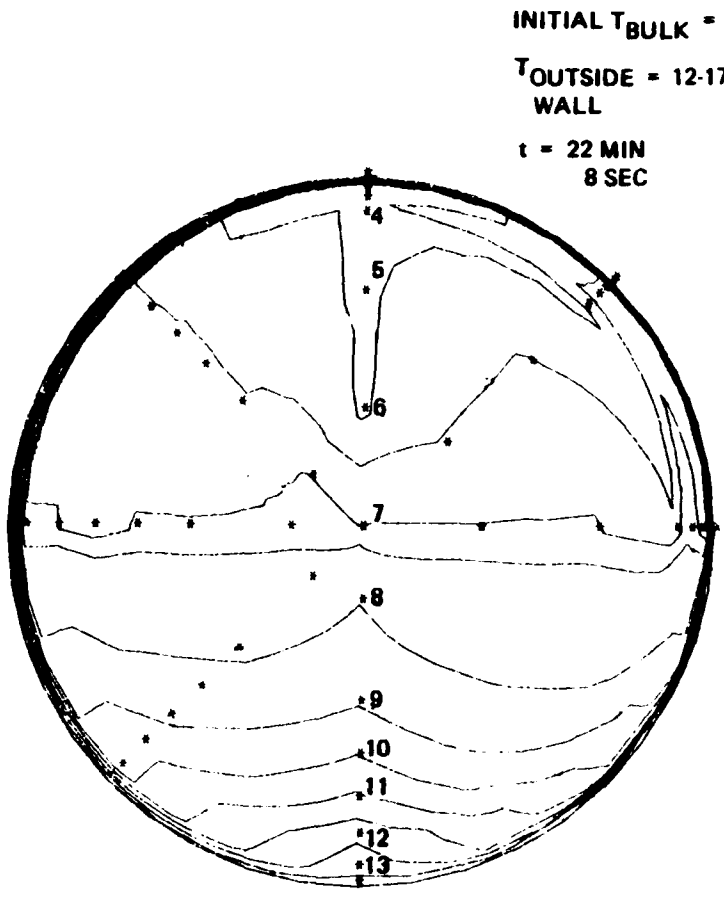

b. *Measured Temperature Distribution 22.1 Minutes After Start of Cooling*

Figure 63. Comparison of Numerical Simulation with Boeing Test Results

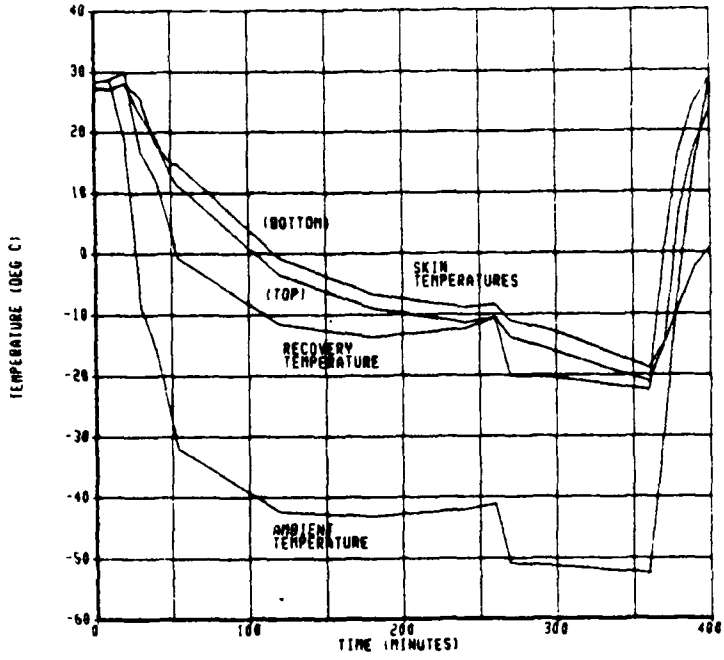

a. NASA Flight Test 1653

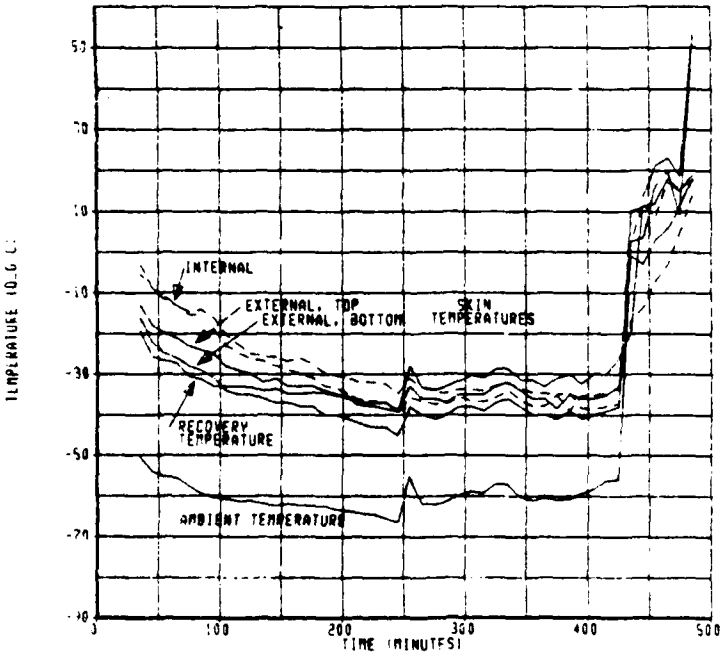

b. NASA Flight Test 1755

Figure 64. NASA Flight Test Temperature Meaurements

noted in the data, the upper skin being about $3^{o}C$ colder. This was attributed to a small ullage in the instrumented airplane fuel tank, allowing the upper skin to more closely approach the adiabatic wall temperature. Ambient and recovery temperatures, altitude, and airspeed taken from the flight test data were used as input to the computer analysis, and the resulting skin and bulk fuel temperature compared to the flight test results, shown in Figures 65 and 66 for Tests 1653 and 1755, respectively.

The L-1011 lower skin temperature was also used in the Boeing test tank to simulate the thermal exposure during NASA Flight Test 1653 in Test 7. Fuel withdrawal was also simulated, beginning 370 minutes into the flight. The tank was 40% full at the end of the flight. The resultant fuel temperatures are compared to the flight test and calculated temperatures in Figure 65, and are presented in thermal profile form in Figures 67. Time did not permit laboratory simulation of NASA Flight Test 1755; a comparison of the thermal profiles obtained during the flight test and those calculated is given in Figure 68.

The bulk temperature shown in the flight test data (Test 1653) is about 3^{o} cooler than in the test simulation. Some of the difference is due to the slightly higher starting temperature in the test tank (about $1.5^{o}C$), some may be due to the cooler upper skin temperature seen in the flight test data, and some may be due to differences in fuel transport properties (conductivity, specific heat), since the differences in composition between the flight test and simulator test fuels were not known. In general, agreement between the flight test and simulation is within 2 to $3^{o}C$; this agreement is excellent considering the error band inherent in instrumentation and differences in properties.

The analytical predictions and simulator results, in turn, were in similarly good agreement with the flight test data with the exception of the end of the portion of the flight when fuel is withdrawn. The ullage size at a given time has to be deduced from examination of the temperature profiles, assumptions of tank geometry, and from reports of fuel quantity as a function of time. Presumably, better agreement could have been reached if actual ullage size had been known.

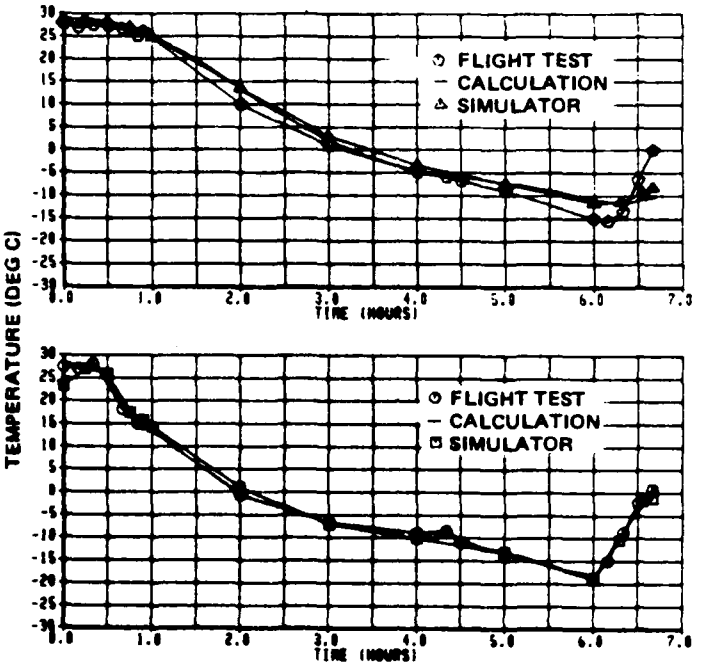

Test 7

Fuel 3

Figure 65. NASA Flight Test 1653; Comparison of Flight Test, Calculated and Simulator Temperatures

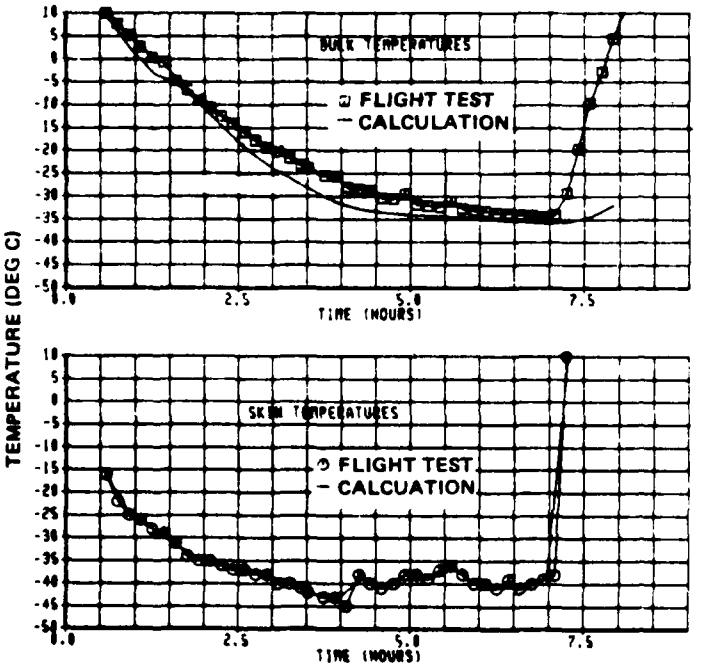

Figure 66. NASA Flight Test 1755; Comparison of Flight Test and Calculated Temperatures

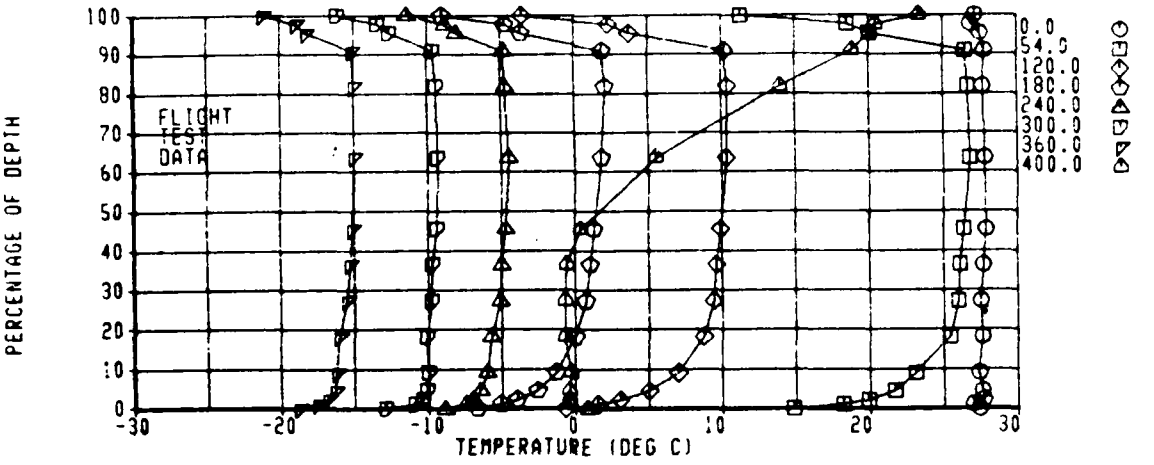

a. Flight Test Data

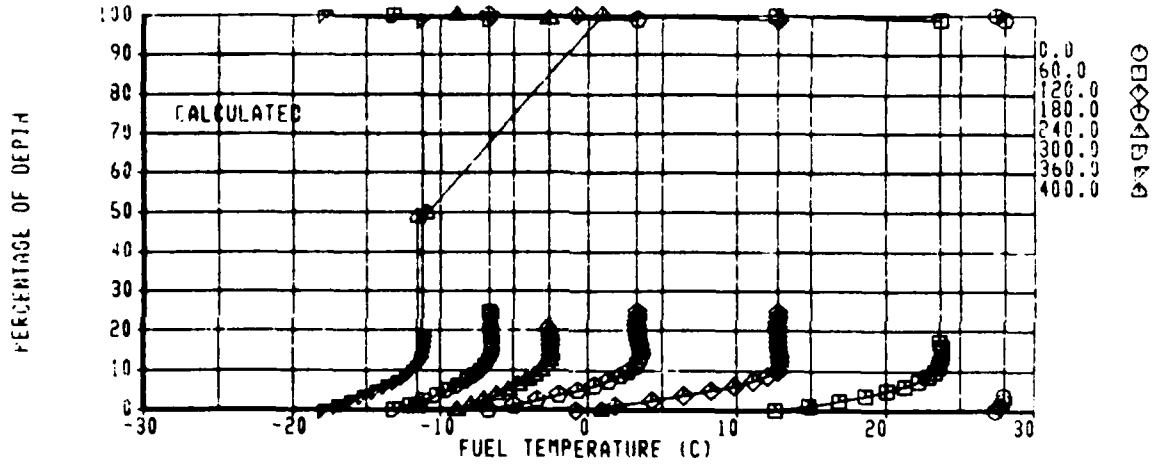

b. Calculation

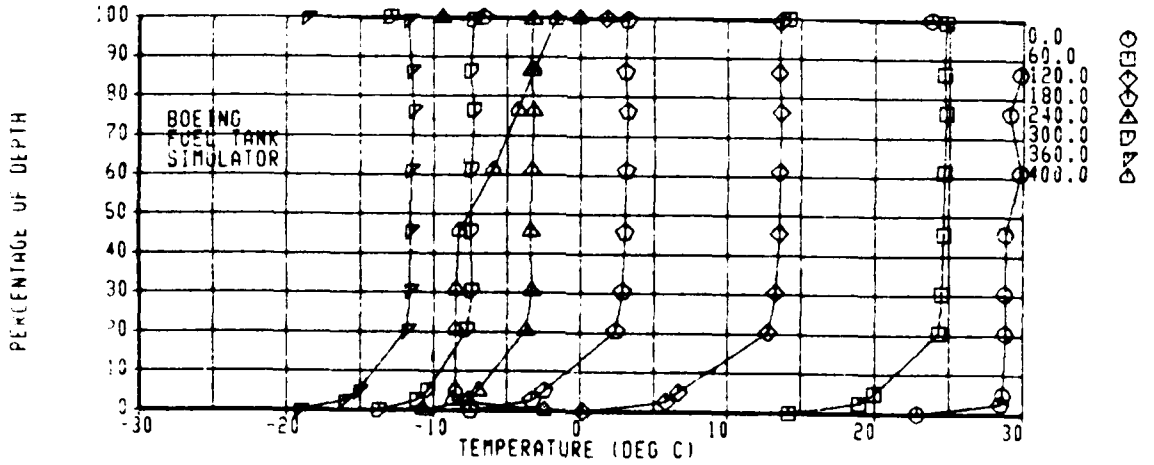

c. Test 7, Fuel 3

Figure 67. Thermal Profiles During NASA Flight Test 1653

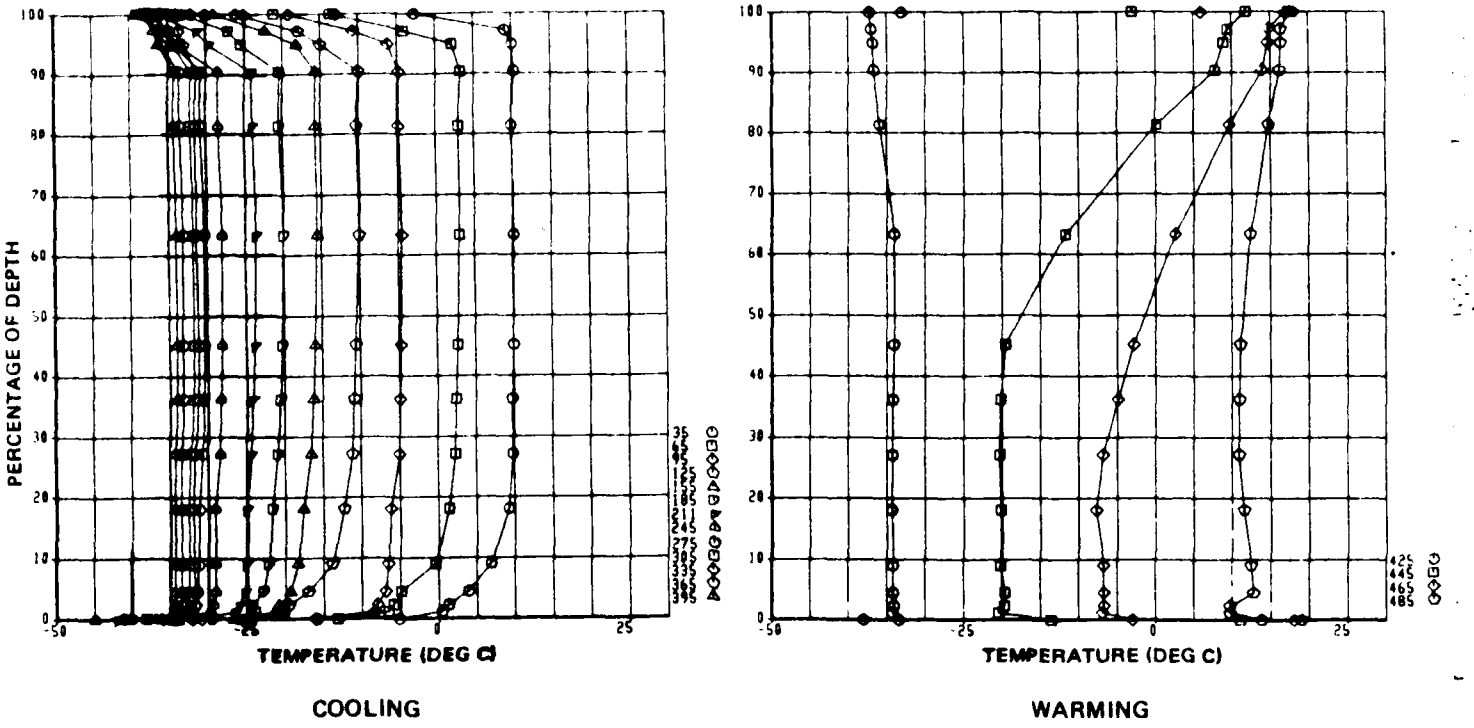

a. Flight Test Data

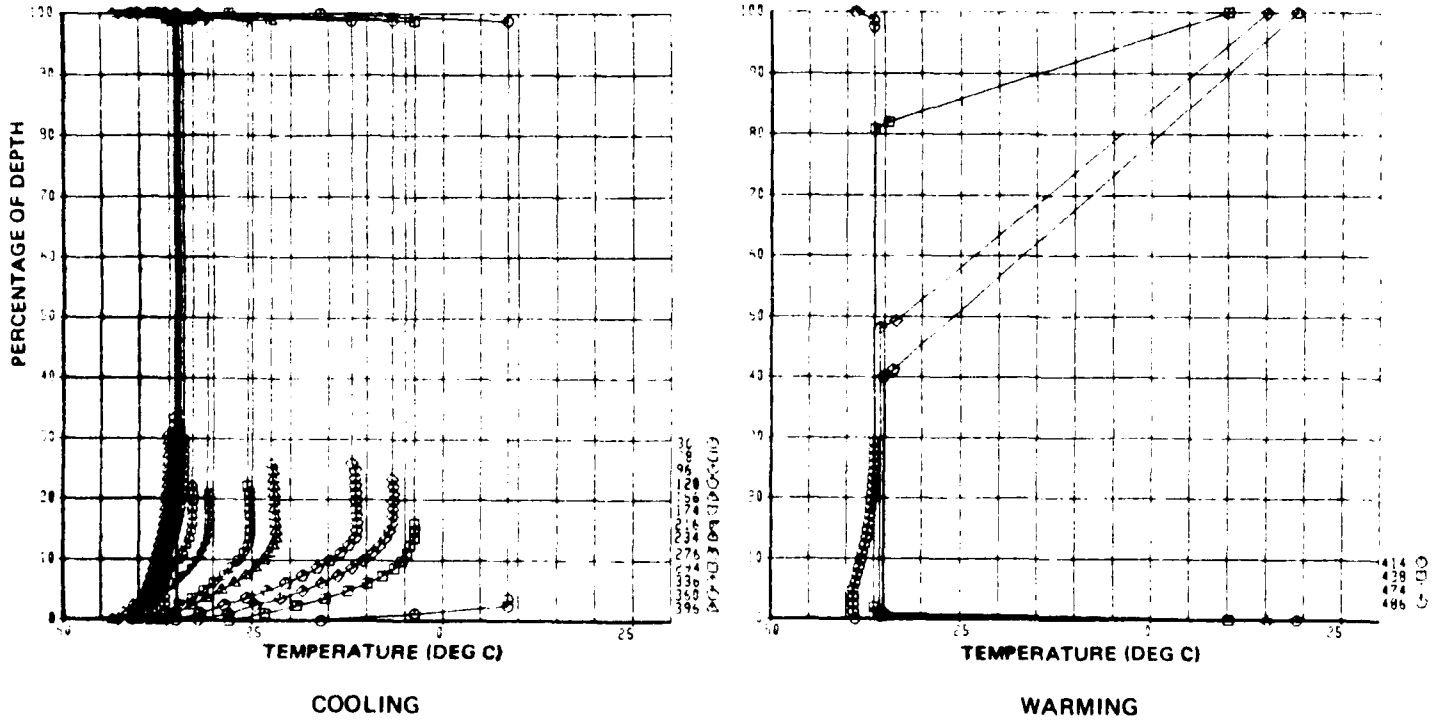

b. Calculation

Figure 68. Thermal Profiles During NASA Flight Test 1755

c. Drainability and Pumpability Tests

Drainability and pumpability of frozen, or partially frozen fuel was also explored. In the past, following a typical experimental simulation, normal test procedure had been to perform a level gravity drain of the test tank at a fixed skin temperature (the last temperature prior to drain) to determine the quantity of non-flowable fuel. Gravity draining was terminated when the fuel drain rate became less than 1/4 lb per minute. Next, the fuel tank simulator was tilted to allow liquid trapped by fuel tank structure to escape, generally removing a considerable amount of liquid fuel. After all of the liquid fuel had been gravity drained from the tank, the boost pump was operated to try to extract additional fuel thereby testing the pumpability of the sometimes slurry-like residual fuel. Only 2 - 3% of the undrained fuel was pumpable probably because flow blockage by the frozen fuel restricted flow in the suction line leading to pump cavitation. Although no attempt was made to pump the slushy frozen fuel while substantial amounts of liquid fuel remained in the tank, slurry (liquid/solid) formations were observed to flow during gravity drain indicating some solid entrainment. Based on this observation, it was speculated that bulk liquid flow induced by a boost pump could enhance the pumpability of the slush and thereby reduce the amount of hold-up.

The latter speculation was investigated in Tests 8, 9, and 10 by comparing gravity drain and boost pump drain hold-up. In the comparison tests, the fuel was given identical thermal conditioning (or as nearly as experimental procedures allowed, Figures 69 and 70) until a solid/liquid mixture existed; the drain tests were then performed. To ensure that external heat flow through the drain lines was minimized, both the gravity and boost pump drain lines were insulated. The insulation was inadvertently left off of the drain lines during tests 8a and 8b. The lines were insulated in tests 8c and 8d. Although the difference in the heat loss is not obvious from the holdup measurements, there does appear to have been some effect on the shape of the thermal profile to cause the development of a larger, better defined conduction zone.

The holdup visible on the upper and lower tank surfaces following each fuel drain was generally about the same in appearance; a 1 to 2 inch thick layer of frozen fuel covered the surfaces with mounds where stringers or other

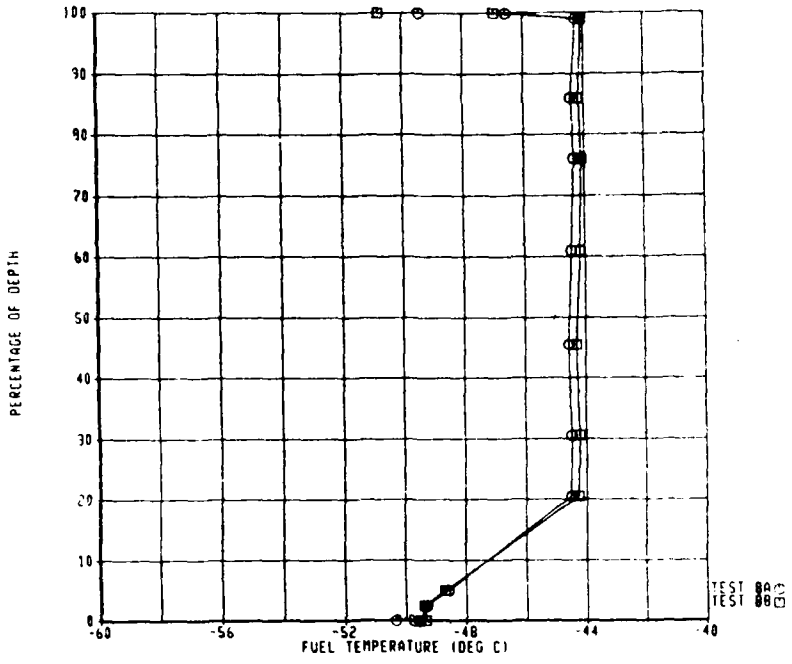

a. Tests 8a and 8b, Fuel 3

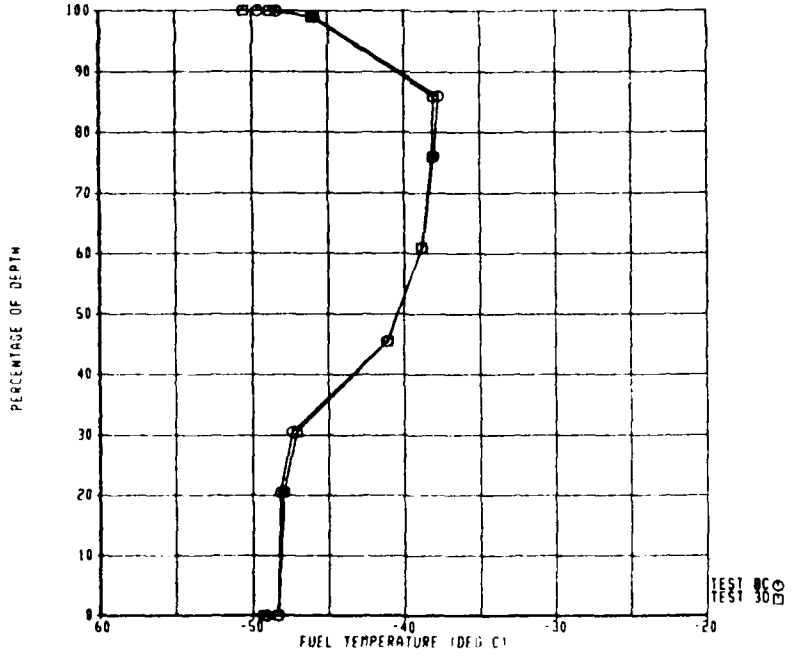

b. Tests 8c and 8d, Fuel 3

Figure 69. Temperature Profiles At Time of Drain

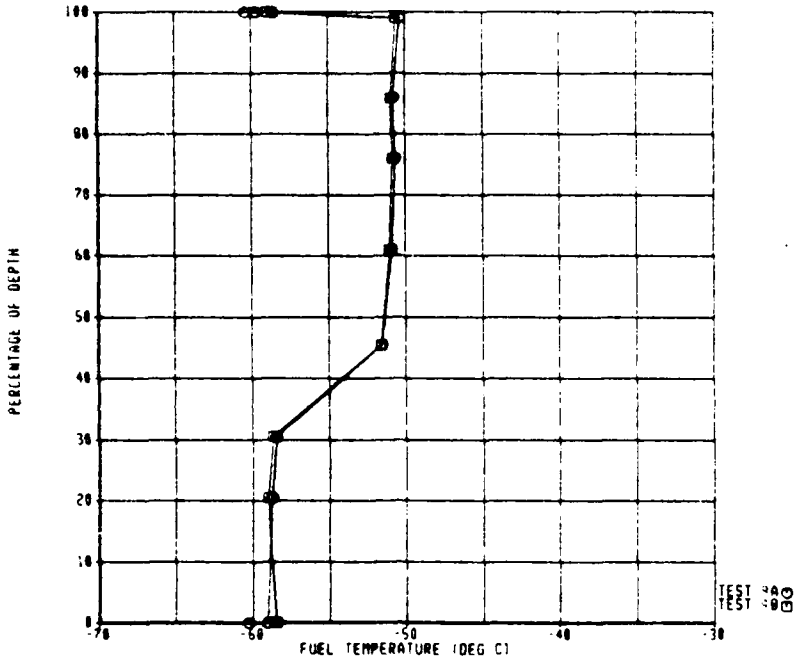

a. Tests 9a and 9b, Fuel 4

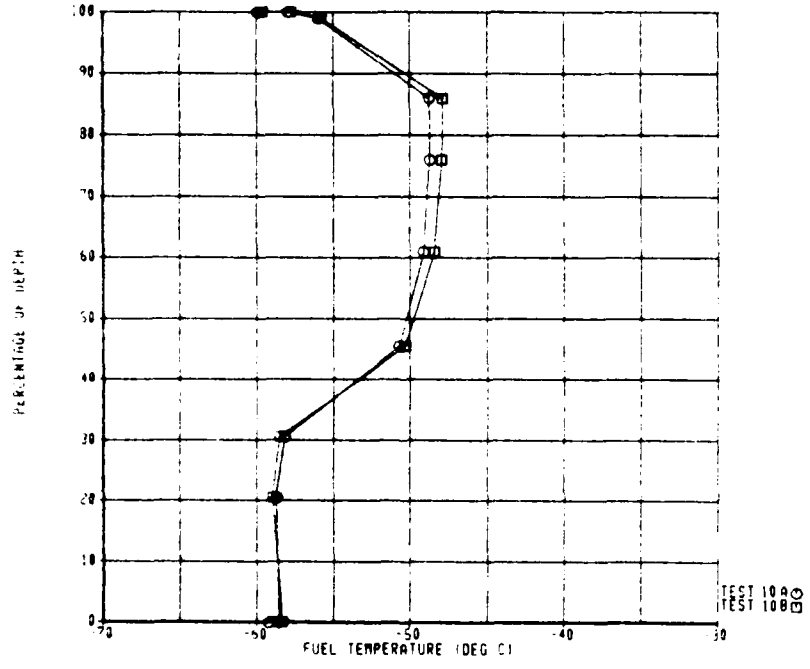

b. Tests 10a and 10b, Fuel 5

Figure 70. Thermal Profiles At Time of Drain

structure was present. The results of these tests indicate no significant advantage to using the boost pump to determine holdup quantities as opposed to the earlier procedure of gravity draining the tank. However, although "tilt" draining is possible inflight, from a practical standpoint the comparison might better be made between the horizontal gravity drain and the boost pump drain results. In this view, there is a clear advantage to pumping the fuel over gravity draining. It may be important to note that while slushy frozen fuel is normally observed in a transparent section of the drain line (downstream of the insulated section) during gravity draining, none was seen in any of the four boost pump drain tests. This indicates that the boost pump energy re-liquified the fuel during the brief drain time.

d. Fuel Composition Effects

It has been supposed that two fuels with identical freeze points but different compositions might produce differing amounts of holdup at temperatures below the freeze point. Fuel numbers 5 and 6 both had a measured freeze point of $-50^{o}C$ (Table 7), and essentially identical holdup characteristics in Shell-Thornton tests (Figures 46e and 46f).

Tests 9 and 10 in the fuel tank simulator suggest differences in the transport properties of the two fuels, which caused the paraffinic fuel to cool more rapidly (Figure 71) and to produce a larger quantity of holdup than the naphthenic fuel (Table 8). Throughout the first 3-4 hours of cooling the naphthenic fuel was consistently about $5\text{-}8^{o}C$ warmer than the paraffinic fuel, even accounting for the slight difference in skin temperature histories between tests. The calculated bulk fuel temperature falls between the measured fuel temperatures, presumably because a mixture of paraffinic and naphthenic fuel samples was used to develop the JP-8 fuel property data.

5. DISCUSSION

Good agreement was shown between the calculated fuel temperatures and experimental data, verifying the importance of

- using accurate fuel property data in the calculation procedure, particularly at low temperatures

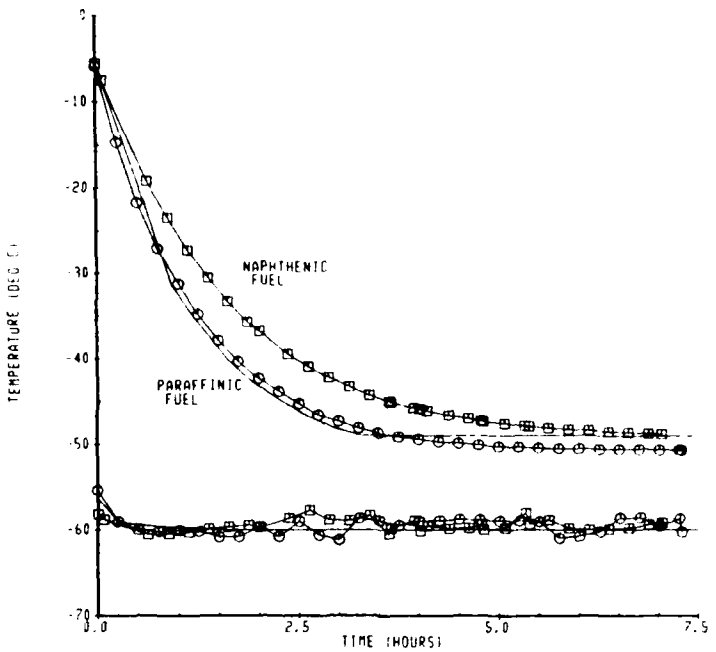

Figure 71. Comparison of Experimental and Analytical Results

- o including a freezing model when the skin temperature is at or below the fuel freezing point for accurate prediction of fuel temperatures

Without these, temperature predictions will be artificially low, resulting in high estimates of fuel holdup.

It can be concluded from Tests 1 and 2 that the allowable freeze point for thick wing tanks zero percent holdup criterion is between $-46^{o}C$ and $-51^{o}C$ based on the holdup remaining in the tank at the end of the 24-hour conditioning period. Analysis performed to determine the exact freeze point shows that $-50^{o}C$ is the limiting value. None of the thin wing missions studied involved such severe thermal exposure as the KC-135 at Eielson AFB, therefore, $-50^{o}C$ is also acceptable for the smaller airplanes. If thin wing aircraft were to experience this thermal exposure, however, the results of Test 6 indicate that a significant amount of holdup would develop even with the $-51^{o}C$ freeze point fuel.

Of great significance are the results of the flight test data comparison. Not only was it possible to use the actual ambient conditions recorded inflight as input to the computer program and accurately predict both fuel tank skin and fuel temperatures, but also to obtain similarly good agreement between the flight test data temperatures and those recorded in the Boeing fuel tank simulator. This is the first opportunity to check the validity of the assumptions made in the development of the one-dimensional computer program, and the results were gratifying.

The implication of the drainability/pumpability tests is that significantly more fuel can be extracted from a tank containing frozen fuel by pumping than by gravity draining, and in fact, some of the frozen material can be melted by the action of pumping. The data also suggests that fuel composition may influence freezing characteristics to a degree; of the two fuels (having identical freeze points) tested, the paraffinic fuel cooled more rapidly than the naphthenic fuel. It is unknown, however, whether such a difference would be observable in an airplane, where tank size, structure, and flow passages would interact with the fuel and with the heat transfer processes.

The only remaining limitation of the 1-D model is the fact that it does not accurately predict the shape of the conduction layer of the fuel. The transition between the regions controlled by conduction and convection is generally sharper than observed in tests, and the calculated conduction layer does not extend as far into the fuel. The reason is that mass transfer due to buoyancy of the transition region has not been accounted for in the analysis for the purpose of simplicity. In other words, the cool fuel returning from the top of the tank by means of the convection cells can interact with the fuel at the transition between the conductive and convective layers and become stably stratified with fuel of equal or lower temperature in the conduction layer, causing the conduction layer to grow more quickly than by pure conduction; this effect has been neglected. To accomplish more exact prediction of the shape, a more complex model, such as the one used to study heat transfer in cylindrical tanks would be needed. In spite of this limitation, the 1-D model has proved to be a very effective tool for predicting heat transfer from fuel, with accuracy proven by the test data comparisons, including instances when the boundary conditions (skin temperatures) dictate that fuel freezing will occur.

Significant progress was made in the study of the 2-D, cylindrical tank problem. Temperatures and heat transfer characteristics of the cylindrical system were sufficiently well matched with the analytical predictions to show that the initial assumptions of two-dimensional fluid behavior were valid. Future work should show improvement, especially as better data becomes available from the cylindrical tank simulator for comparison, and as fuel freezing and ullage models are added to the computer program. In terms of the results of this study, portions of the fuel were observed by analysis to cool even more rapidly than fuel in an internal wing tank (almost $65^{o}C$ in one hour). Considering the A-10 and KC-135, both of which have external tanks and are based at Eielson AFB, the $-50^{o}C$ thermal exposure which determines the fuel freeze point requirement for internal fuel tanks imposes an equal limitation for external, cylindrical tanks.

SECTION IV
FACTORS AFFECTING MAXIMUM ALLOWABLE FUEL FREEZE POINT

Prior to drawing conclusions on an acceptable freeze point, the probability of interference with flight operation as a function of fuel freeze point was estimated for each airplane. In addition, consideration was given to the impact of unusual flight operations on the specification of a freeze point, and to changes in current operating procedures which could allow the use of aviation turbine fuels with higher freeze points. Potential airplane problems which can result from fuel freezing are discussed below.

While the observations made are intended to be general in nature, each airplane fuel system is unique. What may be acceptable in one fuel system may not be in another. It therefore behooves a fuel system designer to assure adequate performance of his fuel system in the presence of some frozen fuel.

1. POTENTIAL AIRPLANE PROBLEMS

Problems associated with the use of higher freeze point fuels are loss of available fuel due to hold-up (fraction of nonpumpable fuel in the tank) and malfunction of fuel system hardware, such as boost pumps, fuel filters, and ejector-scavenge pumps during operation at temperatures where frozen fuel can accumulate on the tank surfaces.

Internal surfaces of airplane integral fuel tanks are not smooth because of wing structural members (laterally aligned stringers and vertically aligned ribs). The stringers are bridged by the ribs which divide each tank into bays. Holes cut in the bottom wing tank stringers provide fuel transfer in the fore and aft directions, thus minimizing quantities of fuel which may become trapped between these members. These holes are usually elliptical in shape and for structural reasons are located with their centroid at the mid point of the stringer (2 to 4 cm from the bottom of the tank). Fore and aft transfer may also be provided by rectangular slots approximately 1/4 cm high at the base of the stringers.

The transmission of semi-solid (slushy) fuel through an airplane fuel system is only possible if it can be assured that various fuel system components,

such as boost pumps, fuel filters, ejector pumps, etc. will function according to fuel system design specifications.

a. Boost Pump Performance

Boost pumps are located in the fuel tanks to minimize the airplane unusable fuel; therefore, they are usually near the low points of the tanks. The boost pump is required to provide adequate inlet pressure to the engine feed pump throughout the flight envelope. Boost pumps often have a suction inlet screen (4 to 20 mesh) to prevent ingestion of relatively large debris such as nuts and bolts. Typical boost pump inlet plumbing is shown in Figure 72. Flapper check valves (Figure 73), installed in the ribs adjacent to the boost pump bays, restrict fuel flow outboard during airplane maneuvers. Fuel commonly flows due to gravity through openings in the ribs and stringers to the bay containing the boost pump inlet. One of the major concerns in using higher freeze point fuels is the restriction of these flow paths during low temperature flights. For example, frozen fuel accumulation around a flapper check valve (Figure 73) may prevent it from opening.

As demonstrated in cold fuel simulator tests performed in this study and Reference 30, the existence of frozen fuel in a tank does not mean that pumps cannot supply fuel to the engines. This finding is supported by earlier tests (References 35 and 36) under isothermal conditions, which demonstrated that fuels are pumpable at temperatures substantially below their freeze point and in some cases below their pour point. While the fuel temperature profile in the latter tests did not properly represent expected airplane tank temperatures (where variations between the bulk fuel temperature and the tank skin can be as high as $20^{o}C$ or more) they and the other tests show the fallacy of using the freeze point as the flowability criterion.

The most serious threat posed by low temperature fuel on satisfactory pump performances is frozen fuel accumulation sufficient to block the boost pump inlet; since the boost pumps are normally turned on prior to engine start and operate continuously during the flight, this type of blockage is unlikely as long as liquid fuel exists in the tanks. In the event the boost pumps were not operated until later in the mission, it would be possible to block the inlets with frozen fuel; if the boost pumps were then switched on, the

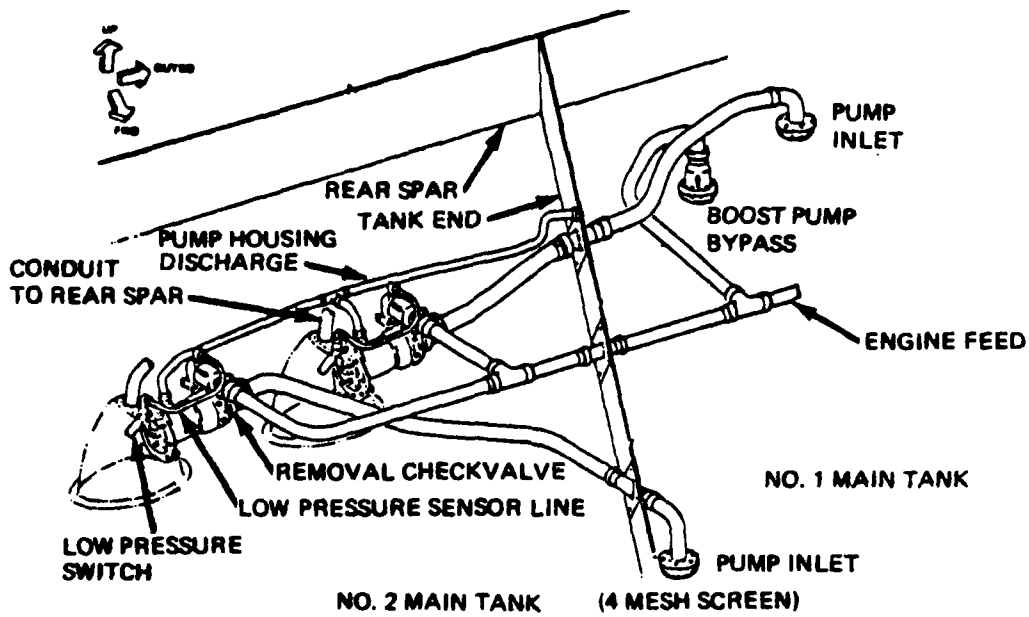

Figure 72. Schematic of Boost Pump Plumbing (B-747 Airplane)

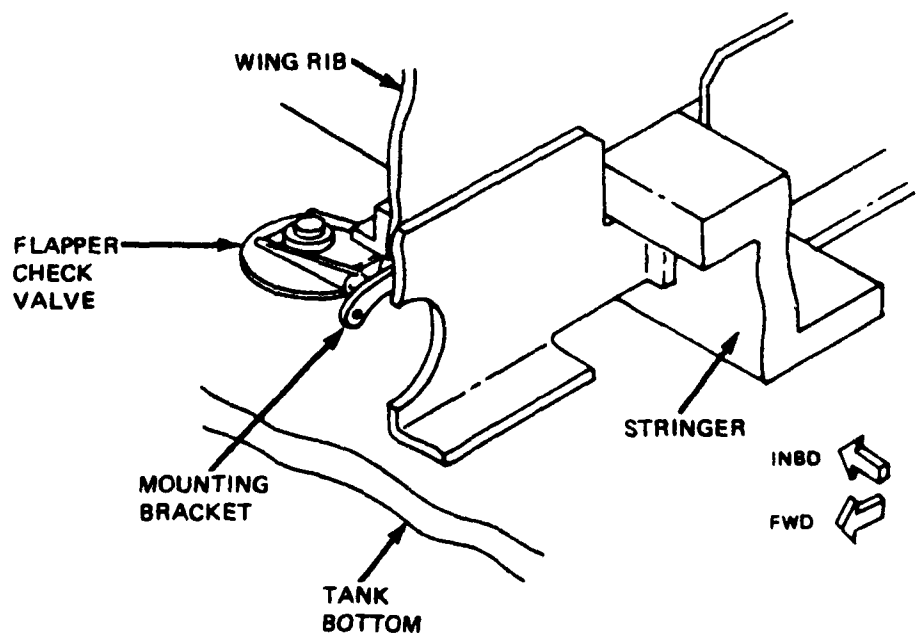

Figure 73. Flapper Check Valve Installation

limiting shear stress of the matrix may not be overcome by pump suction (Reference 33). In the event that boost pumps become inoperative during flight (as in an electric power failure), the engine fuel pump will attempt to suction feed through the boost pump bypass (Figure 72). However, it is likely that the same blockage possibility would also prevail in the suction feed line since it is of similar design and located at approximately the same level as the boost pump inlet.

b. Engine Feed Filter Plugging

In pumping slushy fuel, the mean particle size of the solid fraction would be reduced by large shear forces in the pump and the temperature of the fuel might increase by 1/4 to 1/2^{o}C due to friction losses. Since this temperature increase would be insufficient to eliminate the solid fraction, there is a possibility that the low pressure (engine feed) filter could be blocked with frozen fuel. However, these filters (10 to 40μ) are pre-heated, usually by an engine oil heat exchanger, to prevent water ice blockage. The heaters are typically sized to provide a fuel outlet temperature a few degrees higher than 0^{o}C. Obviously, filter plugging by frozen fuel would not be a problem as long as the anti-icing heaters were in operation and the fuel was totally liquid at 0^{o}C.

c. Ejector Pump Performance

Some fuel systems include ejector pumps to prevent water accumulations, to scavenge fuel or to transfer fuel from one tank to another. The motive flow for these pumps is provided by the boost pump discharge. During cold fuel pumpability tests performed recently (Reference 37), ejector pumps generally operated satisfactorily when pumping out tanks containing relatively high amounts of hold-up (e.g. 30%). The most vulnerable point for blockage in these pumps is the primary nozzle throat since this is the minimum flow area. (A typical throat diameter for airplane ejector pumps is approximately 0.18 cm.) However, since fuel blockage of jet pumps was not a problem in these tests, the shear stresses generated in the fuel by the boost pump must have been sufficient to reduce the mean particle size of the solid fraction to below that of the nozzle throat diameter.

2. HOLDUP GUIDELINES

At present there is a need for a guideline of acceptable holdup level for higher freeze point fuels. While acceptable levels will depend on the particular airplane design, fuel type, mission, and fluid motion during flight, a general all-inclusive guideline would make it easier to arrive at a suitable low temperature flowability criterion. In the airplanes studied, a uniform layer of frozen fuel approximately 0.7 cm thick on top and bottom surfaces did not obstruct the fuel transfer holes or block flapper check valves and the residual fuel could flow or be pumped as normal. This level corresponded to an average of 3% of the tank volume.

One approach to defining the allowable holdup level for a given fuel tank is to equate it to the amount of unusable fuel specified for that tank. These levels are listed in Table 10 for the critical tanks identified in Section II.2.

A more refined approach was also developed using the Boeing FTS (Fuel Tank Simulator) computer graphics program (Reference 38). FTS displays the fuel surface for a given tank geometry and a specified fuel quantity. Pump inlets and gravity drain openings, (obtained from airplane drawings and technical orders, References 5 through 14 and 40 through 45) were located within the tanks and the fuel level adjusted until it was found to just cover the inlet or opening. This was defined to be the maximum allowable holdup quantity; where more than one inlet is present in a tank, a holdup quantity was determined for each. The results of this approach are given in Table 11. Examples of the graphical models of the wing tanks and external (cylindrical) tanks are shown in Figure 74.

3. PROBABILITY OF INTERFERENCE WITH FLIGHT OPERATIONS

"Probability of interference" refers to the frequency of instances in which the presence of frozen fuel would impact airplane performance for a particular route and fuel of known freezing characteristics.

Previous studies revealed that the fifteen lowest temperature histories for a given route have similar trends and all fit within a relatively narrow band (Section II.1.c). A baseline ambient temperature history was established for

Table 10. Fuel Capacity of Study Airplane Critical Tanks

Airplane	Critical Tank	Total Fuel (lb)	Unusable Fuel (lb)	Mass %
A-10	wing	2155.0	117.9	5.47
	external	3954.2	24.2	0.61
B-52	outboard	7545.6	32.8	0.43
	external	4585.0	not given	-
C-141	1/4 main	8221.0	209.6	2.52
F-15	wing	3275.0	26.2	0.80
	external	4015.2	19.7	0.49
KC-135	1/4 reserve	2849.3	6.6	0.23

Table 11. Allowable Holdup Based On Graphics Simulation

Airplane	Critical Tank	Holdup Allowed (lb)	Mass %
A-10	wing	126.1	5.85
	external	35.6	0.90
B-52	outboard		
	pump inlet 2	192.0	2.55
	pump inlet 3	114.3	1.52
	external	46.8	1.02
C-141	1/4 main		
	primary pump	175.5	2.12
	secondary pump	295.3	3.56
F-15	wing	37.6	1.15
	external	28.9	0.72
KC-135	1/4 reserve	7.8	0.27

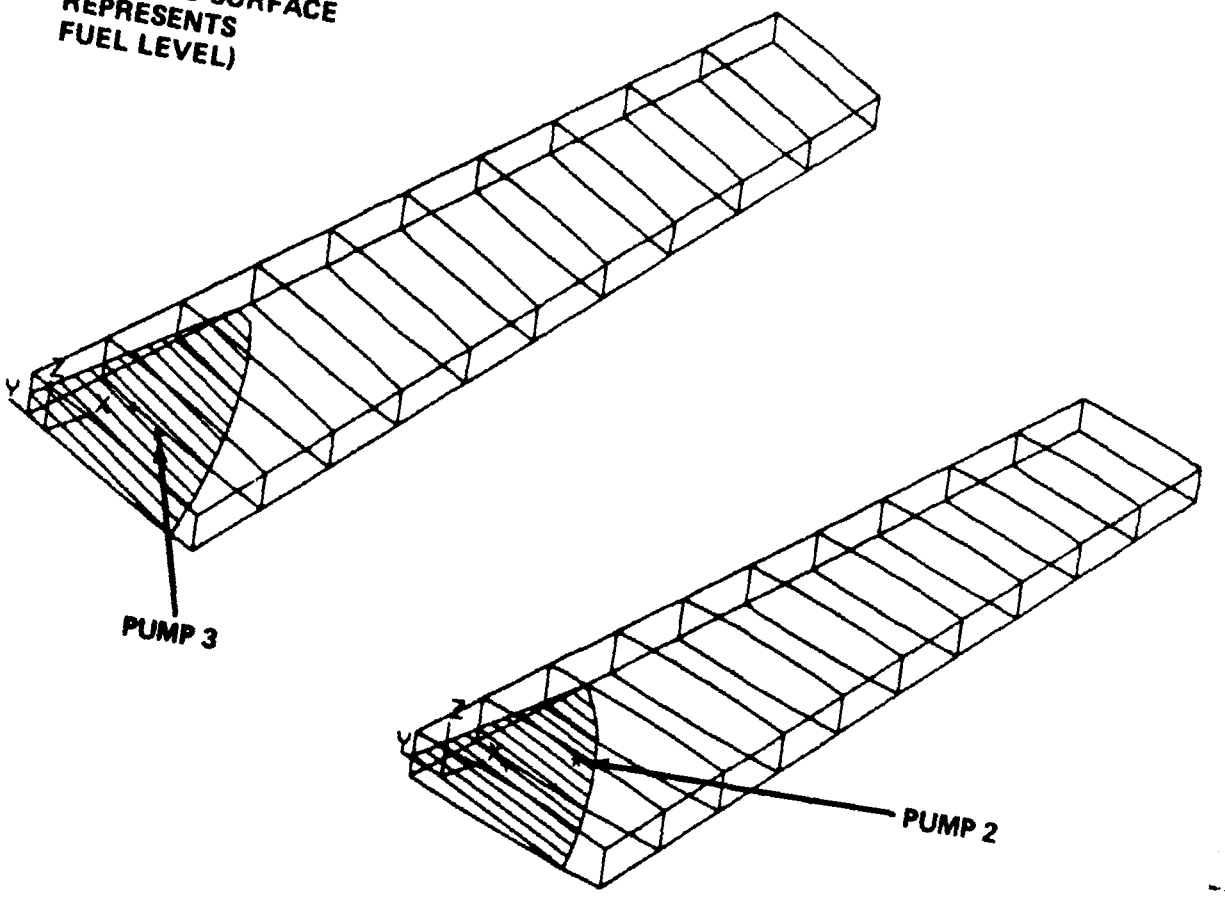

a. B-52 Outboard Wind Tank

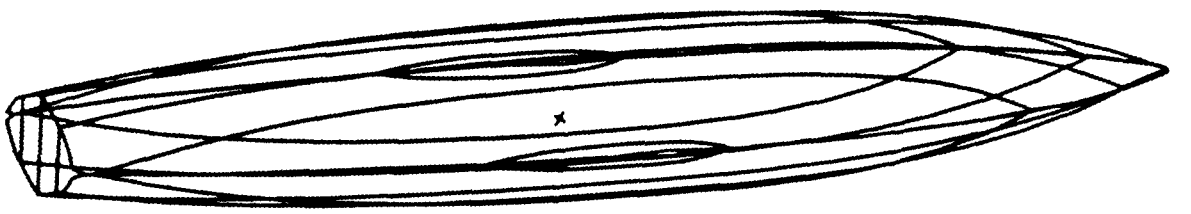

b. B-52 External Tank

Figure 74. Computer Graphics Model Examples

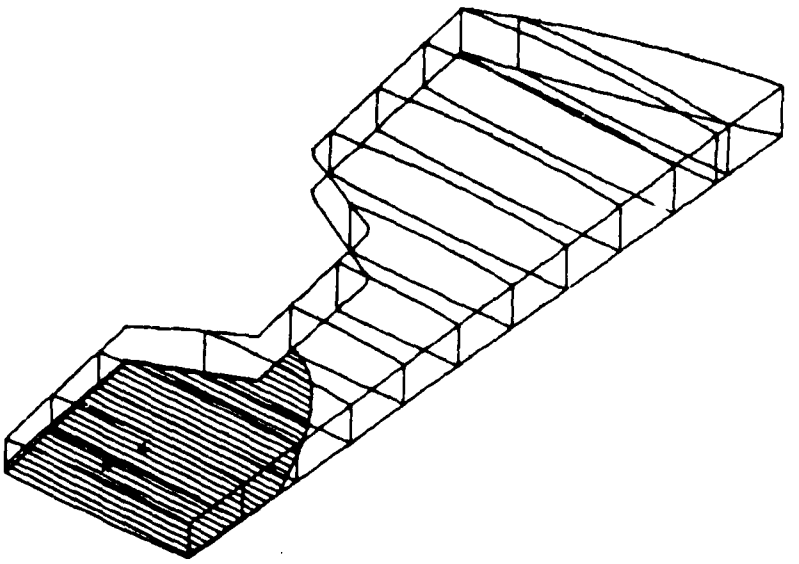

c. C-141 No. 1/4 Main Tank

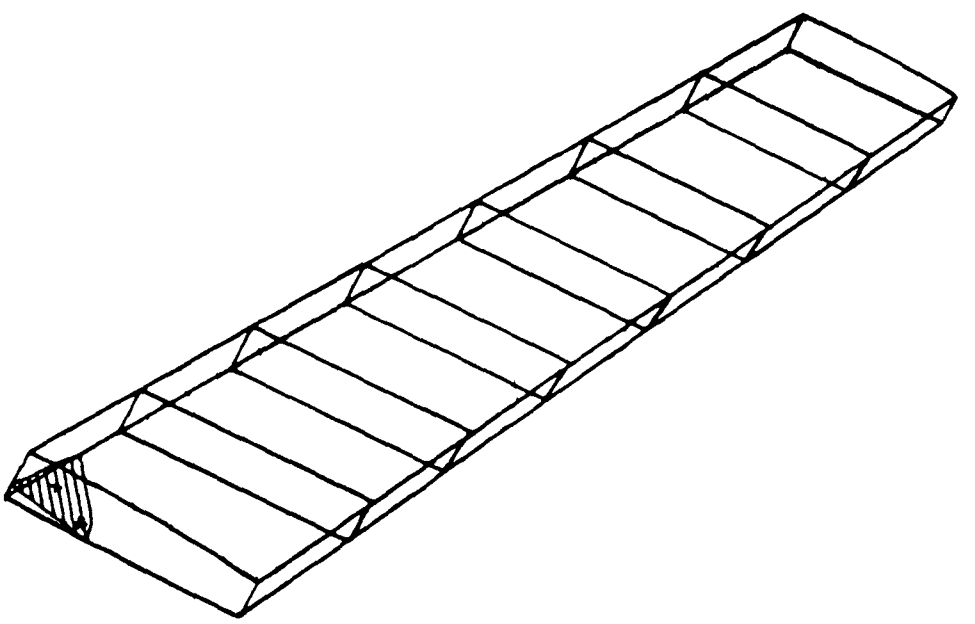

d. KC-135 No. 1/4 Reserve Tank

Figure 74. Computer Graphics Model Examples (Continued)

the most severe route for each study airplane by constructing a mean temperature history through this band of ambient temperature data. To perform the analysis required, calculations were made with the one dimensional computer model using various fuel freeze point temperatures and holdup characteristics. The mean baseline temperature history was then adjusted upward and downward for each fuel freeze point examined to find temperature which would freeze no more than the allowable limit (as defined in Table 11). The average temperature thus determined was then compared with the atmospheric temperature distributions found in the statistical analysis (Section II.3.b) to obtain the probability of encounter of each temperture history, and therefore, the probability of interference for each fuel freeze point considered. This probability is reported as a function of fuel freeze point in Figure 75 through 79, part a.

As an example of the use of the information contained in the figures, consider the following example: A fuel freeze point of $-43^{o}C$ is being evaluated for its acceptability in the A-10. Figure 75 (left) indicates that this is an acceptable fuel for the worst case route, for a temperature history along the route that is $7.3^{o}C$ above the worst baseline temperature history. In other words, for a temperature history $7.3^{o}C$ above the worst case, 5.85% holdup was predicted to develop using a fuel with a freeze point of $-43^{o}C$. Moving to the right, it is found that there is a 25% probability that the $7.3^{o}C$ case will ever be encountered. Since the atmospheric data base covers only the winter months, the probability of interference on a yearly basis is one-fourth of that found in the analysis.

A second, more conservative, approach to determining freeze point suitability is demonstrated in Figures 75 through 79, part b. The approach assumes that the fuel must meet the test of the worst case temperature history, with no more than the acceptable amount of holdup as defined in Table 11. Mission simulations were performed with the computer program to determine the maximum holdup occuring during the mission in the flight for a range of freeze points. The lowest maximum freeze point allowable for the five study airplanes then serves as the basis for a fuel specification which would have zero probability of operational interference. For the five airplanes examined (Table 12), the maximum freeze point under this criterion is $-50^{o}C$ (the lowest in any case).

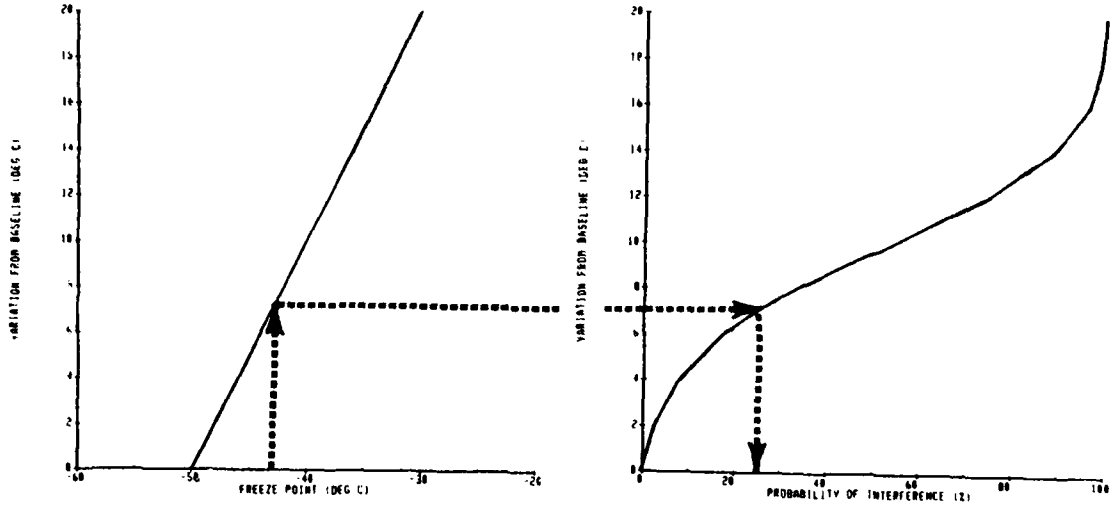

a. Variation From Baseline Temperature vs. Freeze Point and Probability of Interference

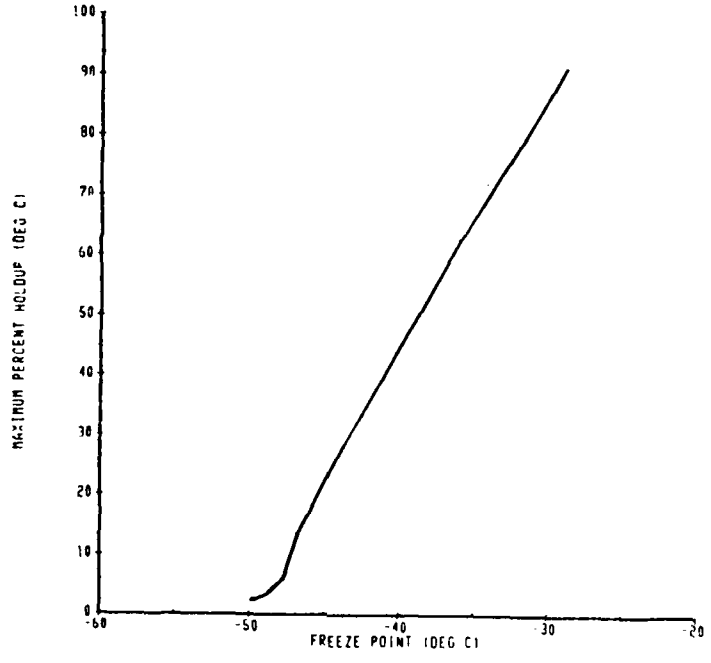

b. Maximum Percent Holdup vs. Freeze Point; Worst Case Cold Day

Figure 75. Allowable Freeze Point Estimation For Most Severe A-10 Mission

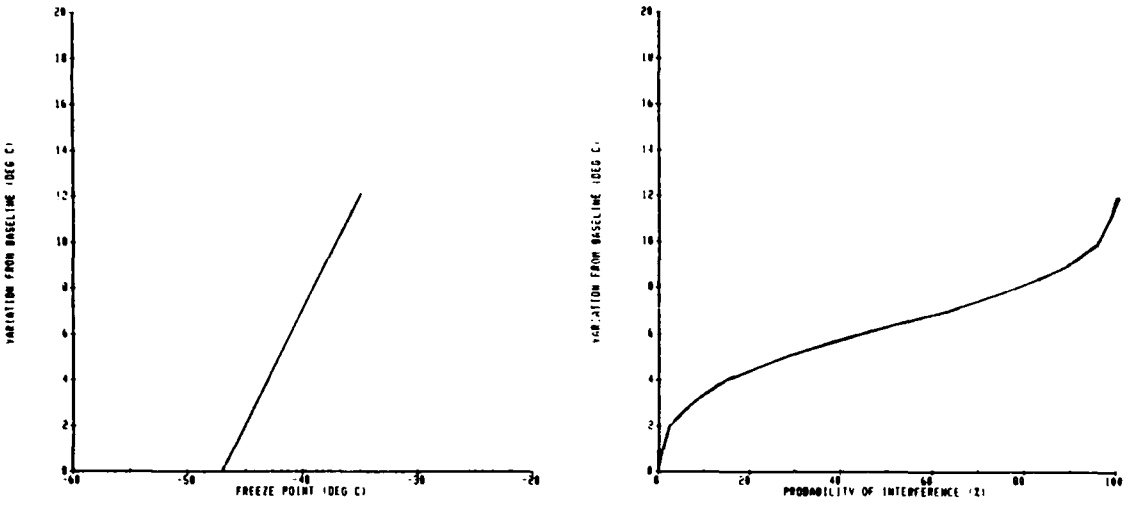

a. Variation From Baseline Temperature versus Freeze Point and Probability of Interference

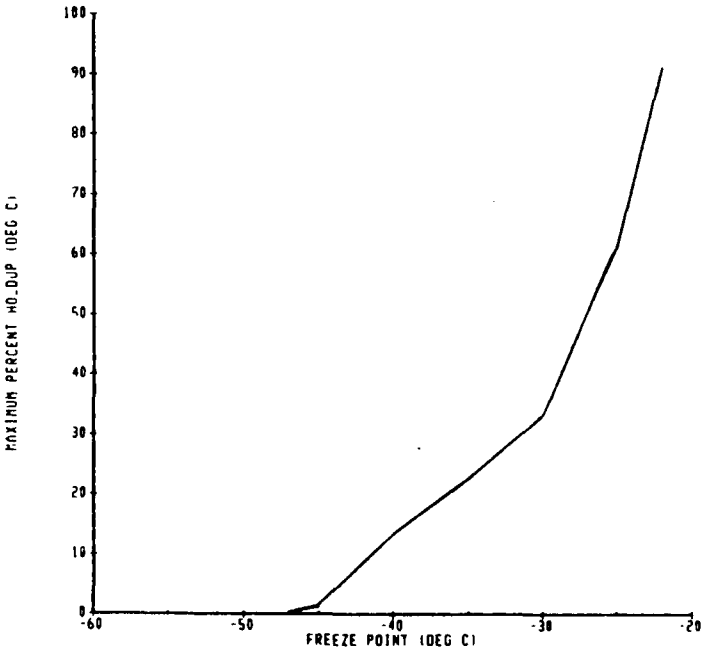

b. Maximum Percent Holdup versus Freeze Point; Worst Case Cold Day

Figure 76. Allowable Freeze Point Estimation For Most Severe B-52 Mission

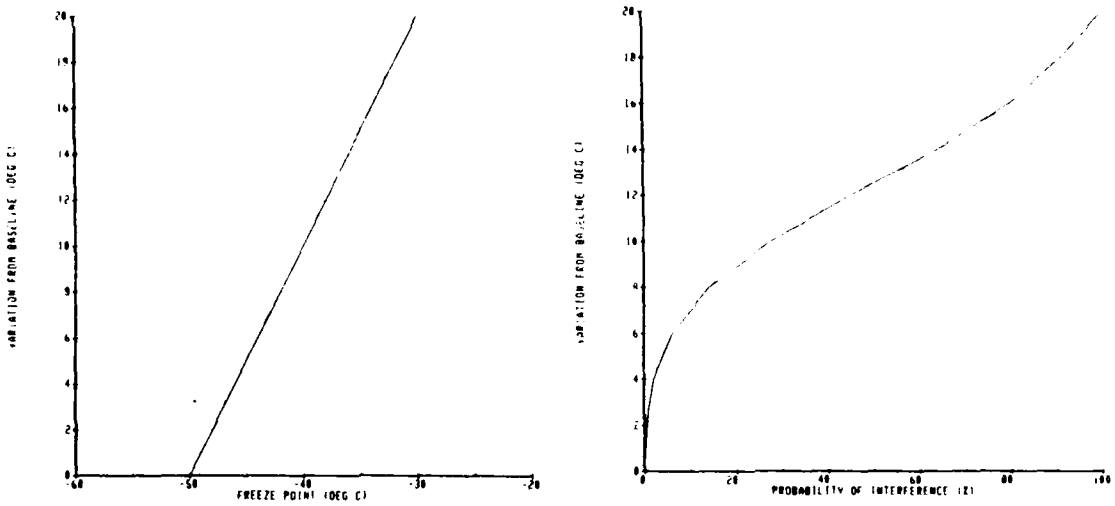

a. Variation From Baseline Temperature versus Freeze Point and Probability of Interference

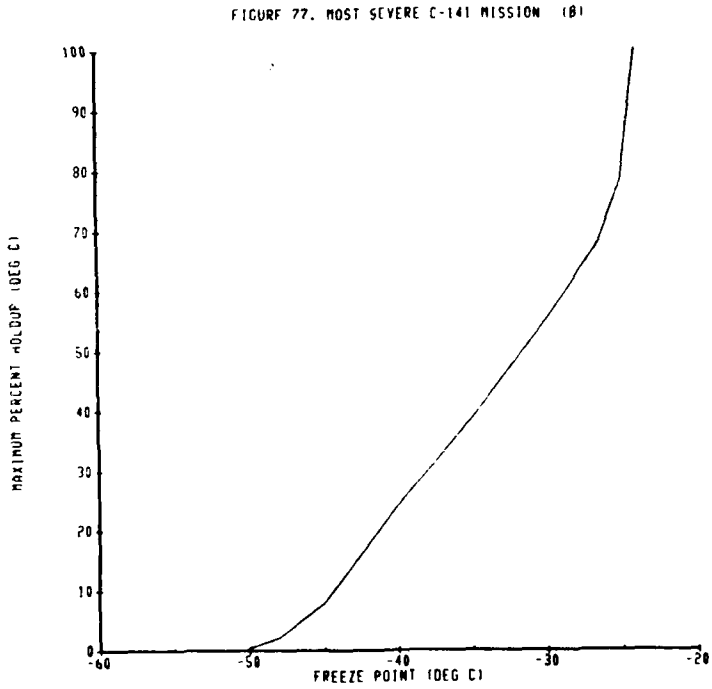

b. Maximum Percent Holdup versus Freeze Point; Worst Case Cold Day

Figure 77. Allowable Freeze Point Estimation For Most Severe C-141 Mission

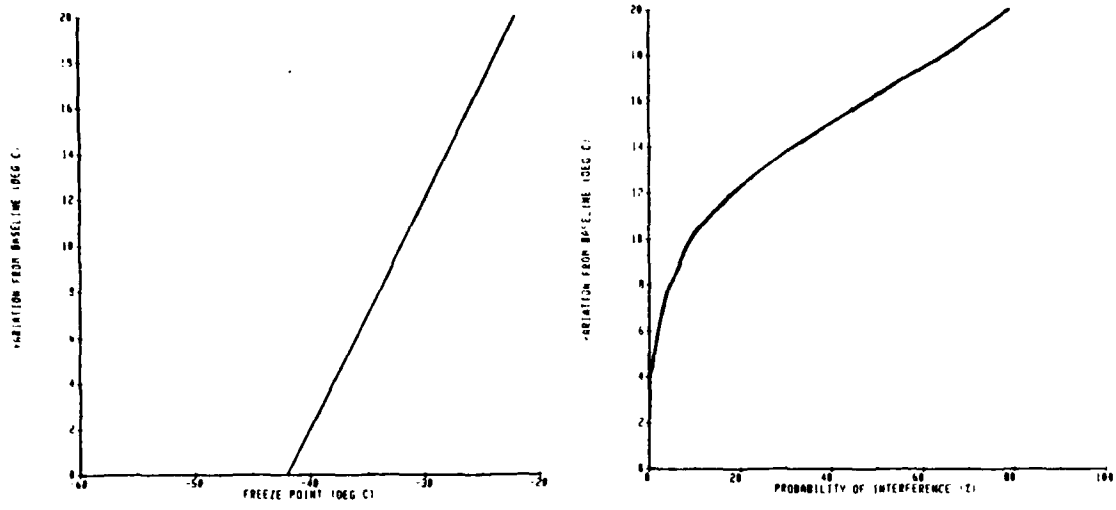

a. Variation From Baseline Temperature versus Freeze Point and Probability of Interference

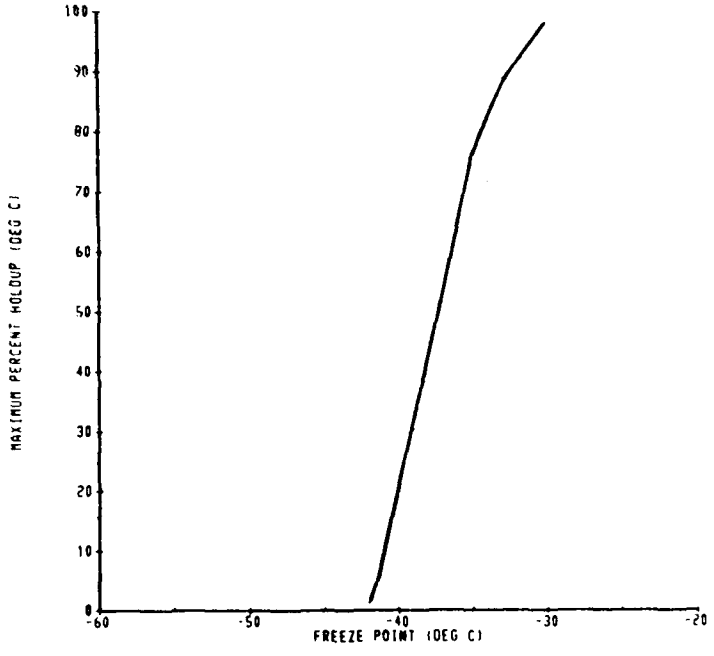

b. Maximum Percent Holdup versus Freeze Point; Worst Case Cold Day

Figure 78. Allowable Freeze Point Estimation For Most Severe F-15 Mission

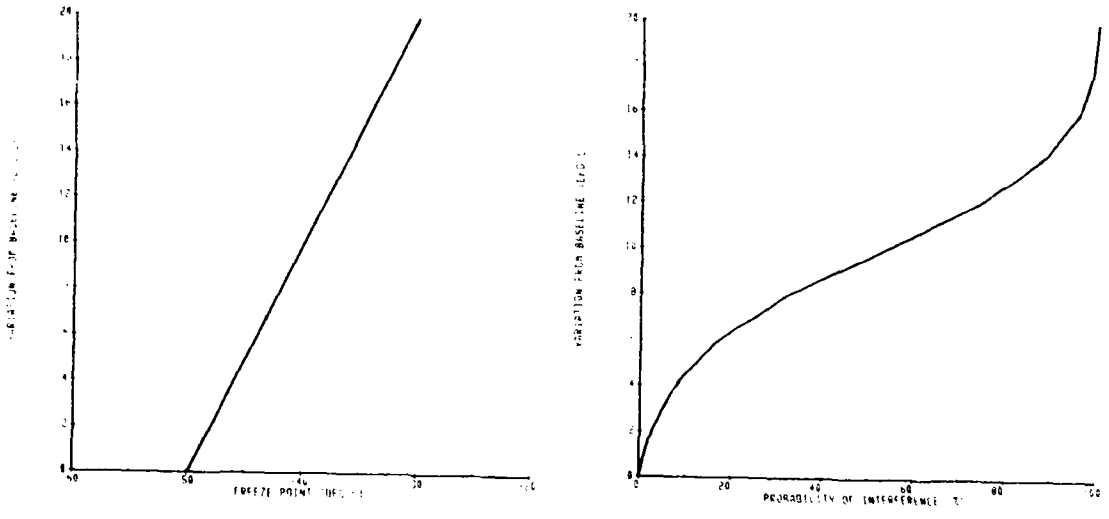

a. Variation From Baseline Temperature versus Freeze Point and Probability of Interference

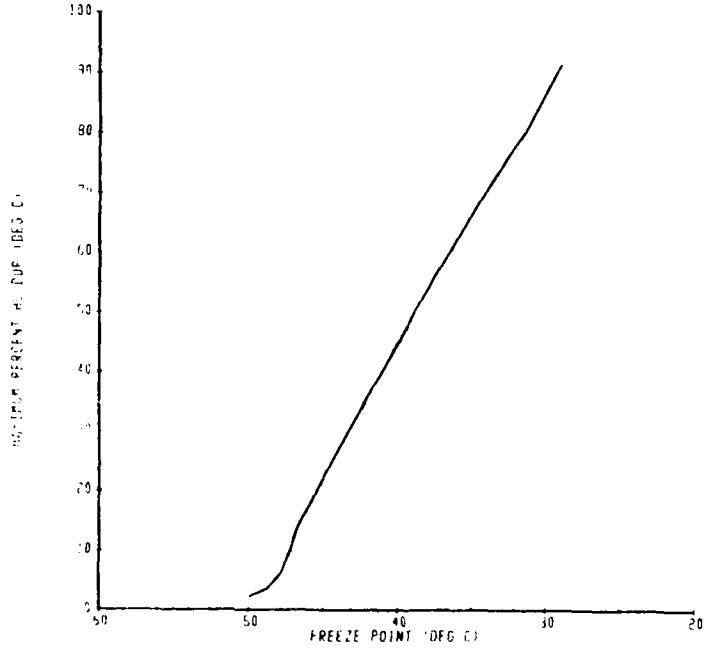

b. Maximum Percent Holdup versus Freeze Point; Worst Case Cold Day

Figure 79. Allowable Freeze Point Estimation For Most Severe KC-135 Mission

Table 12. Maximum Allowable Fuel Freeze Point for Five Study Airplanes (Worst Case, Zero Probability Criteria)

Airplane	Freeze Point (^{o}C)	Determined By (Conditions)
A-10	-50.0	ground
B-52	-47.0	atmospheric
C-141	-50.0	atmospheric
F-15	-42.0	atmospheric
KC-135	-50.0	ground

4. ABNORMAL OPERATING CONDITION ASSESSMENT

Abnormal operating conditions or failure modes which could affect the fuel freeze point requirement include:

- boost pump failure causing the fuel system to revert to suction feed
- an engine failure on a multi-engine airplane resulting in changes in fuel usage sequence
- an engine failure requiring reduced Mach number operation (and hence reduced recovery temperature) for extended periods of time

Many airplane fuel feed systems are designed to revert to suction feed automatically in the event of boost pump failure, using suction generated by the engine driven fuel pump. Cold fuel does not normally create problems with suction feed (assuming no freezing), and in fact suction feed problems are normally associated with hot fuel. The pump inlet and suction feed line inlets are usually separate, and placed about the same distance above the bottom of the tank. For this reason, only slight differences in the availability of the fuel to either of the inlets are likely. However, with frozen fuel there may be larger differences in the amount of fuel that is removable from the tank, based on the drainability/pumpability test results reported in the previous section. Between 1 and 10% more fuel was removable from the test tank with boost pump operation than in suction feed which is analogous to gravity draining.

Crossfeeding of fuel in the event of engine failure is usually a feature of multi-engine airplane designs. If the engine failure does not require the airplane to reduce its speed, no additional problems with frozen fuel should occur. By using the cross feed manifold, the fuel depletion schedule could be identical to flights without engine failure. If reduced speed results from reduced thrust, the remedy is the same as for the general case of reduced airplane speed as discussed below.

Should some circumstance arise where an airplane was required to operate at lower than normal Mach number for an extended period of time, the recovery temperature would be lower, and fuel temperatures will also be reduced. An example of the effect on temperatures of reduced Mach number was prepared using the conditions of KC-135 Track 10, combining the worst case atmospheric temperature day with the actual ground temperatures for the 24 hours preceding that day (Figure 80). Assuming a fuel freeze point of $-50^{o}C$, the increase in holdup predicted is shown in Figure 81 as a function of Mach number decrease. Based on these results, either a lower fuel freeze point or alteration of flight altitude or route of flight might be required. Such procedures are stipulated for commercial airplane operation. One unanswered question concerns the probability of being unable to locate a warmer air mass in time to prevent fuel freezing problems. Further investigations into this issue can be performed with existing analytical tools if there is sufficient interest, and if the flight plan alterations are specified.

5. CURRENT OPERATING PROCEDURE EVALUATION

Current operating procedures and changes that would allow the Air Force to utilize fuels with still higher freeze points were considered.

a. Effect of Mission Changes

Flying at higher Mach numbers when very low temperatures are encountered may be an effective means of avoiding fuel freezing problems. Opposite to the example given above, recovery temperatures and in turn, fuel temperatures, would be increased if an airplane operated at higher than normal Mach numbers for an extended period of time (Figure 82). The conditions of KC-135 Track 10 were again used for the example, even though such increases in Mach number are typically not feasible for this type of airplane. As mentioned above,

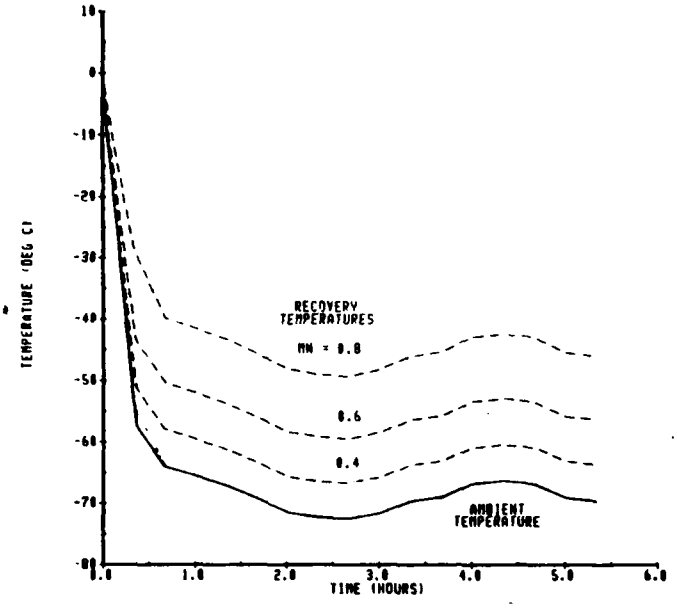

a. *Effect on Recovery Temperature*

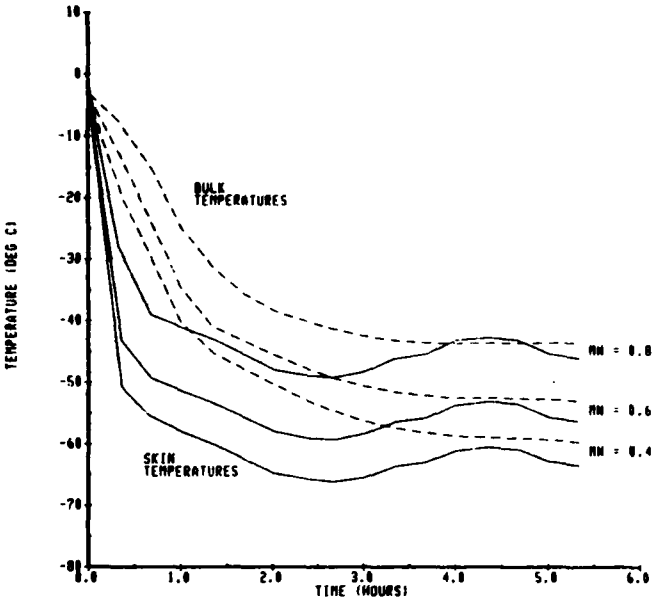

b. *Effect on Skin and Bulk Temperatures*

Figure 80. Effect of Lowering Mach Number

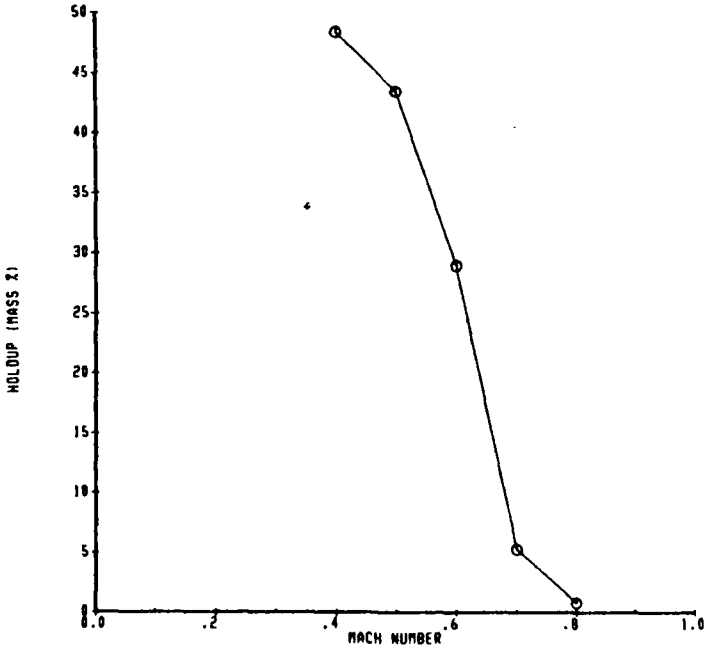

Figure 81. Holdup as a Function of Mach Number

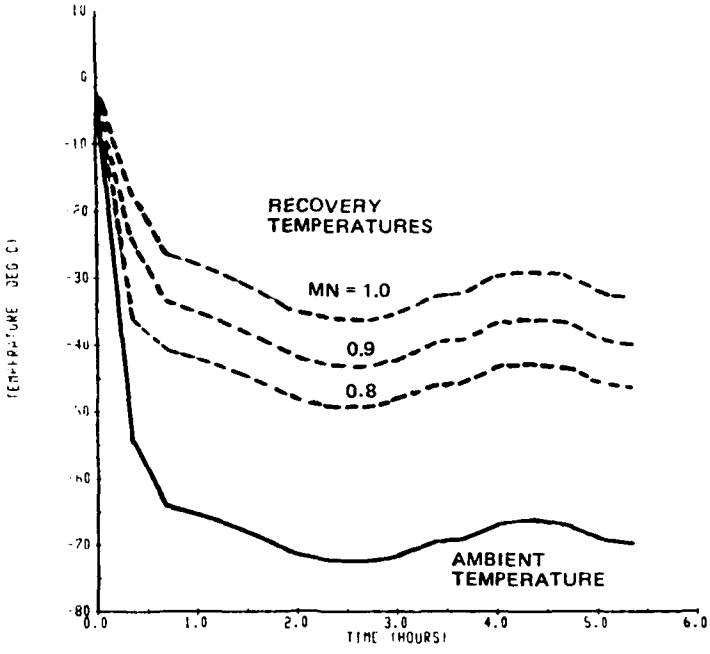

a. Effect on Recovery Temperature

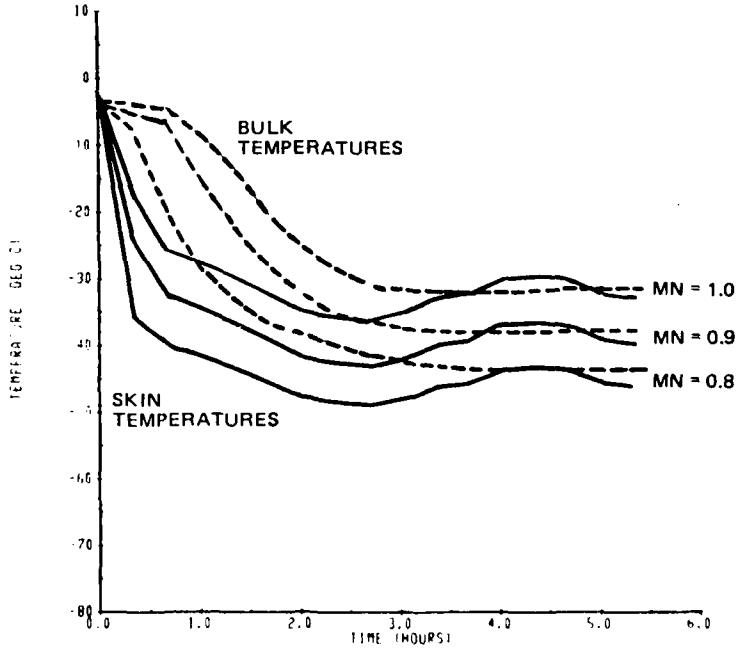

b. Effect on Skin and Bulk Temperatures

Figure 82. Effect of Increasing Mach Number

descending to lower altitudes or altering routes when low temperatures are encountered might be required. Further study of these options could produce useful alternatives.

b. Fuel Treatments

Fuel heating during flight and the addition of flow improver additives are two techniques which have promise for enhancing the flowability of fuel at temperatures below the freeze point.

Fuel heating concepts have been evaluated in other programs (Reference 33 and 37). It has been found that in situations which would produce low hold-up (2%) the effects of fuel heating are small, presumably because of the inability of the heated fuel to penetrate the cold stagnant fuel layer at the bottom of the tank. However, the benefit of fuel heating in high hold-up situations was notable. Without flow distributors to direct the heated fuel along the bottom of the tank, 1% to 2% hold-up may be present along the subfreezing lower tank skin even with relatively high rates of heating. As pointed out earlier, quantities of hold-up of the order of 2% do not appear to be a problem for the airplanes studied. The obvious penalties for using internal tank heaters are additional complexity and weight.

It is common practice to add flow improvers to high density fuels, such as diesel and home heating oil, to help improve flowability at low temperatures. The additives do not alter the freeze point of the fuel but have a pronounced effect on reducing the pour point. For this reason the additives continue to be referred to as pour point depressants. Although some flow improvers have been shown to have negligible effects on kerosene fuels (Reference 33), a recently developed additive (Paradyne, produced by Exxon) was claimed to have utility. Limited experiments have been performed with dilute concentrations of Paradyne mixed with one of the program test fuels (Reference 2). This material produced a marked change in the low temperature flowability curve (Figure 83) and a three-fold reduction in hold-up during cold fuel simulation tests. Paradyne is believed to interfere with the ability of individual fuel crystals to grow and agglomerate into a matrix which can trap substantial amounts of liquid fuel. Further testing of this material is required to determine its effect on a broad range of airplane fuels and to optimize

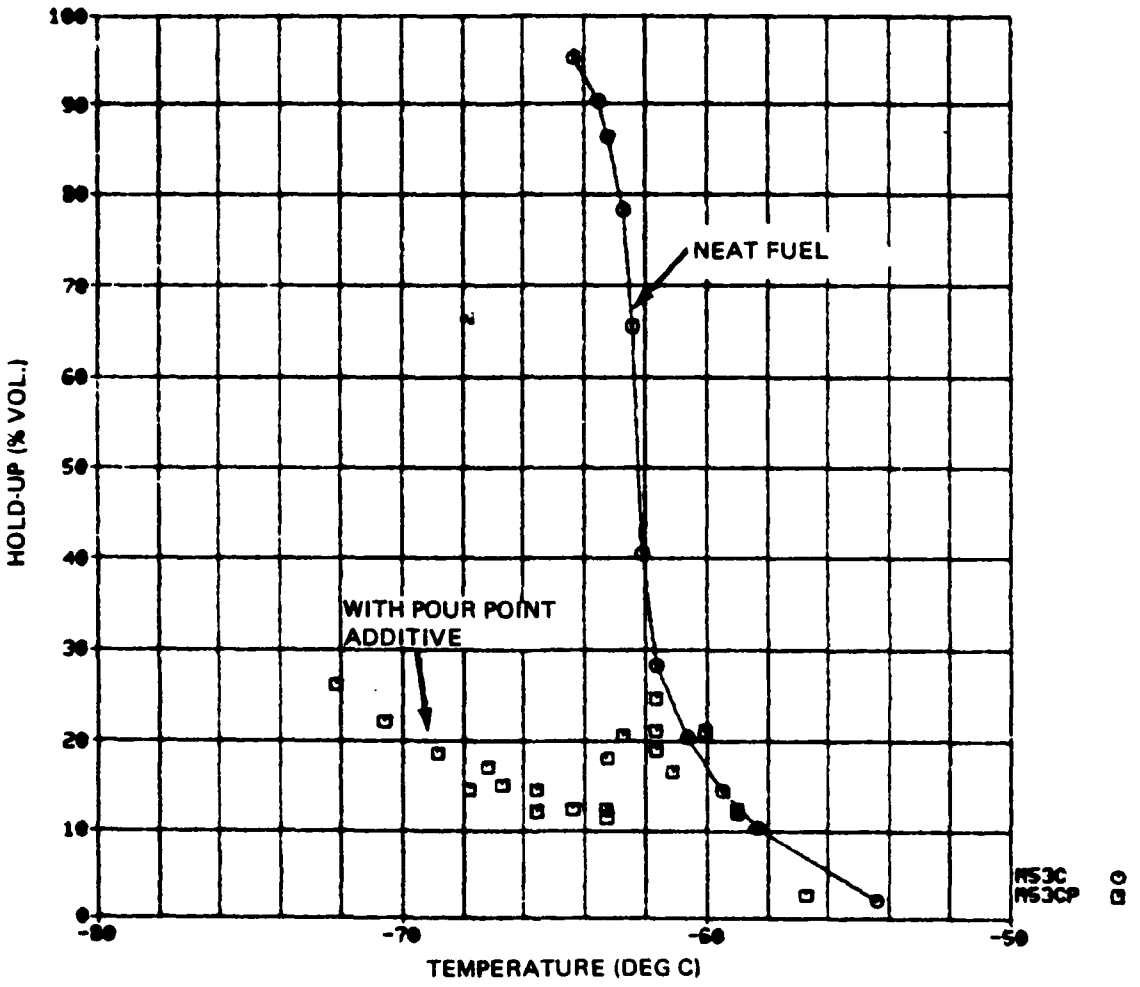

Figure 83. Shell-Thornton Data, Fuel With and Without Pour Point Depressant

concentration levels. Its use might be limited to airplanes required to operate in arctic regions, or when weather forecasts indicated a need.

6. USE OF HIGHER FREEZE POINT FUEL IN EUROPE

A change in the Jet A-1 freeze point specification from -50°C to -47°C has fairly recently become effective. U. S. airplanes in Europe normally use JP-8, which has a freeze point specification of -50°C (Jet A has a freeze point maximum of -40°C) but may have occasion to use Jet A-1. It is therefore, of interest to determine whether the freeze point change will cause any interference problems for European operations. Surface temperature data was reviewed for this purpose.

Shown in Figure 84 are the average and extreme minimum temperatures taken over a number of years for the winter months at northern European USAF bases used by the five study airplanes. Bases in Greenland and Labrador were included for reference. A check of temperatures at a number of other military airfields and joint military/civilian airfields in Europe was made to determine which regions experience the most severe thermal exposures (Figure 85). Locations included in the study are listed in Table 13 (there were too many names to place on the figure).

The lowest average and extreme minimum temperatures were found to have been recorded at the three Swedish airfields, with Lulea/Kallax being the most severe with extreme temperatures as low as-38°C. To ensure that no more severe locations had been overlooked, additional data was obtained for sixteen other airfields within Sweden. Five of these were almost as severe as Lulea/Kallax, but none were worse.

Based on the review of surface temperatures, -47°C is clearly an acceptable, conservative fuel freeze point specification for northern Europe. If only surface temperatures are considered, a freeze point as high as -43°C would not be likely to create any operational difficulties. A complete evaluation of acceptability should also include an examination of:

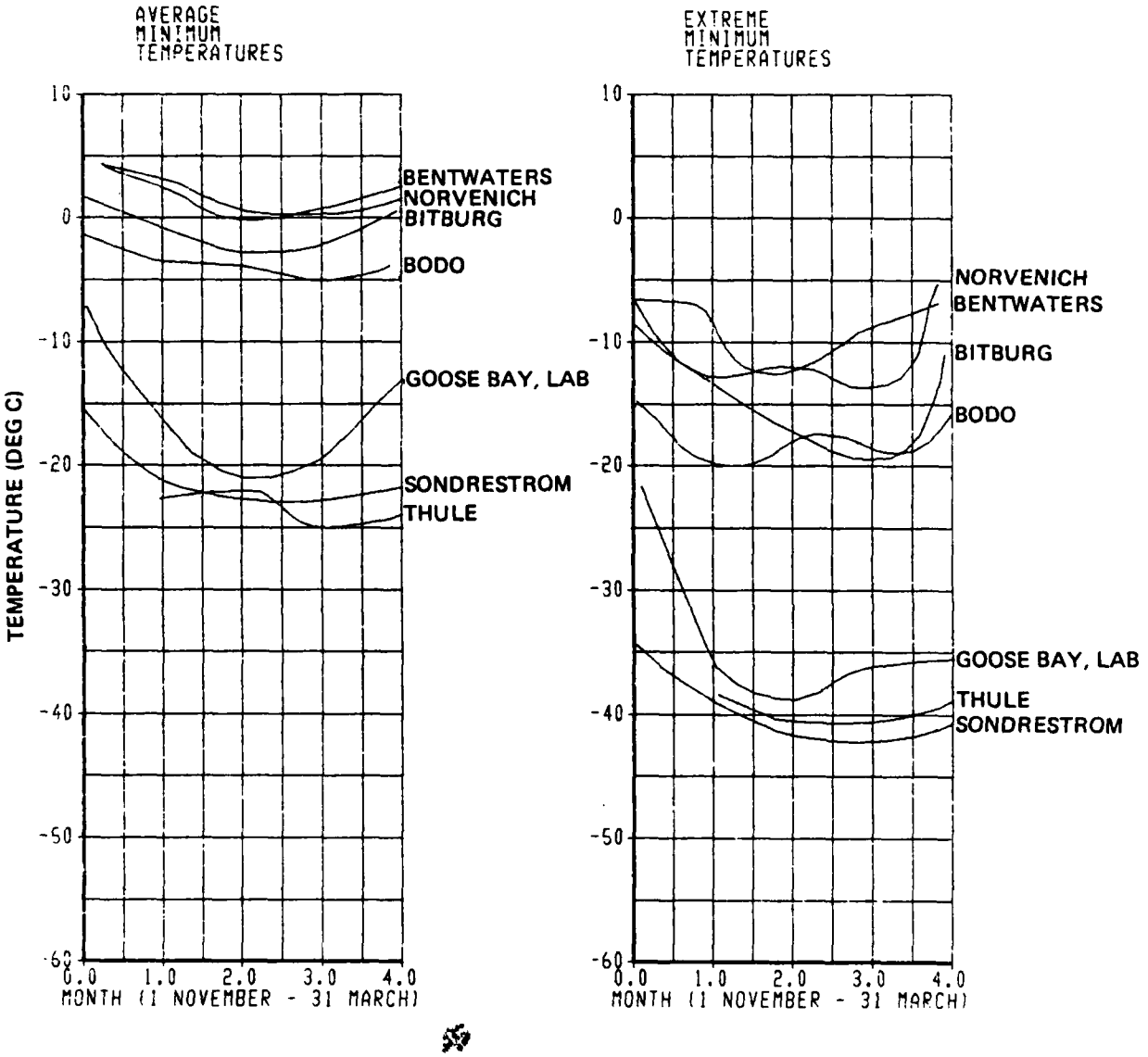

Figure 84. Winter Surface Air Temperatures at Northern European Air Force Bases for Five Study Airplanes

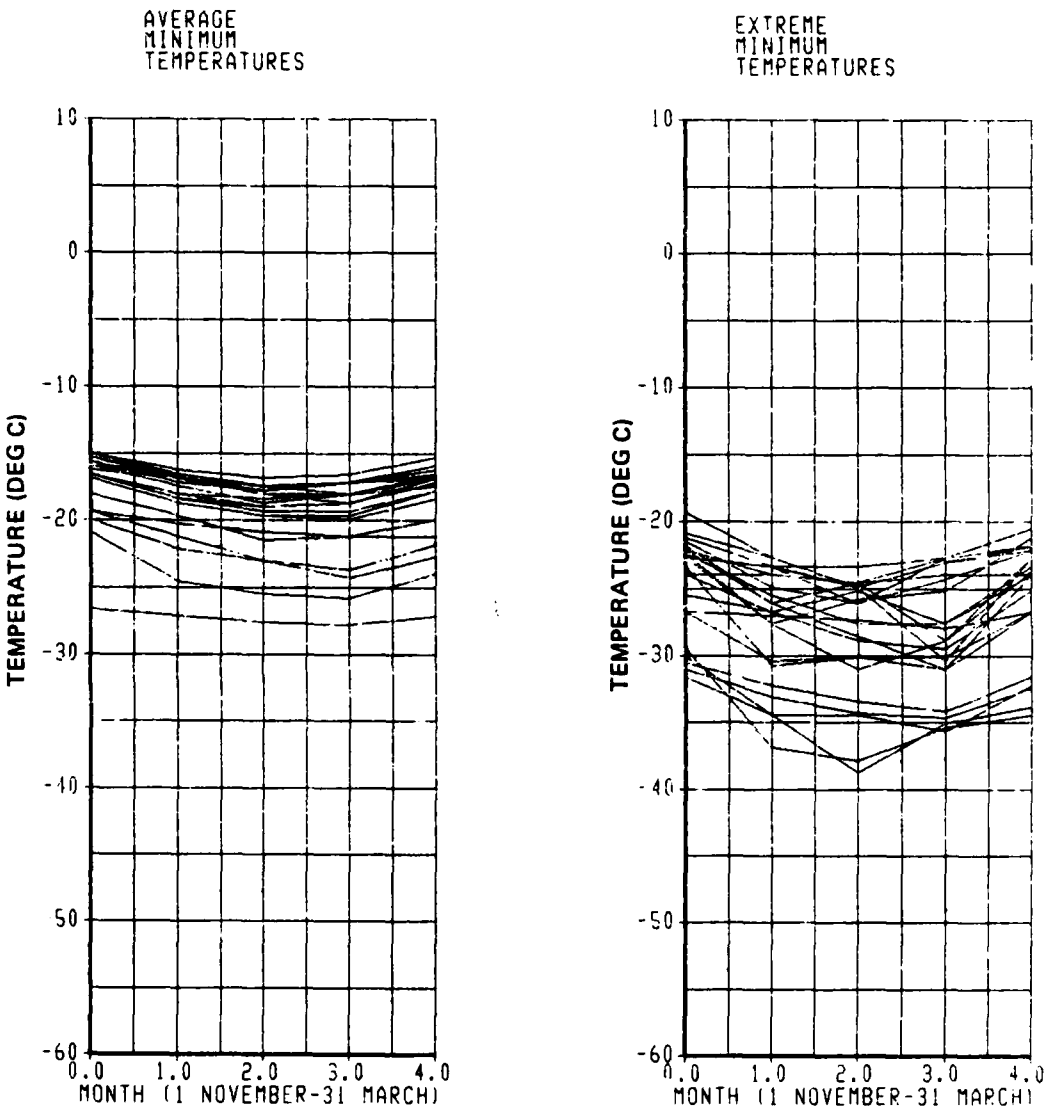

Figure 85. Winter Surface Air Temperatures at Additional Northern European Air Fields

Table 13. Airfields Used in Review of Temperatures in Northern Europe

Belgium

- Brussels National
- Liege Bierset

France

- Lognac - Chateaubernard
- Mont - de - Marsan
- Reims/Champagne
- Strasburg/Entzheim
- Tours/St. Symphorien

Germany

- Hahn
- Ramstein
- Sembach
- Zweibrucken

Netherlands

- Deelen
- Eindhoven

Norway

- Banak
- Stavanger/Sola
- Trondheim/Vaerne

Sweden

- Borlange
- Lulea/Kallax
- Ostersund/Froson

United Kingdom

- Fairford
- Greenham Common
- Marham
- Woodbridge

- o the fuel systems of the airplanes in question

- o the specifics of the missions to be flown in or from northern Europe (routes, altitudes, and airspeeds)

A number of relevant facts are known from experience with atmospheric temperatures for the missions of the five study airplanes:

- o Most of the routes studied traverse latitudes across the U.S. and Canada that are as far or further north than those which cross Europe (Figures 1, 2, 3, and 6).

- o Up to an altitude of 40,000 feet, mean atmospheric temperatures across Europe all during the winter months are quite similar across the U.S. northern tier and Canada, including Alaska. Above 40,000 feet, mean temperatures are lower across Europe. Surface temperatures for the same period of time have already been shown more severe in the U.S. than in Europe.

- o Of the ten original B-52 routes studied, eight terminated Europe; none of these was notably severe.

With the similarity of atmospheric temperature, it is possible to conclude that $-48^{o}C$ would be an acceptable maximum freeze point specification for Europe with the assumption that the presence of frozen fuel is not allowed. A freeze point of $-47^{o}C$ would also be acceptable, given a small probability, estimated to be less than 1.0%, of operational interference from fuel freezing during the winter months.

SECTION V
CONCLUSIONS AND RECOMMENDATIONS

1. CONCLUSIONS

Extensive analytical and experimental studies were conducted to establish the maximum allowable fuel freeze point which will ensure satisfactory operation of all USAF airplane fleets. The results revealed that the maximum allowable fuel freeze point for a general purpose aviation turbine fuel for Air Force airplanes operating in the northern hemisphere is -50°C. This conclusion is based on a systematic study of the probability of fuel freezing during ground and inflight exposures to extremely low air temperatures. The study included:

- o determining the lowest inflight temperature exposures by simulating flights of five different USAF airplanes on low temperature routes using a 15-year data base of atmospheric properties

- o defining the lowest ground temperature exposures for northern latitude air bases

- o performing experiments in a low temperature fuel test apparatus to measure fuel holdup based on the inflight and ground temperatures obtained above

- o refining a one-dimensional computer code by validating fuel temperature and holdup predictions with test data

The study confirmed that the -58°C specification limit for JP-4 fuel may be relaxed, and that an earlier finding (Reference 1) that a specification limit between -43°C and -46°C would be acceptable was not all inclusive. The limiting case was found to be exposure to the extremely low ground temperatures possible at Eielson AFB, Alaska, where temperatures may remain at about -50°C for a 24-hour period creating the potential for fuel freezing with fuels having freeze points higher than -50°C. The above conclusion (-50°C maximum freeze point) assumes that the presence of frozen fuel is not acceptable at any time. Since ground temperatures at Eielson AFB were the limiting case, the possibility of interference with airplane operations with -50°C freeze point fuel is eliminated.

Even when the effect of ground temperatures at Eielson AFB is neglected in the analysis, -50°C again proved to be the freeze point limitation (using the zero holdup allowable criterion) based on the inflight temperature predictions for C-141 Track 10. The exposure of the airplane to the low temperature extreme (<-50°C) during the mission is, however, relatively brief. If the development of some holdup were to be allowed during ground exposure, as in the case of Eielson AFB, or during a short portion of the flight, as with the C-141 mission, a freeze point of -48°C could be recommended. In both instances, warming and thawing of the fuel would have occurred well before the point during the flight at which fuel withdrawal began.

The freeze point specification for Jet A-1, -47°C, was determined to be acceptable for European operations based on a study of surface temperature data. Limited consideration of atmospheric data indicated that a freeze point of -48°C would satisfy all operational requirements, but that -47°C is also acceptable if a small probability of interference (less than 1%) is considered reasonable.

A number of advancements were made in the ability to model the behavior of low temperature fuels:

- a more complete definition of low temperature fuel properties was established, including phase change effects
- the one-dimensional fuel thermal analysis was refined to include the low temperature fuel properties and was more completely validated by additional experimental data
- promising initial results were obtained for two-dimensional cooling studies applicable to external cylindrical fuel tanks
- a technique was developed to statistically analyze airplane low temperature exposures in combination with fuel tank physical characteristics to predict the probability of interference of airplane operations as a function of fuel freeze point

- greater insight was obtained into drainability and pumpability of partially frozen fuel

- a maximum freeze point acceptable for Europe has been clearly established based on the examination of ground temperatures; further study of the atmospheric data given specific airplanes and missions to determine whether any isolated areas of extreme low temperature exist

For future use in assessing the acceptability of higher freeze point fuels, a method was developed to provide an estimate of whether a fuel with a given freeze point will cause operational interference. Data was assembled for the worst case mission of each study airplane; caution should therefore be used in the application of this approach because it is mission specific. The maximum acceptable freeze point was determined analytically for the worst case mission. Increments of temperature were then added to the worst case temperature history, and new acceptable freeze points determined for each incremented temperature history. Using the statistical data for each route, the probability of encountering each incremented temperature history was determined, which can also be interpreted as probability of operational interference.

2. RECOMMENDATIONS

A number of follow-on studies are appropriate to more fully understand the relationship between fuel freeze point and potential operational problems. Some of these are:

- further check refine the one-dimensional thermal analysis when further flight test data becomes available, ideally including the performance of verification tests in the low temperature simulator

- continue development of the two and three dimensional codes for external fuel tanks

- further investigate the effect of fuel chemical composition on the heat transfer characteristics of the fuel

- investigate the effect of fuel tank construction and materials on fuel freezing and holdup

- o further evaluate the effect of mission changes (changing altitude, airspeed, or route) on minimizing the effects of severe low temperature exposure

- o establish maximum allowable fuel freeze points as a function of geographical location to determine the feasibility and payoff of using special fuels at specific locations

- o determine the effect of mixing various fuels on fuel freezing phenomena; that is, if a special, low freeze point fuel were used for problem bases such as Eielson AFB, what treatment would be required for an airplane landing at the base loaded with a standard, higher freeze point fuel - could the special fuel be added to the standard fuel to reduce the effective freeze point? If so, in what proportion?

REFERENCES

1. McConnell, P.M., L. A. Massmann, G. M. Peterson, and F. F. Tolle, "Fuel/Engine/Airframe Trade-off Study - Operational Effects of Increased Freeze Point Fuels," Boeing Military Airplane Company prepared for Air Force Aero Propulsion Laboratory, AFWAL-TR-82-2067, August 1982.

2. McConnell, P.M., and L. A. Massmann, "Operational Effects of Increased Freeze Point Fuels in Thin Wing Aircraft, "Boeing Military Airplane Company prepared for Air Force Aero Propulsion Laboratory, AFWAL-TR-82-2087, September 1982.

3. Peck, G. M., "Advanced Fuel System Technology For Utilizing Broadened Property Aircraft Fuels," prepared for the Twelfth Congress of the International Council of Aeronautical Sciences, NASA-TM-81538, October 1984.

4. Dickson, J. C. and L. P. Karvelas, "Impact of Fuel Properties on Jet Fuel Availability," Bonner & Moore Associates, Inc., prepared for Air Force Aero Propulsion Laboratory, AFAPL-TR-76-7, April 1976.

5. USAF T.O. 1B-52H-1, "B-52H Flight Manual," revisions through 15 July 1981.

6. USAF T.O. 1B-52G-2 -2, "Ground Handling, Servicing, and Airframe Maintenance," revisions through 30 October 1977.

7. USAF T.O.1C-141A-1, "C141A Flight Manual," revisions through 10 November 1983.

8. USAF T.O. 1C-141A-2-5, "C-141A Fuel System," revisions through 15 April 1975.

9. USAF TO.0.1C-135(K)A-1, "KC-135 Flight Manual," revisions through 10 August 1984.

10. USAF T.O. 1C-135(K)A-2-5-1, "KC-135 Fuel System," revisions through 27 April 1979.

11. USAF T.O. 1A-10A-1, "A-10A Flight Manual," revisions through 10 June 1982.

12. USAF T.O. 1A-10A-1, "A-10A Fuel System," revisions through 10 June 1982.

13. USAF T.O. 1F-15A-1, "F-15A/B Flight Manual," revisions through 15 January 1982.

14. USAF T.O.1F-15A-2-12 "Fuel System," revisions through 1 February 1981.

15. Shapiro, H. H., "The Dynamics and Thermodynamics of Compressible Fluid Flow, Volume II," Ronald Press Company, 1954.

16. Schlichting, H., "Boundary Layer Theory," 6th Edition, McGraw-Hill Book Company, Inc., 1968.

17. Friedman, R., NASA letter to Boeing Military Airplane Company (F. F. Tolle), dated 24 May 1983.

18. Coordinating Research Council, Inc., "Handbook of Aviation Fuel Properties" CRC Report No. 530, 1983.

19. Schmidt, J. E., and A. M. Momenthy, "Properties of Common Fuels," Boeing Commercial Airplane Company (draft).

20. Exxon Company, "Data Book for Designers," September 1973.

21. Gavin, D. L., and Moynihan, C. T., "Specific Heats of Hydrocarbon Fuels, "Preliminary Data - Rensselaer Polytechnic Institute, Materials Engineering Department Research Supported by NASA-Lewis Research Center, 2 February 1983.

22. Moynihan, C. T., Mossedegh, R., and Bruce, A. J., "Determination of the Mass Fraction of Crystals in Partly Frozen Fuel," draft submitted to Analytical Chemistry, RPI Materials, Engineering Department, July 1983.

23. Mossedegh, R., Bruce, A. J., and Moynihan, C. T., "Specific Heats of Six Jet Fuel Kerosenes Above and Below the Melting Point," Technical Report No. 1 Under Navy Contract N00140-83-C-6056, 6 January 1984.

24. Boeing Design Manual 29.143, "Thermal Conductivity," Commercial Airplane Company, 10-19-66.

25. Eckert, E. R. G. and R. M. Drake, "Heat and Mass Transfer, "Second Edition, McGraw-Hill Book Company, Inc., 1959.

26. IP217/66 Tentative Shell-Thornton, Journal of Institute of Petroleum, Volume 48 (467) pgs 388-390, November 1962.

27. Spalding, D. B., "A General Purpose Computer Program for Multi-Dimensional One and Two Phase Flow," Mathematics and Computers in Simulation (North Holland Press) Vol XXIII, 267-276 (1981).

28. Markatos, N. C. and Pericleous, C. A., "Laminar and Turbulent Natural Convection in an Enclosed Cavity", Natural Convection in Enclosures HTD-Vol 26, (ASME, New York) 1983.

29. Launder, B. E. and D. B. Spalding, "Mathematical Models of Turbulence," Academic Press, New York, 1972.

30. Patankar, S. V., "Numerical Heat Transfer and Fluid Flow," Hemisphere Publishing Corp., New York, 1980.

31. Gary, J. H., and Handwerk, G. E., "Chemical Processing and Engineering, Volume 5: Petroleum Refining and Economics - Technology and Economics," Published by Marcel Dekker, Inc., 1975.

32. Peterson, G. N., "Low Temperature Jet Fuel Study," Boeing Military Airplane Company prepared for Coordinating Research Council, Low Temperature Flow Performance of Aviation Turbine Fuels Group, Boeing Document Number D180-25483-1, September 1979.

33. Friedman, R., NASA letter to Boeing Military Airplane Company (F. F. Tolle), dated 13 January 1982.

34. Friedman, R., NASA letter to Boeing Military Airplane Company (L. A. Desmarais), dated 18 July 1983.

35. Strawson, H., "Using Turbine Fuels at Low Temperatures," Shell Aviation News, Volume 210; 8-12 (1955).

36. Ford, P. T. and Robertson, A. G., "Jet Fuels Redefining the Low Temperatures Requirements," Shell Aviation News, V.441; 22-27 (1977).

37. Stockemer, F. J. and Dean, R. L., "Additional Experiments on Flowability Improvements of Aviation Fuels at Low Temperatures," NASA CR 167912, 1982.

38. Davis, R. N., "Fuel Tank Simulator (FTS) Computer Graphics Program," Boeing Document D6-48770, September 1779.

39. Friedman, R., "High Freezing Point Fuels Used for Aviation Turbine Engines," NASA TM 79015 (1979).

40. USAF T.O. 1A-10A-2-28MS-1, "Fuel System," revisions through 30 August 1981.

41. USAF T.O. 1B-52G-2-5GA-1, "Fuel System," revisions through 27 April 1984.

42. USAF T.O. 1C-141A-3, "Structural Repair Instructions," revisions through 23 January 1978.

43. "Study Guide, C-141 Aircraft Systems," 1 October 1969.

44. USAF T.O. 1F-15A-2-2-2, "Ground Handling and Servicing," revisions through 15 July 1981.

45. USAF T.O. 1F-15A-4-5, "(IPB) Fuel System, Engine and Related Systems," revisions through 15 June 1984.

APPENDIX A
ROUTE DATA

The data presented show latitude, longitude, altitude, and airspeed for the airplane along each route studied. The sign conventions are as follows:

	+	-
Latitude	north	south
Longitude	east	west

The sources of route data were discussed in Section 2.1; this section includes:

Table A-1a. B-52 Track 1

LATITUDE (DEG)	LONGITUDE (DEG)	ALTITUDE (FT)	AIRSPEED (KNOTS)
48.0	-101.0	35000	444
80.0	-110.0	35000	444
87.0	-130.0	35000	444
86.0	127.0	35000	444
75.0	120.0	35000	444
70.0	115.0	250	360
60.0	115.0	250	360
55.0	112.0	250	360
52.0	112.0	250	360
51.0	113.0	250	360
CIRCLE			
51.0	115.0	250	360
51.0	116.0	250	360
50.0	118.0	250	360
50.0	120.0	22000	444
38.0	127.0	0	0

Table A-1b. B-52 Track 3

LATITUDE (DEG)	LONGITUDE (DEG)	ALTITUDE (FT)	AIRSPEED (KNOTS)
48.0	- 97.0	35000	444
80.0	- 80.0	35000	444
81.0	- 25.0	35000	444
78.0	18.0	35000	444
68.0	18.0	35000	444
68.0	18.0	250	360
63.0	20.0	250	360
53.0	29.0	250	360
61.0	33.0	250	360
61.0	35.0	250	360
58.0	35.0	250	360
58.0	39.0	250	360
57.0	40.0	250	360
CIRCLE			
57.0	38.0	250	360
57.0	37.0	250	360
56.0	36.0	250	360
56.0	25.0	250	360
61.0	35.0	250	360
63.0	29.0	250	360
65.0	25.0	0	0

Table A-1c. B-52 Track 4

LATITUDE (DEG)	LONGITUDE (DEG)	ALTITUDE (FT)	AIRSPEED (KNOTS)
48.0	- 97.0	35000	444
80.0	-100.0	35000	444
88.0	-120.0	35000	444
84.0	47.0	35000	444
78.0	47.0	35000	444
78.0	47.0	250	360
68.0	47.0	250	360
66.0	46.0	250	360
61.0	45.0	250	360
60.0	44.0	250	360
59.0	42.0	250	360
CIRCLE			
58.0	41.0	250	360
60.0	41.0	250	360
61.0	38.0	250	360
62.0	38.0	250	360
64.0	32.0	250	360
65.0	25.0	0	0

Table A-2a. C-141 Track 1

LATITUDE (DEG)	LONGITUDE (DEG)	ALTITUDE (FT)	AIRSPEED (KNOTS)
61.25	-149.77	39000	424
61.20	-150.20	39000	424
60.80	-161.80	39000	424
60.40	-164.40	39000	424
59.70	-170.00	39000	424
57.40	-180.00	39000	424
53.50	170.00	39000	424
50.00	160.00	39000	424
49.70	150.00	39000	424
40.30	145.00	39000	424
38.90	143.20	39000	424
37.20	141.00	39000	424
36.70	140.30	39000	424
36.50	139.90	39000	424
35.60	139.40	39000	424
35.80	139.40	39000	424

Table A-2b. C-141 Track 8

LATITUDE (DEG)	LONGITUDE (DEG)	ALTITUDE (FT)	AIRSPEED (KNOTS)
61.25	-149.77	39000	424.5
61.60	-149.97	39000	424.5
64.80	-148.02	39000	424.5
66.60	-145.27	39000	424.5
69.20	-141.00	39000	424.5
69.60	-140.19	39000	424.5
74.50	-130.00	39000	424.5
78.50	-110.00	39000	424.5
80.00	- 85.00	39000	424.5
80.60	- 69.34	39000	424.5
77.30	- 40.00	39000	424.5
75.00	- 30.00	39000	424.5
71.00	- 20.00	39000	424.5
69.00	- 16.42	39000	424.5
65.00	- 11.50	39000	424.5
61.00	- 8.00	39000	424.5
58.22	- 6.19	39000	424.5
55.04	- 1.72	39000	424.5
53.65	1.50	39000	424.5
53.17	3.00	39000	424.5
53.09	3.29	39000	424.5
52.34	5.10	39000	424.5
51.95	6.65	39000	424.5
51.92	6.79	39000	424.5
51.72	7.59	39000	424.5
51.67	7.97	39000	424.5
50.45	8.35	39000	424.5
50.42	9.25	39000	424.5
50.29	8.85	39000	424.5
50.04	8.57	39000	424.5

Table A-2c. C-141 Track 10

LATITUDE (DEG)	LONGITUDE (DEG)	ALTITUDE (FT)	AIRSPEED (KNOTS)
76.53	- 68.70	39000	424.5
74.84	- 68.57	39000	424.5
73.00	- 68.65	39000	424.5
72.77	- 68.67	39000	424.5
71.00	- 68.60	39000	424.5
70.47	- 68.59	39000	424.5
65.00	- 68.50	39000	424.5
63.74	- 68.47	39000	424.5
58.10	- 68.44	39000	424.5
54.00	- 70.59	39000	424.5
53.20	- 70.92	39000	424.5
52.00	- 72.14	39000	424.5
49.80	- 74.50	39000	424.5
45.89	- 74.39	39000	424.5
45.00	- 74.20	39000	424.5
42.75	- 73.80	39000	424.5
41.77	- 73.60	39000	424.5
40.94	- 72.80	39000	424.5
40.52	- 72.80	39000	424.5
39.90	- 73.54	39000	424.5
39.10	- 74.80	39000	424.5

Table A-3a. KC-135 Track 3

LATITUDE (DEG)	LONGITUDE (DEG)	ALTITUDE (FT)	AIRSPEED (KNOTS)
48.0	- 97.0	35000	444
74.9	- 80.0	35000	444
77.4	- 82.0	35000	444
74.9	- 80.0	35000	444
48.0	- 97.0	0	0

Table A-3b. KC-135 Track 5

LATITUDE (DEG)	LONGITUDE (DEG)	ALTITUDE (FT)	AIRSPEED (KNOTS)
48.0	-101.0	35000	444
62.2	-102.8	35000	444
63.7	-103.0	35000	444
48.0	-101.0	0	0

Table A-3c. KC-135 Track 10

LATITUDE (DEG)	LONGITUDE (DEG)	ALTITUDE (FT)	AIRSPEED (KNOTS)
64.4	-147.0	35000	444
80.0	-155.7	35000	444
85.6	24.2	35000	444
83.5	30.0	35000	444
85.6	24.2	35000	444
80.0	-155.8	35000	444
64.4	-147.0	0	0

Table A-4a. A-10 Track 1

LATITUDE (DEG)	LONGITUDE (DEG)	ALTITUDE (FT)	AIRSPEED (KNOTS)
64.67	-147.12	22000	245
65.30	-146.52	22000	245
68.80	-141.00	22000	245
71.20	-135.00	16000	245
72.70	-130.00	16000	245
73.88	-125.00	17000	245
74.82	-120.00	17000	245
75.53	-115.00	22000	245
76.12	-110.00	22000	245
76.55	-105.00	22000	245
76.85	-100.00	22000	245
77.07	- 95.00	22000	245
77.02	- 90.00	22000	245
77.18	- 85.00	22000	245
77.10	- 80.00	22000	245
76.53	- 68.70	22000	245
75.80	- 60.00	22000	245
75.13	- 54.58	22000	245
74.58	- 51.05	17000	245
73.55	- 45.67	17000	245
72.15	- 40.00	22000	245
70.53	- 35.00	22000	245
68.45	- 30.00	22000	245
65.78	- 25.20	17000	245
63.98	- 22.60	22000	245
61.00	- 12.57	22000	245
60.00	- 10.00	22000	245
52.13	1.45	0	0

Table A-4b. A-10 Track 2

LATITUDE (DEG)	LONGITUDE (DEG)	ALTITUDE (FT)	AIRSPEED (KNOTS)
37.08	- 76.58	18000	245
42.35	- 71.00	18000	245
43.82	- 66.08	18000	245
47.13	- 55.00	18000	245
48.00	- 50.00	18000	245
49.17	- 45.00	18000	245
50.00	- 40.00	18000	245
50.00	- 35.00	18000	245
50.00	- 30.00	18000	245
50.00	- 25.00	18000	245
50.00	- 20.00	18000	245
50.00	- 15.00	18000	245
50.00	- 10.00	18000	245
50.13	- 5.63	18000	245
52.13	1.45	0	0

Table A-4c. A-10 Track 3

LATITUDE (DEG)	LONGITUDE (DEG)	ALTITUDE (FT)	AIRSPEED (KNOTS)
64.67	-147.12	26000	300
68.45	-155.28	26000	300
68.73	-156.10	6000	300
69.03	-156.90	6000	300
68.73	-156.10	6000	300
68.45	-155.28	26000	300
65.33	-148.30	26000	300
64.67	-147.12	0	0

Table A-4d. A-10 Track 4

LATITUDE (DEG)	LONGITUDE (DEG)	ALTITUDE (FT)	AIRSPEED (KNOTS)
64.67	-147.12	15000	210
65.40	-148.43	15000	210
65.33	-148.30	15000	210
65.40	-148.43	15000	210
65.33	-148.30	15000	210
65.40	-148.43	15000	210
65.33	-148.30	15000	210
65.40	-148.43	15000	210
65.33	-148.30	15000	210
65.40	-148.43	15000	210
65.33	-148.30	15000	210
65.40	-148.43	15000	210
65.33	-148.30	15000	210
65.40	-148.43	15000	210
65.33	-148.30	15000	210
65.40	-148.43	15000	210
65.33	-148.30	15000	210
65.40	-148.43	15000	210
65.33	-148.30	15000	210
65.40	-148.43	15000	210
65.33	-148.30	15000	210
65.40	-148.43	15000	210
65.33	-148.30	15000	210
65.40	-148.43	15000	210
65.33	-148.30	15000	210
65.40	-148.43	15000	210
65.33	-148.30	15000	210
65.40	-148.43	15000	210
65.33	-148.30	15000	210
65.40	-148.43	15000	210
65.33	-148.30	15000	210
65.40	-148.43	15000	210
65.33	-148.30	15000	210
65.40	-148.43	15000	210
65.33	-148.30	15000	210
65.40	-148.43	15000	210
65.33	-148.30	15000	210
65.40	-148.43	15000	210
65.33	-148.30	15000	210
65.40	-148.43	15000	210
65.33	-148.30	15000	210
65.40	-148.43	15000	210
65.33	-148.30	15000	210
65.40	-148.43	15000	210

Table A-4d. A-10 Track 4

LATITUDE (DEG)	LONGITUDE (DEG)	ALTITUDE (FT)	AIRSPEED (KNOTS)
65.33	-148.30	15000	210
65.40	-148.43	15000	210
65.33	-148.30	15000	210
65.40	-148.43	15000	210
65.33	-148.30	15000	210
65.40	-148.43	15000	210
65.33	-148.30	15000	210
65.40	-148.43	15000	210
65.33	-148.30	15000	210
65.40	-148.43	15000	210
65.33	-148.30	15000	210
65.40	-148.43	15000	210
65.33	-148.30	15000	210
65.40	-148.43	15000	210
65.33	-148.30	15000	210
65.40	-148.43	15000	210
65.33	-148.30	15000	210
65.40	-148.43	15000	210
65.33	-148.30	15000	210
65.40	-148.43	15000	210
65.33	-148.30	15000	210
65.40	-148.43	15000	210
65.33	-148.30	15000	210
65.40	-148.43	15000	210
65.33	-148.30	15000	210
65.40	-148.43	15000	210
65.33	-148.30	15000	210
65.40	-148.43	15000	210
65.33	-148.30	15000	210
65.40	-148.43	15000	210
65.33	-148.30	15000	210
65.40	-148.43	15000	210
65.33	-148.30	15000	210
65.40	-148.43	15000	210
65.33	-148.30	15000	210
65.40	-148.43	15000	210
65.33	-148.30	15000	210
65.40	-148.43	15000	210
65.33	-148.30	15000	210
65.40	-148.43	15000	210
65.33	-148.30	15000	210
65.40	-148.43	15000	210
65.33	-148.30	15000	210
65.40	-148.43	15000	210

Table A-4d. A-10 Track 4

LATITUDE (DEG)	LONGITUDE (DEG)	ALTITUDE (FT)	AIRSPEED (KNOTS)
65.33	-148.30	15000	210
65.40	-148.43	15000	210
65.33	-148.30	15000	210
65.40	-148.43	15000	210
65.33	-148.30	15000	210
65.40	-148.43	15000	210
65.33	-148.30	15000	210
65.40	-148.43	15000	210
65.33	-148.30	15000	210
65.40	-148.43	15000	210
65.33	-148.30	15000	210
65.40	-148.43	15000	210
65.33	-148.30	15000	210
65.40	-148.43	15000	210
65.33	-148.30	15000	210
65.40	-148.43	15000	210
65.33	-148.30	15000	210
65.40	-148.43	15000	210
65.33	-148.30	15000	210
65.40	-148.43	15000	210
65.33	-148.30	15000	210
64.92	-147.52	15000	210
64.67	-147.12	0	0

Table A-4e. A-10 Track 5

LATITUDE (DEG)	LONGITUDE (DEG)	ALTITUDE (FT)	AIRSPEED (KNOTS)
64.67	-147.12	6000	205
67.52	-152.93	6000	205
64.90	-147.50	6000	205
64.67	-147.12	0	0

Table A-4f. A-10 Track 6

LATITUDE (DEG)	LONGITUDE (DEG)	ALTITUDE (FT)	AIRSPEED (KNOTS)
64.67	-147.12	6000	320
67.23	-152.28	6000	320
65.03	-147.73	6000	320
64.67	-147.12	0	0

Table A-4g. A-10 Track 7

LATITUDE (DEG)	LONGITUDE (DEG)	ALTITUDE (FT)	AIRSPEED (KNOTS)
40.65	- 86.13	26000	300
45.70	- 86.13	26000	300
46.12	- 86.13	6000	300
46.53	- 86.13	6000	300
46.12	- 86.13	6000	300
45.70	- 86.13	26000	300
41.48	- 86.13	26000	300
30.65	- 86.13	0	0

Table A-4h. A-10 Track 8

LATITUDE (DEG)	LONGITUDE (DEG)	ALTITUDE (FT)	AIRSPEED (KNOTS)
40.65	- 86.13	15000	210
41.57	- 86.13	15000	210
41.48	- 86.13	15000	210
41.57	- 86.13	15000	210
41.48	- 86.13	15000	210
41.57	- 86.13	15000	210
41.48	- 86.13	15000	210
41.57	- 86.13	15000	210
41.48	- 86.13	15000	210
41.57	- 86.13	15000	210
41.48	- 86.13	15000	210
41.57	- 86.13	15000	210
41.48	- 86.13	15000	210

Table A-4h. A-10 Track 8

LATITUDE (DEG)	LONGITUDE (DEG)	ALTITUDE (FT)	AIRSPEED (KNOTS)
41.57	- 86.13	15000	210
41.48	- 86.13	15000	210
41.57	- 86.13	15000	210
41.48	- 86.13	15000	210
41.57	- 86.13	15000	210
41.48	- 86.13	15000	210
41.57	- 86.13	15000	210
41.48	- 86.13	15000	210
41.57	- 86.13	15000	210
41.48	- 86.13	15000	210
41.57	- 86.13	15000	210
41.48	- 86.13	15000	210
41.57	- 86.13	15000	210
41.48	- 86.13	15000	210
41.57	- 86.13	15000	210
41.48	- 86.13	15000	210
41.57	- 86.13	15000	210
41.48	- 86.13	15000	210
41.57	- 86.13	15000	210
41.48	- 86.13	15000	210
41.57	- 86.13	15000	210
41.48	- 86.13	15000	210
41.57	- 86.13	15000	210
41.48	- 86.13	15000	210
41.57	- 86.13	15000	210
41.48	- 86.13	15000	210
41.57	- 86.13	15000	210
41.48	- 86.13	15000	210
41.57	- 86.13	15000	210
41.48	- 86.13	15000	210
41.57	- 86.13	15000	210
41.48	- 86.13	15000	210
41.57	- 86.13	15000	210
41.48	- 86.13	15000	210
41.57	- 86.13	15000	210
41.48	- 86.13	15000	210
41.57	- 86.13	15000	210
41.48	- 86.13	15000	210
41.57	- 86.13	15000	210
41.48	- 86.13	15000	210
41.57	- 86.13	15000	210
41.48	- 86.13	15000	210
41.57	- 86.13	15000	210
41.48	- 86.13	15000	210

Table A-4h. A-10 Track 8

LATITUDE (DEG)	LONGITUDE (DEG)	ALTITUDE (FT)	AIRSPEED (KNOTS)
41.57	- 86.13	15000	210
41.48	- 86.13	15000	210
41.57	- 86.13	15000	210
41.48	- 86.13	15000	210
41.57	- 86.13	15000	210
41.48	- 86.13	15000	210
41.57	- 86.13	15000	210
41.48	- 86.13	15000	210
41.57	- 86.13	15000	210
41.48	- 86.13	15000	210
41.57	- 86.13	15000	210
41.48	- 86.13	15000	210
41.57	- 86.13	15000	210
41.48	- 86.13	15000	210
41.57	- 86.13	15000	210
41.48	- 86.13	15000	210
41.57	- 86.13	15000	210
41.48	- 86.13	15000	210
41.57	- 86.13	15000	210
41.48	- 86.13	15000	210
41.57	- 86.13	15000	210
41.48	- 86.13	15000	210
41.57	- 86.13	15000	210
41.48	- 86.13	15000	210
41.57	- 86.13	15000	210
41.48	- 86.13	15000	210
41.57	- 86.13	15000	210
41.48	- 86.13	15000	210
41.57	- 86.13	15000	210
41.48	- 86.13	15000	210
41.57	- 86.13	15000	210
41.48	- 86.13	15000	210
41.57	- 86.13	15000	210
41.48	- 86.13	15000	210
41.57	- 86.13	15000	210
41.48	- 86.13	15000	210
41.57	- 86.13	15000	210
41.48	- 86.13	15000	210
41.57	- 86.13	15000	210
41.48	- 86.13	15000	210
41.57	- 86.13	15000	210
41.48	- 86.13	15000	210
41.57	- 86.13	15000	210

Table A-4h. A-10 Track 8

LATITUDE (DEG)	LONGITUDE (DEG)	ALTITUDE (FT)	AIRSPEED (KNOTS)
41.48	- 86.13	15000	210
41.57	- 86.13	15000	210
41.48	- 86.13	15000	210
41.57	- 86.13	15000	210
41.48	- 86.13	15000	210
41.57	- 86.13	15000	210
41.48	- 86.13	15000	210
41.57	- 86.13	15000	210
41.48	- 86.13	15000	210
40.97	- 86.13	15000	210
40.65	- 86.13	0	0

Table A-4i. A-10 Track 9

LATITUDE (DEG)	LONGITUDE (DEG)	ALTITUDE (FT)	AIRSPEED (KNOTS)
40.65	- 86.13	6000	205
44.40	- 86.13	6000	205
40.93	- 86.13	6000	205
40.65	- 86.13	0	0

Table A-4j. A-10 Track 10

LATITUDE (DEG)	LONGITUDE (DEG)	ALTITUDE (FT)	AIRSPEED (KNOTS)
40.65	- 86.13	6000	320
44.03	- 86.13	6000	320
41.10	- 86.13	6000	320
40.65	- 86.13	0	0

Table A-5a. F-15 Track 1

LATITUDE (DEG)	LONGITUDE (DEG)	ALTITUDE (FT)	AIRSPEED (KNOTS)
46.33	- 87.38	29000	480
46.37	- 79.42	29000	480
47.43	- 75.28	29000	480
48.33	- 71.00	29000	480
50.22	- 66.27	29000	480
53.45	- 60.00	29000	480
55.00	- 50.00	29000	480
55.00	- 45.00	29000	480
55.00	- 40.00	29000	480
55.00	- 35.00	29000	480
55.00	- 30.00	29000	480
55.50	- 25.00	29000	480
56.00	- 20.00	29000	480
56.00	- 15.00	29000	480
56.00	- 10.00	29000	480
55.43	- 5.70	29000	480
49.95	6.55	0	0

Table A-5b. F-15 Track 2

LATITUDE (DEG)	LONGITUDE (DEG)	ALTITUDE (FT)	AIRSPEED (KNOTS)
61.25	-149.77	29000	480
61.00	-151.00	29000	480
59.62	-156.50	29000	480
59.23	-157.80	29000	480
59.00	-158.55	29000	480
58.65	-162.07	29000	480
57.38	-165.00	29000	480
55.42	-168.97	29000	480
54.83	-170.00	29000	480
53.45	-175.00	29000	480
51.75	-180.00	29000	480
49.00	175.00	29000	480
47.65	170.00	29000	480
46.00	165.00	29000	480
44.00	160.00	29000	480
41.70	155.00	29000	480
39.00	150.00	29000	480
37.37	145.00	29000	480
36.73	140.35	29000	480
35.27	136.92	29000	480
33.57	130.45	0	0

Table A-5c. F-15 Track 3

LATITUDE (DEG)	LONGITUDE (DEG)	ALTITUDE (FT)	AIRSPEED (KNOTS)
61.25	-149.77	39000	500
69.10	-156.62	39000	500
62.57	-150.65	39000	500
61.25	-149.77	0	0

Table A-5d. F-15 Track 4

LATITUDE (DEG)	LONGITUDE (DEG)	ALTITUDE (FT)	AIRSPEED (KNOTS)
61.25	-146.77	30000	500
66.50	-153.85	30000	500
63.88	-151.58	30000	500
63.22	-151.12	15000	500
61.90	-150.20	15000	500
61.25	-146.77	0	0

Table A-5e. F-15 Track 5

LATITUDE (DEG)	LONGITUDE (DEG)	ALTITUDE (FT)	AIRSPEED (KNOTS)
61.25	-149.77	30000	500
69.10	-156.60	30000	500
69.73	-157.37	15000	500
68.48	-155.88	15000	500
67.82	-155.15	30000	500
65.23	-152.70	30000	500
64.58	-152.17	15000	500
61.93	-150.22	15000	500
61.25	-149.77	0	0

Table A-5f. F-15 Track 6

LATITUDE (DEG)	LONGITUDE (DEG)	ALTITUDE (FT)	AIRSPEED (KNOTS)
61.25	-149.77	39000	500
76.40	-170.50	39000	500
76.93	-172.25	27000	500
78.97	178.58	27000	500
78.48	-178.83	39000	500
63.90	-151.63	39000	500
63.23	-151.13	15000	500
61.92	-150.20	15000	500
61.25	-149.77	0	0

Table A-5g. F-15 Track 7

LATITUDE (DEG)	LONGITUDE (DEG)	ALTITUDE (FT)	AIRSPEED (KNOTS)
48.27	-101.28	39000	500
54.58	- 92.33	39000	500
49.48	-100.00	39000	500
48.27	-101.28	0	0

Table A-5h. F-15 Track 8

LATITUDE (DEG)	LONGITUDE (DEG)	ALTITUDE (FT)	AIRSPEED (KNOTS)
48.27	-101.28	30000	500
52.60	- 95.63	30000	500
50.55	- 98.60	30000	500
50.02	- 99.30	15000	500
48.95	-100.68	15000	500
48.27	-101.28	0	0

Table A-5i. F-15 Track 9

LATITUDE (DEG)	LONGITUDE (DEG)	ALTITUDE (FT)	AIRSPEED (KNOTS)
48.27	-101.28	30000	500
54.58	- 92.32	30000	500
55.05	- 91.45	15000	500
54.08	- 93.18	15000	500
53.60	- 94.02	30000	500
51.58	- 97.12	30000	500
51.07	- 97.87	15000	500
48.95	-100.68	15000	500
48.27	-101.28	0	500

Table A-5j. F-15 Track 10

LATITUDE (DEG)	LONGITUDE (DEG)	ALTITUDE (FT)	AIRSPEED (KNOTS)
48.27	-101.28	39000	500
59.78	- 80.32	39000	500
60.15	- 79.22	27000	500
61.57	- 74.30	27000	500
61.23	- 75.57	39000	500
51.58	- 97.12	39000	500
51.07	- 97.87	15000	500
48.95	-100.68	15000	500
48.27	-101.28	0	0

Table A-6a. NASA GASP Data - 25 Nov 1978

LATITUDE (DEG)	LONGITUDE (DEG)	ALTITUDE (FT)	AIRSPEED (KNOTS)
26.7	50.6	35000.0	478.0
29.5	44.0	35000.0	478.0
32.0	37.5	35000.0	478.0
35.0	30.0	35000.0	478.0
38.9	16.0	35000.0	478.0
39.0	15.0	37000.0	478.0
40.7	7.0	37000.0	478.0
41.8	-2.0	37000.0	478.0
42.5	-7.0	37000.0	478.0
42.7	-8.0	35000.0	478.0
43.0	-9.0	35000.0	478.0
43.2	-12.0	35000.0	478.0
43.6	-15.0	35000.0	478.0
43.8	-17.5	37000.0	478.0
44.0	-18.0	41000.0	478.0
44.2	-26.0	41000.0	478.0
44.7	-34.0	41000.0	478.0
45.5	-43.0	41000.0	478.0
46.2	-52.5	41000.0	478.0
46.4	-57.0	41000.0	478.0
46.0	-59.0	43000.0	478.0
45.8	-60.5	44000.0	478.0
43.2	-68.0	43000.0	478.0
43.6	-69.0	43000.0	478.0
40.6	-73.8	0.0	0.0

Table A-6b. NASA GASP Data - 1 Dec 1978

LATITUDE (DEG)	LONGITUDE (DEG)	ALTITUDE (FT)	AIRSPEED (KNOTS)
26.7	50.6	35250.0	478.0
29.2	43.0	35250.0	478.0
31.8	36.0	35250.0	478.0
36.0	32.5	35250.0	478.0
41.1	26.0	35250.0	478.0
43.3	20.0	35250.0	478.0
44.0	18.0	39000.0	478.0
47.8	15.0	39000.0	478.0
51.6	5.0	39000.0	478.0
54.7	-5.0	39000.0	478.0
57.0	-15.0	39000.0	478.0
57.7	-27.5	39000.0	478.0
56.8	-40.0	39000.0	478.0
54.5	-52.0	39000.0	478.0
54.2	-53.0	42900.0	478.0
51.7	-58.0	42900.0	478.0
47.8	-65.0	42900.0	478.0
43.0	-72.0	42900.0	478.0
42.5	-73.0	42900.0	478.0
40.6	-73.8	0.0	0.0

APPENDIX B FUEL USAGE SEQUENCE

The fuel usage sequences were extracted from USAF Technical Orders (References 5-14, and 40-45), the contents of this section are as follows:

TABLE B-1

Typical B-52 Fuel Consumption Procedure

1	TAKEOFF		
	Aft Body	to Engines	1,2
	No. 2 Main	to Engines	3,4
	No. 3 Main	to Engines	5,6
	Ctr Wing	to Engines	7,8
2	CLIMB		
	Aft Body	to Engines	1,2,3,4
	Ctr Wing	to Engines	5,6,7,8
3	Aft Body	to Engines	1,2,3,4
	Fwd Body	to Engines	5,6,7,8
4	Mid Body	to Engines	
5	Aft Body (Down to 13,000=)	to All Engines	
6	Aft Body	to Engines	1,2,7,8
	No. 2 Main	to Engines	3,4
	No. 3 Main	to Engines	5,6,
7	Main Tanks (To Green Bond in Mains 1 & 4)	to All Engines	
8	L. H. External	to Engines	1,2
	No. 2 Main	to Engines	3,4
	No. 3 Main	to Engines	5,6
	R.H. External	to Engines	7,8
9	L.H. Outboard 5,000=)	to Engines	1,2
	No. 2 Main 5,000=	to Engines	3,4
	No. 3 Main 5,000=	to Engines	5,6
	R.H. Outboard 5,000=	to Engines	7,8
10	L.H. Outboard	to Engines	1,2,3,4
	R.H. Outboard	to Engines	5,6,7,8
11	Main Tanks	to All Engines	

AD-A152 801 FUEL FREEZE POINT INVESTIGATIONS(U) BOEING MILITARY AIRPLANE CO SEATTLE WA L A DESMARAIS ET AL. JUL 84 D180-28285-1 AFWAL-TR-84-2049 F33615-82-C-2262 3/3

UNCLASSIFIED F/G 21/4 NL

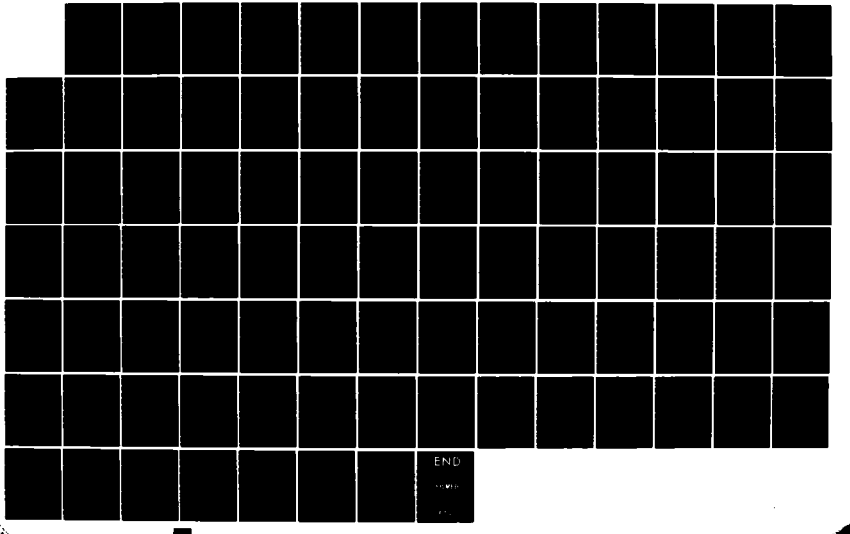

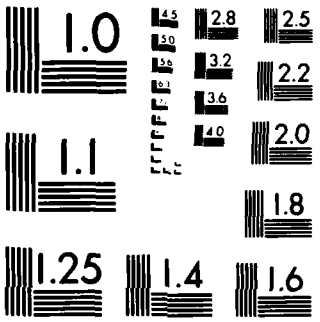

TABLE B-2.

C-141 FUEL USAGE SEQUENCE

The sequence for normal fuel usage is:

1. For take-off, use tank-to-engine feed from auxiliary tanks. Burn approximately 1,050 pounds per tank.

2. Use fuel equally from extended range tanks until empty.

3. Use fuel equally from auxiliary tanks until auxiliary tanks No. 2 and No. 3 are empty.

4. Use fuel equally from auxiliary tanks No. 1 and No. 4 and main tanks No. 2 and No. 3 until auxiliary tanks No. 1 and No. 4 are empty.

5. Use fuel equally from all main tanks.

Table B-3.

C-135 Fuel Management Sequence

❶ TOTAL RAMP FUEL							FUEL VALVE POSITIONS	FLIGHT CONDITION	FUEL QUANTITY AND TANK USE
UP to 50,000	50,000 to 72,000	72,000 to 99,500	99,500 to 109,500	109,500 to 119,500	119,500 to 136,000	136,000 or greater			
1	1	1	1	1	1	1	1, 3, & 4, Tank to Engine, 2 Tank to Manifold	START ENGINES, TAXI and TAKEOFF	Mains 1, 2, 3, and 4 ❷
			2	2	2	2	1, 2, 3 & 4 Tank to Manifold	ENROUTE CLIMB and CRUISE	10,000 lb from Center Wing
					3	3		CRUISE	10,000 lbs from Aft Body
						4			Start with Forward Body and use in ratio of 1 lb from Forward Body and 1-1/2 lb from Aft Body. Do not exceed 6700 lb from Forward Body or 10,000 lb from Aft Body. Use until empty. ❻
					4				Forward Body, use until empty ❻
			3	3	5				Aft Body, use until empty
2	2	2	4	4	6	5			Center Wing retain 10,000 lb until after final takeoff. This step may be deleted if the desired cg for takeoff can be maintained.
2A	2A	2A	4A	4A	6A	5A			Center Wing, use until empty ❸
	3	3	5	5	7	6			Use tanks 1 & 4 to all engines until quantities in 1 & 1R equal quantity in 2, and quantity in 4 & 4R equal quantity in 3
	4	4	6	6	8	7	1R & 4R Open	❹	Drain reserves 1 & 4
3	5	5	7	7	9	8	1, 3 & 4 Tank to Engine, 2 Tank to Manifold	LANDING ❺	Use until completion of mission

❶ Determine ramp fuel aboard, select appropriate column, and follow indicated steps

❷ Whenever the airplane gross weight is greater than the maximum brake release gross weight for takeoff, fuel must be used from a body tank during ground operation.

❸ Sequence of this step dependent upon mission takeoff requirements

❹ Do not accomplish at G.W. in excess of 240,000 lb for 1 ▶ 15 or 245,000 lb for 16 ▶ (2.5 g)
Do not accomplish at G.W. in excess of 268,000 lb for 1 ▶ 15 or 293,000 lb for 16 ▶ (2.0 g)

❺ For any TAKEOFF or LANDING with less than 10,500 lb in any main tank, all valves Tank to Manifold and all boost pumps ON

❻ Retaining some forward body fuel may be required for CG control.

TABLE B-4

A-10 FUEL MANAGEMENT SEQUENCE

The sequence for normal fuel usage is:

1. Use fuel from wing tanks until quantity in either tank drops by approximately 400 lb. Fuel feeds from external tanks to refill wings. Repeat cycle until external tanks and wing tanks are empty.

2. Wing tank boost pumps operate at higher pressure and override main tank pumps to automatically empty the wing tanks first.

3. External tanks will feed automatically if fuselage tank quantity falls below 500 lb.

TABLE B-5

F-15 FUEL MANAGEMENT SEQUENCE

The sequence for normal fuel usage is:

1. Fuel transfers from Tank 1 and wing tanks (simultaneously) into Tanks 2, 3A, and 3B to keep these full.

2. External tanks feed into Tank 1 after fuel level in Tank 1 reaches approximately 1560 lb. until external tanks are empty.

3. Wing external tanks empty first, fuel transferred to centerline tank when not refueling internal tanks.

4. After fuel level reaches 1560 lb. in Tank 1, fuel is used from wing tanks until empty.

5. Use fuel from Tank 1 until empty, then finally from Tanks 2, 3A, and 3B until empty.

TABLE B-6

CRITICAL TANK FUEL USAGE

	TANK DEPTH (IN)	TIME (HRS)	ULLAGE DEPTH (IN)	PERCENT OF TOTAL
B-52	18.0	0.0	0.0	0.0
	Start of Withdrawal	14.6	0.0	0.0
		15.43	9.0	50.0
		15.65	17.0	94.4
C-141	19.5	0.0	0.0	0.0
	Start of Withdrawal	8.73	0.0	0.0
		10.00	11.7	60.0
		11.90	18.5	94.9
KC-135	15.0	0.0	0.0	0.0
	Start of Withdrawal	5.20	0.0	0.0
		5.48	14.0	93.3
A-10	17.5	0.0	0.0	0.0
(Track 1)		0.08	0.91	5.0
		12.37	0.91	5.0
		14.52	16.5	94.0
		15.30	16.5	94.0
F-15	8.9	0.0	0.0	0.0
(Track 3)		0.53	4.7	52.8
		1.11	8.4	94.0
		2.00	8.4	94.0

APPENDIX C ATMOSPHERIC TEMPERATURE EXPOSURE AND STATISTICAL ANALYSIS

Four figures are included to define the thermal exposure and statistical analysis of each route:

a 15 Worst Case Cold Days
b Worst Case Cold Day
c Number of Exceedances
d Number of Encounters

Figure C-1. B-52 Track 1

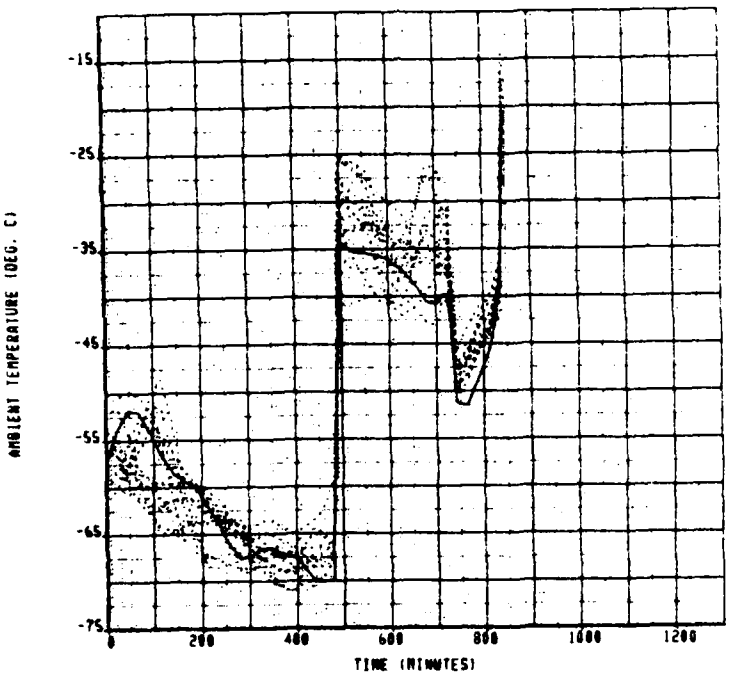

a. 15 Worst Case Cold Days

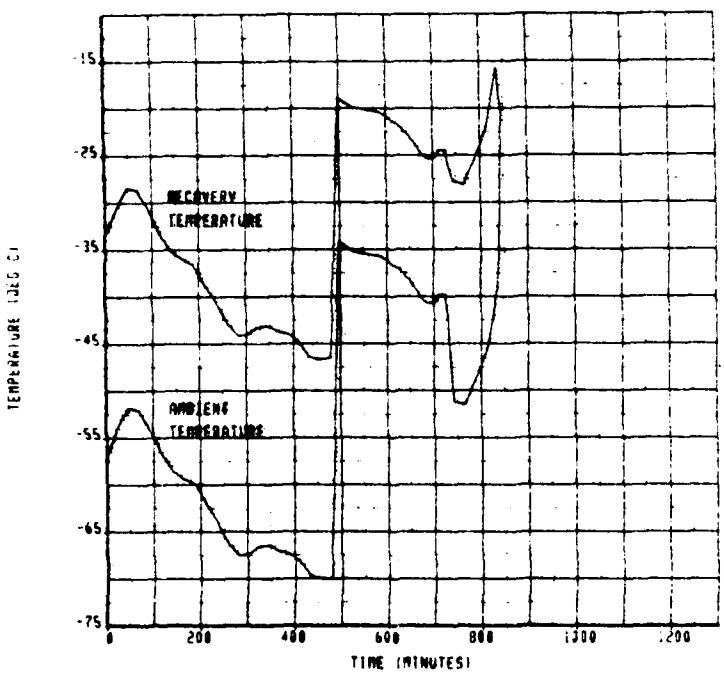

b. Worst Case Cold Day

B-52 TRACK 1

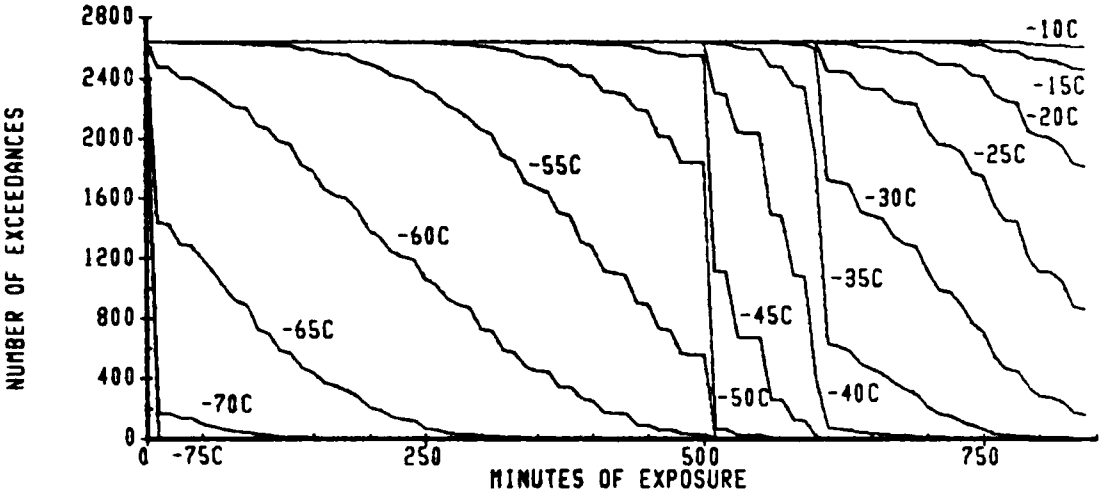

c. Number of Exceedances

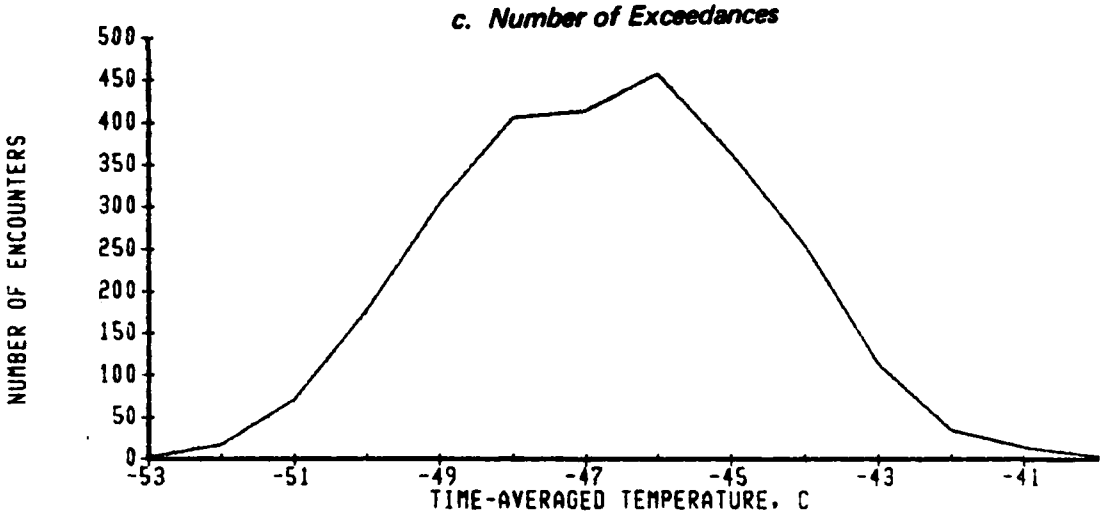

d. Number of Encounters

CALC		17MAY83	REVISED	DATE	B-52 TRACK 1	
CHECK						
APPD.						
APPD.					THE BOEING COMPANY	PAGE 191

Figure C-2. B-52 Track 3

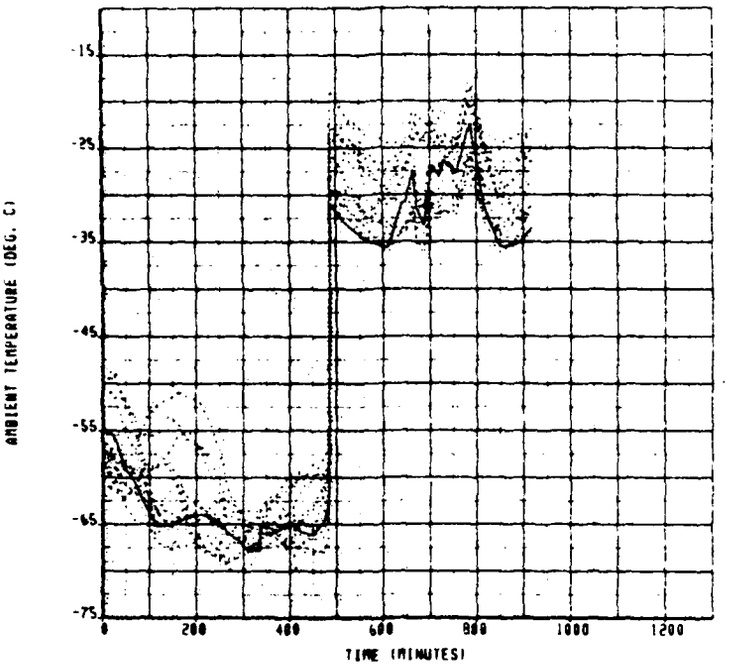

a. 15 Worst Case Cold Days

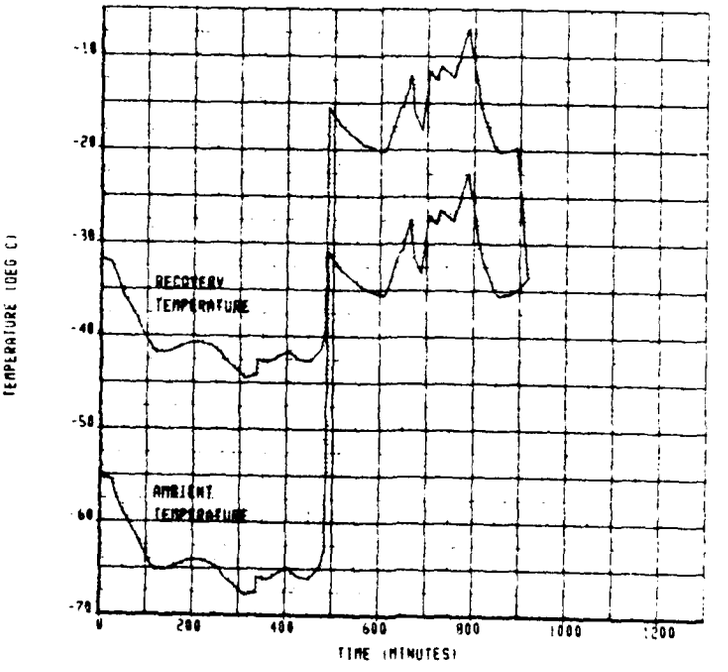

b. Worst Case Cold Day

B-52 TRACK 3

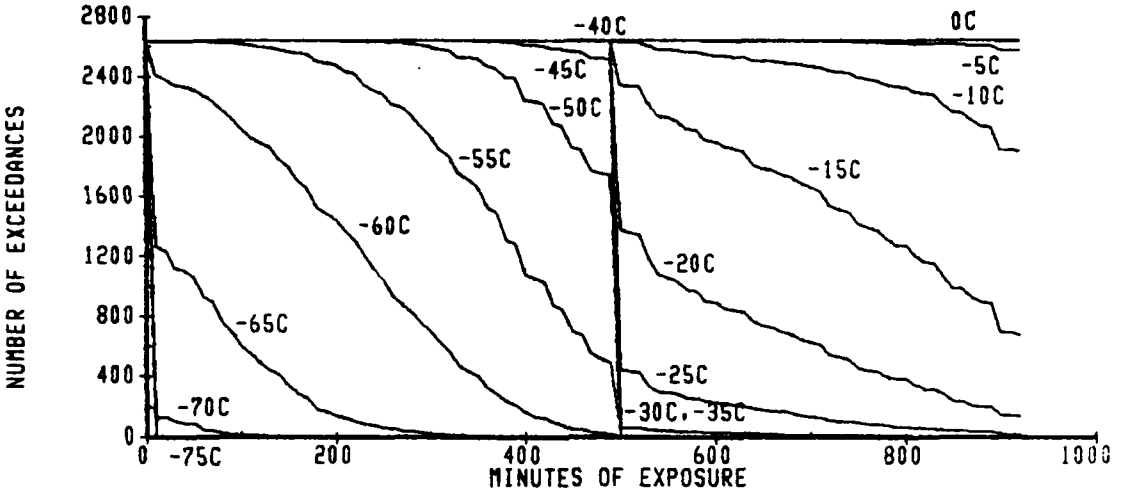

c. Number of Exceedances

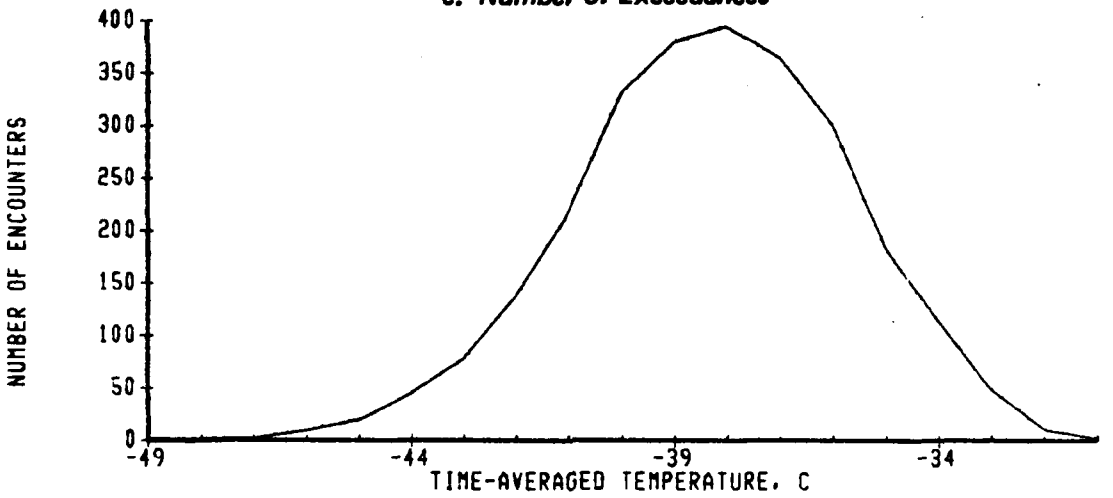

d. Number of Encounters

CALC		17MAY83	REVISED	DATE	B-52 TRACK 3	
CHECK						
APPD.						
APPD.					THE BOEING COMPANY	PAGE 193

Figure C-3. B-52 Track 4

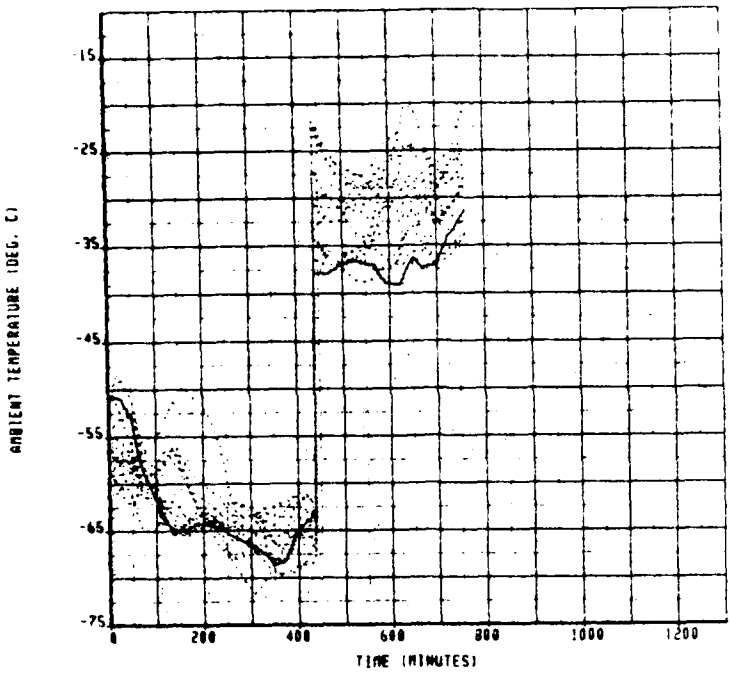

a. 15 Worst Case Cold Days

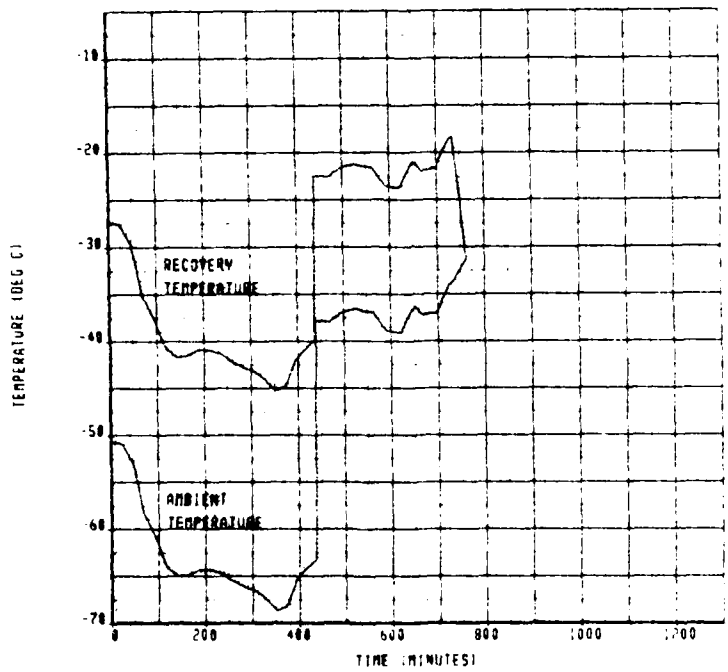

b. Worst Case Cold Day

B-52 TRACK 4

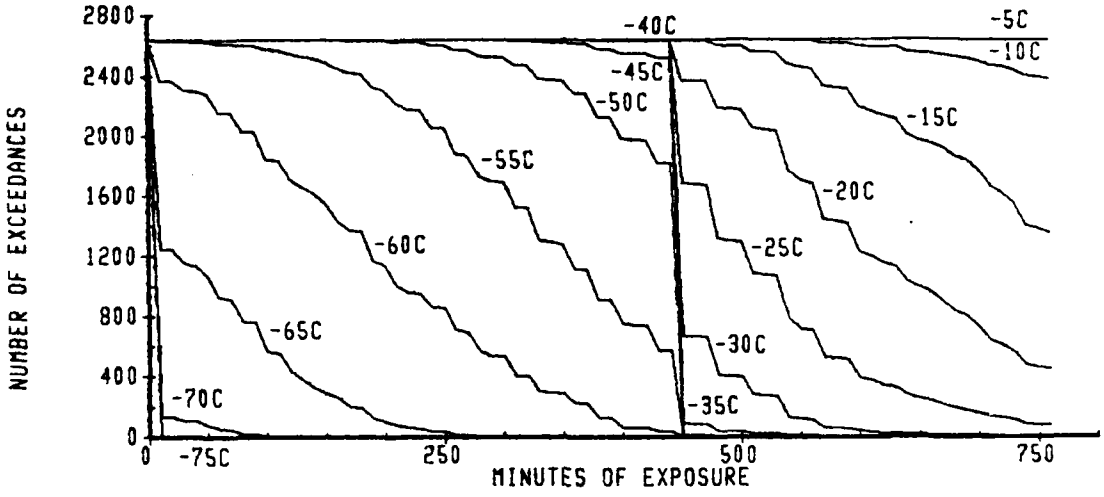

c. Number of Exceedances

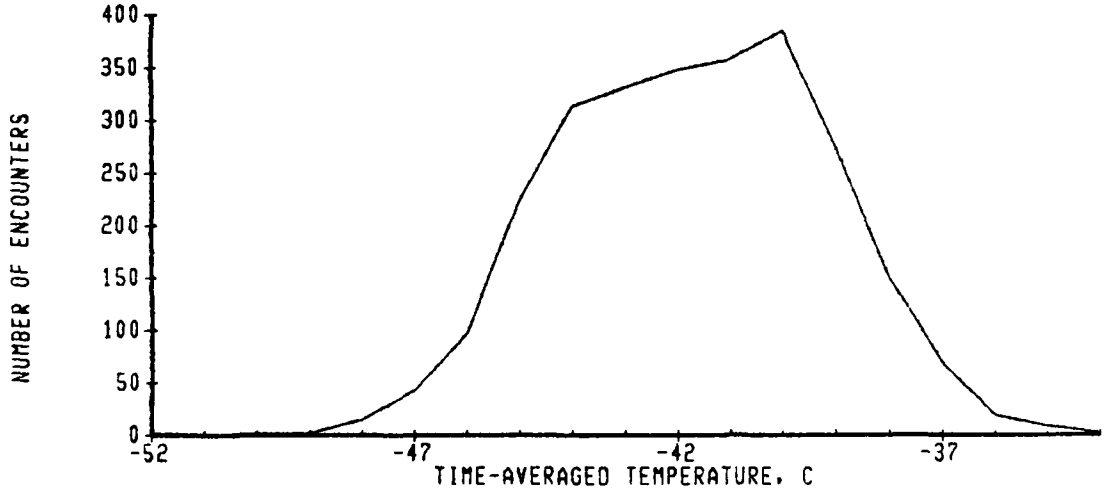

d. Number of Encounters

CALC		17MAY83	REVISED	DATE	B-52 TRACK 4	
CHECK						
APPD.						
APPD.					THE BOEING COMPANY	PAGE 195

Figure C-4. C-141 Track 1

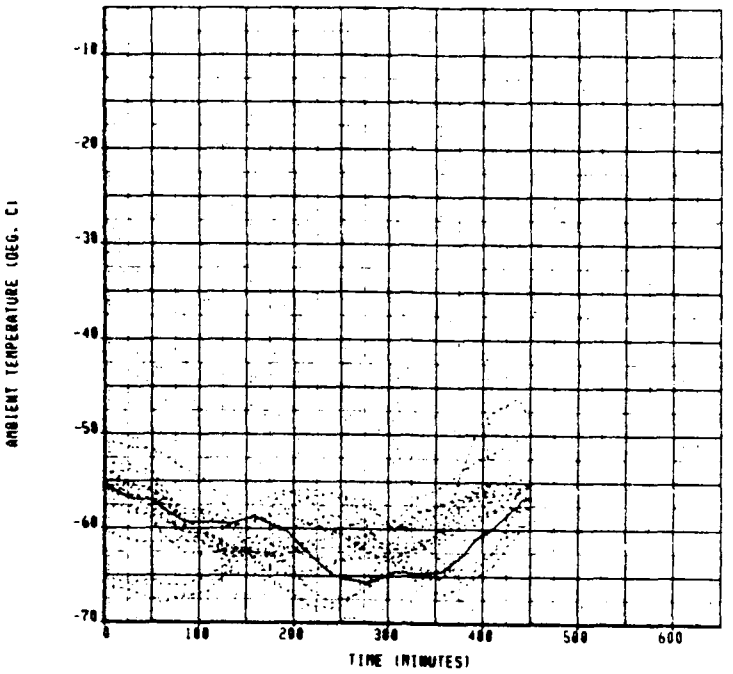

a. 15 Worst Case Cold Days

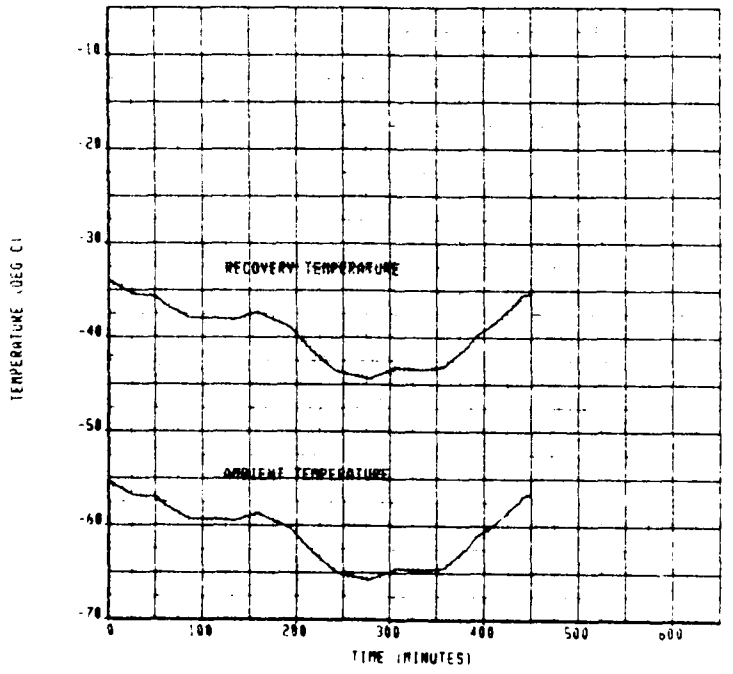

b. Worst Case Cold Day

C-141 TRACK 1

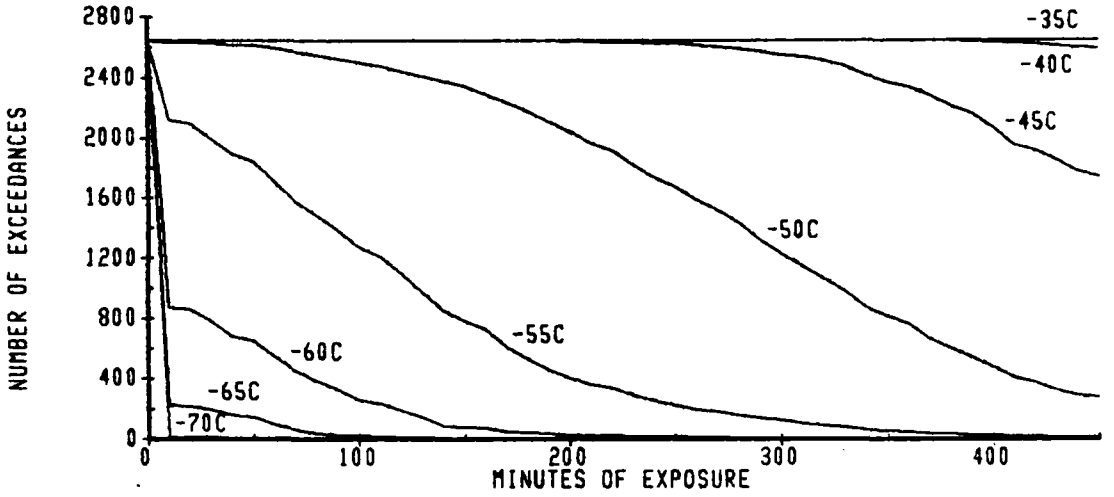

c. Number of Exceedances

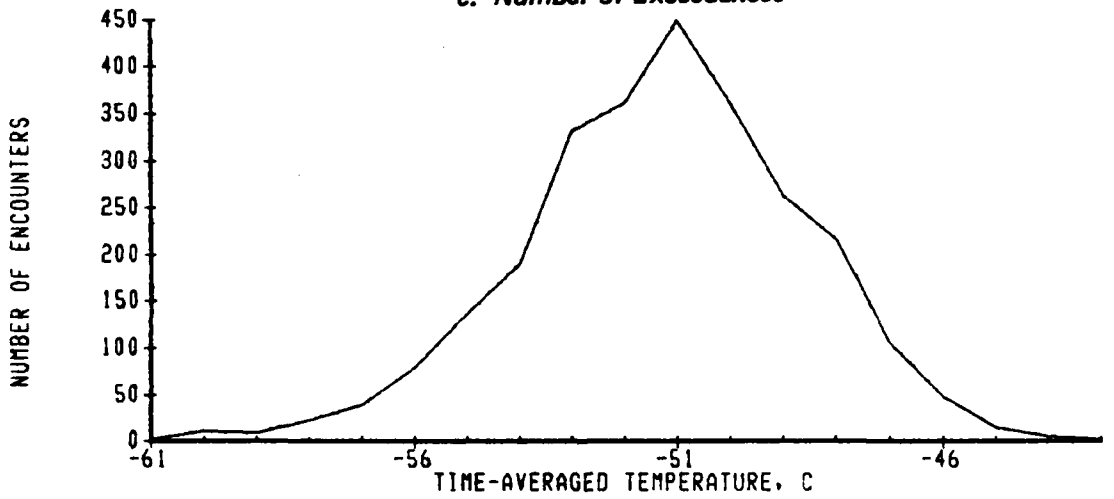

d. Number of Encounters

CALC		13MAY83	REVISED	DATE	C-141 TRACK 1	
CHECK						
APPD.						
APPD.					THE BOEING COMPANY	PAGE 197

Figure C-5. C-141 Track 8

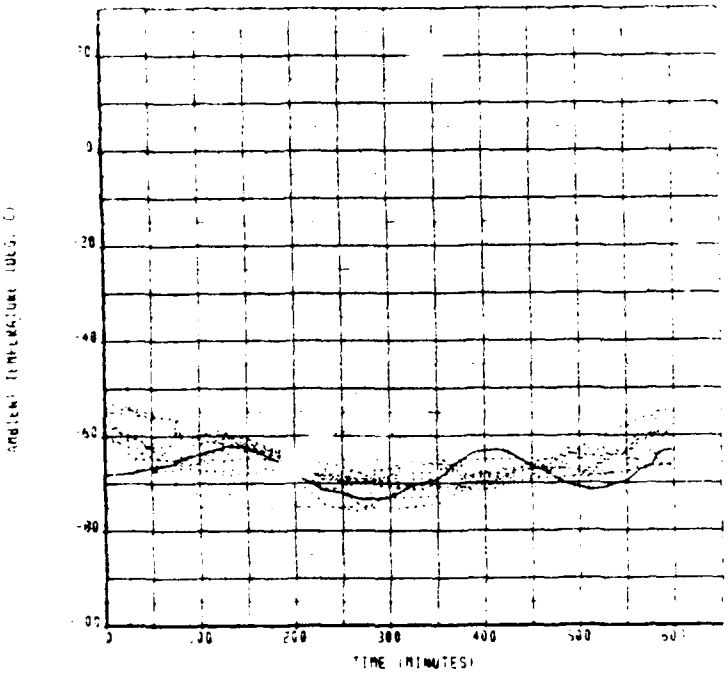

a. 15 Worst Case Cold Days

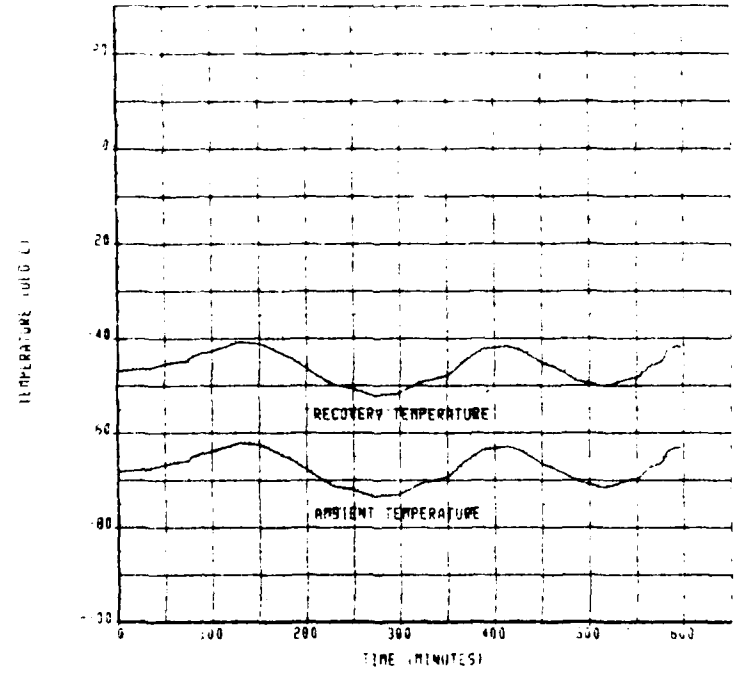

b. Worst Case Cold Day

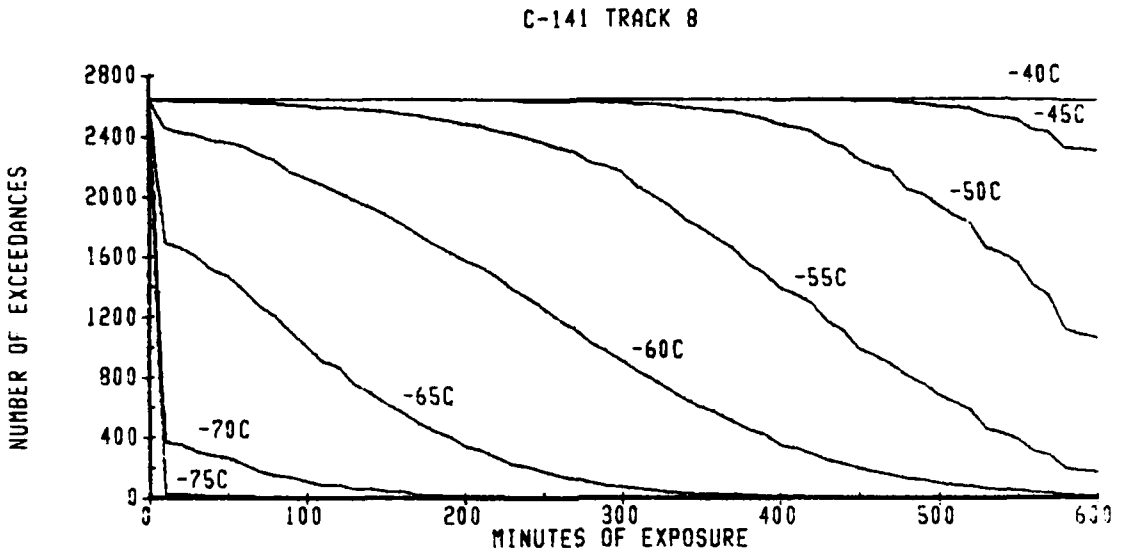

c. Number of Exceedances

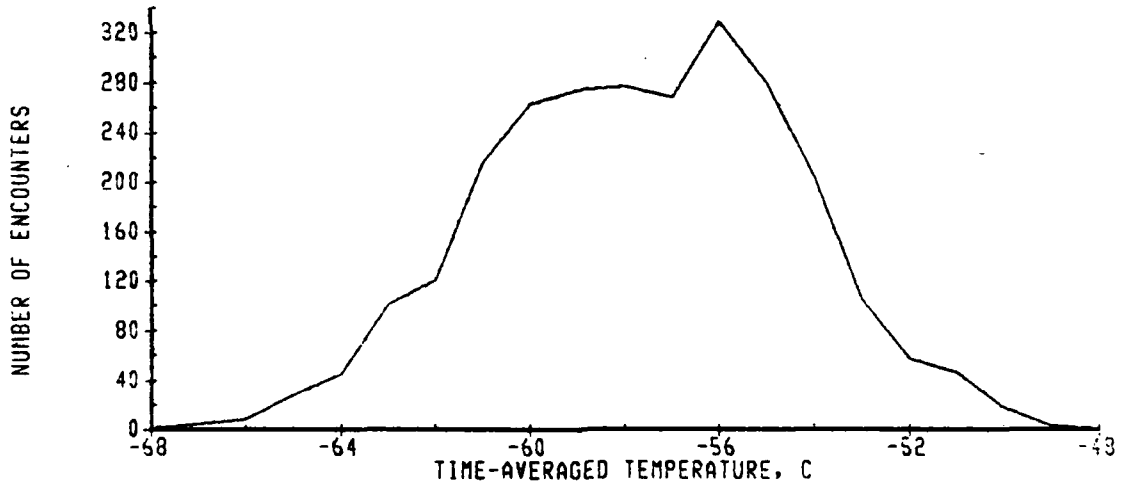

d. Number of Encounters

Figure C-6. C-141 Track 10

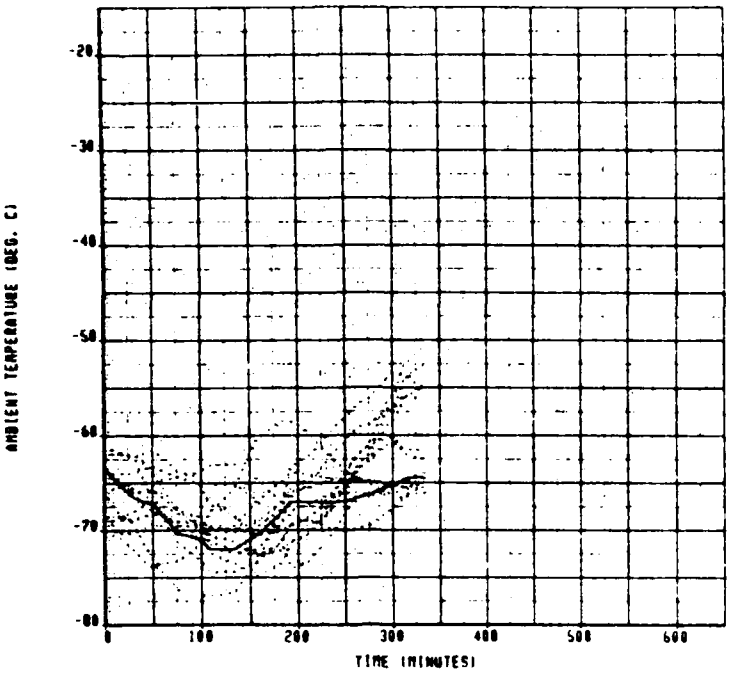

a. 15 Worst Case Cold Days

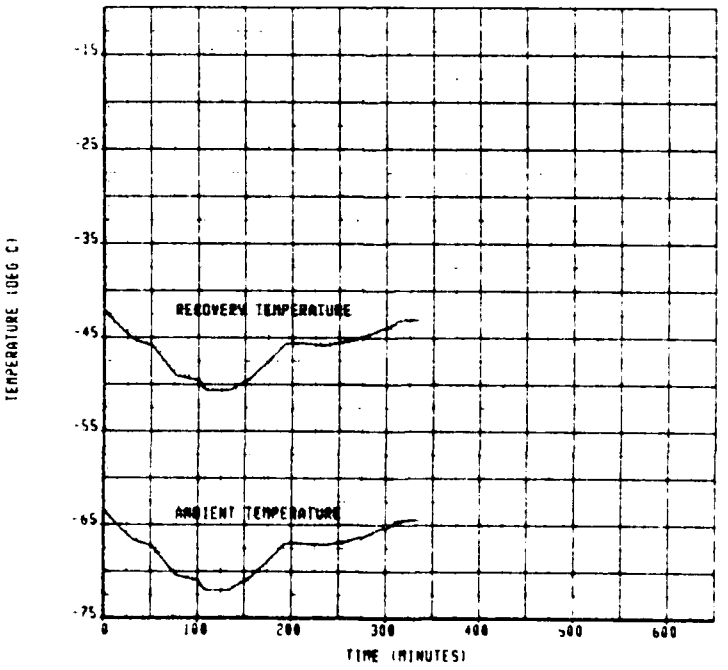

b. Worst Case Cold Day

C-141 TRACK 10

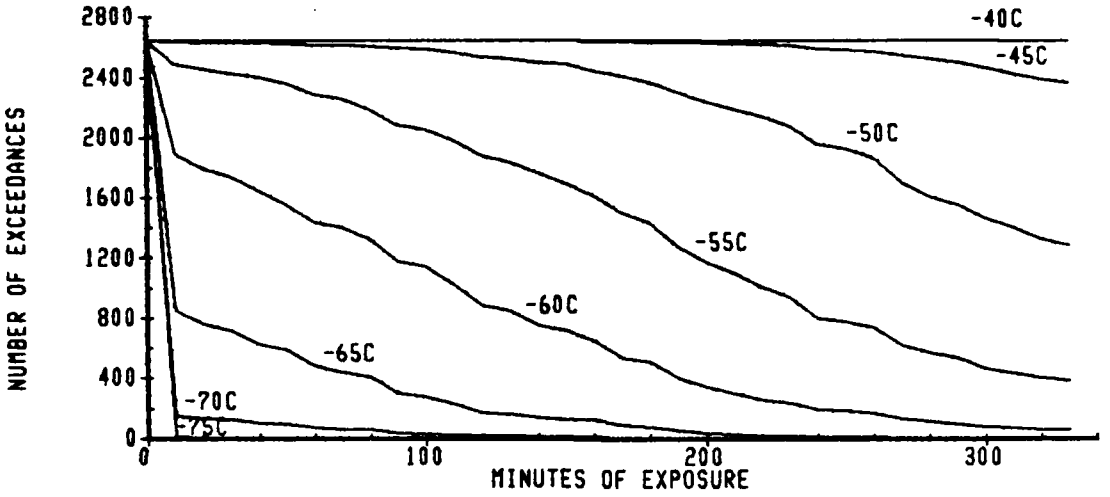

c. Number of Exceedances

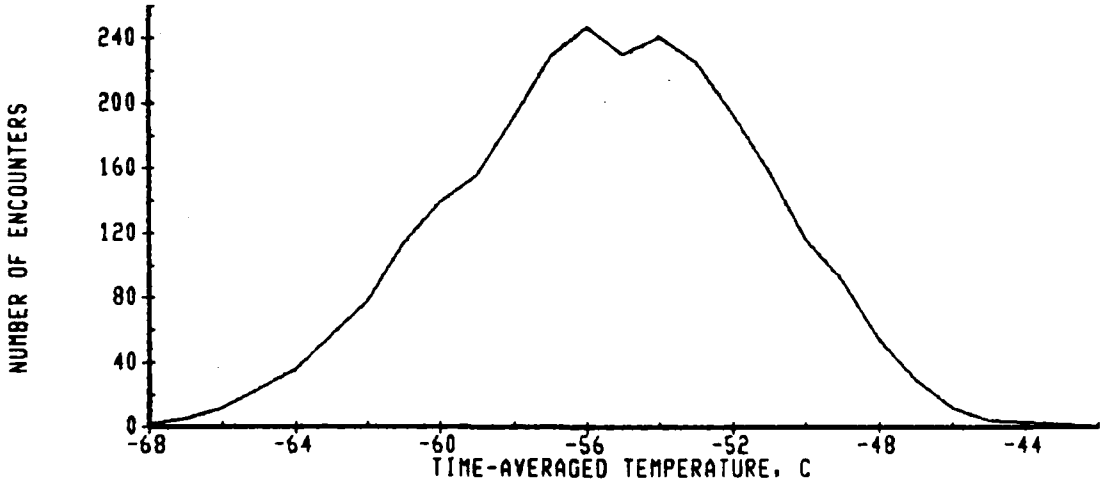

d. Number of Encounters

CALC		13MAY83	REVISED	DATE	C-141 TRACK 10	
CHECK						
APPD.						
APPD.					THE BOEING COMPANY	PAGE 201

Figure C-7. KC-135 Track 3

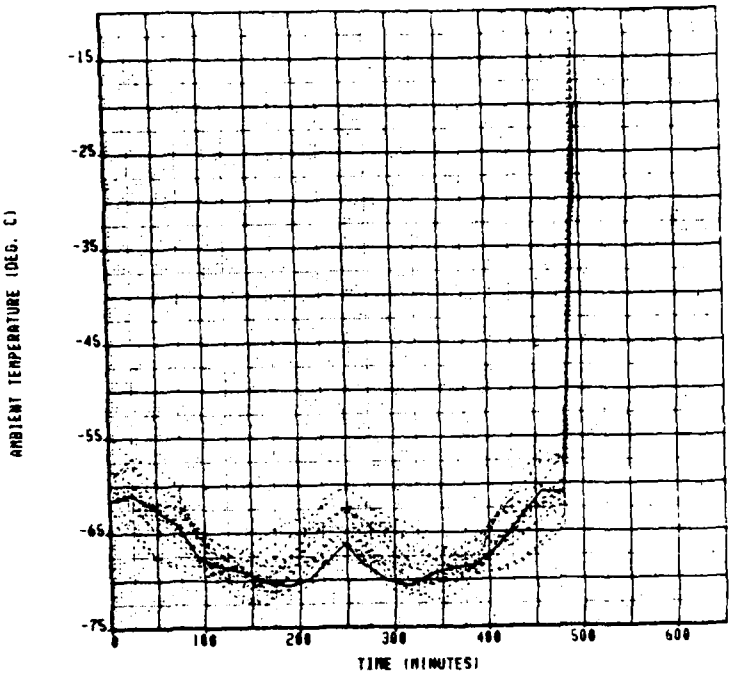

a. 15 Worst Case Cold Days

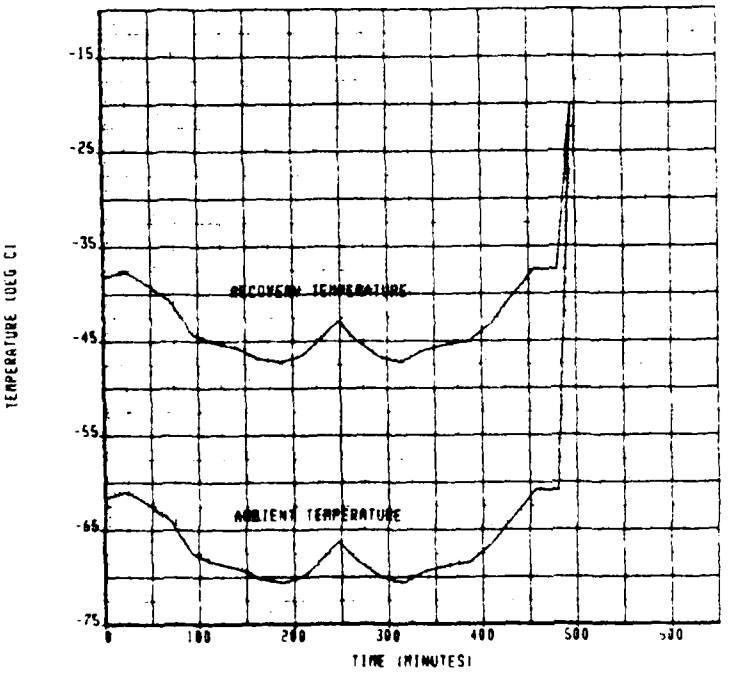

b. Worst Case Cold Day

KC-135 TRACK 3

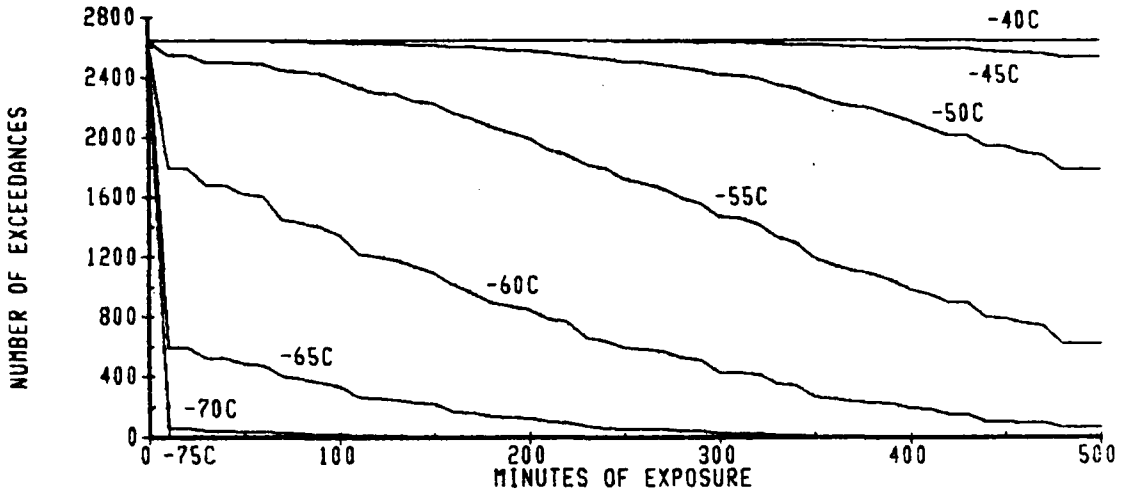

c. Number of Exceedances

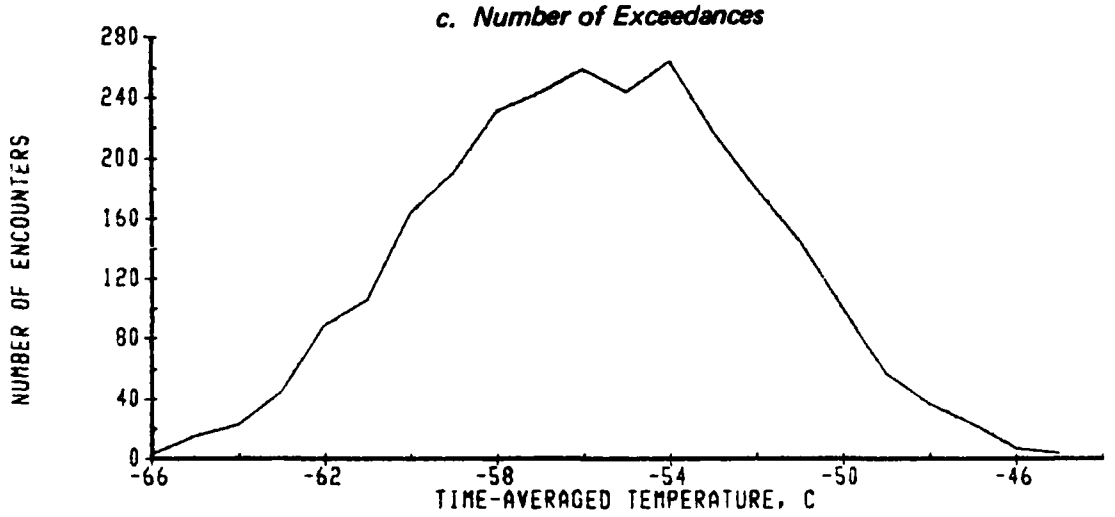

d. Number of Encounters

CALC		13MAY83	REVISED	DATE	KC-135 TRACK 3	
CHECK						
APPD.						
APPD.					THE BOEING COMPANY	PAGE 203

Figure C-8. KC-135 Track 5

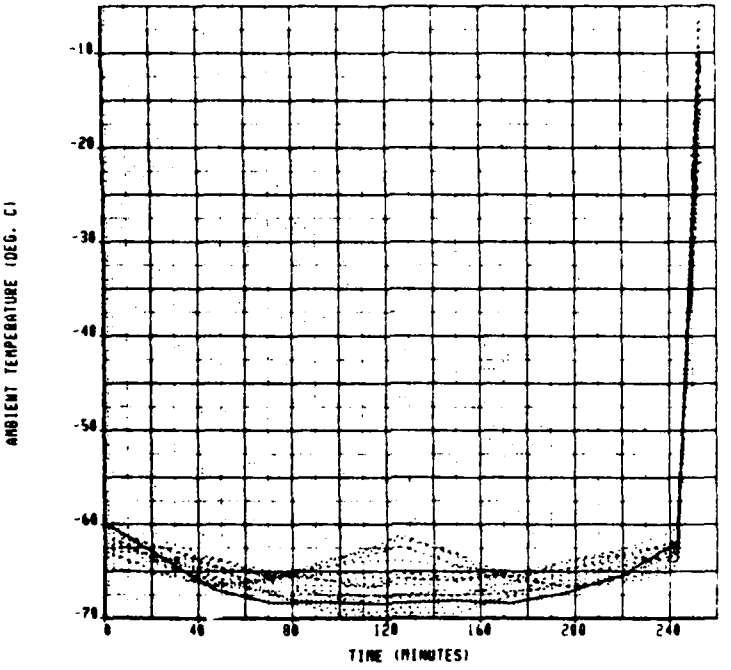

a. 15 Worst Case Cold Days

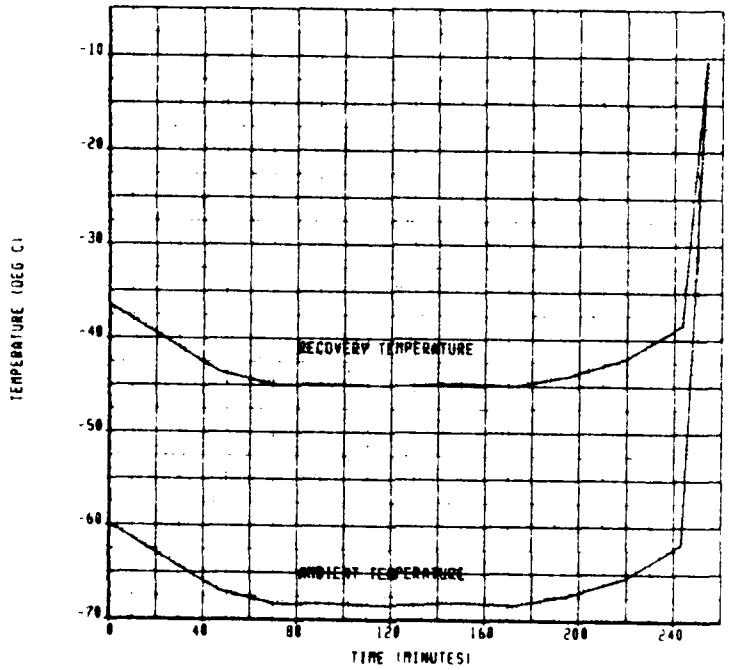

b. Worst Case Cold Day

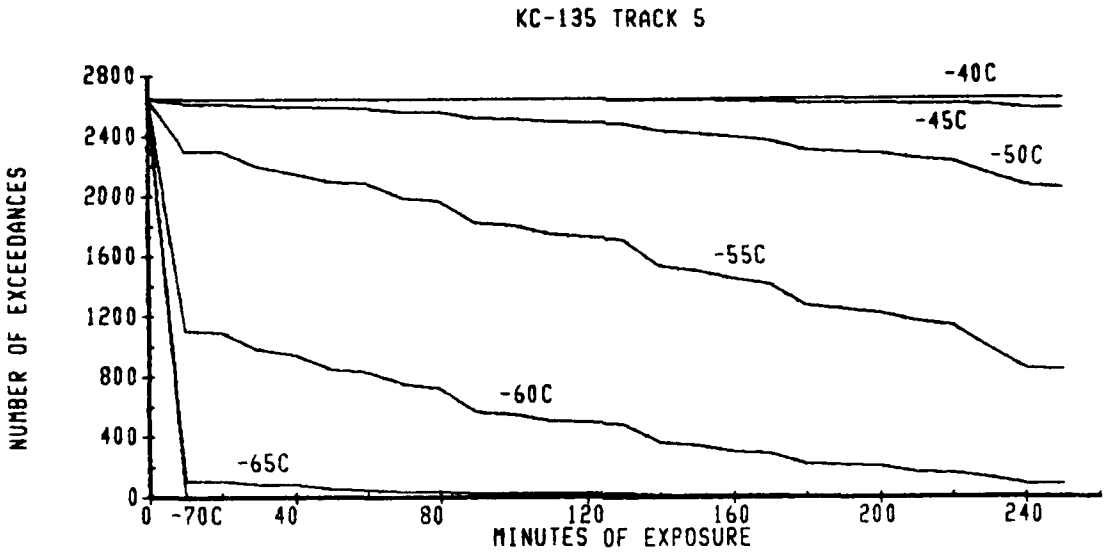

c. Number of Exceedances

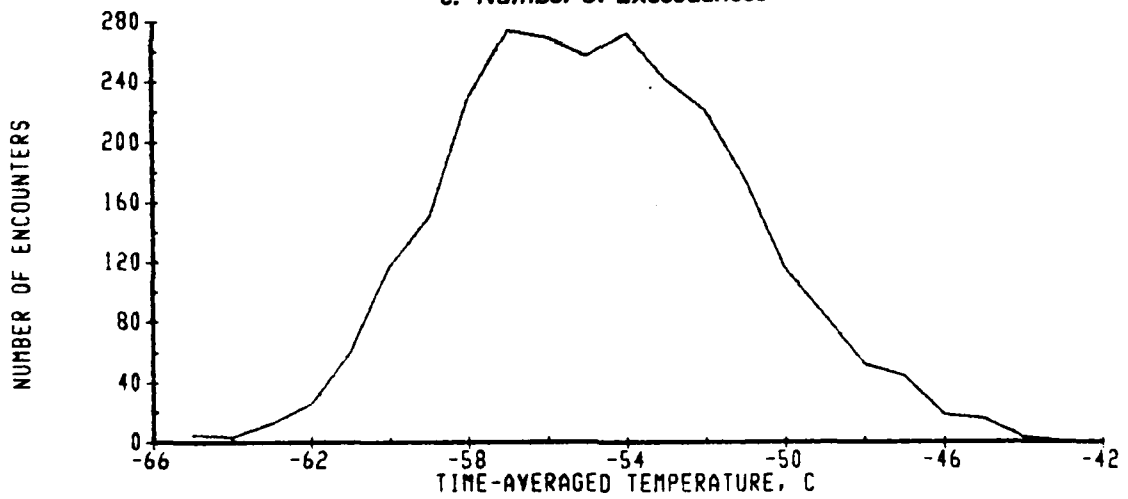

d. Number of Encounters

CALC		13MAY83	REVISED	DATE	KC-135 TRACK 5	
CHECK						
APPD.						
APPD.					THE BOEING COMPANY	PAGE 205

Figure C-9. KC-135 Track 10

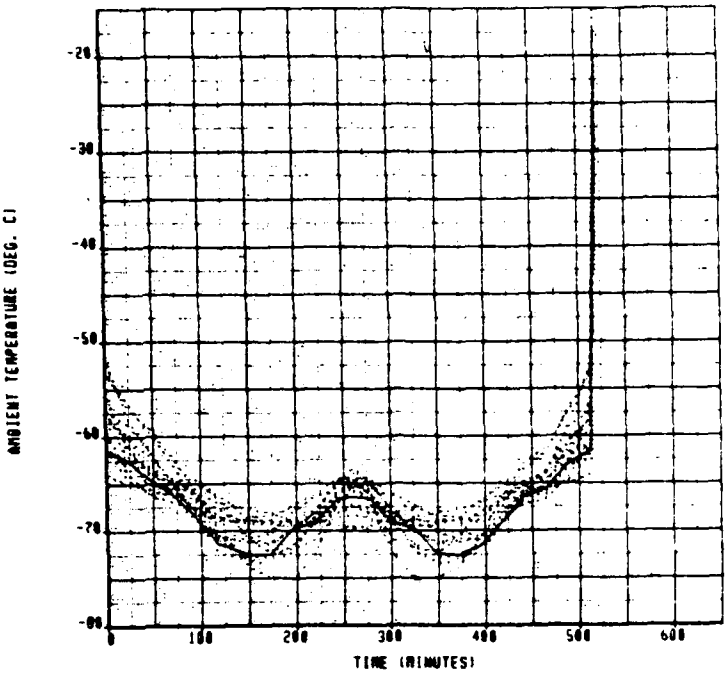

a. 15 Worst Case Cold Days

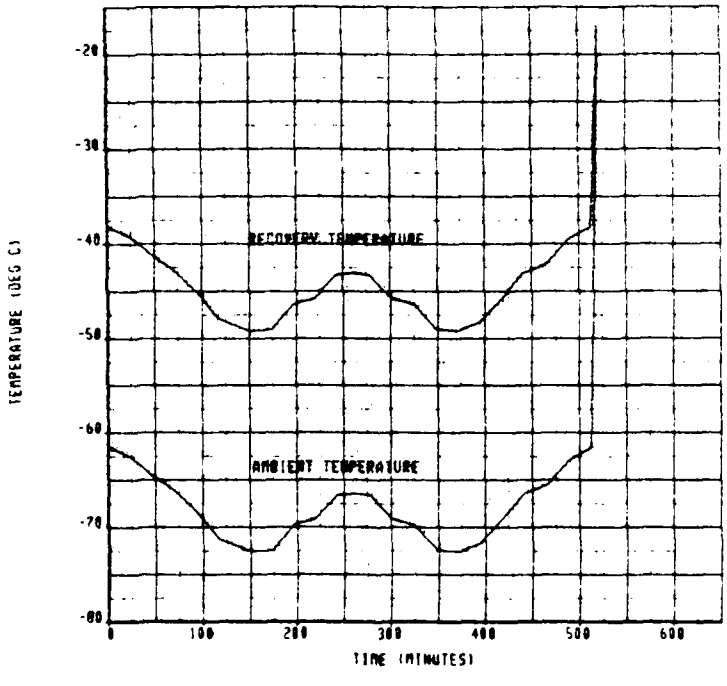

b. Worst Case Cold Day

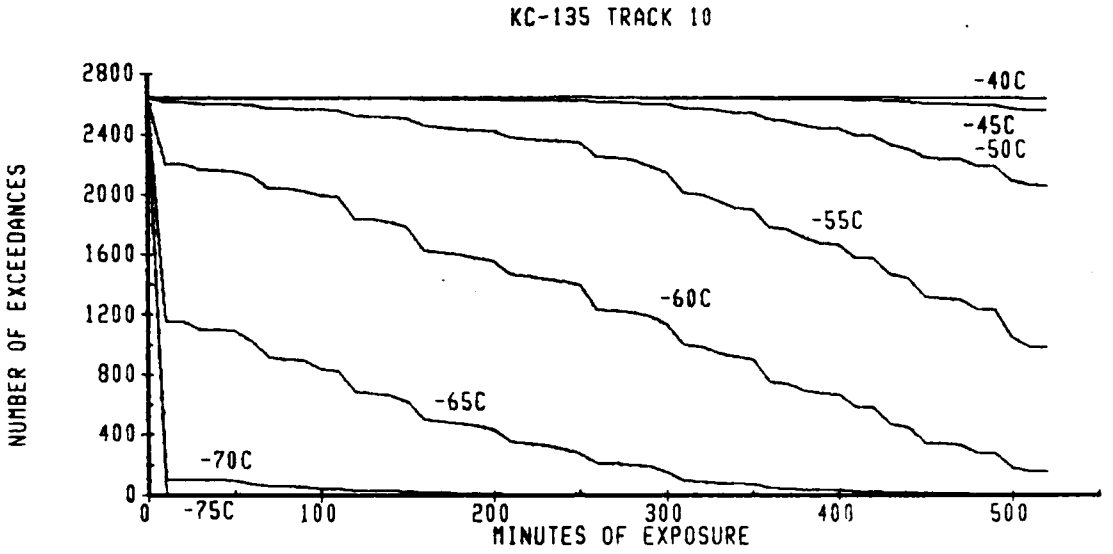

c. Number of Exceedances

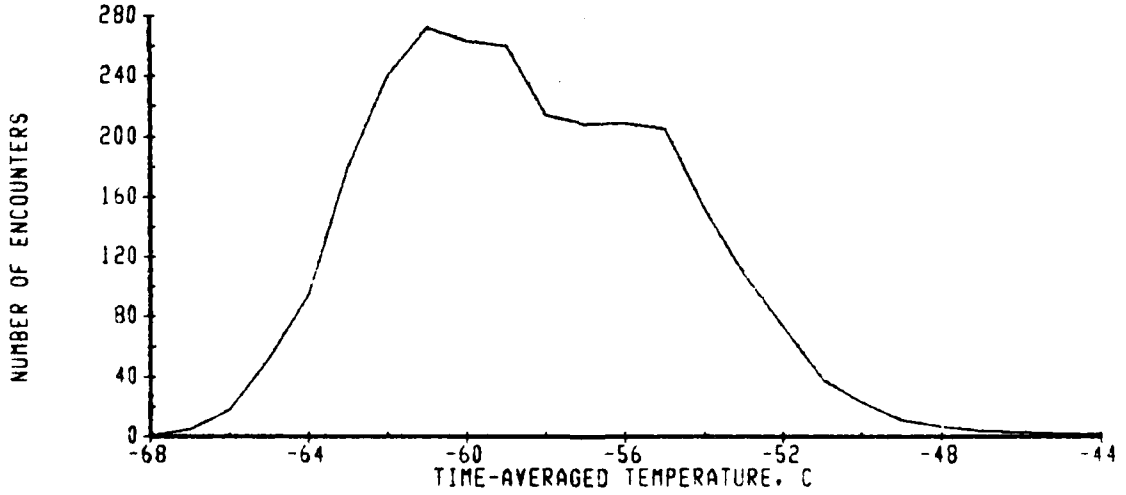

d. Number of Encounters

Figure C-10. A-10 Track 1

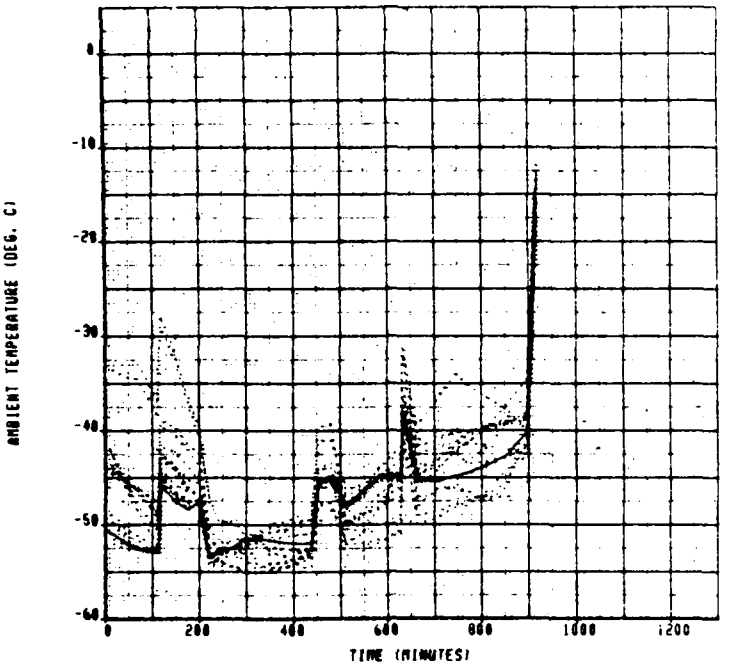

a. 15 Worst Case Cold Days

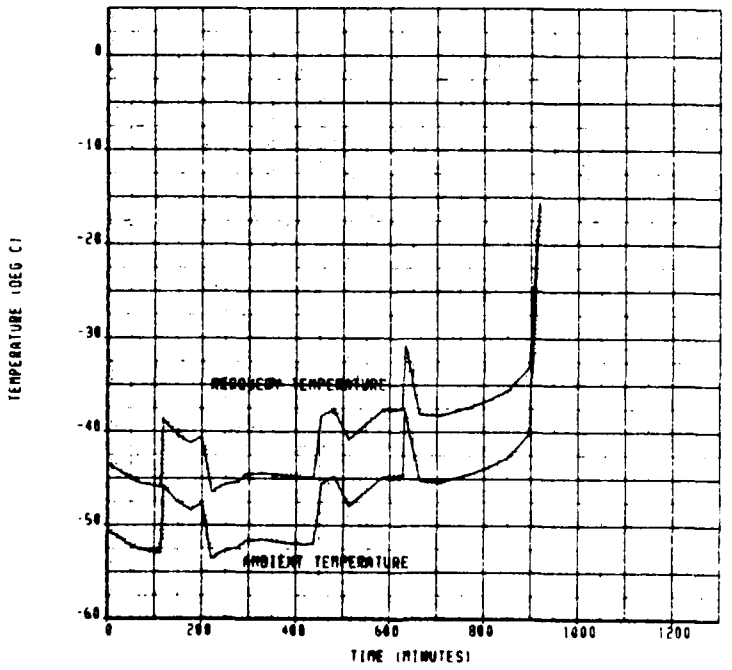

b. Worst Case Cold Day

A-10 TRACK 1

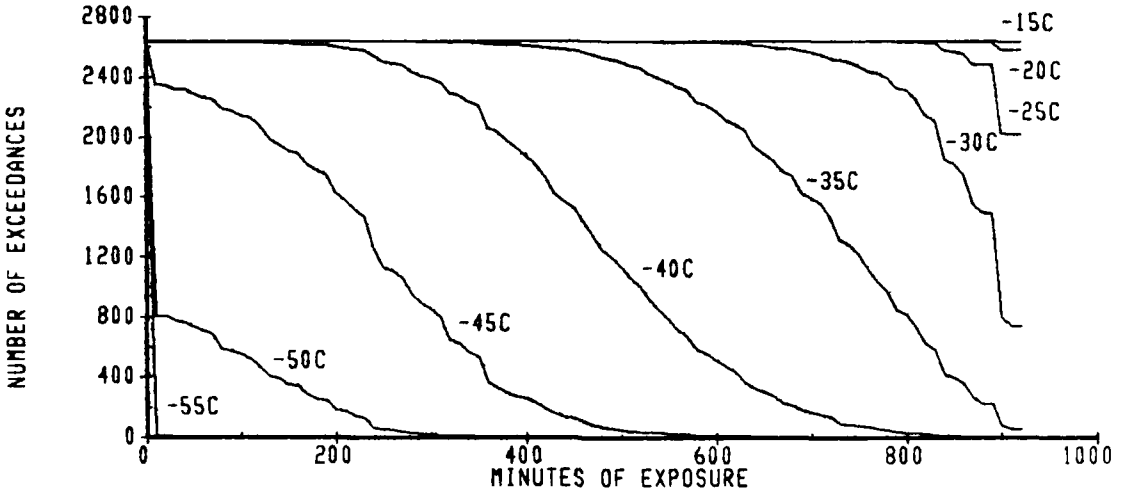

c. Number of Exceedances

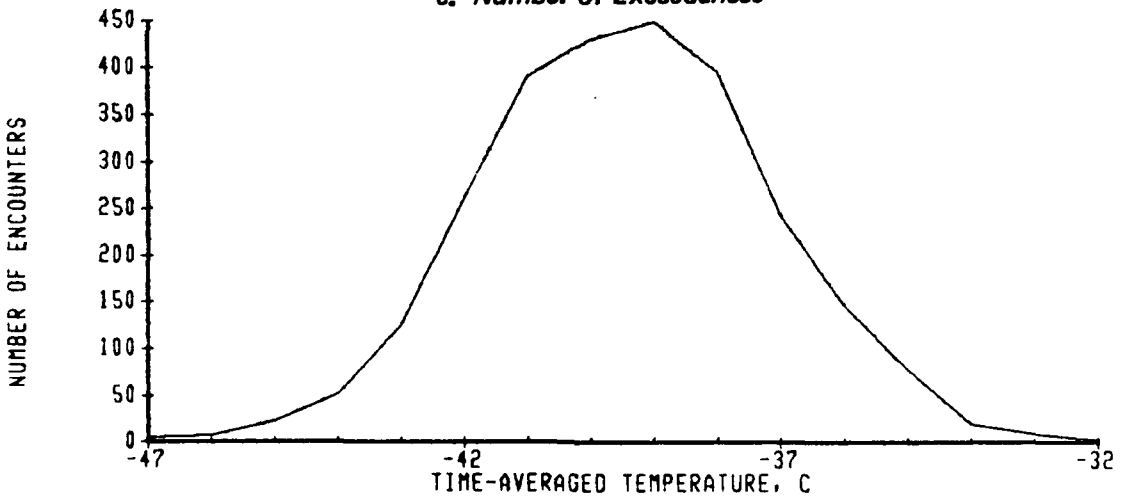

d. Number of Encounters

Figure C-11. A-10 Track 2

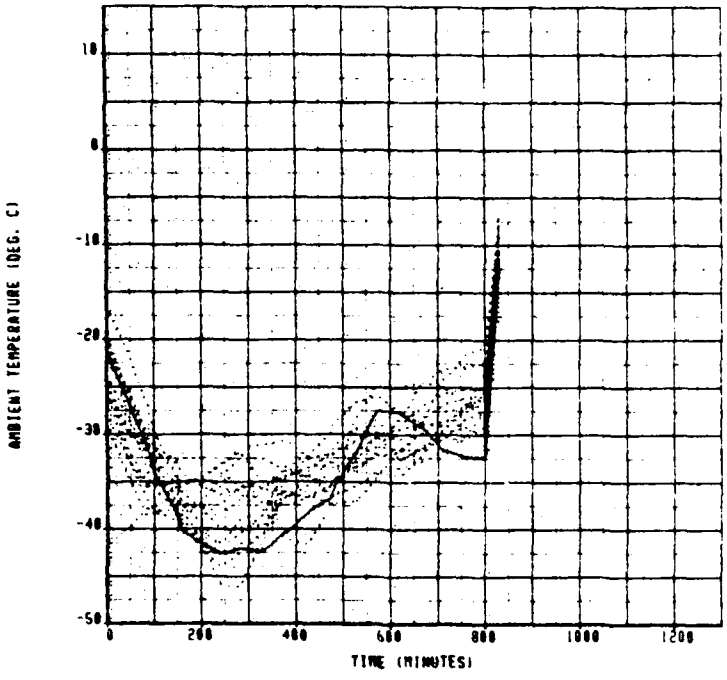

a. 15 Worst Case Cold Days

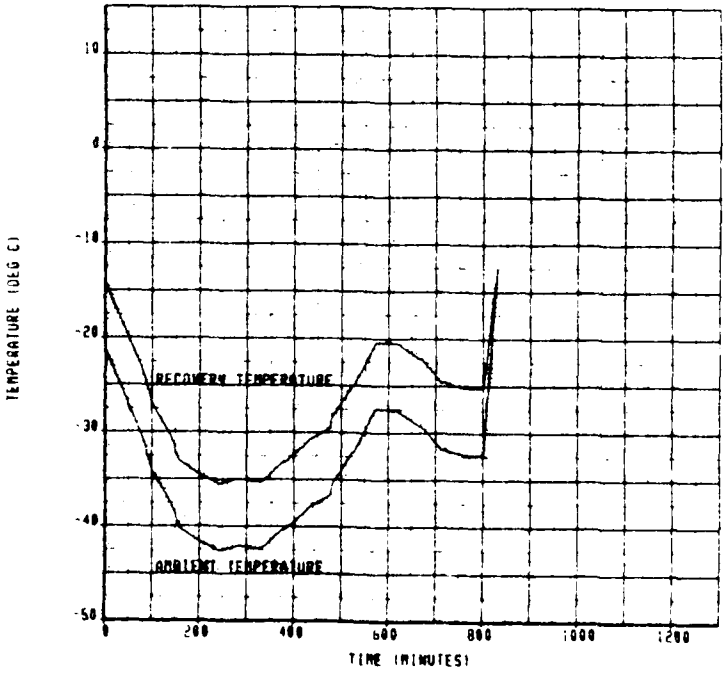

b. Worst Case Cold Day

A-10 TRACK 2

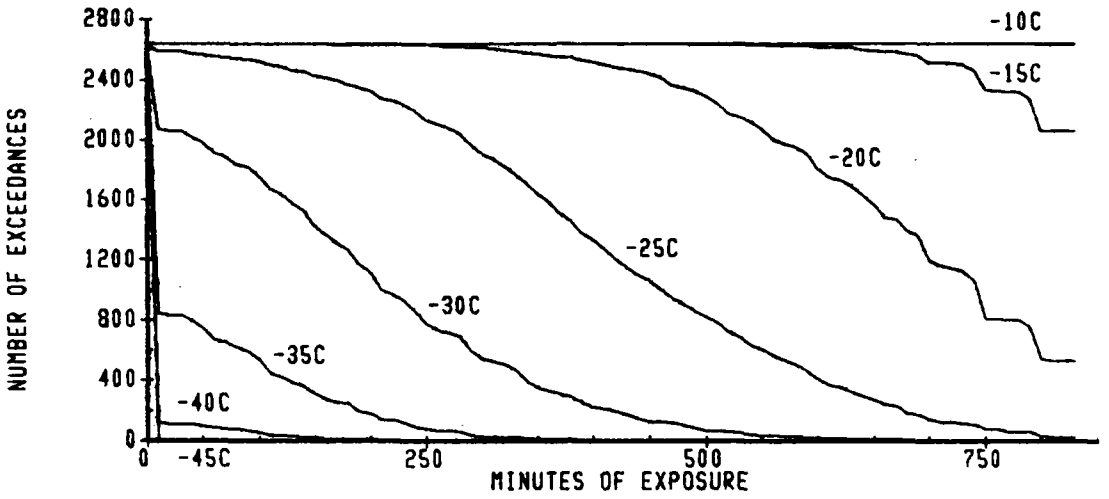

c. Number of Exceedances

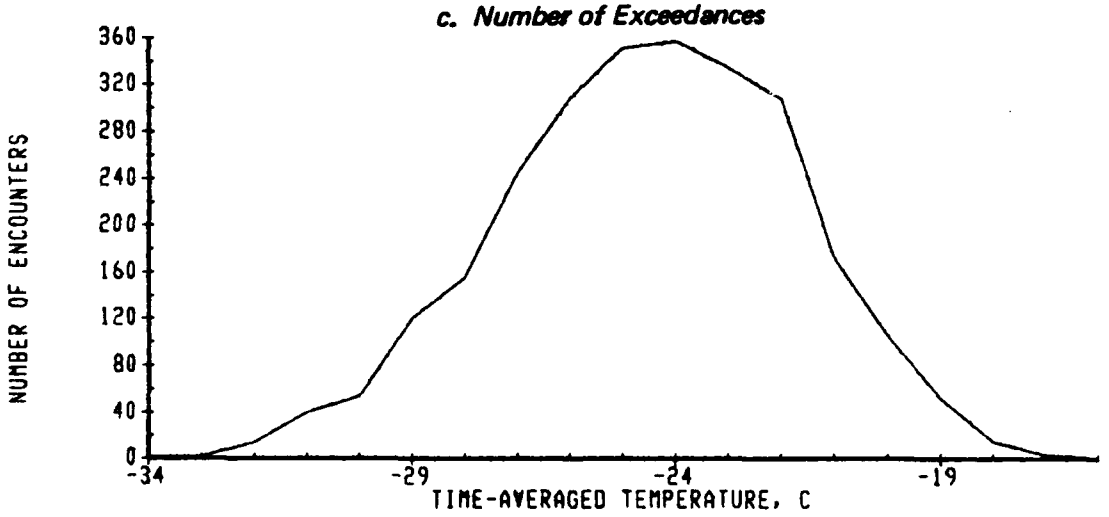

d. Number of Encounters

Figure C-12. A-10 Track 3

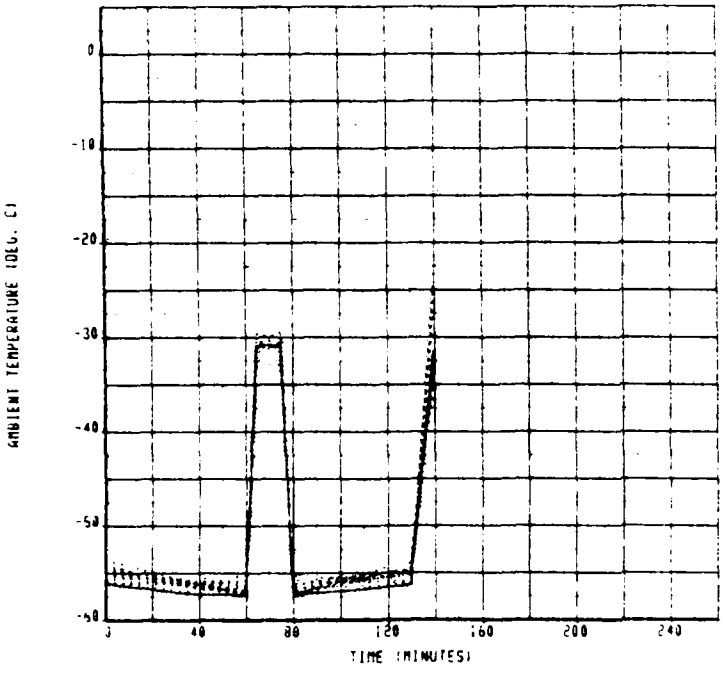

a. 15 Worst Case Cold Days

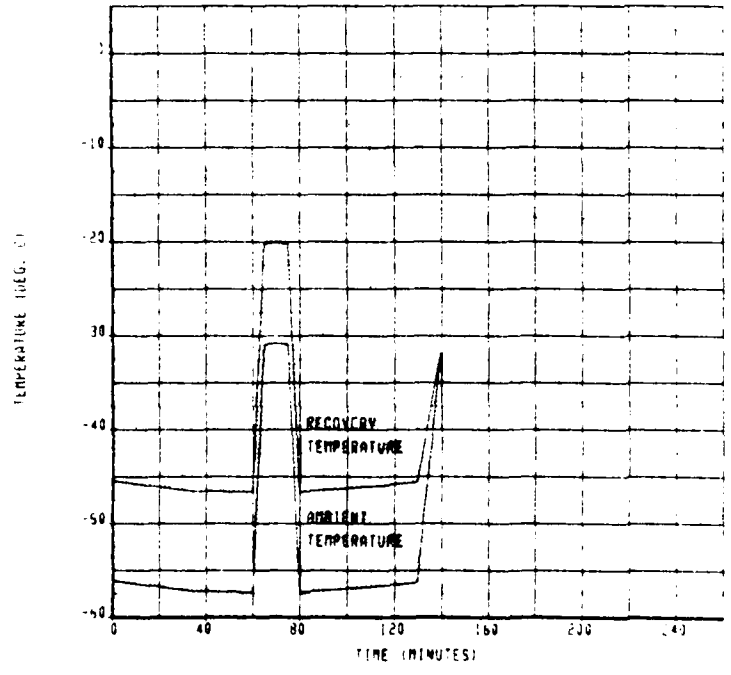

b. Worst Case Cold Day

A-10 TRACK 3

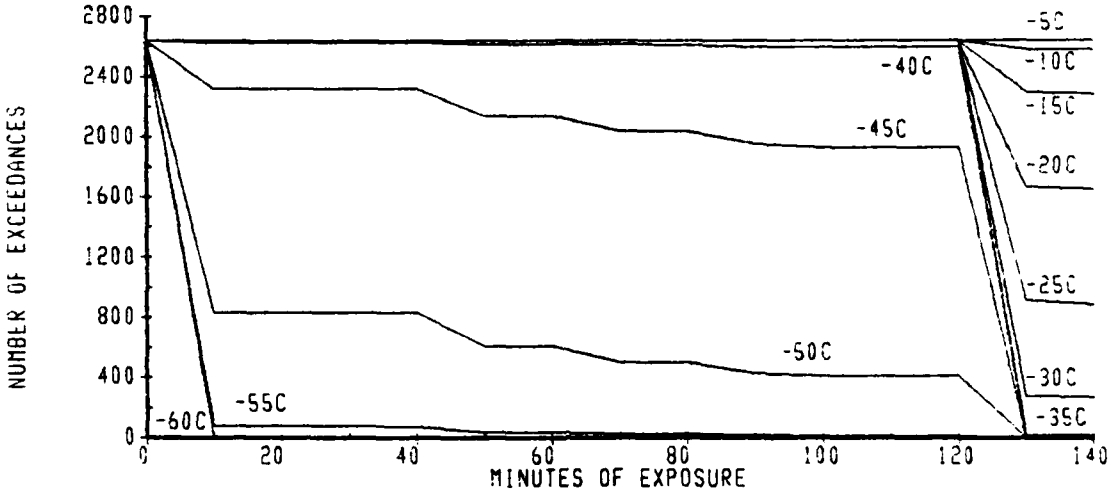

c. Number of Exceedances

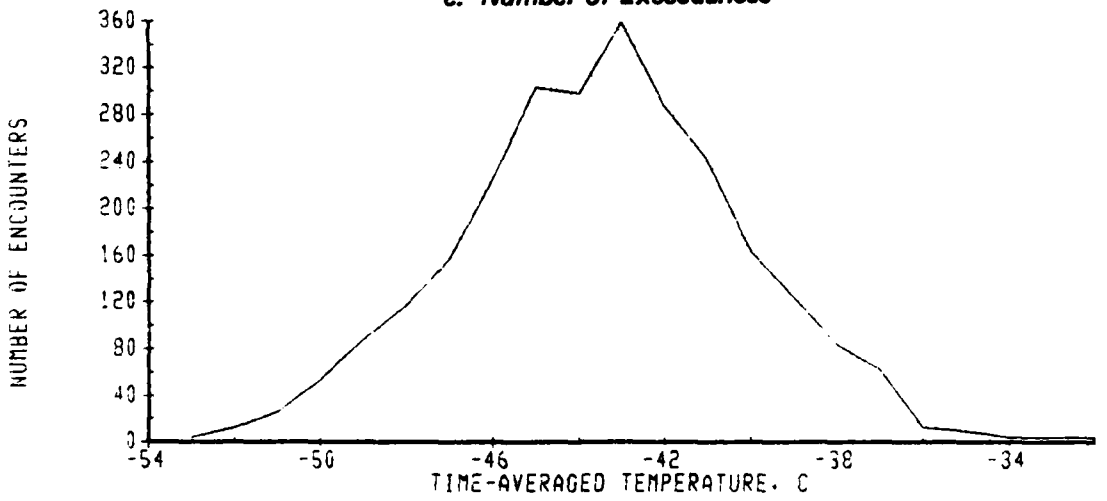

d. Number of Encounters

Figure C-13. A-10 Track 4

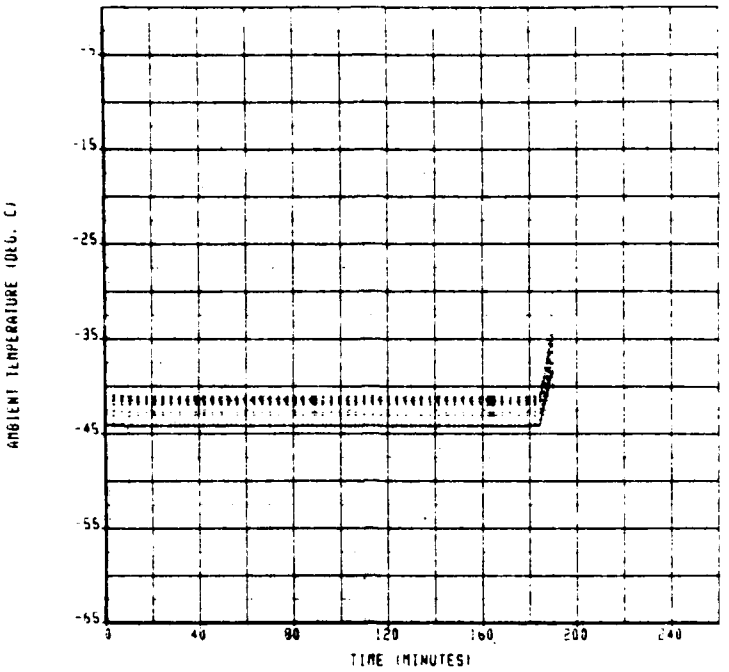

a. 15 Worst Case Cold Days

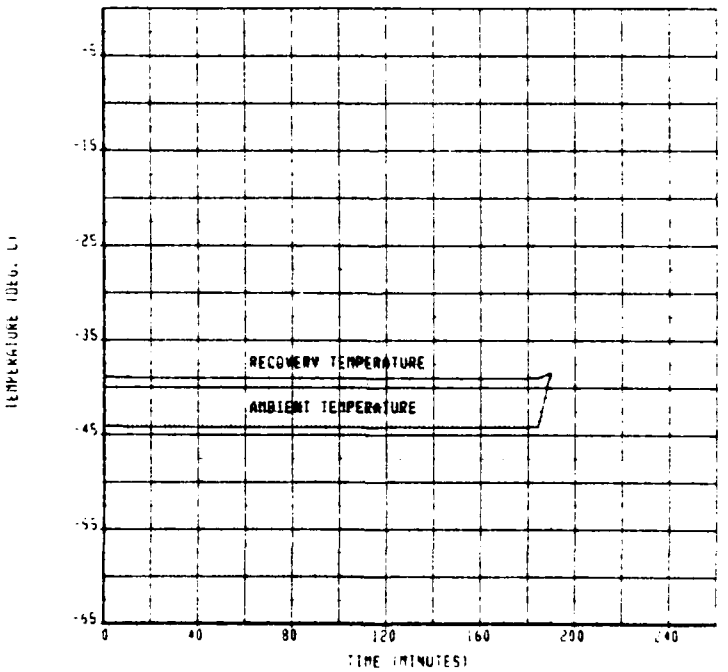

b. Worst Case Cold Day

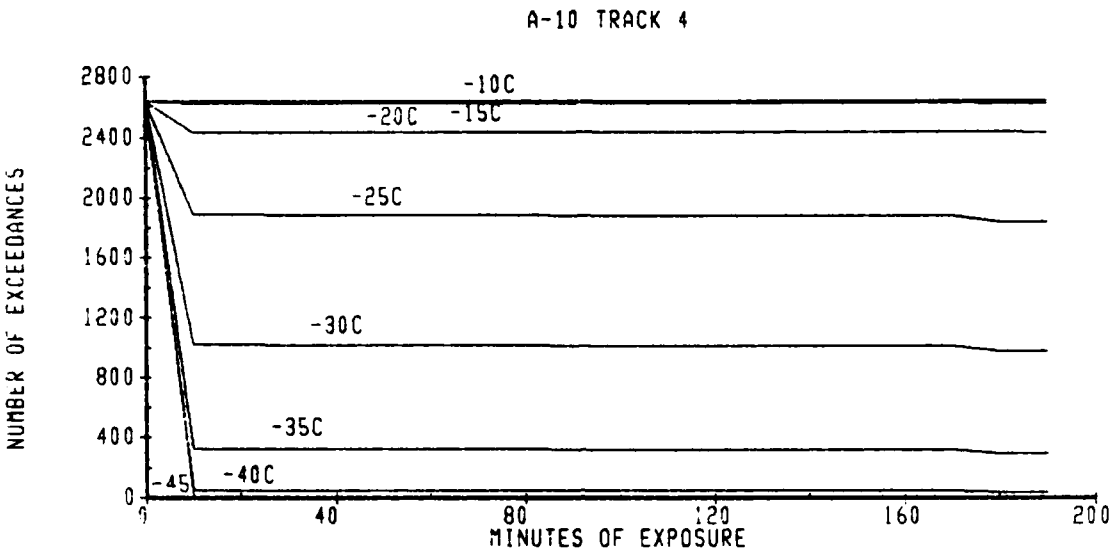

c. Number of Exceedances

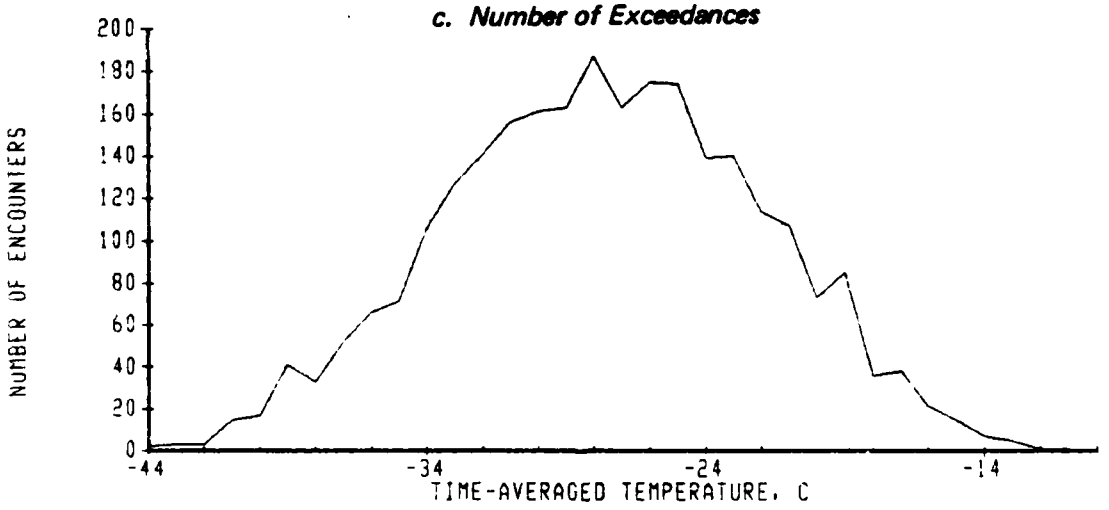

d. Number of Encounters

Figure C-14. A-10 Track 5

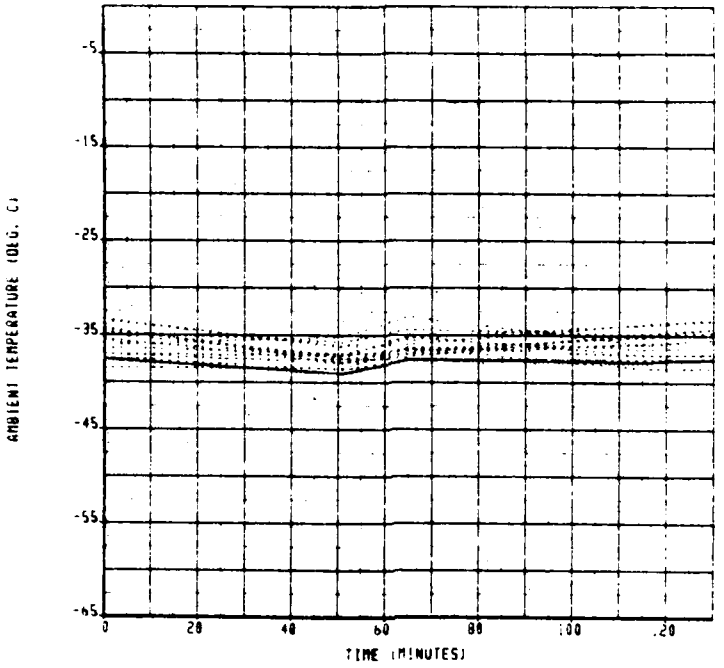

a. 15 Worst Case Cold Days

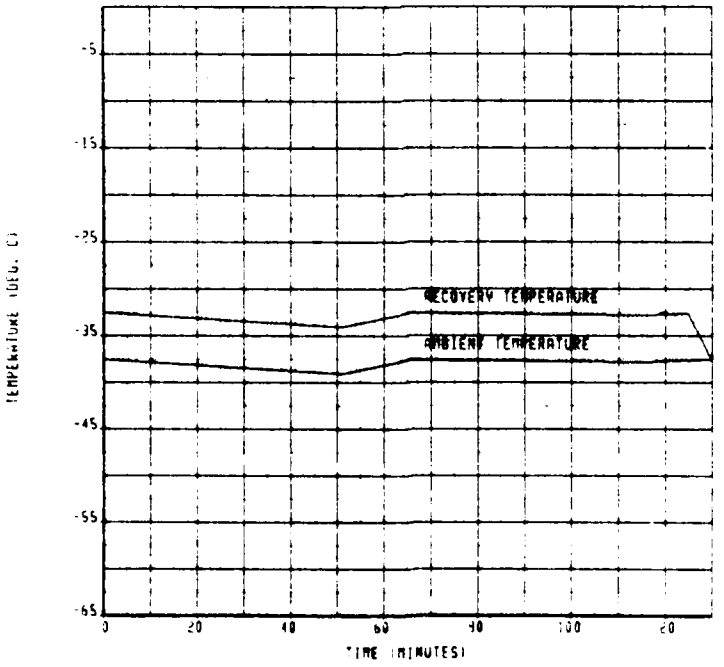

b. Worst Case Cold Day

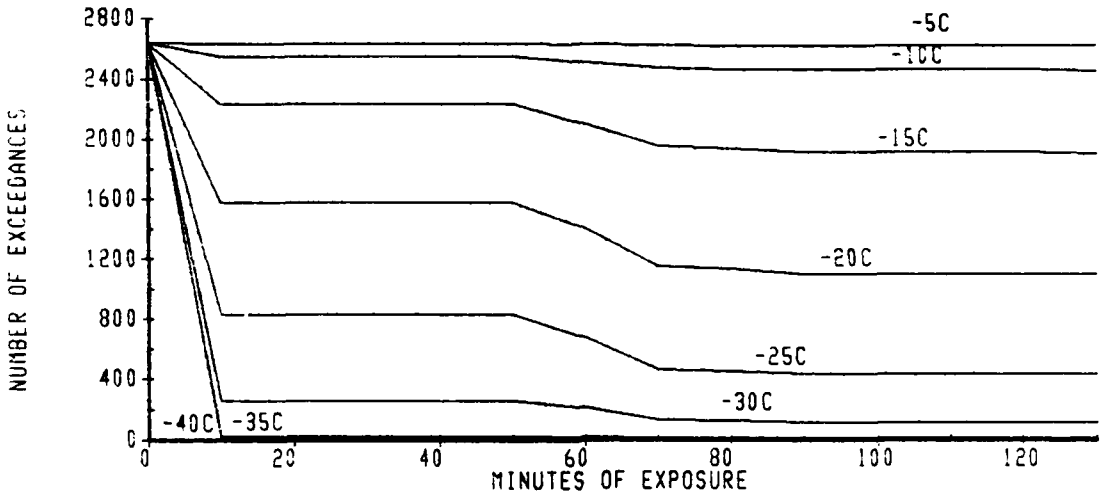

c. Number of Exceedances

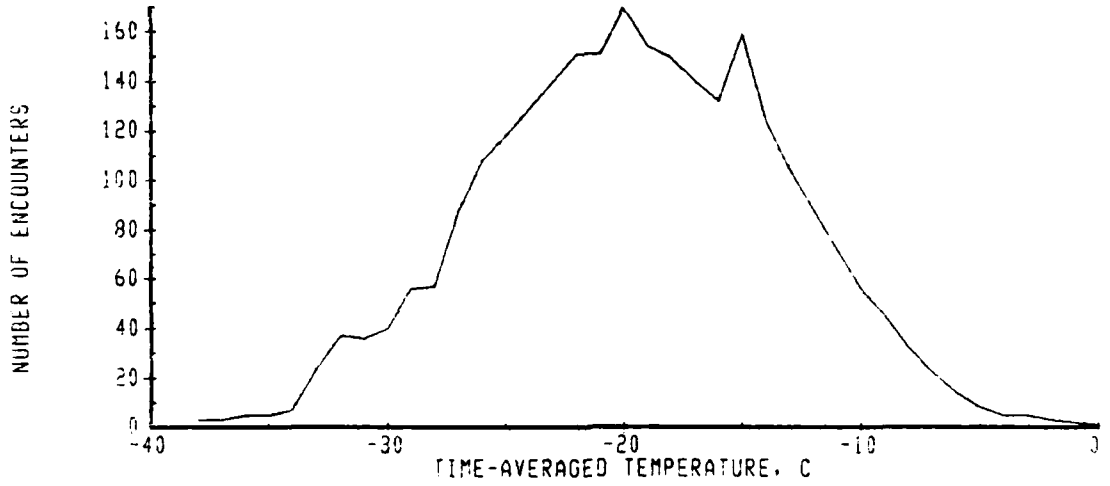

d. Number of Encounters

Figure C-15. A-10 Track 6

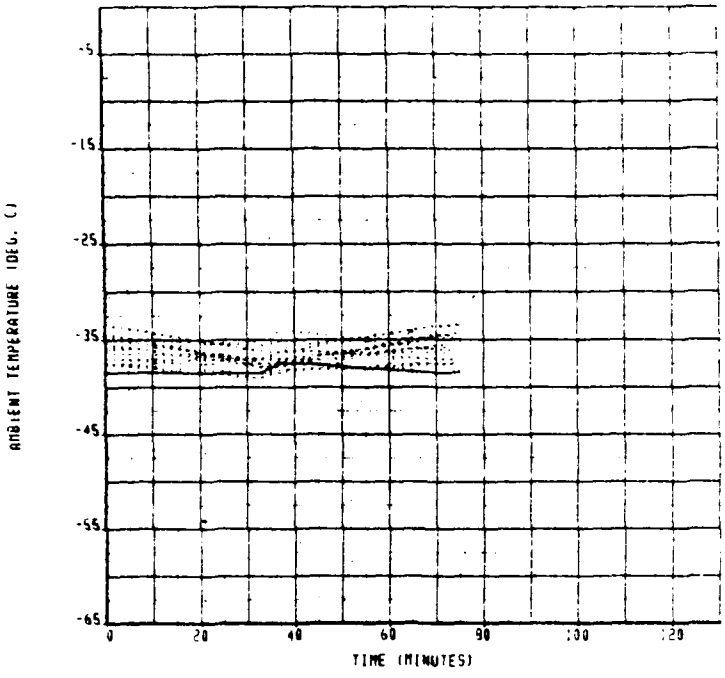

a. 15 Worst Case Cold Days

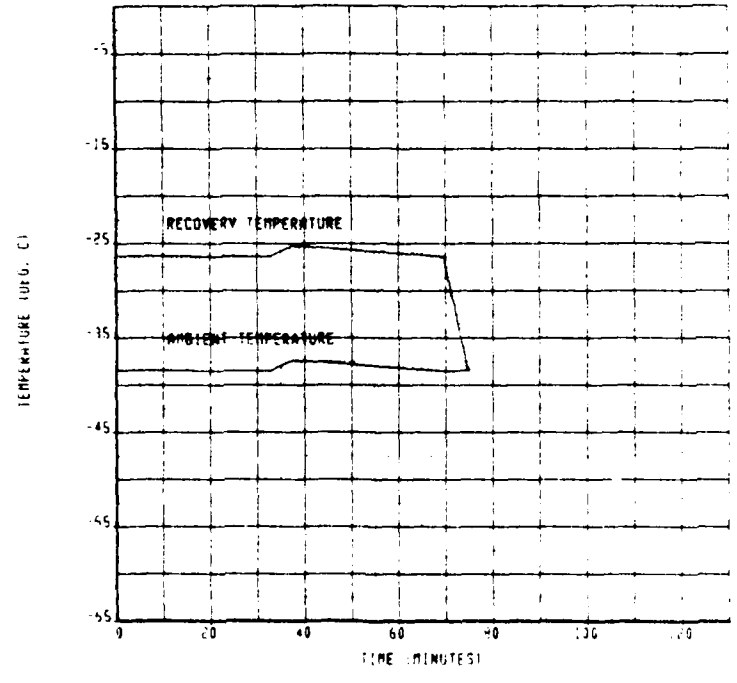

b. Worst Case Cold Day

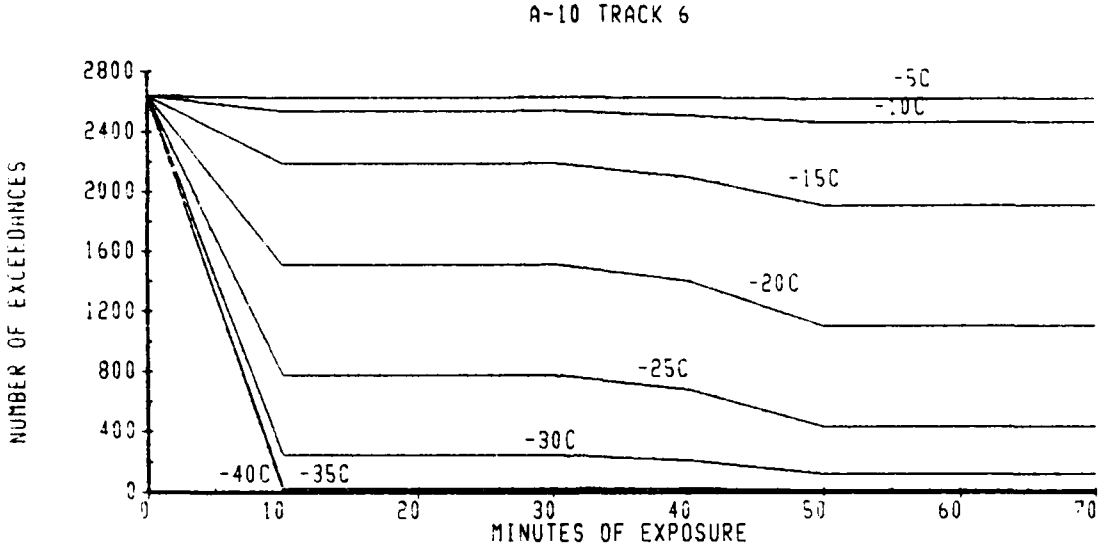

c. Number of Exceedances

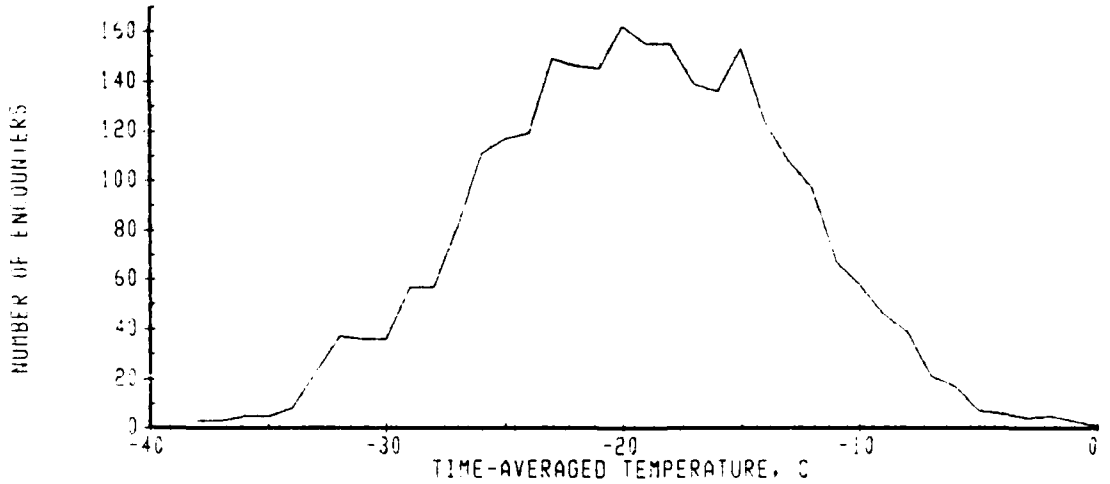

d. Number of Encounters

Figure C-16. A-10 Track 7

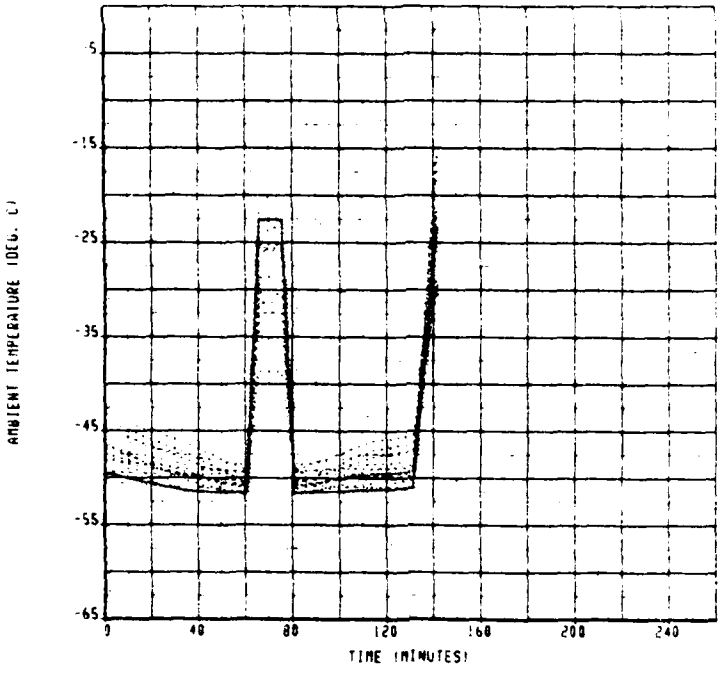

a. 15 Worst Case Cold Days

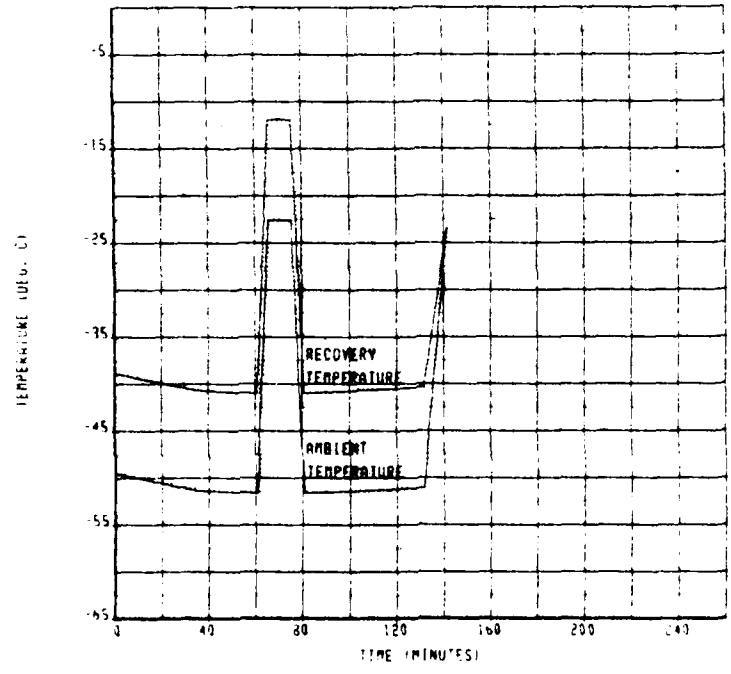

b. Worst Case Cold Day

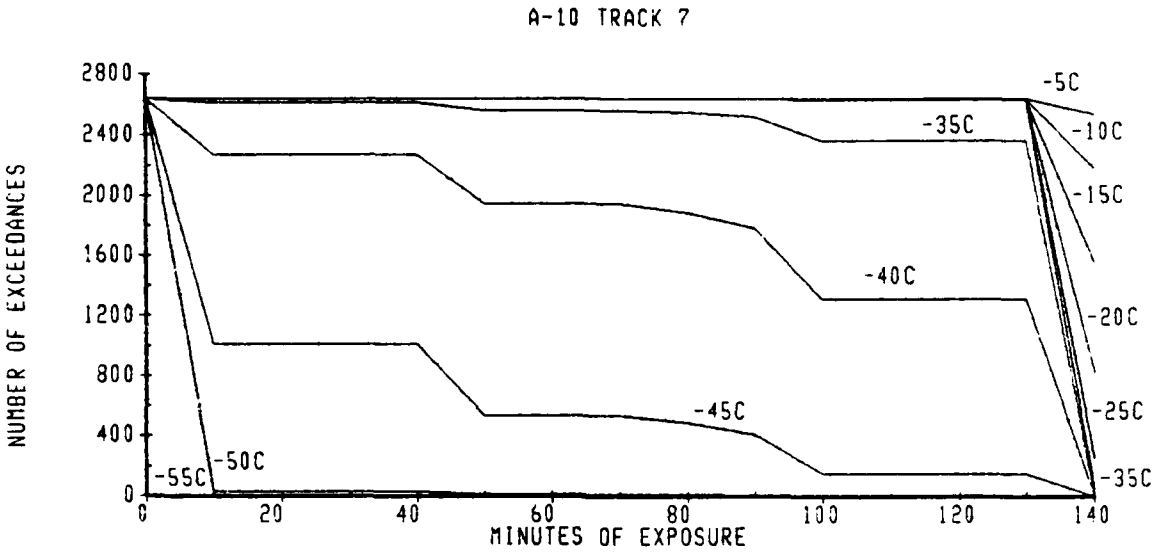

c. Number of Exceedances

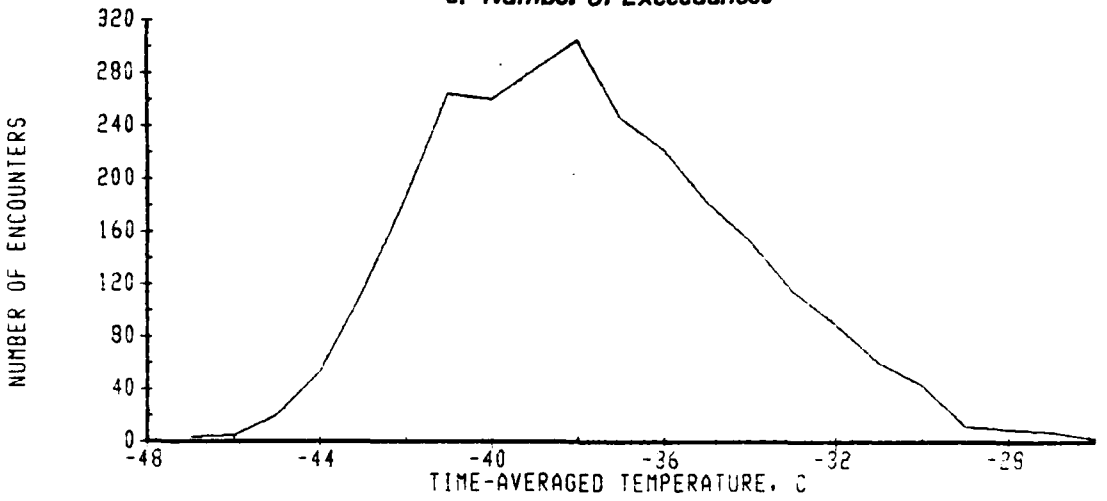

d. Number of Encounters

Figure C-17. A-10 Track 8

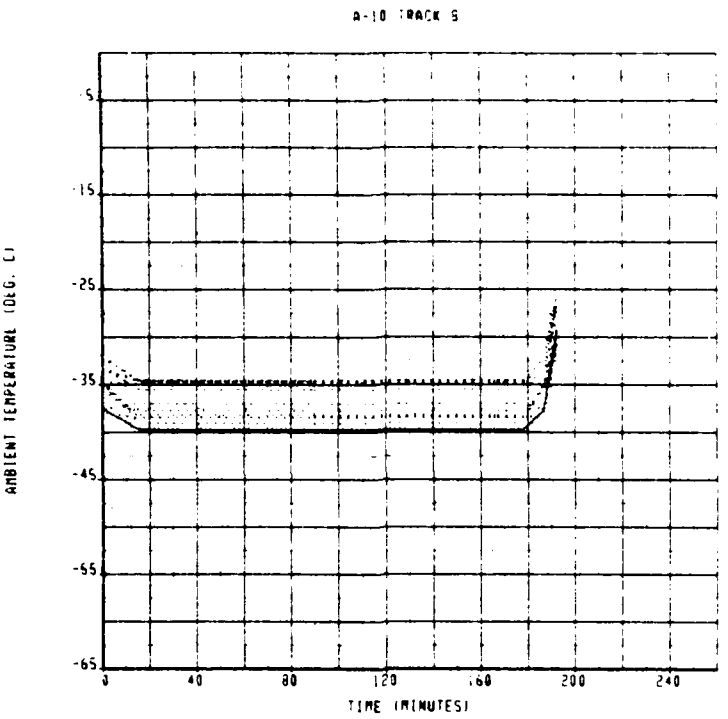

a. 15 Worst Case Cold Days

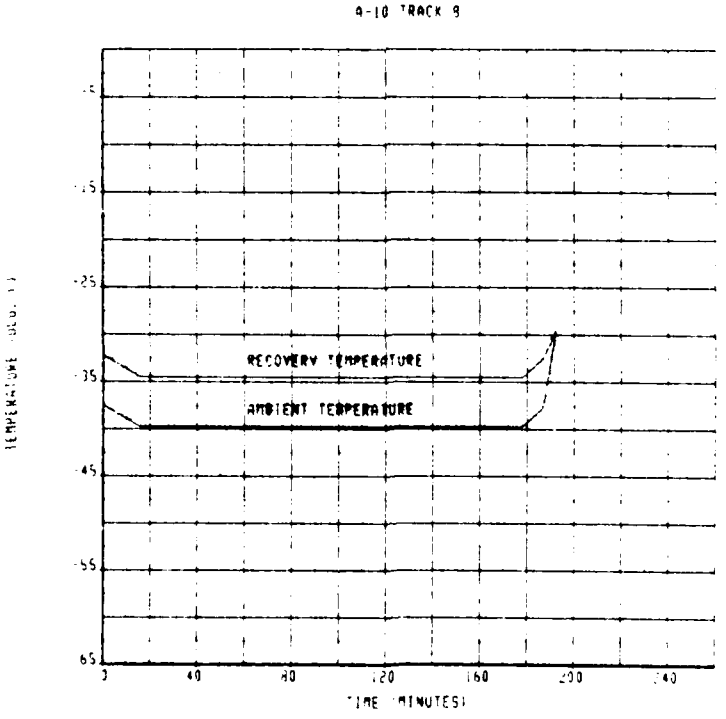

b. Worst Case Cold Day

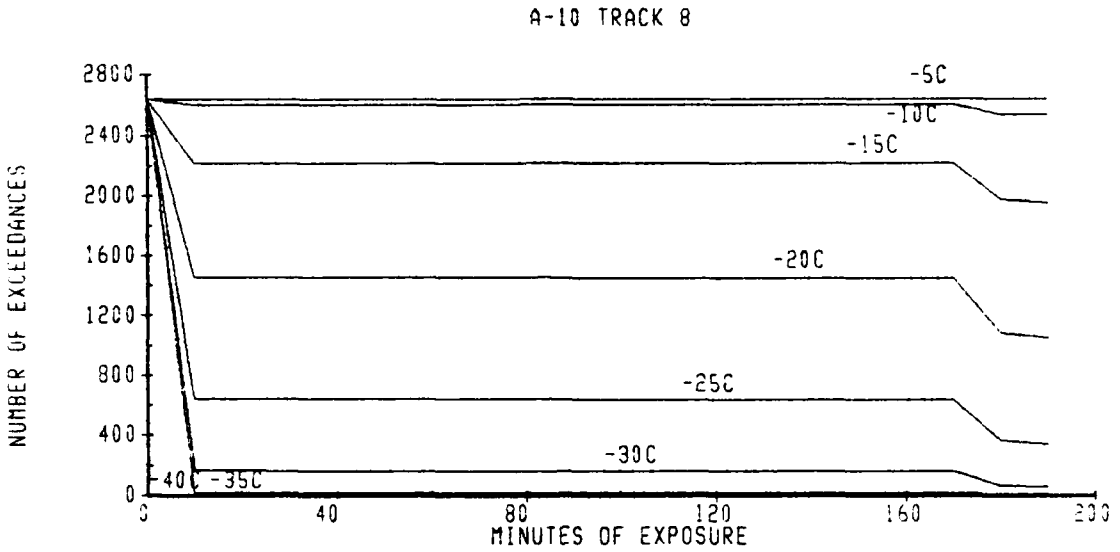

c. Number of Exceedances

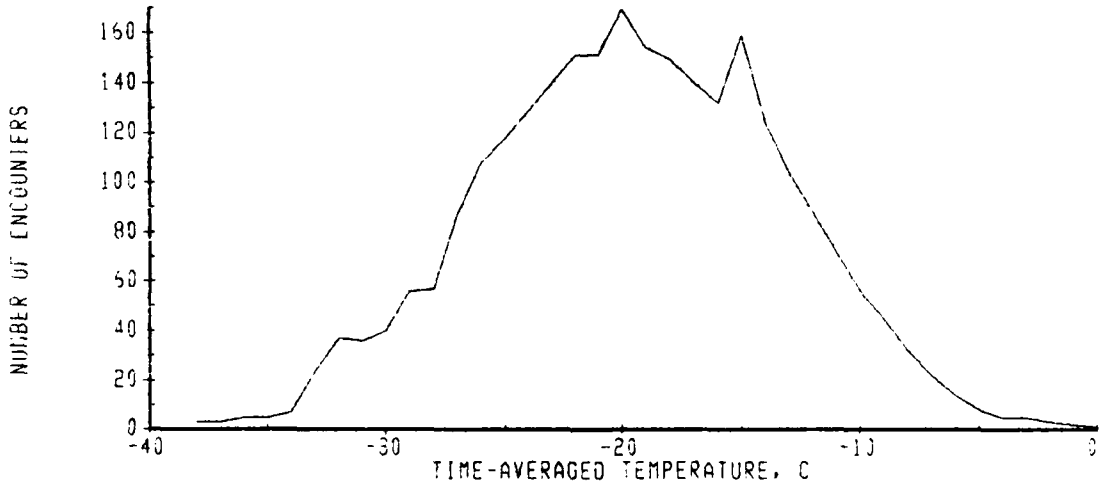

d. Number of Encounters

Figure C-18. A-10 Track 9

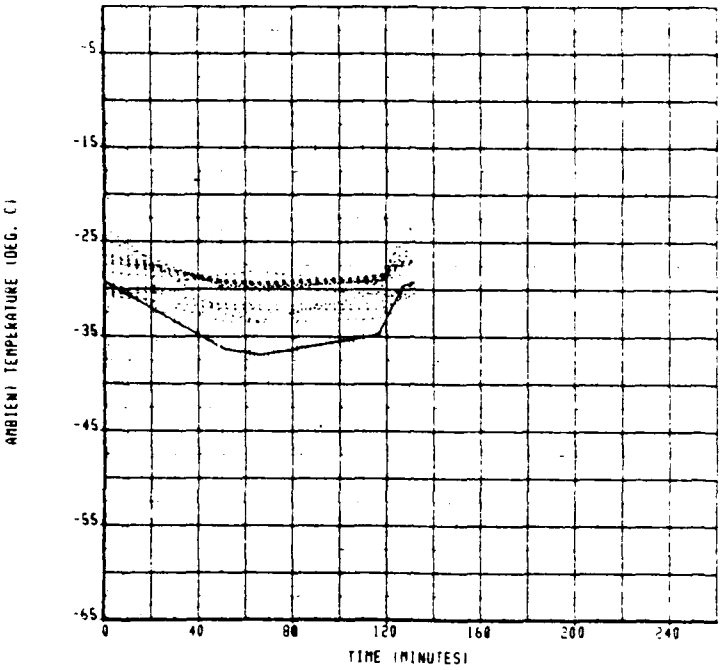

a. 15 Worst Case Cold Days

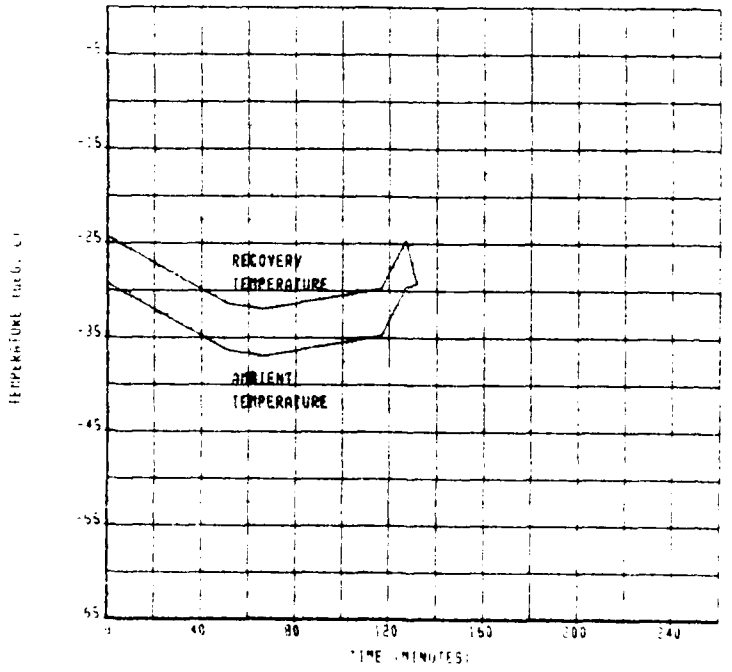

b. Worst Case Cold Day

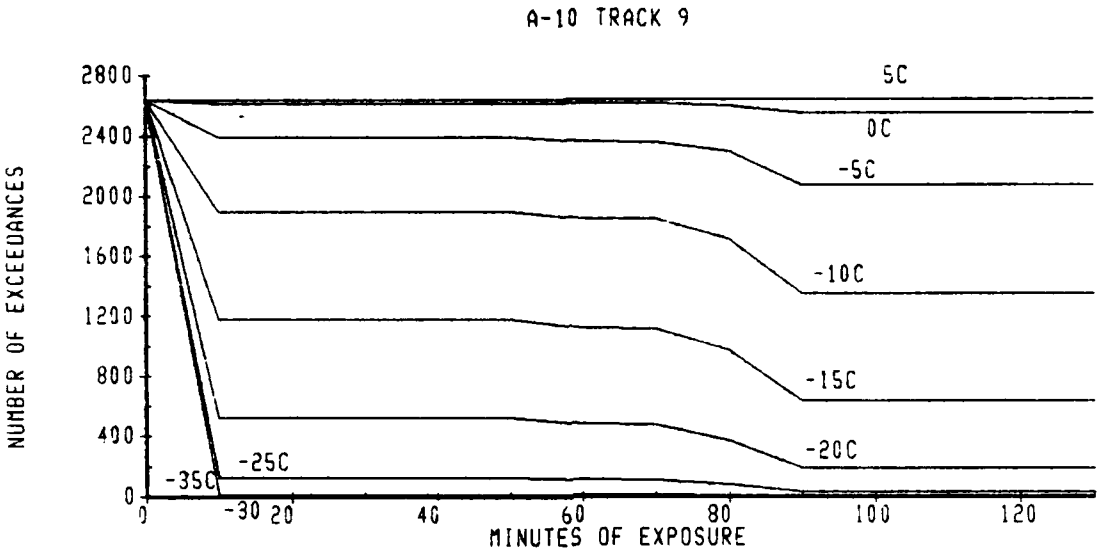

c. Number of Exceedances

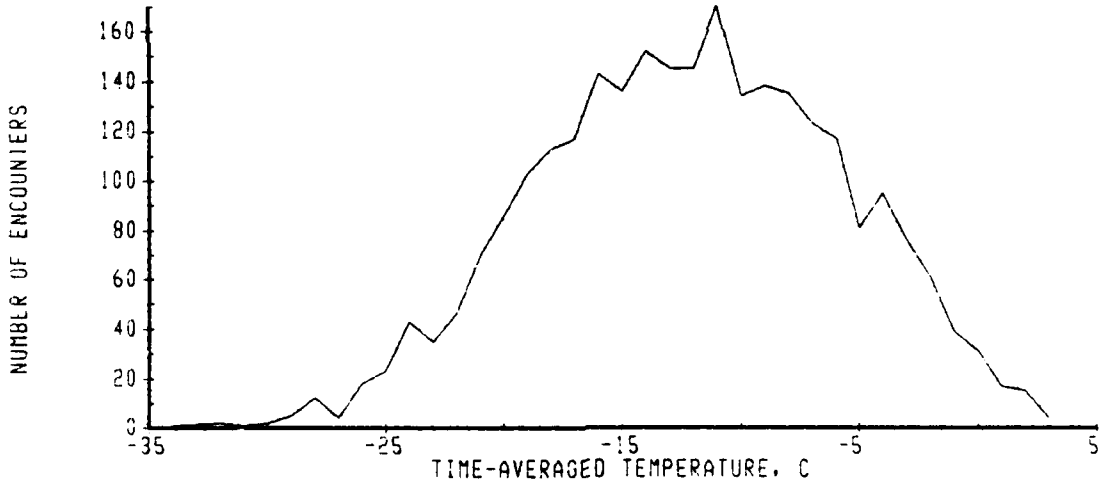

d. Number of Encounters

CALC		19JUL83	REVISED	DATE	A-10 TRACK 9
CHECK					
APPD.					
APPD.					THE BOEING COMPANY
					PAGE 225

Figure C-19. A-10 Track 10

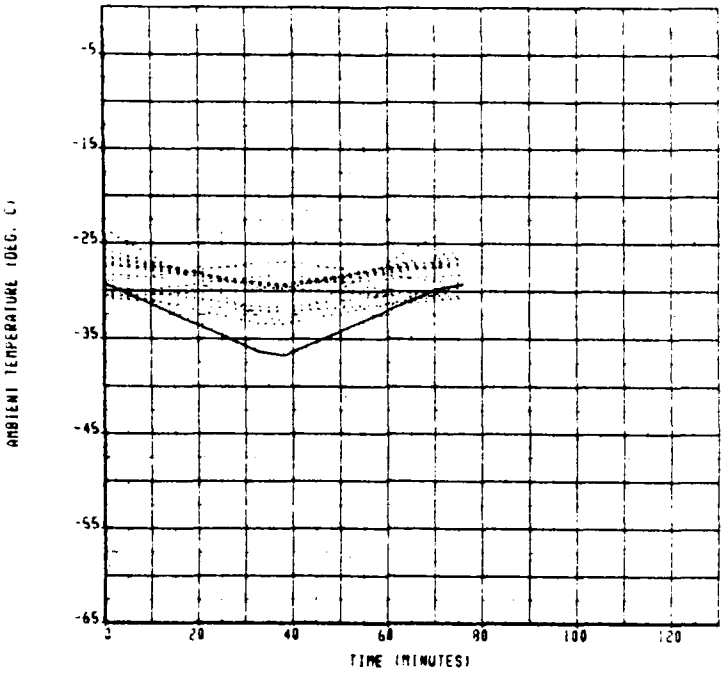

a. 15 Worst Case Cold Days

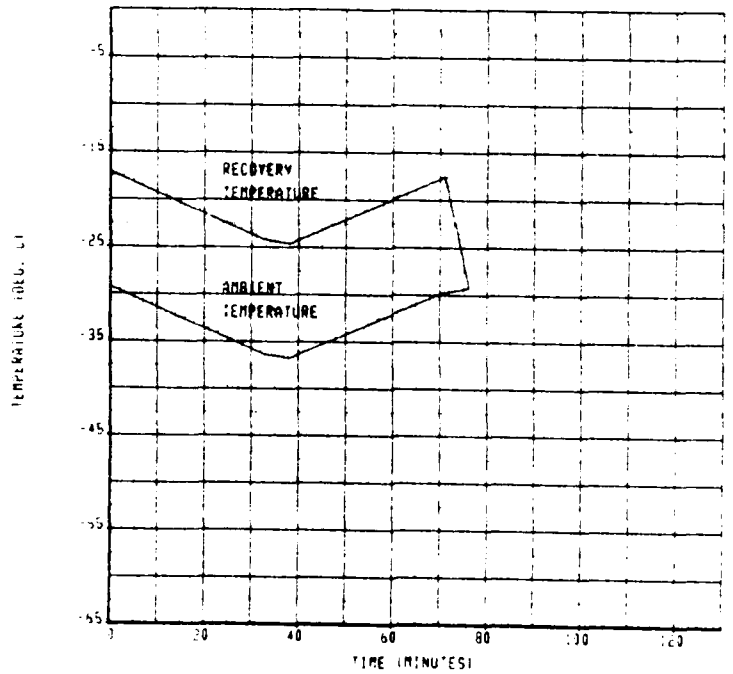

b. Worst Case Cold Day

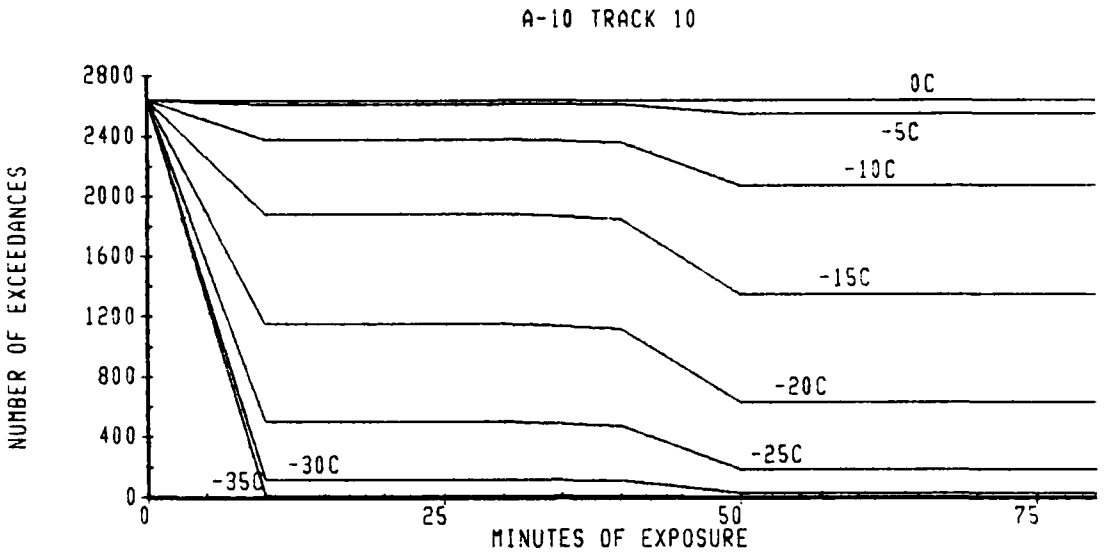

c. Number of Exceedances

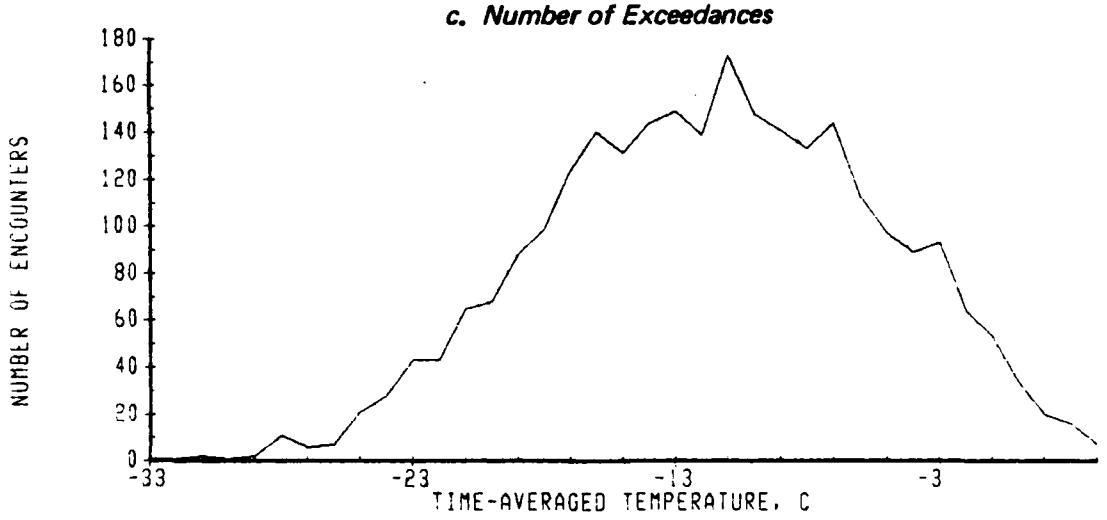

d. Number of Encounters

CALC		19JUL83	REVISED	DATE	A-10 TRACK 10	
CHECK						
APPD.						
APPD.					THE BOEING COMPANY	PAGE 227

Figure C-20. F-15 Track 1

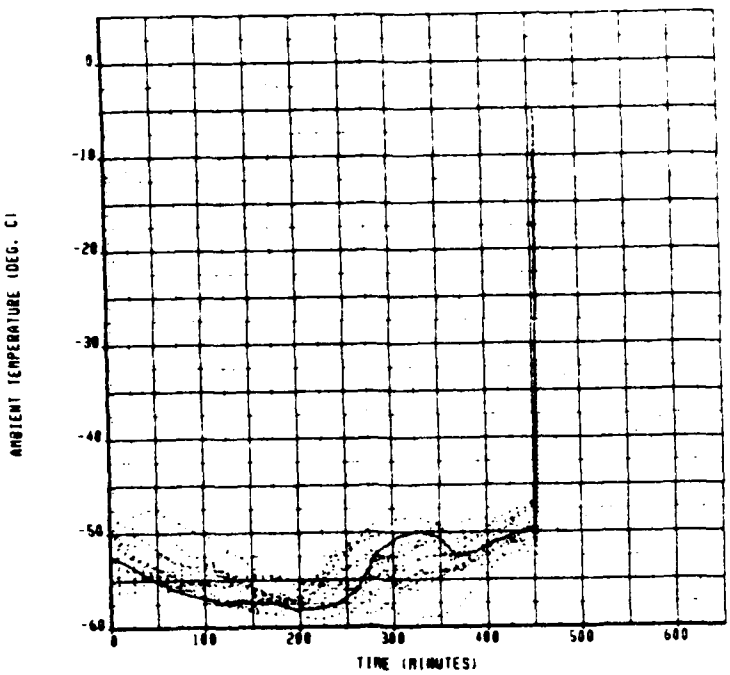

a. 15 Worst Case Cold Days

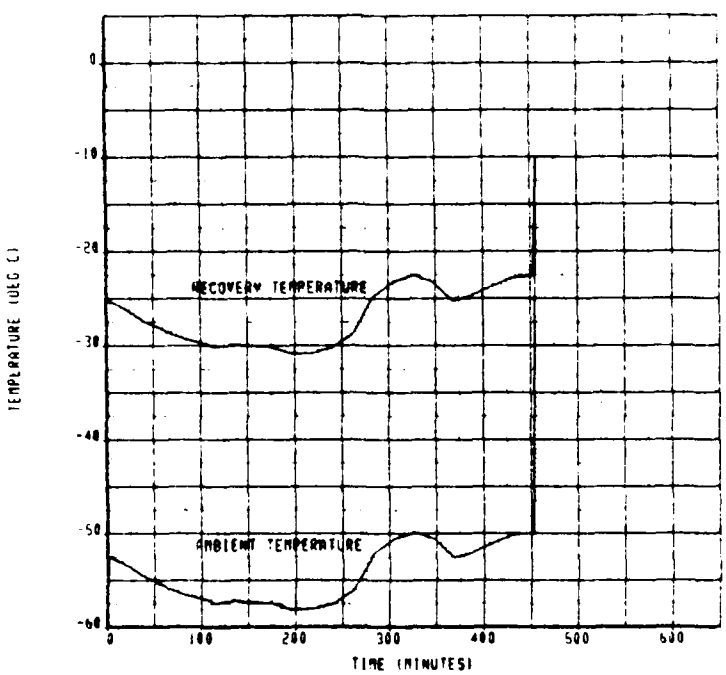

b. Worst Case Cold Day

F-15 TRACK 1

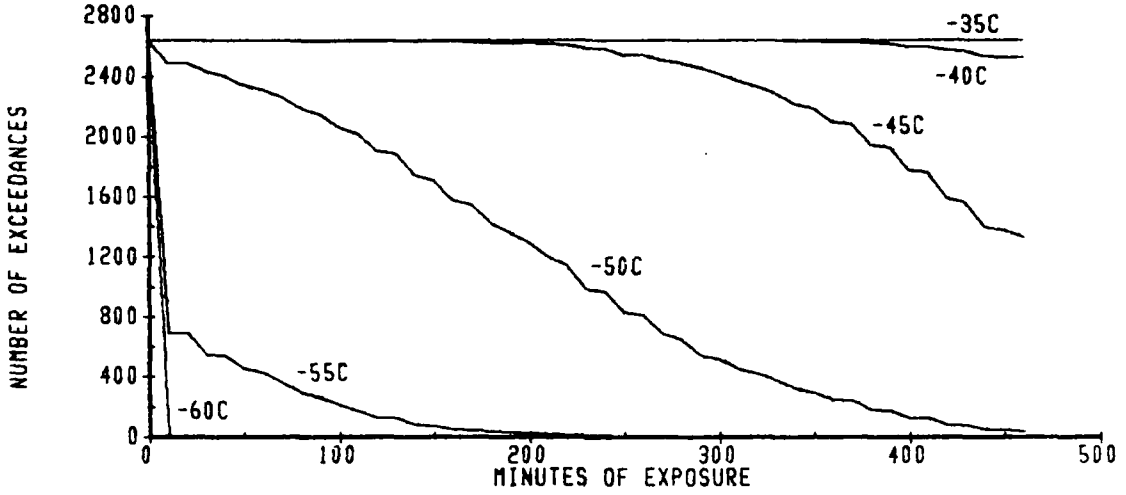

c. Number of Exceedances

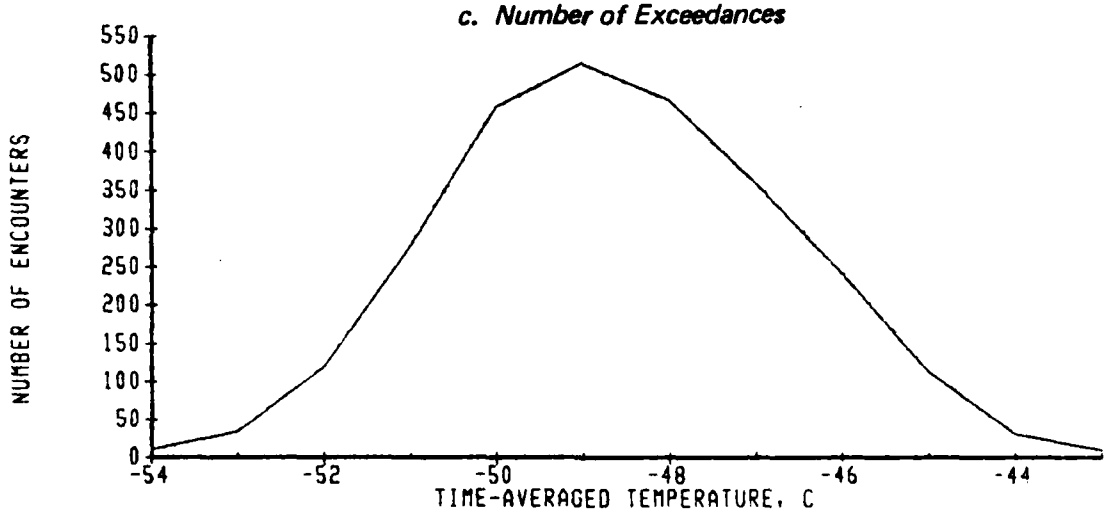

d. Number of Encounters

Figure C-21. F-15 Track 2

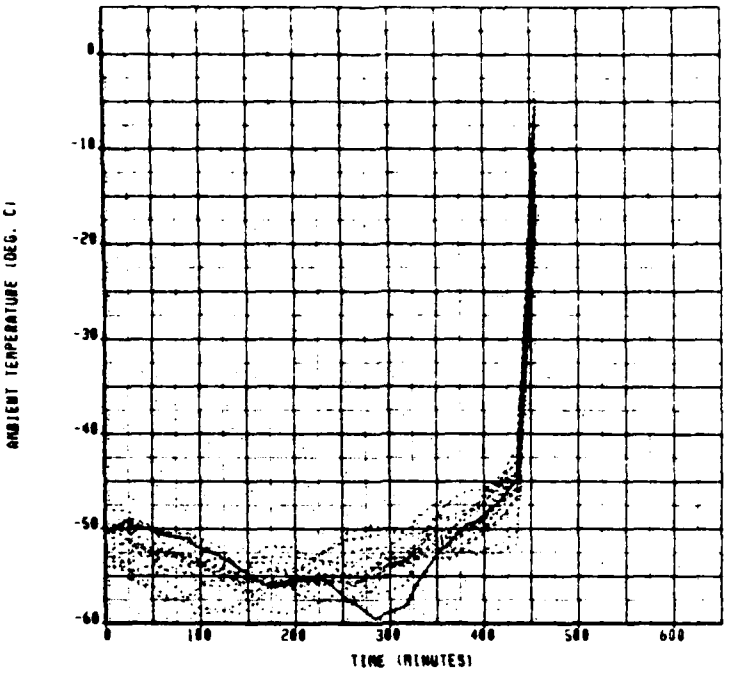

a. 15 Worst Case Cold Days

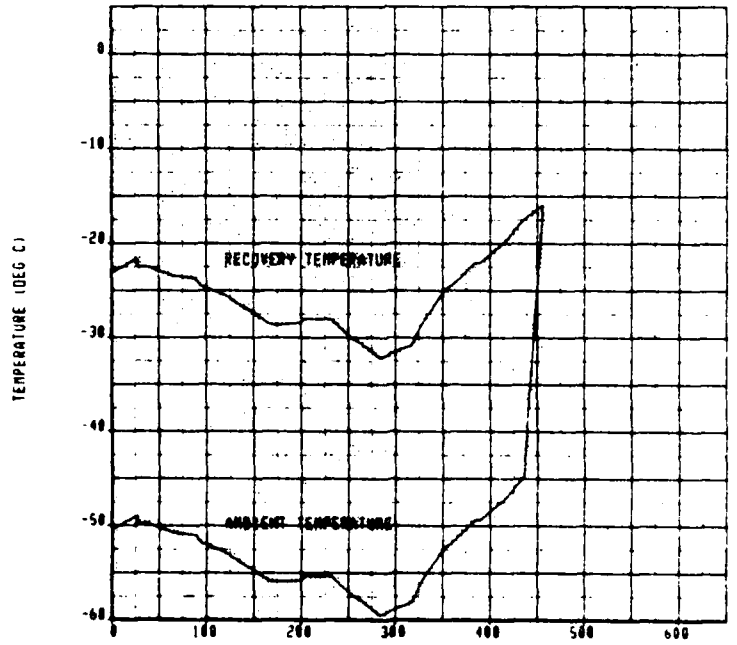

b. Worst Case Cold Day

F-15 TRACK 2

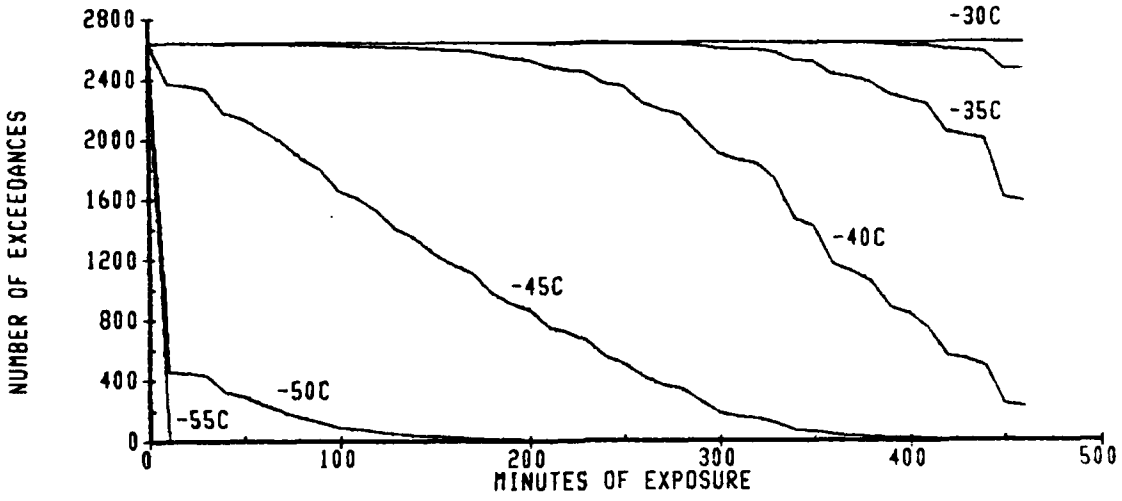

c. Number of Exceedances

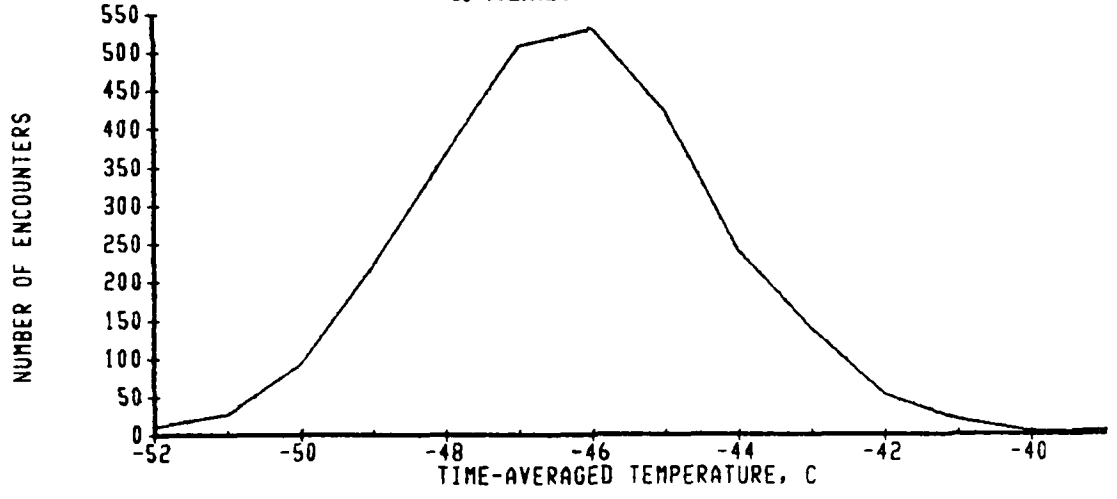

d. Number of Encounters

Figure C-22. F-15 Track 3

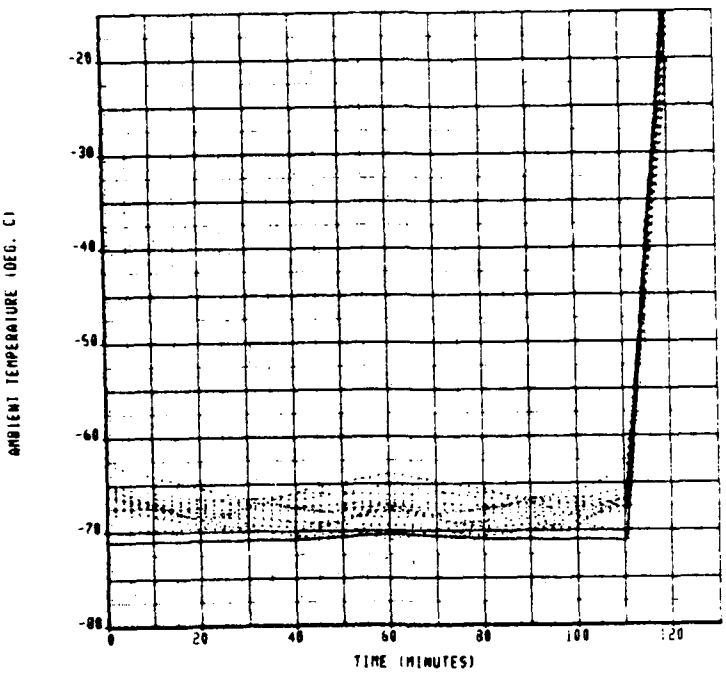

a. 15 Worst Case Cold Days

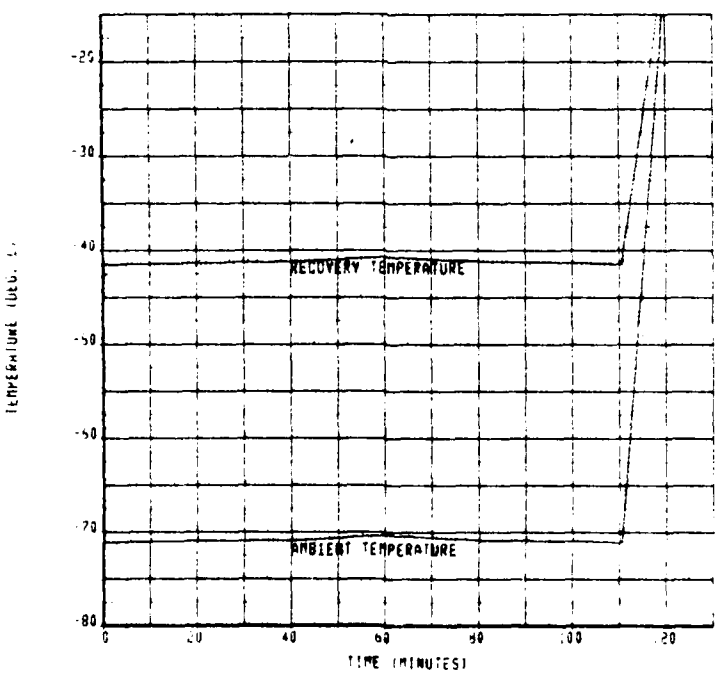

b. Worst Case Cold Day

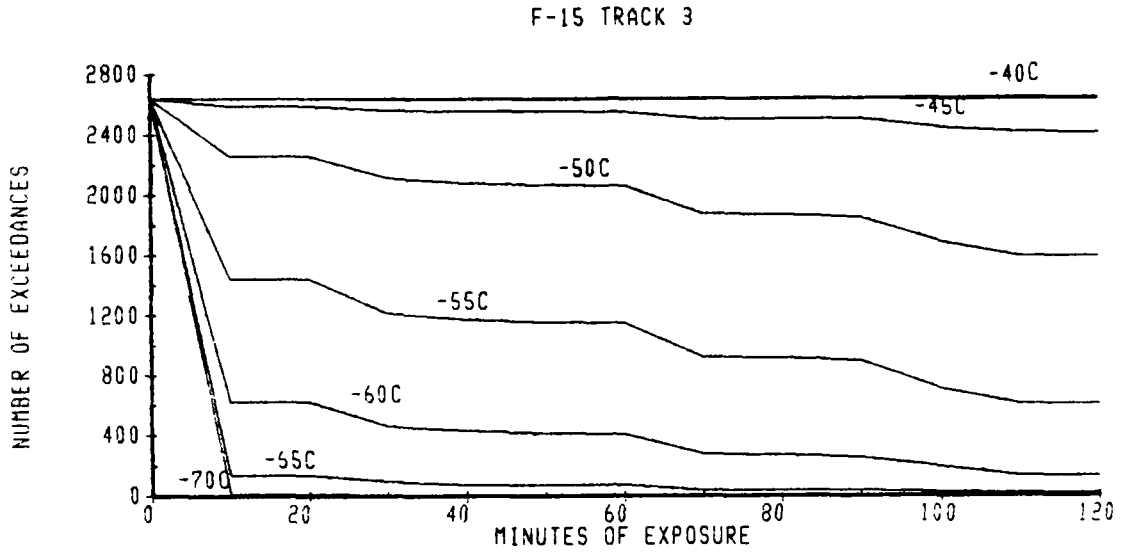

c. Number of Exceedances

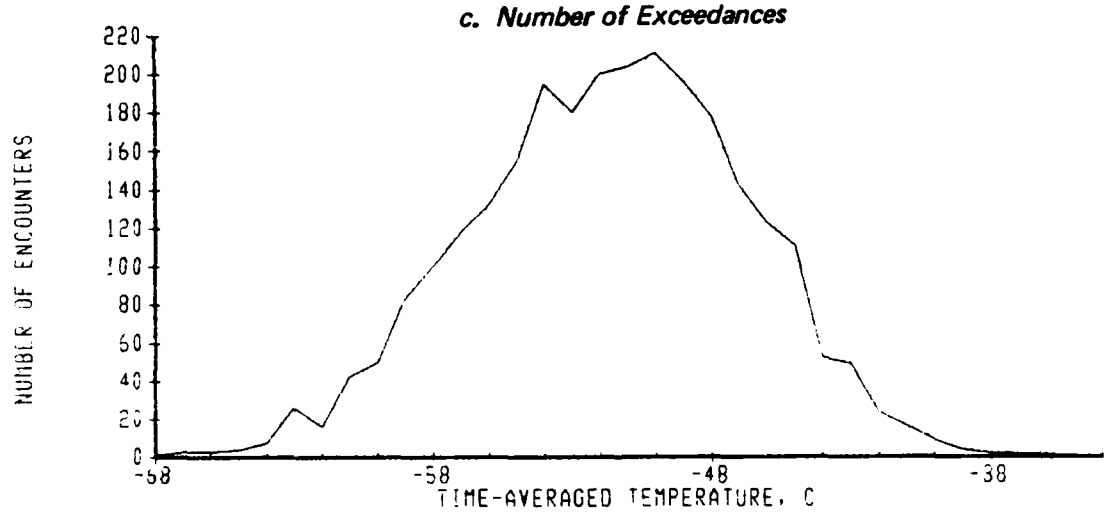

d. Number of Encounters

Figure C-23. F-15 Track 4

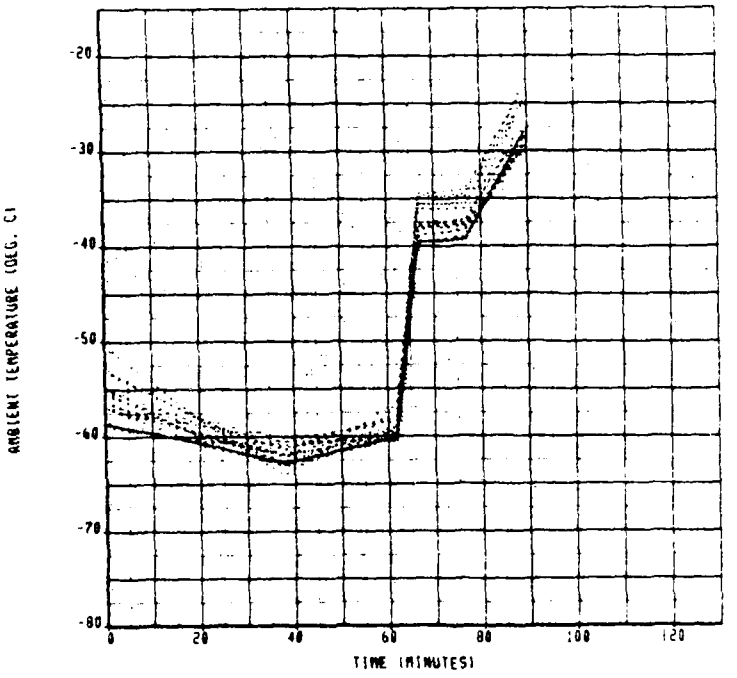

a. 15 Worst Case Cold Days

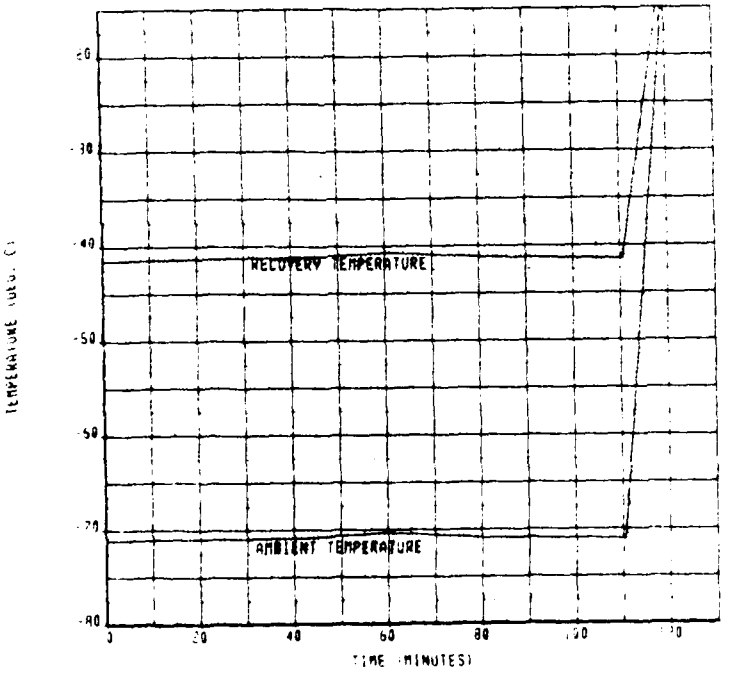

b. Worst Case Cold Day

F-15 TRACK 4

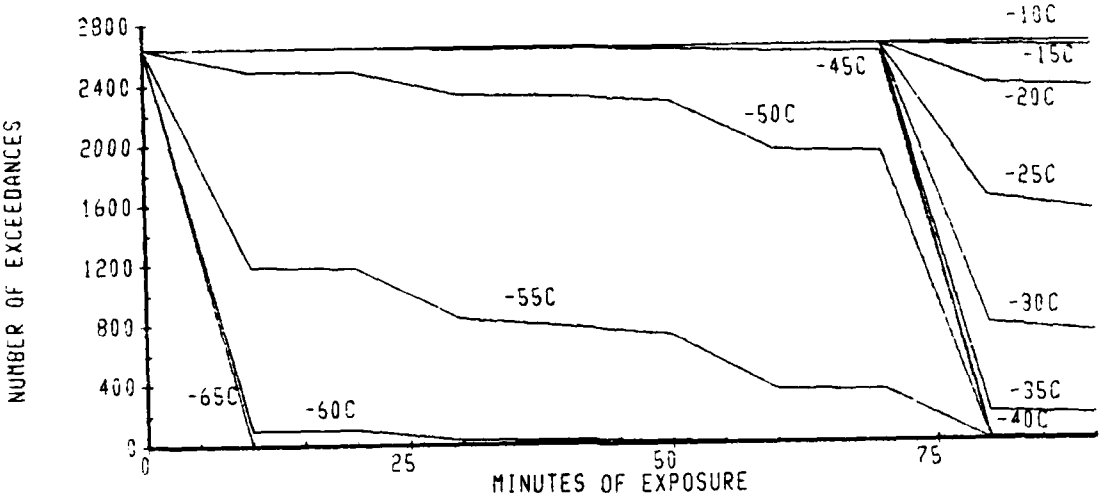

c. Number of Exceedances

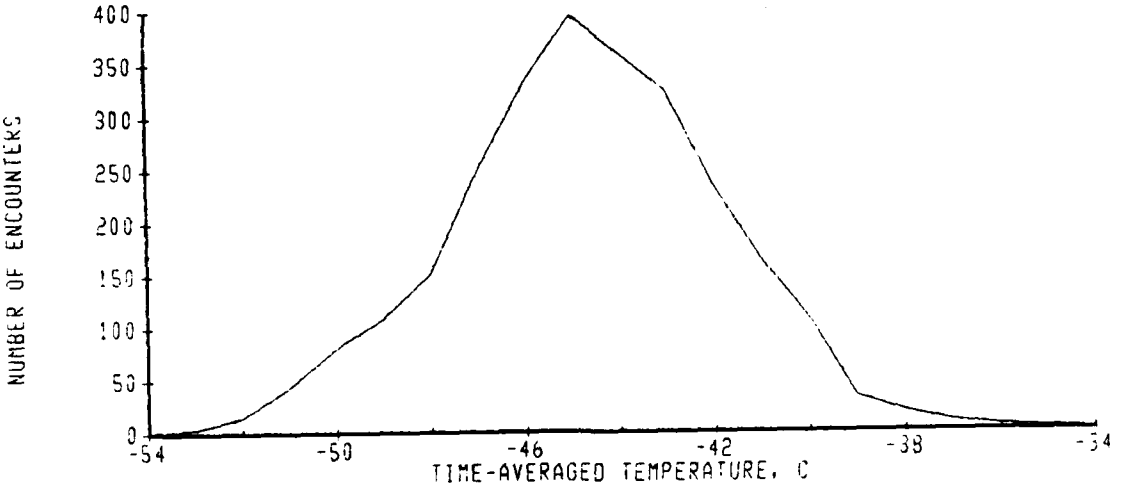

d. Number of Encounters

CALC		19JUL83	REVISED	DATE	F-15 TRACK 4	
CHECK						
APPD.						
APPD.					THE BOEING COMPANY	PAGE 235

Figure C-24. F-15 Track 5

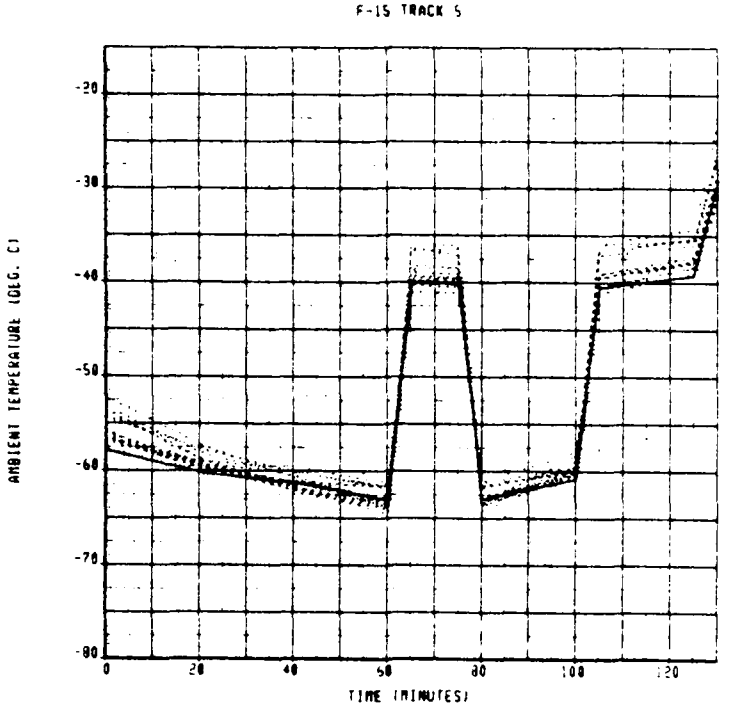

a. 15 Worst Case Cold Days

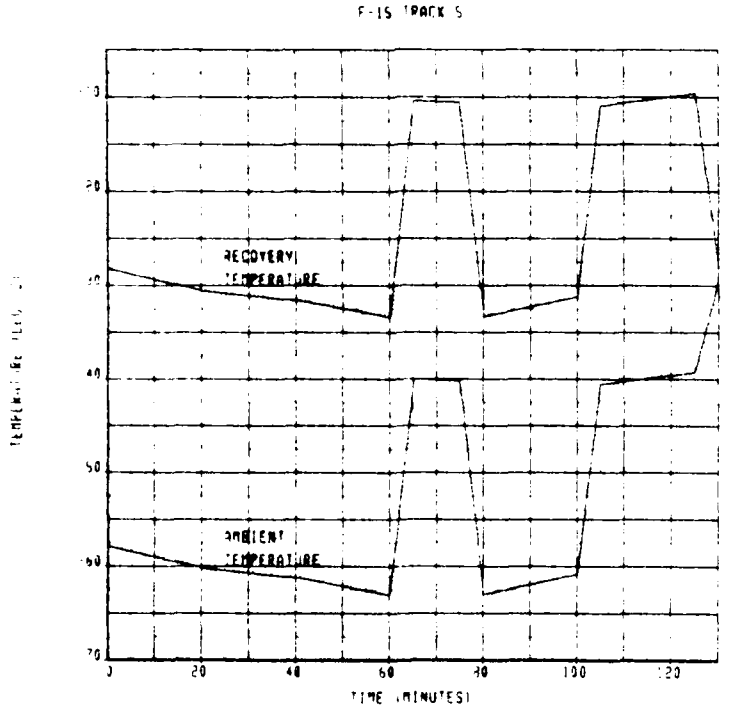

b. Worst Case Cold Day

F-15 TRACK 5

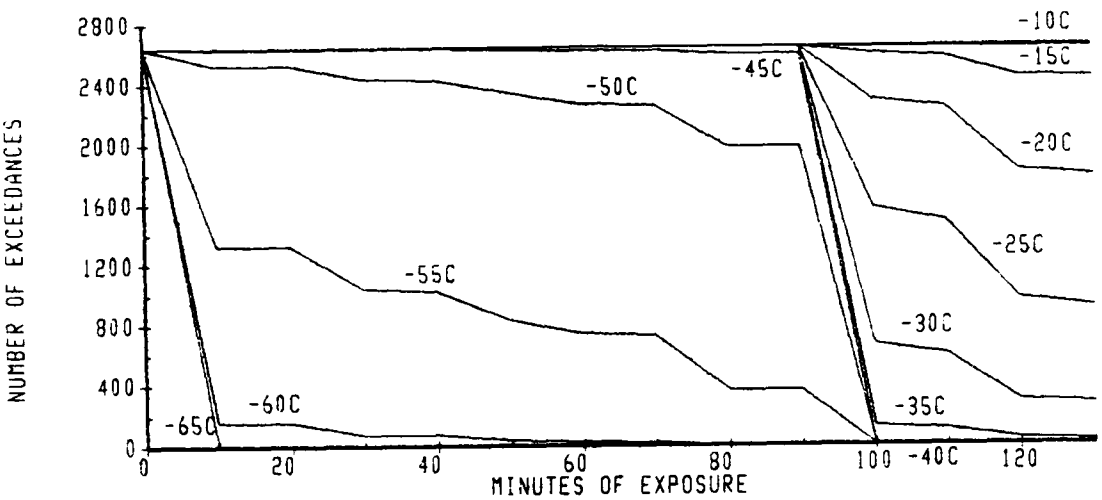

c. Number of Exceedances

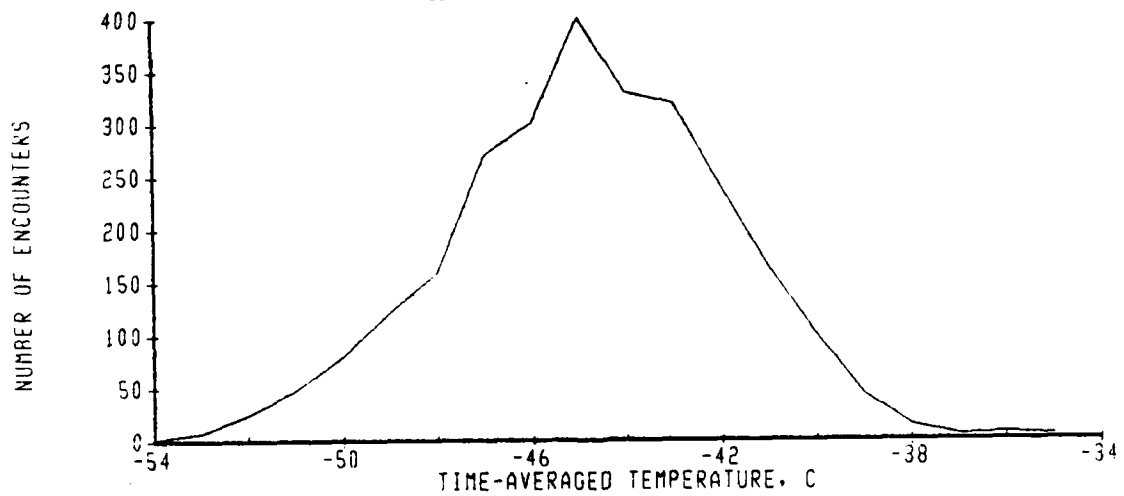

d. Number of Encounters

Figure C-25. F-15 Track 6

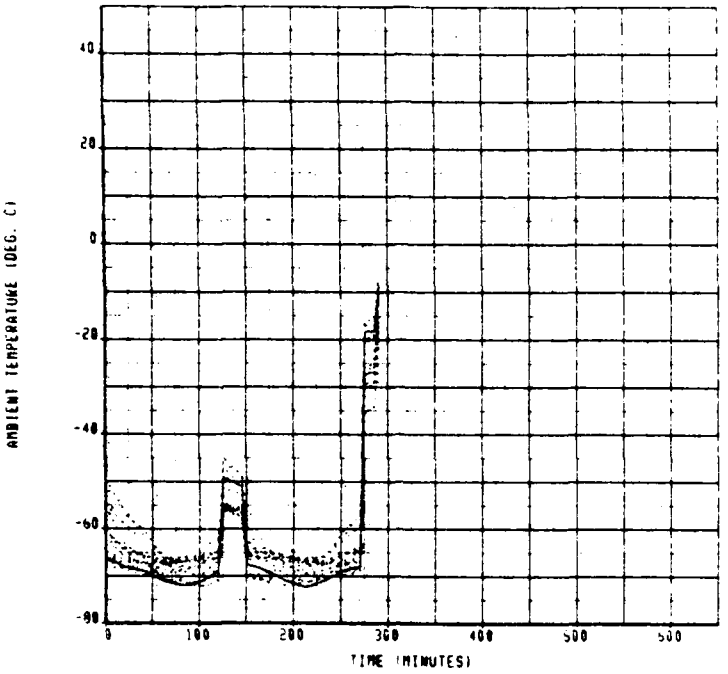

a. 15 Worst Case Cold Days

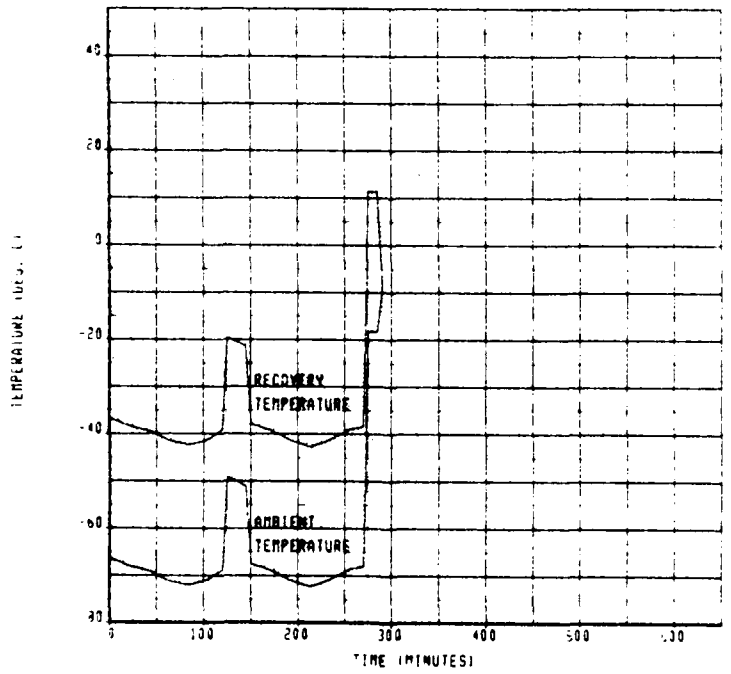

b. Worst Case Cold Day

F-15 TRACK 6

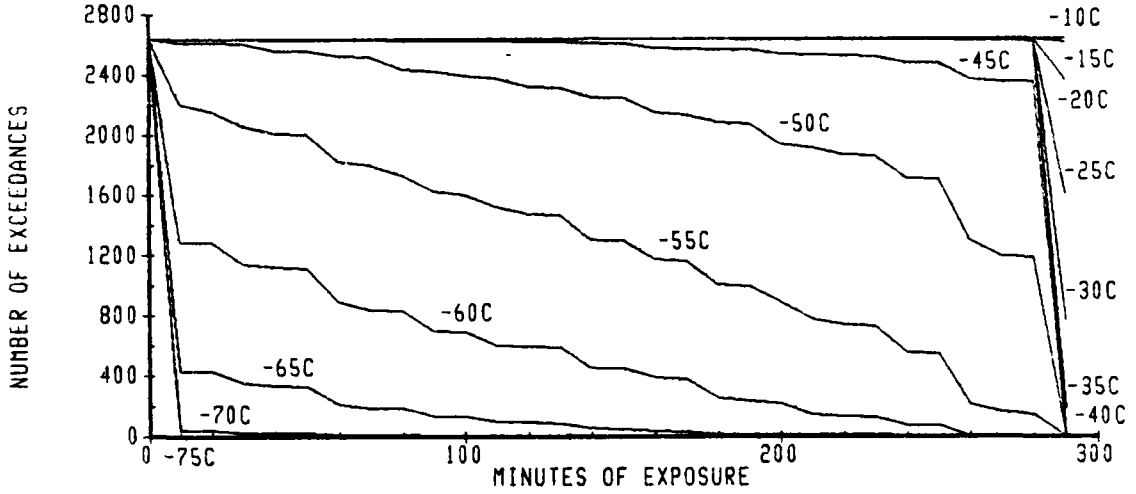

c. Number of Exceedances

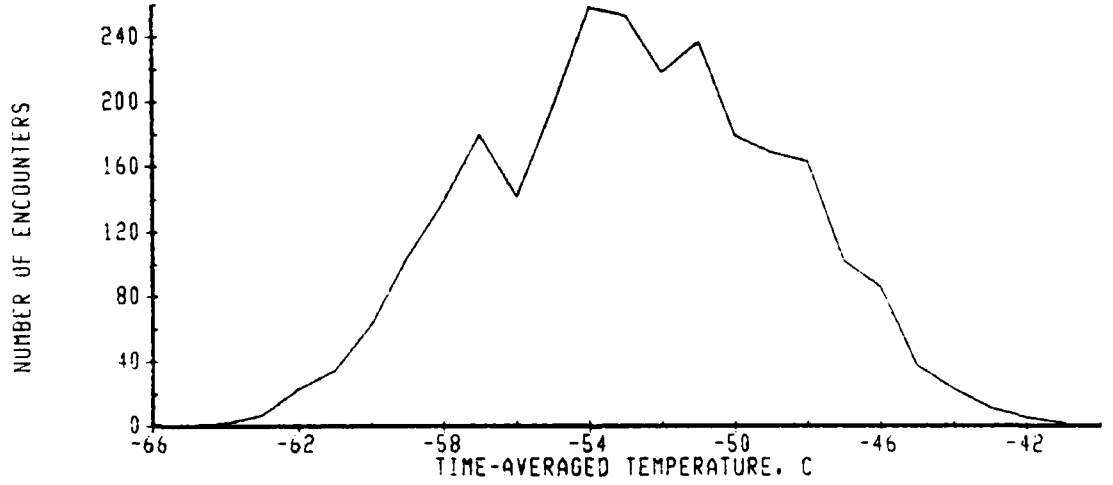

d. Number of Encounters

Figure C-26. F-15 Track 7

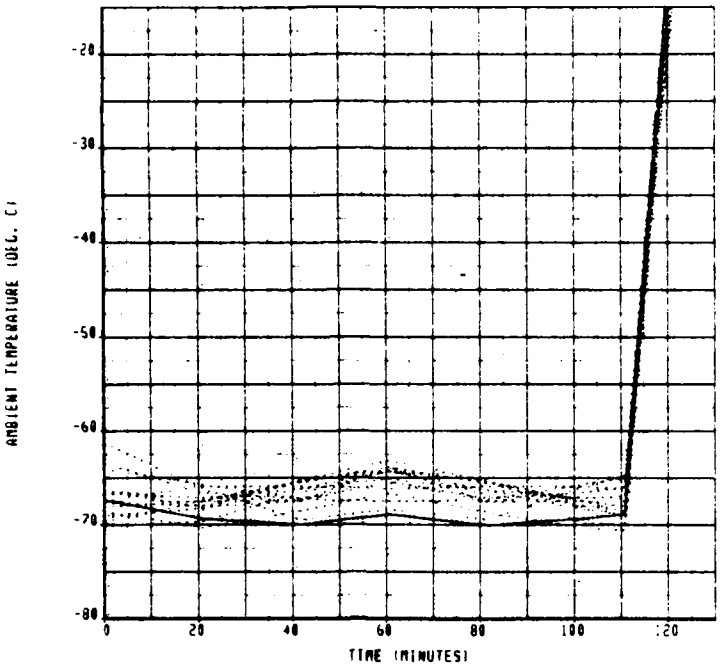

a. 15 Worst Case Cold Days

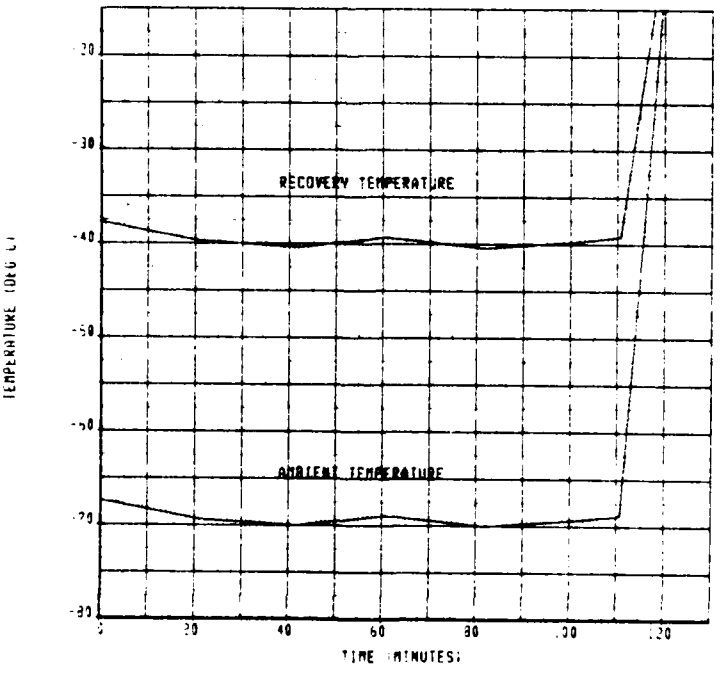

b. Worst Case Cold Day

F-15 TRACK 7

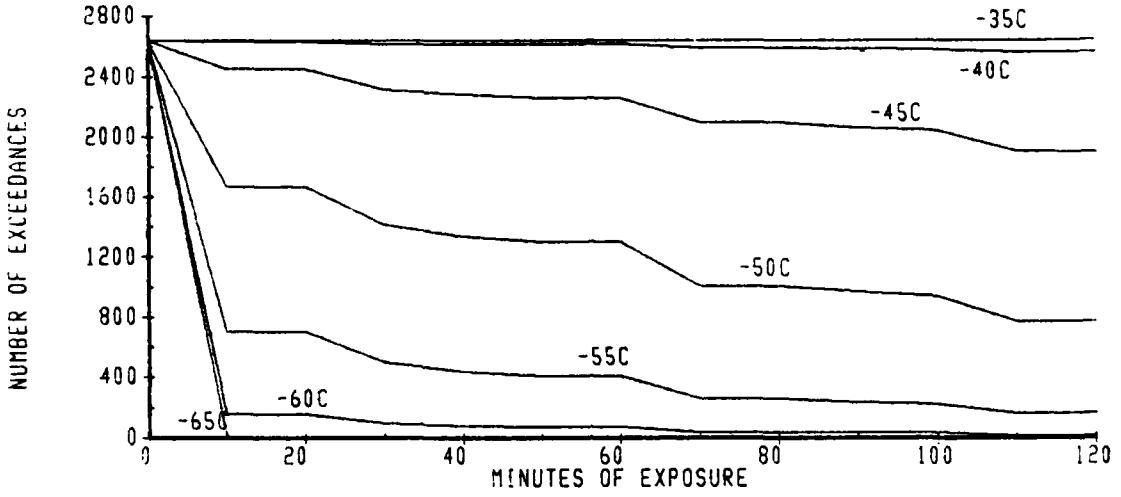

c. Number of Exceedances

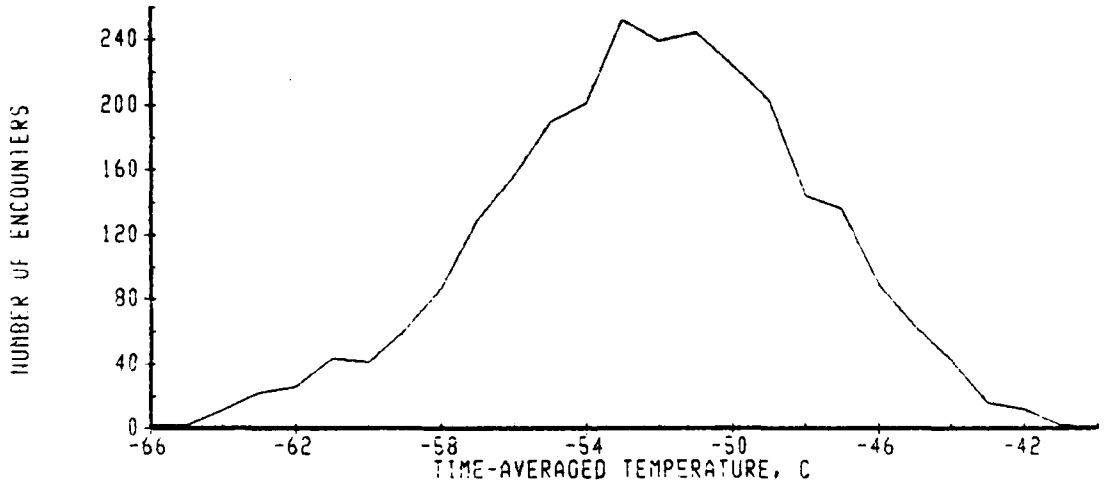

d. Number of Encounters

DRLG		14-JUL83	REVISED	DATE	F-15 TRACK 7
CHECK					
APPD.					
APPD.					THE BOEING COMPANY

Figure C-27. F-15 Track 8

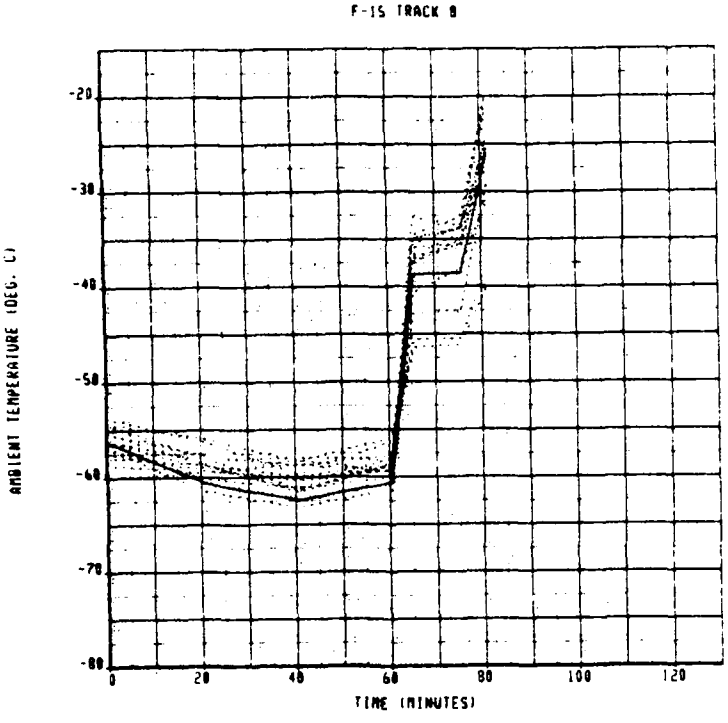

a. 15 Worst Case Cold Days

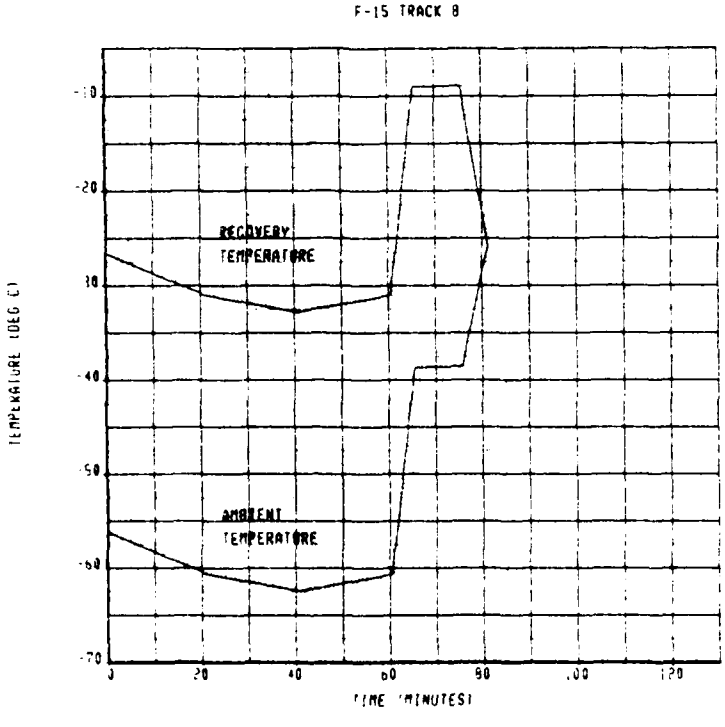

b. Worst Case Cold Day

F-15 TRACK 8

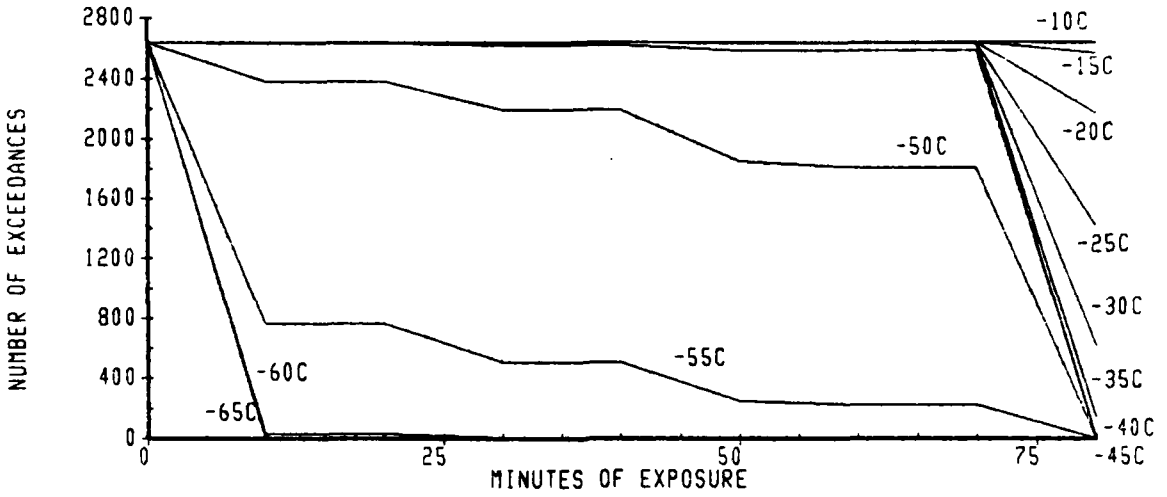

c. Number of Exceedances

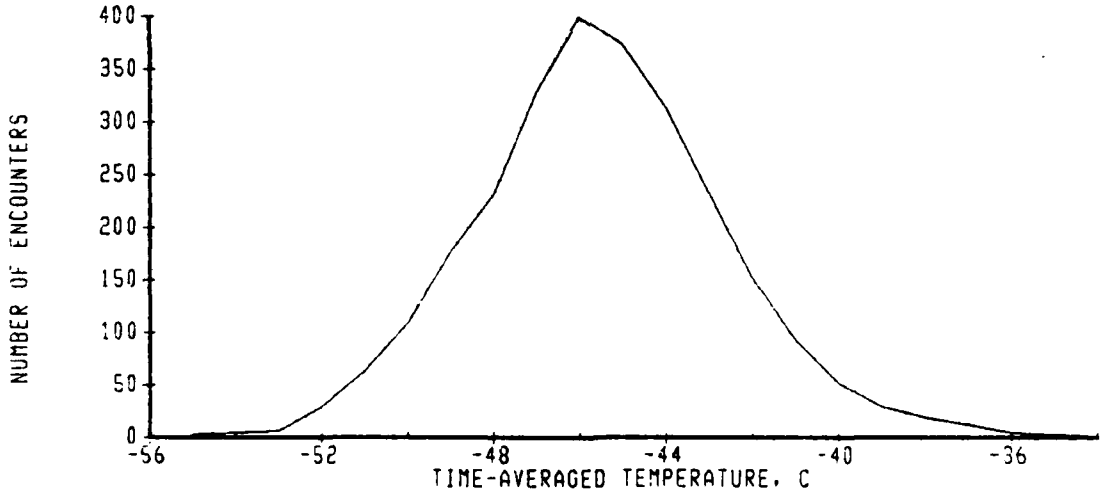

d. Number of Encounters

Figure C-28. F-15 Track 9

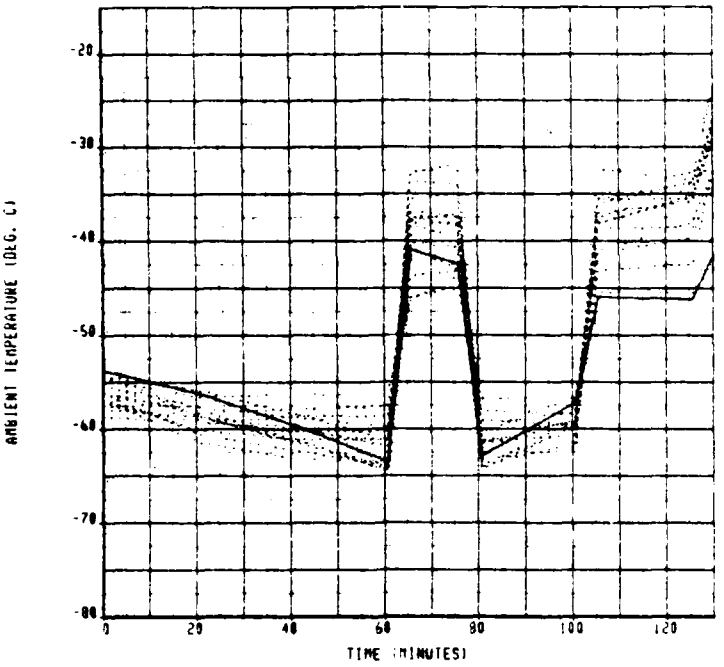

a. 15 Worst Case Cold Days

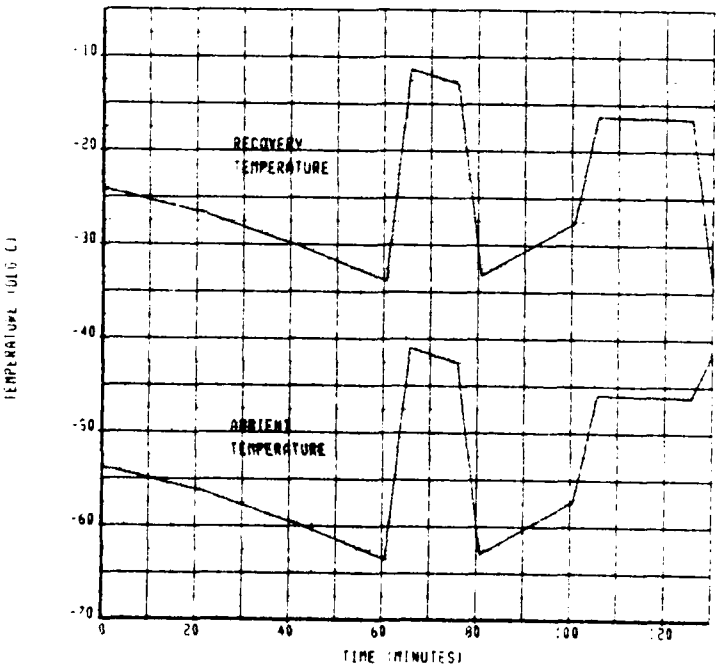

b. Worst Case Cold Day

F-15 TRACK 9

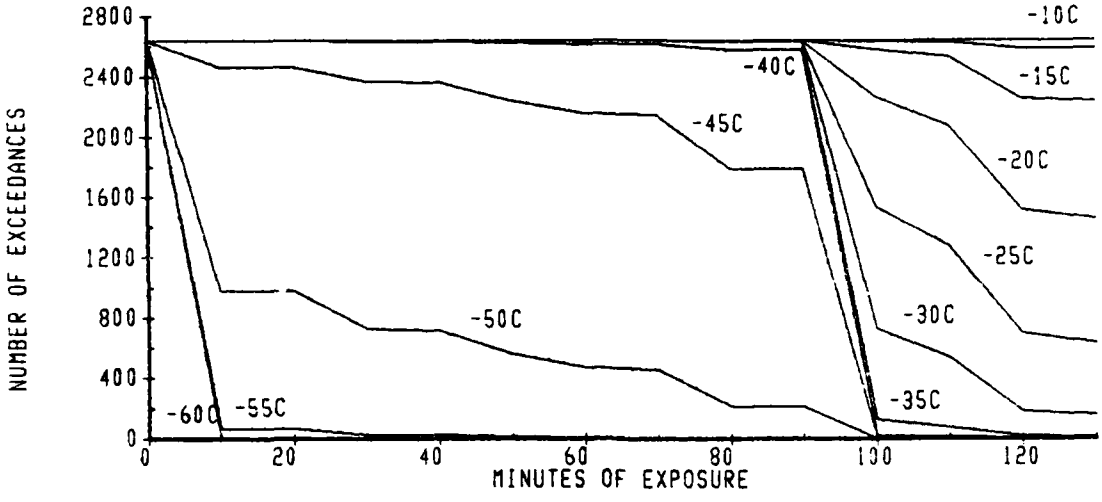

c. Number of Exceedances

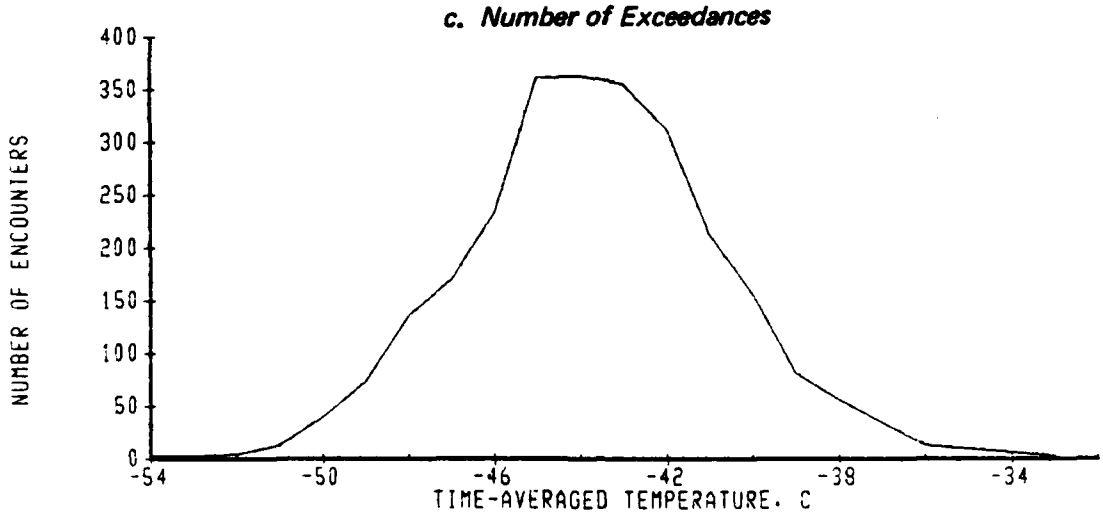

d. Number of Encounters

Figure C-29. F-15 Track 10

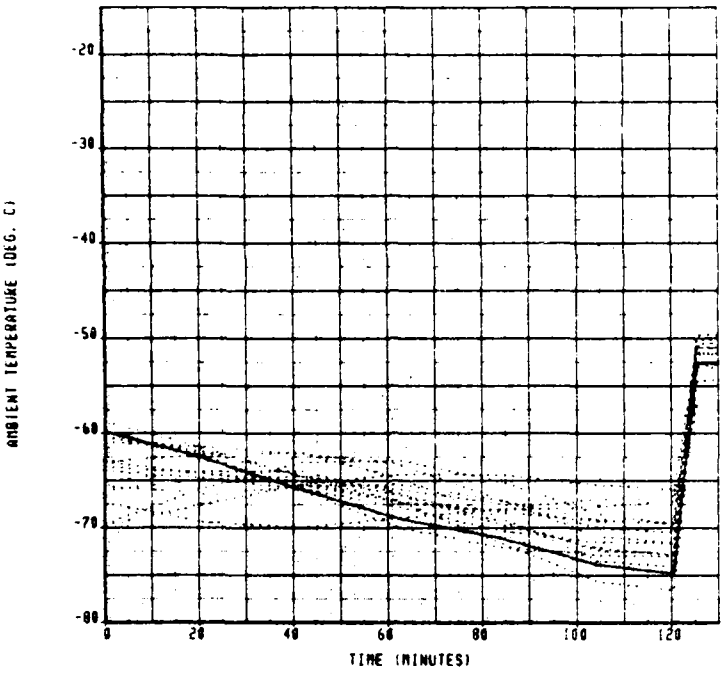

a. 15 Worst Case Cold Days

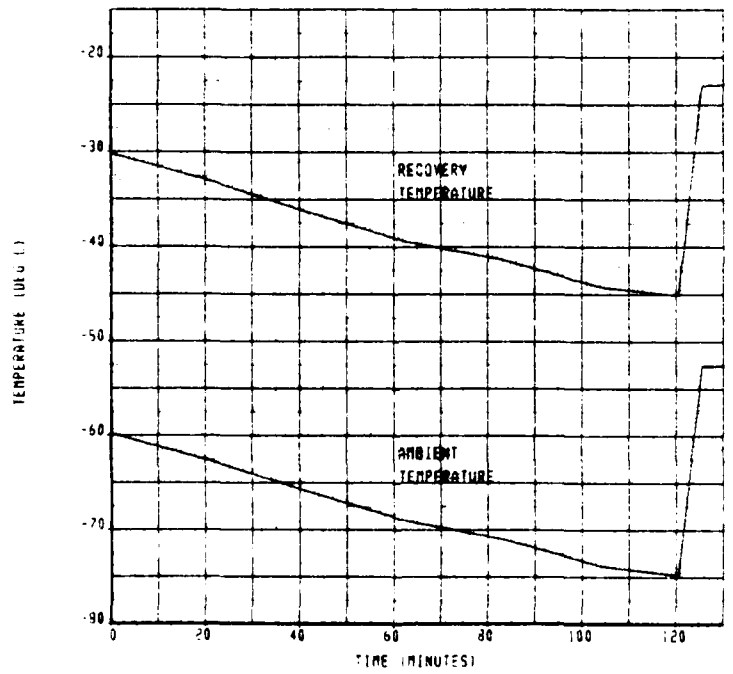

b. Worst Case Cold Day

F-15 TRACK 10

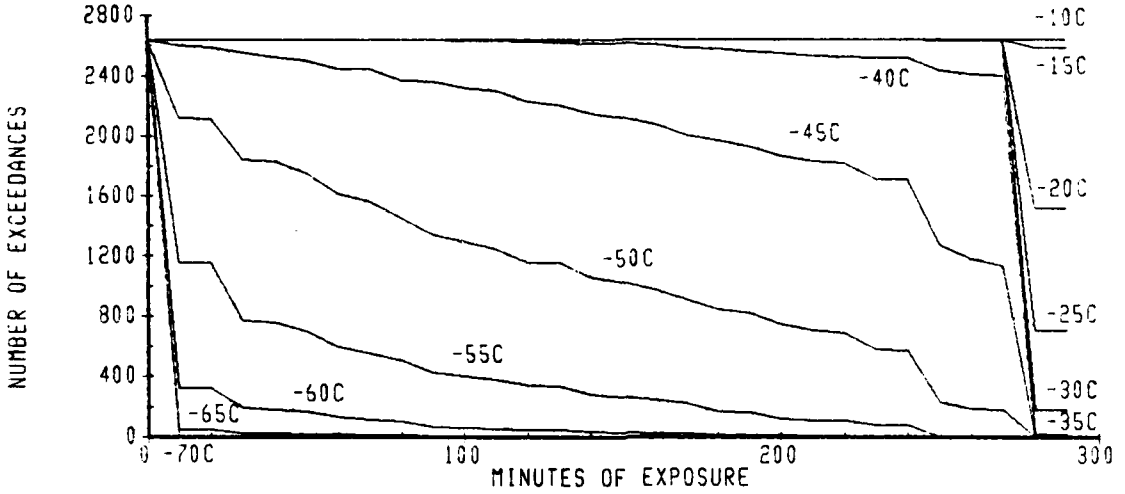

c. Number of Exceedances

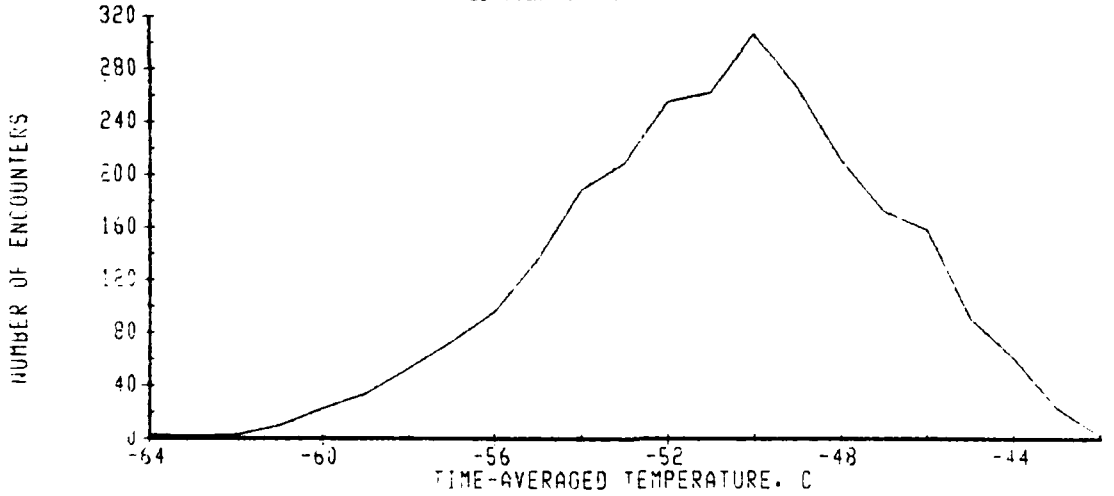

d. Number of Encounters

APPENDIX D GROUND TEMPERATURE EXPOSURE AND STATISTICAL ANALYSIS

Two figures define the thermal exposure and statistical trends of each base:

a 10 Worst Case 24-Hour Periods
b Time - Averaged Temperature Frequency Distribution

Figure D-1. Eielson AFB, Alaska

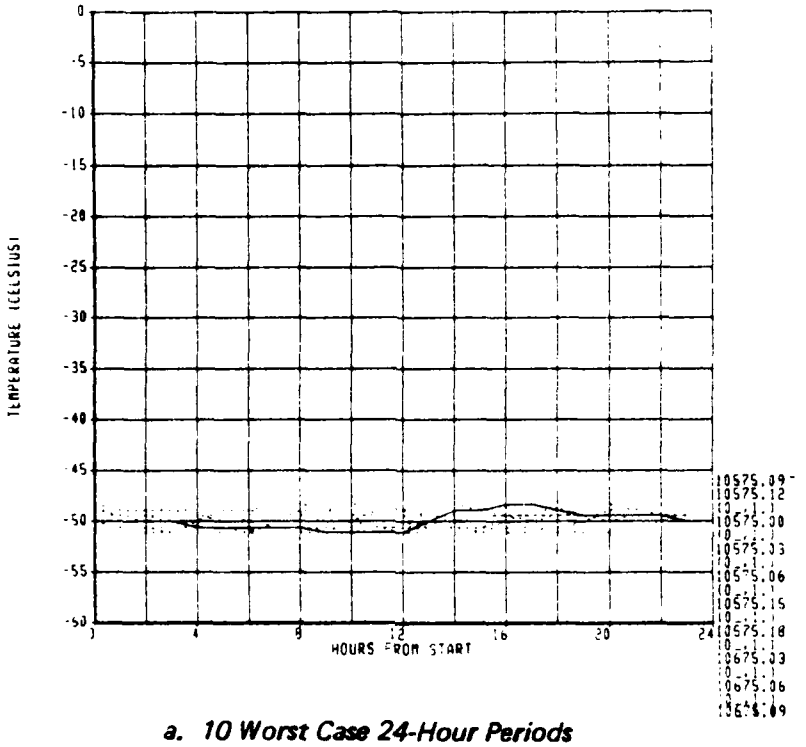

a. 10 Worst Case 24-Hour Periods

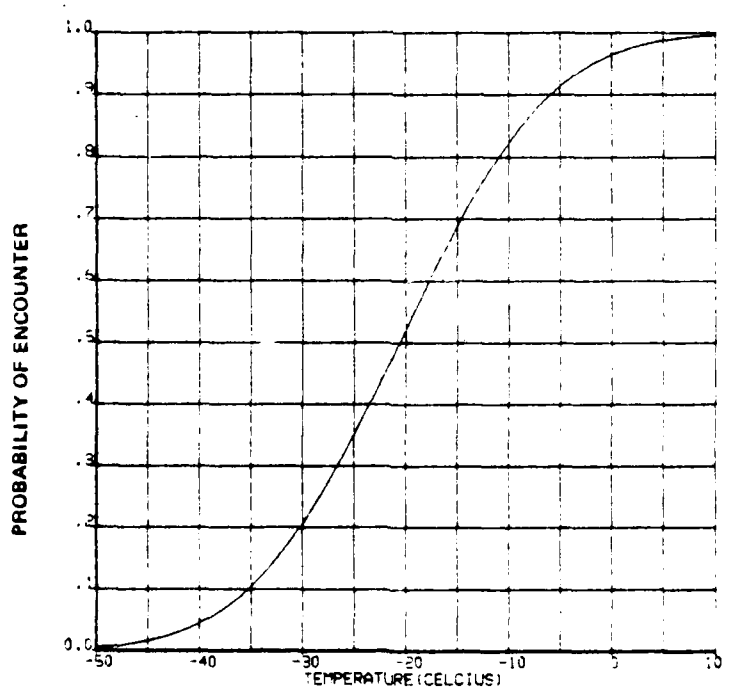

b. Time - Averaged Temperature Frequency Distribution

Figure D-2. Elmendorf AFB, Alaska

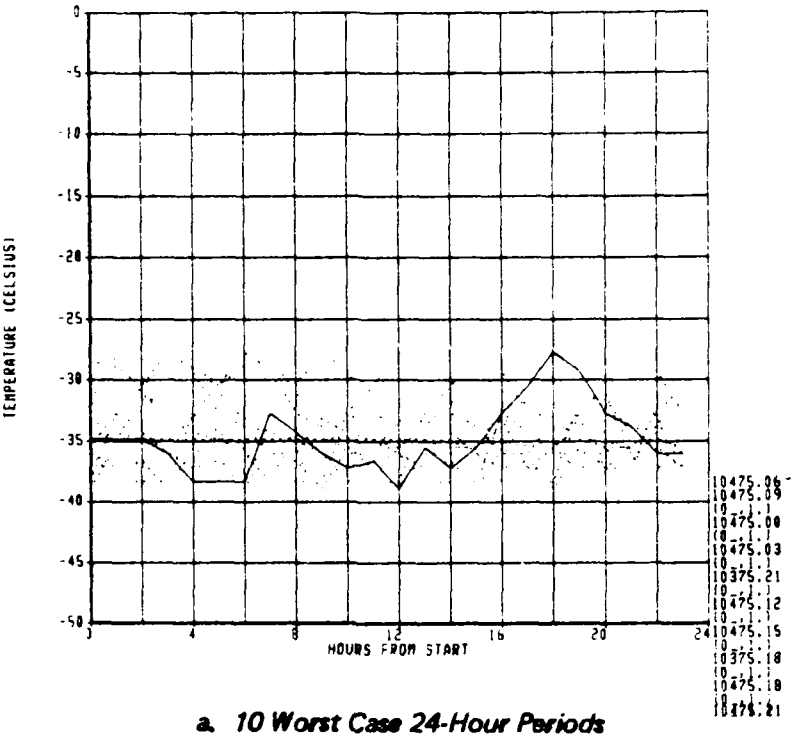

a. 10 Worst Case 24-Hour Periods

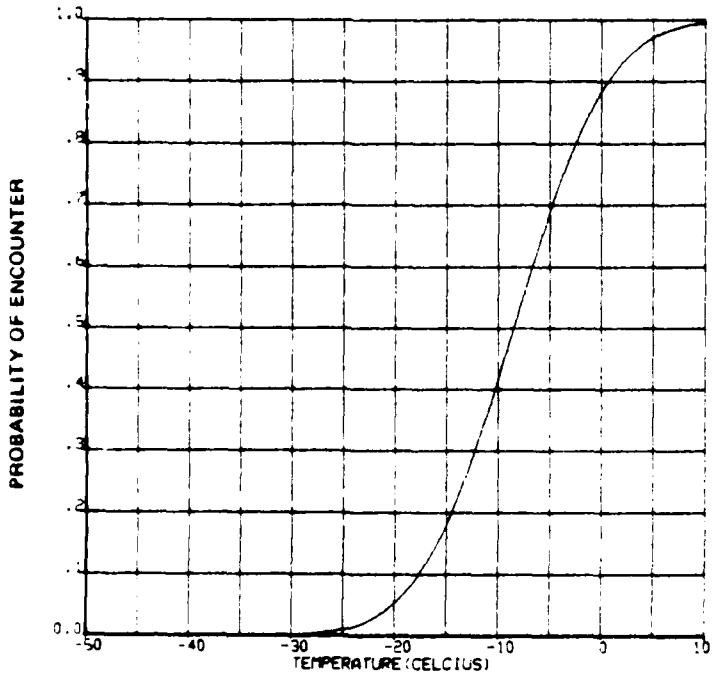

b. Time - Averaged Temperature Frequency Distribution

Figure D-3. Grand Forks AFB, North Dakota

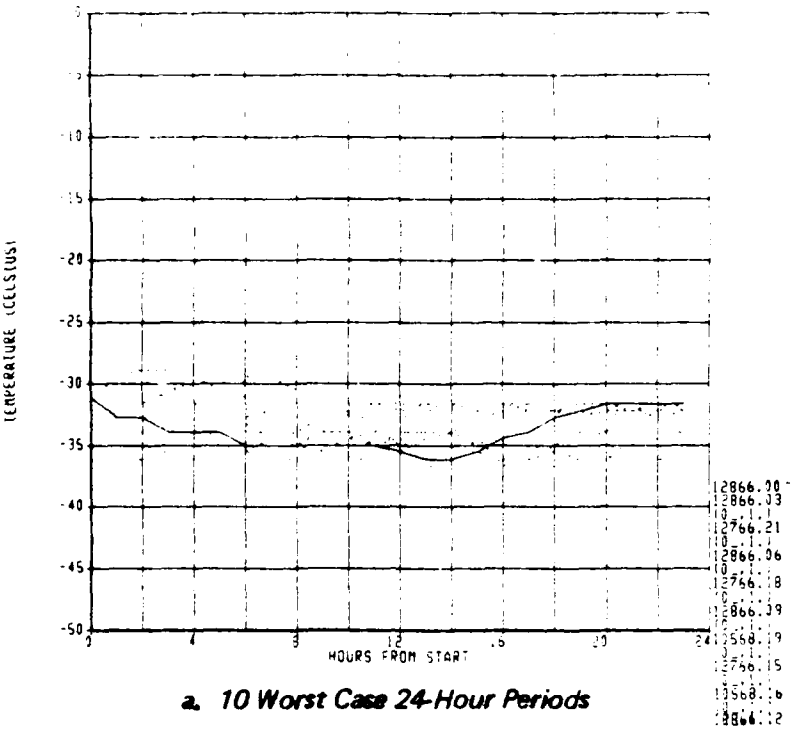

a. 10 Worst Case 24-Hour Periods

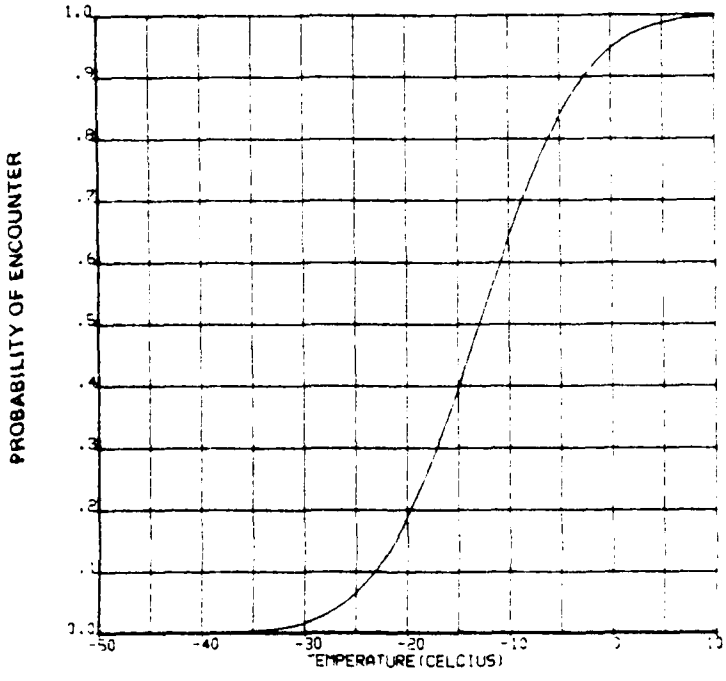

b. Time - Averaged Temperature Frequency Distribution

Figure D-4. Grissom AFB, Indiana

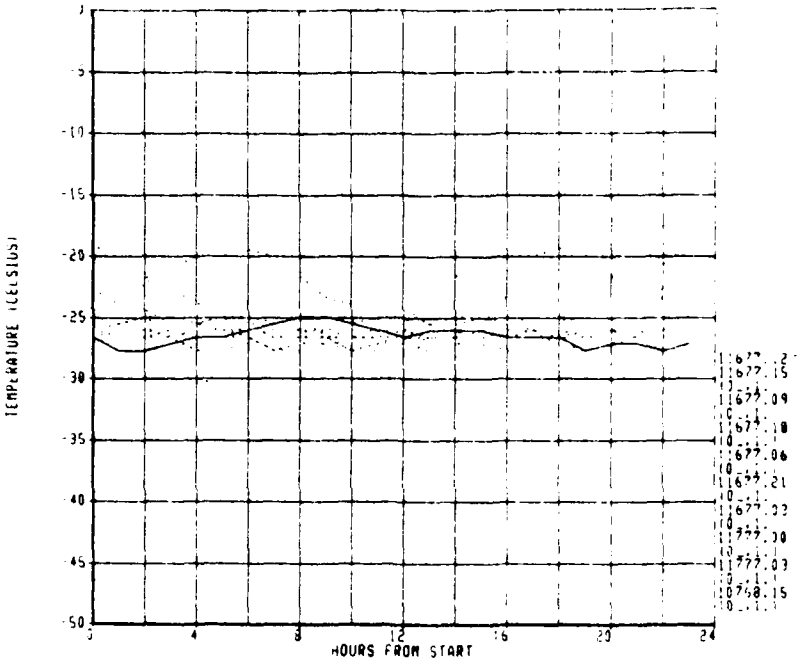

a. 10 Worst Case 24-Hour Periods

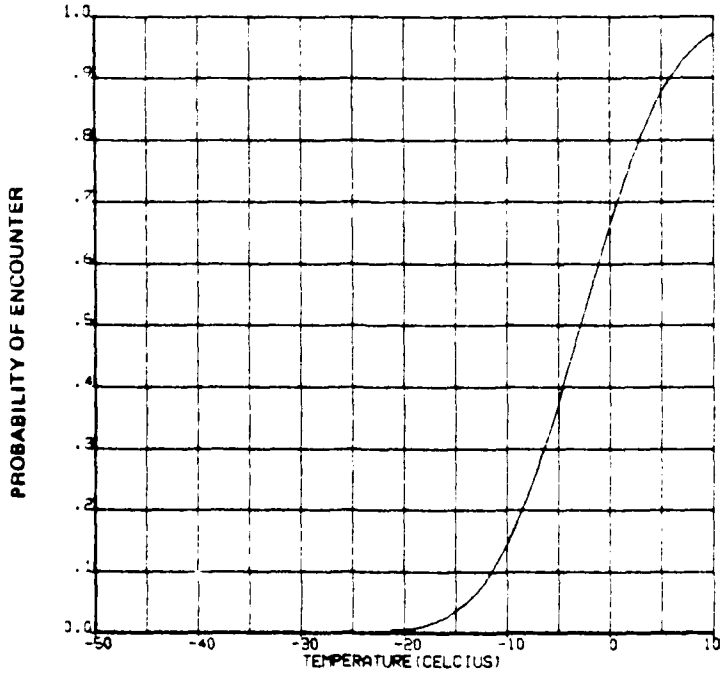

b. Time - Averaged Temperature Frequency Distribution

Figure D-5. Hancock Field, New York

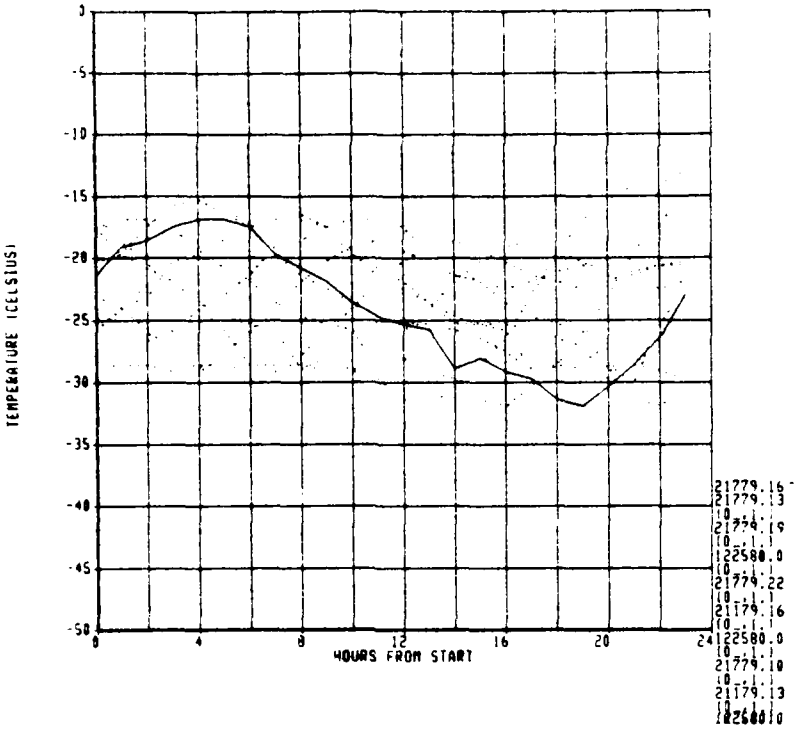

a. 10 Worst Case 24-Hour Periods

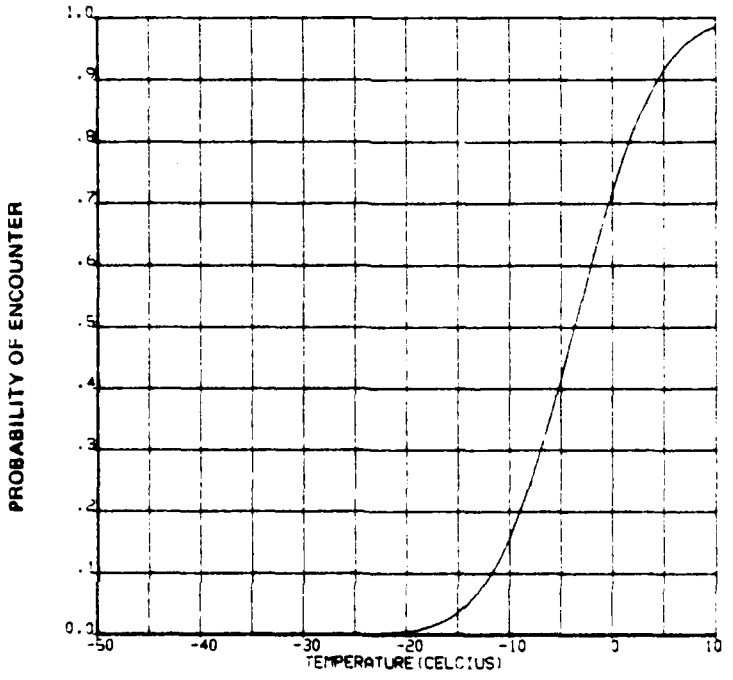

b. Time - Averaged Temperature Frequency Distribution

Figure D-6. Minot AFB, North Dakota

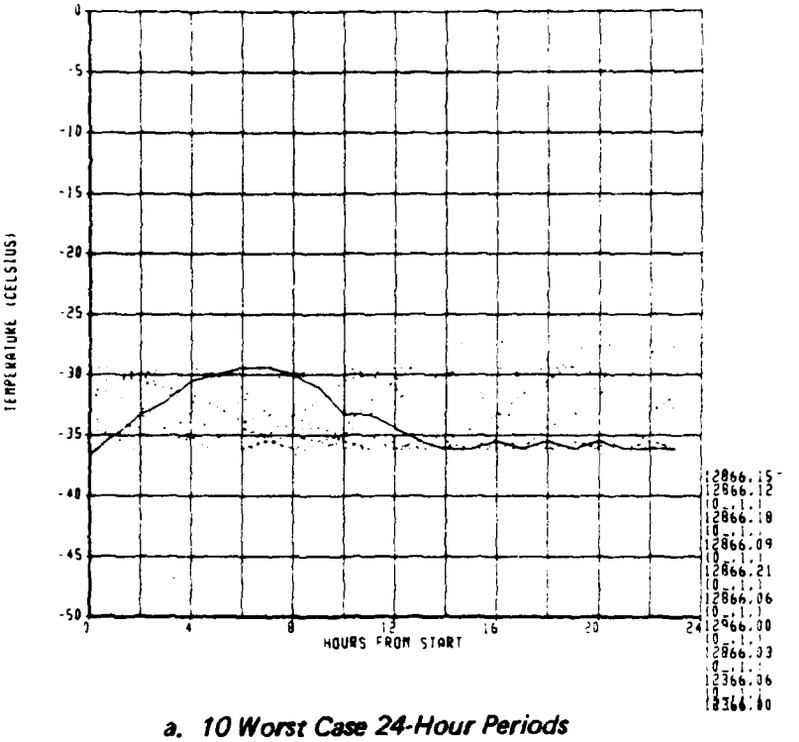

a. 10 Worst Case 24-Hour Periods

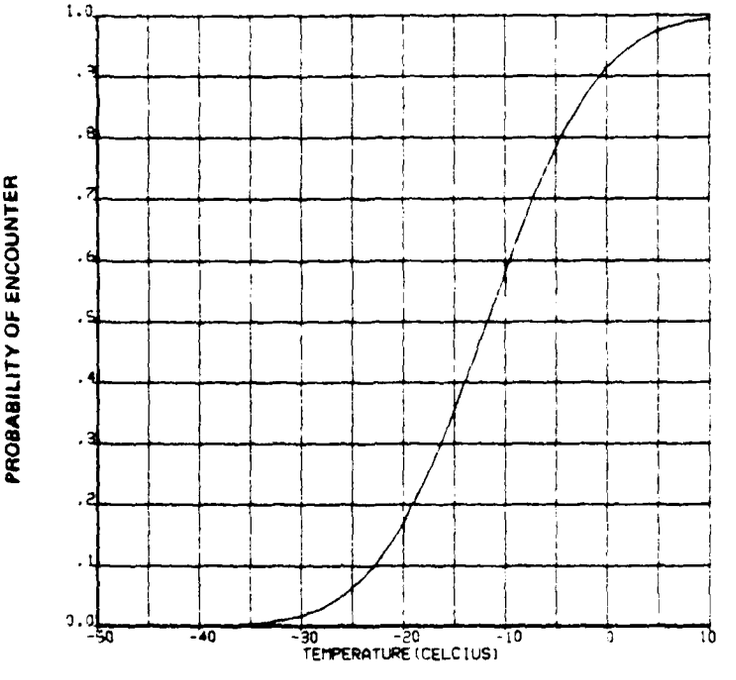

b. Time - Averaged Temperature Frequency Distribution

Figure D-7 Sondrestrom AFB, Greenland

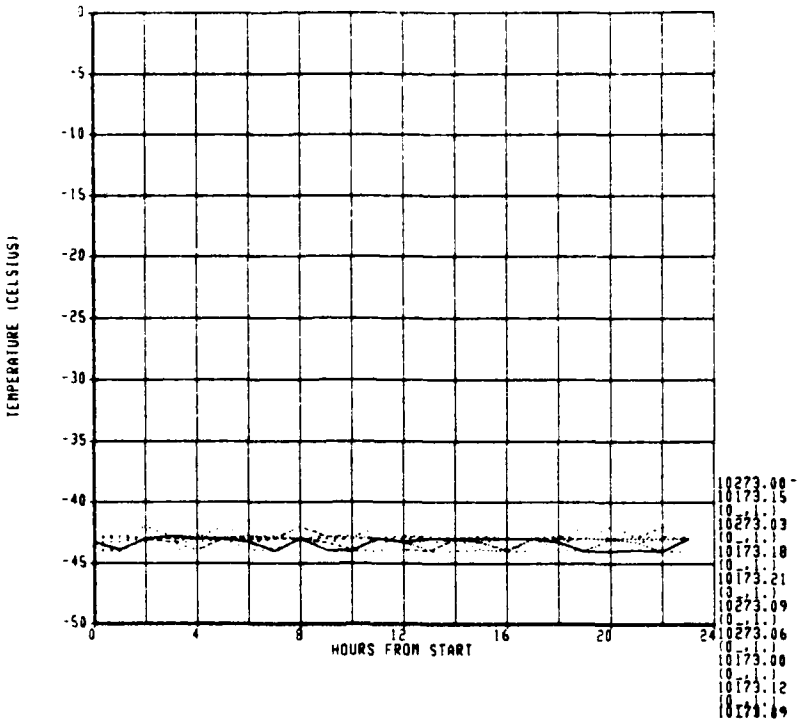

a. 10 Worst Case 24-Hour Periods

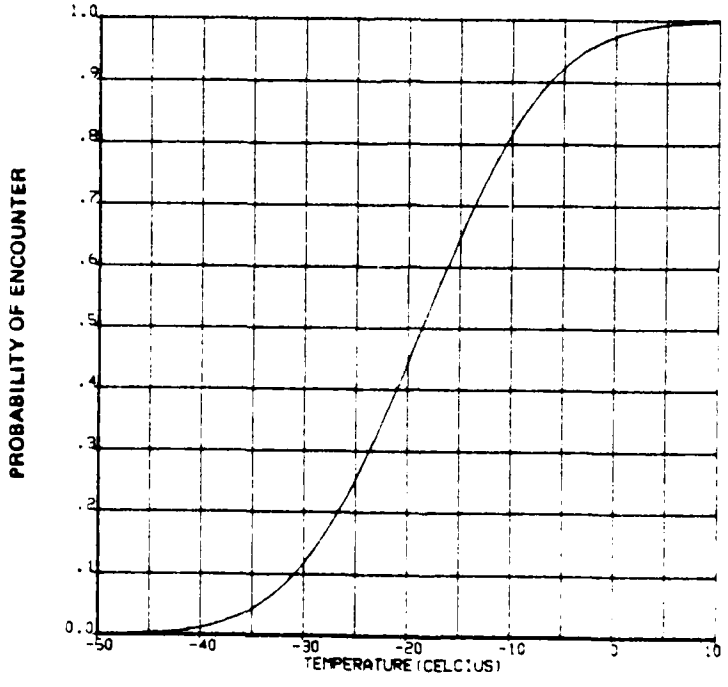

b. Time - Averaged Temperature Frequency Distribution

Figure D-8. Thule AFB, Greenland

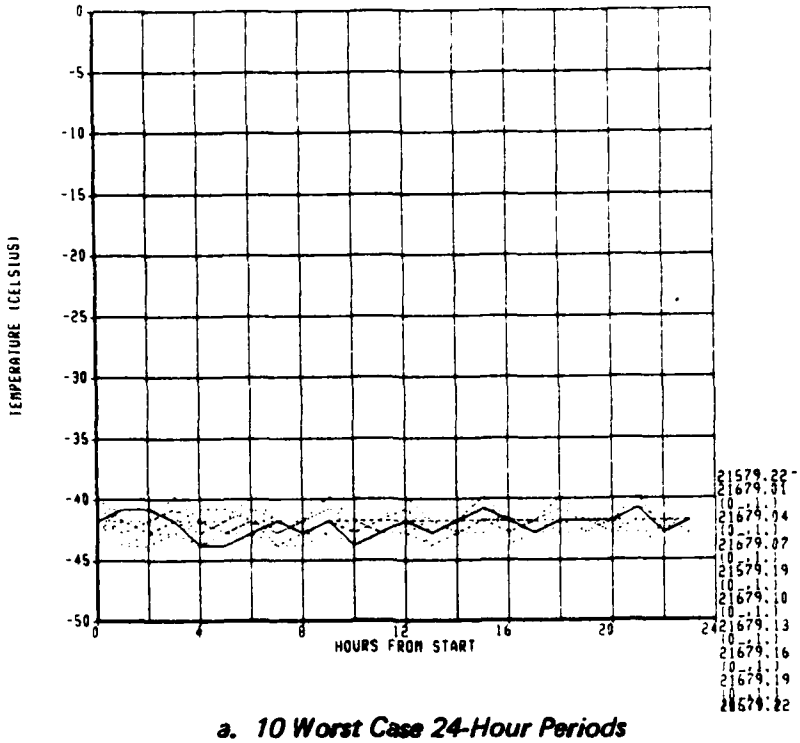

a. 10 Worst Case 24-Hour Periods

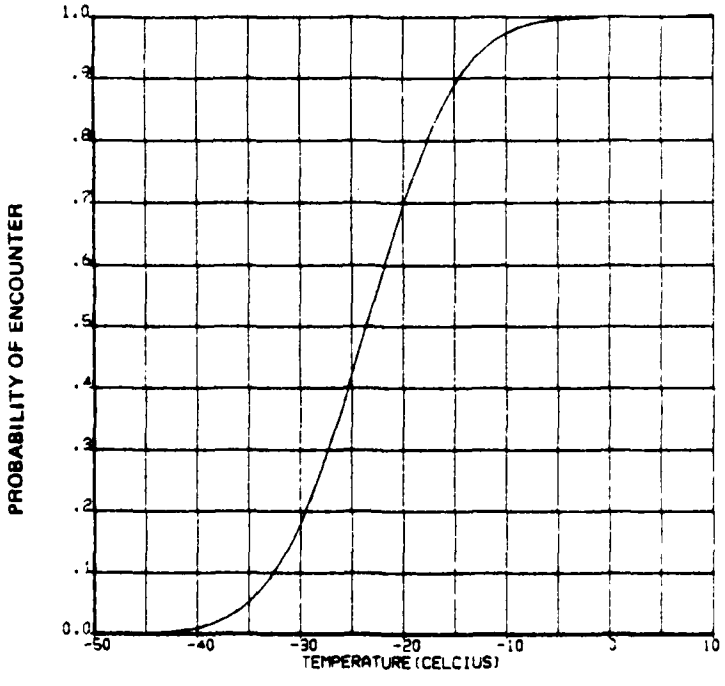

b. Time - Averaged Temperature Frequency Distribution

APPENDIX E FUEL CHARACTERIZATION DATA

Data in this section include the characterization data for the fuels used in the fuel property development phase.

FUEL JP-4, Shale-Derived (81-POSF-114)
MILITARY SPECIFICATION MIL-T-5624L#1

FUEL TYPE DESCRIPTION	SPEC	METHOD	RESULT
Composition			
Aromatics (vol % max)	25.0	D1319	5.8
Olefins (vol % max)	5.0	D1319	0.5
Sulfur, total (wt % max)	0.4	D1266	0.0
Acidity, total (mg KOH/g max)	0.015	D3242	-
Hydrogen Content (wt % min)	13.6	D1018	14.74
Volatility			
Distillation (^{o}C max)	-	D86	-
Initial BP	not limited	-	-3
10%	not limited	-	88
20%	145	-	99
50%	190	-	142
90%	245	-	231
95%	-	-	241
End Point	270	-	255
Residue (vol % max)	1.5	-	-
Loss (vol % max)	1.5	-	-
Flash Point (^{o}C min)	-	D93	10
Density (API @ 15^{o}C min-max)	45-57	D1298	54.8
Gravity Specific (kg/l at 15^{o}C min-max)	0.751-0.802	D1298	-
Fluidity			
Freeze Point, (^{o}C max)	-58.0	D2386	-67
Viscosity (@ -20^{o}C, cst max)	-	D445	-
Temperature (@ 12 cst, ^{o}C)	-	-	-
Combustion			
Aniline-Gravity Product (min)	5250	D1405	
Net Heat of Combustion (BTU/lb min)	18400	D240	18804
Smoke Point (mm min)	20.0	D1322	28.0
Corrosion			
Copper Strip (2 hr @ 100^{o}C max)	1-b	D130	1-a
Stability			
JFTOT, Breakpoint Temp. (^{o}C)	-	-	-
Contaminants			
Existent Gum (mg/100 max)	7.0	D381	-
Particulates (mg/liter max)	1.0	D2276	-
WSIM (min)	70	D2550	-
Additives			
Anti-Icing (vol %)	0.1-0.15	-	-
Corrosion Inhibitor (lb/1000 bbl min-max)	3-8	-	-
Antioxidant (lb/1000 bbl min-max)	6.0-8.4	-	-
Composition Data Available	No		

FUEL JP-5, Shale-Derived (81-POSF-117)
MILITARY SPECIFICATION MIL-T-5624L#1

FUEL TYPE DESCRIPTION	SPEC	METHOD	RESULT
Composition			
Aromatics (vol % max)	25.0	D1319	16.0
Olefins (vol % max)	5.0	D1319	1.2
Sulfur, total (wt % max)	0.4	D1266	0.0
Acidity, total (mg KOH/g max)	0.015	D3242	-
Hydrogen Content (wt % min)	13.5	D1018	13.83
Volatility			
Distillation (^{o}C max)	-	D86	-
Initial BP	not limited	-	134
10%	205	-	164
20%	not limited	-	181
50%	not limited	-	220
90%	not limited	-	254
95%	-	-	260
End Point	290	-	268
Residue (vol % max)	1.5	-	1.0
Loss (vol % max)	1.5	-	1.0
Flash Point (^{o}C min)	-	D93	56
Density (API @ 15^{o}C min-max)	36-58	D1298	43.6
Gravity Specific (kg/l at 15^{o}C min-max)	0.788-0.845	D1298	-
Fluidity			
Freeze Point, (^{o}C max)	-58.0	D2386	-45
Viscosity (@ -20^{o}C, cst max)	-	D445	-
Temperature (@ 12 cst, ^{o}C)	-	-	-
Combustion			
Aniline-Gravity Product (min)	4500	D1405	-
Net Heat of Combustion (BTU/lb min)	18300	D240	18804
Smoke Point (mm min)	19.0	D1322	28.0
Corrosion			
Copper Strip (2 hr @ 100^{o}C max)	1-b	D130	1-b
Stability			
JFTOT, Breakpoint Temp. (^{o}C)	-	-	-
Contaminants			
Existent Gum (mg/100 max)	7.0	D381	-
Particulates (mg/liter max)	1.0	D2276	-
WSIM (min)	85	D2550	-
Additives			
Anti-Icing (vol %)	0.1-0.15	-	-
Corrosion Inhibitor (lb/1000 bbl min-max)	7.5-16.0	-	-
Antioxidant (lb/1000 bbl min-max)	6.0-8.4	-	-
Composition Data Available	No		

FUEL JP-4 (82-POSF-125)
MILITARY SPECIFICATION MIL-T-5624#1

FUEL TYPE DESCRIPTION	SPEC	METHOD	RESULT
Composition			
Aromatics (vol % max)	25.0	D1319	12.2
Olefins (vol % max)	5.0	D1319	1.7
Sulfur, total (wt % max)	0.4	D1266	0.013
Acidity, total (mg KOH/g max)	0.015	D3242	0.01
Hydrogen Content (wt % min)	13.6	D1018	-
Volatility			
Distillation (^{o}C max)	-	D86	-
Initial BP	not limited	-	138
10%	not limited	-	214
20%	145	-	237
50%	190	-	286
90%	245	-	418
95%	-	-	-
End Point	270	-	454
Residue (vol % max)	1.5	-	1.0
Loss (vol % max)	1.5	-	0.0
Flash Point (^{o}C min)	-	D93	-
Density (API @ 15^{o}C min-max)	45-57	D1298	53.3
Gravity Specific (kg/l at 15^{o}C min-max)	0.751-0.802	D1298	-
Fluidity			
Freeze Point, (^{o}C max)	-58.0	D2386	-61
Viscosity (@ -20^{o}C max)	-	D445	-
Temperature (@ 12 cst, ^{o}C)	-	-	-
Combustion			
Aniline-Gravity Product (min)	5250	D1405	6662
Net Heat of Combustion (BTU/lb min)	18400	D240	-
Smoke Point (mm min)	20.0	D1322	-
Corrosion			
Copper Strip (2 hr @ 100^{o}C max)	1-b	D130	1-a
Stability			
JFTOT, Breakpoint Temp. (^{o}C)	-	-	-
Contaminants			
Existent Gum (mg/100 max)	7.0	D381	0.3
Particulates (mg/liter max)	1.0	D2276	0.53
WSIM (min)	70	D2550	88
Additives			
Anti-Icing (vol %)	0.1-0.15	-	0.12 (Union Carbide)
Corrosion Inhibitor (lb/1000 bbl min-max)	3-8	-	-
Antioxidant (lb/1000 bbl min-max)	6.0-8.4	-	-
Composition Data Available	Yes		

FUEL JP-4 (82-POSF-159)
MILITARY SPECIFICATION MIL-T-5624L#1

FUEL TYPE DESCRIPTION	SPEC	METHOD	RESULT
Composition			
Aromatics (vol % max)	25.0	D1319	12.4
Olefins (vol % max)	5.0	D1319	1.2
Sulfur, total (wt % max)	0.4	D1266	0.02
Acidity, total (mg KOH/g max)	0.015	D3242	-
Hydrogen Content (wt % min)	13.6	D1018	14.4
Volatility			
Distillation (^{o}C max)	-	D86	-
Initial BP	not limited	-	27
10%	not limited	-	83
20%	145	-	115
50%	190	-	149
90%	245	-	180
95%	-	-	186
End Point	270	-	213
Residue (vol % max)	1.5	-	-
Loss (vol % max)	1.5	-	-
Flash Point (^{o}C min)	-	D93	-
Density (API @ 15^{o}C min-max)	45-57	D1298	54.6
Gravity Specific (kg/l at 15^{o}C min-max)	0.751-0.802	D1298	0.7603
Fluidity			
Freeze Point, (^{o}C max)	-58.0	D2386	-
Viscosity (@ -20^{o}C max)	-	D445	-
Temperature (@ 12 cst, ^{o}C)	-	-	-
Combustion			
Aniline-Gravity Product (min)	5250	D1405	-
Net Heat of Combustion (BTU/lb min)	18400	D240	-
Smoke Point (mm min)	20.0	D1322	28
Corrosion			
Copper Strip (2 hr @ 100^{o}C max)	1-b	D130	-
Stability			
JFTOT, Breakpoint Temp. (^{o}C)	-	-	-
Contaminants			
Existent Gum (mg/100 max)	7.0	D381	-
Particulates (mg/liter max)	1.0	D2276	-
WSIM (min)	70	D2550	-
Additives			
Anti-Icing (vol %)	0.1-0.15	-	-
Corrosion Inhibitor (lb/1000 bbl min-max)	3-8	-	-
Antioxidant (lb/1000 bbl min-max)	6.0-8.4	-	-
Composition Data Available	Yes		

FUEL JP-8 (82-POSF-168)
MILITARY SPECIFICATION MIL-T-83133A

FUEL TYPE DESCRIPTION	SPEC RQMT	METHOD	RESULT
Composition			
Aromatics (vol % max)	25.0	D1319	-
Olefins (vol % max)	5.0	D1319	-
Sulfur, total (wt % max)	0.3	D1266	-
Acidity, total (mg KOH/g max)	0.015	D3242	-
Hydrogen Content (wt % min)	13.5	D1018	-
Volatility			
Distillation (^{o}C max)	-	D86	-
Initial BP	not limited	-	-
10%	205	-	-
20%	not limited	-	-
50%	not limited	-	-
90%	not limited	-	-
End Point	300	-	-
Residue (vol % max)	1.5	-	-
Loss (%)	1.5	-	-
Flash Point (^{o}C min)	38.0	D56	-
Density (API @ 15^{o}C min-max)	37.0-51.0	D287	-
Gravity Specific (kg/l at 15^{o}C min-max)	0.775-0.840	D1298	-
Fluidity			
Freeze Point (^{o}C max)	-50	D2386	-
Viscosity (@ -20^{o}C cst. max)	-	D445	-
Temperature (@ 12 cst ^{o}C)	-	-	-
Combustion			
Aniline-Gravity Product (min)	-	-	-
Net Heat of Combustion (BTU/lb min)	18400	D240	-
Smoke Point (mm min)	19	D1322	-
Corrosion			
Copper Strip (2 hr @ 100^{o}C max)	1-b	D130	-
Stability			
JFTOT, Breakpoint Temp. (^{o}C)	-	-	-
Contaminants			
Existent Gum (mg/100 ml max)	7.0	D381	-
Particulates (mg/liter max)	1.0	D2276	-
WSIM (min)	70	D2550	-
Additives			
Anti-Icing (vol %)	0.1-0.15	-	-
Corrosion Inhibitor, (lb/1000 bbl)	-	-	-
Antioxidant, (lb/1000 bbl min-max)	6.0-8.4	-	-
Composition Data Available	No		

FUEL JP-8 (82-POSF-445)
MILITARY SPECIFICATION MIL-T-83133A

FUEL TYPE DESCRIPTION	SPEC RQMT	METHOD	RESULT
Composition			
Aromatics (vol % max)	25.0	D1319	16.8
Olefins (vol % max)	5.0	D1319	2.1
Sulfur, total (wt % max)	0.3	D1266	0.11
Acidity, total (mg KOH/g max)	0.015	D3242	0.002
Hydrogen Content (wt % min)	13.5	D1018	13.79
Volatility			
Distillation (^{o}C max)	-	D86	-
Initial BP	not limited	-	182
10%	205	-	202
20%	not limited	-	207
50%	not limited	-	221
90%	not limited	-	248
End Point	300	-	266
Residue (vol % max)	1.5	-	1.0
Loss (%)	1.5	-	1.0
Flash Point (^{o}C min)	38.0	D56	54
Density (API @ 15^{o}C min-max)	37.0-51.0	D287	42.3
Gravity Specific (kg/l at 15^{o}C min-max)	0.775-0.840	D1298	0.8142
Fluidity			
Freeze Point (^{o}C max)	-50	D2386	-44
Viscosity (@ -20^{o}C cst max)	-	D445	1.67
Temperature (@ 12 cst ^{o}C)	-	-	-
Combustion			
Aniline-Gravity Product (min)	-	-	7793
Net Heat of Combustion (BTU/lb min)	18400	D240	18591
Smoke Point (mm min)	19	D1322	26.0
Corrosion			
Copper Strip (2 hr @ 100^{o}C max)	1-b max	D130	1-a
Stability			
JFTOT, Breakpoint Temp. (^{o}C)	-	-	-
Contaminants			
Existent Gum (mg/100 ml max)	7.0	D381	0.0
Particulates (mg/liter max)	1.0	D2276	0.5
WSIM (min)	70	D2550	-
Additives			
Anti-Icing (vol %)	0.1-0.15	-	0.14
Corrosion Inhibitor, (lb/1000 bbl)	-	-	-
Antioxidant, (lb/1000 bbl min-max)	6.0-8.4	-	-
Composition Data Available	No		

FUEL JP-4 (82-POSF-447)
MILITARY SPECIFICATION MIL-T-5624L#1

FUEL TYPE DESCRIPTION	SPEC	METHOD	RESULT
Composition			
Aromatics (vol % max)	25.0	D1319	-
Olefins (vol % max)	5.0	D1319	-
Sulfur, total (wt % max)	0.4	D1266	0.03
Acidity, total (mg KOH/g max)	0.015	D3242	0.002
Hydrogen Content (wt % min)	13.6	D1018	14.46
Volatility			
Distillation (^{o}C max)	-	D86	-
Initial BP	not limited	-	61
10%	not limited	-	97
20%	145	-	110
50%	190	-	148
90%	245	-	228
95%	-	-	-
End Point	270	-	255
Residue (vol % max)	1.5	-	1.0
Loss (vol % max)	1.5	-	1.0
Flash Point (^{o}C min)	-	D93	-
Density (API @ 15^{o}C min-max)	45-57	D1298	54.3
Gravity Specific (kg/l at 15^{o}C min-max)	0.751-0.802	D1298	0.7616
Fluidity			
Freeze Point, (^{o}C max)	-58.0	D2386	-64
Viscosity (@ -20^{o}C max)	-	D445	0.7864
Temperature (@ 12 cst, ^{o}C)	-	-	-
Combustion			
Aniline-Gravity Product (min)	5250	D1405	-
Net Heat of Combustion (BTU/lb min)	18400	D240	18747
Smoke Point (mm min)	20.0	D1322	25.0
Corrosion			
Copper Strip (2 hr @ 100^{o}C max)	1-b	D130	1-a
Stability			
JFTOT, Breakpoint Temp. (^{o}C)	-	-	-
Contaminants			
Existent Gum (mg/100 max)	7.0	D381	0.8
Particulates (mg/liter max)	1.0	D2276	0.1
WSIM (min)	70	D2550	96
Additives			
Anti-Icing (vol %)	0.1-0.15	-	0.07
Corrosion Inhibitor (lb/1000 bbl min-max)	3-8	-	-
Antioxidant (lb/1000 bbl min-max)	6.0-8.4	-	-
Composition Data Available	Yes		

FUEL JP-8, Shale-Derived (82-POSF-562)
MILITARY SPECIFICATION MIL-T-83133A

FUEL TYPE DESCRIPTION	SPEC RQMT	METHOD	RESULT
Composition			
Aromatics (vol % max)	25.0	D1319	22.2
Olefins (vol % max)	5.0	D1319	1.6
Sulfur, total (wt % max)	0.3	D1266	0.0
Acidity, total (mg KOH/g max)	0.015	D3242	0.007
Hydrogen Content (wt % min)	13.5	D1018	13.6
Volatility			
Distillation (^{o}C max)	-	D86	-
Initial BP	not limited	-	180
10%	205	-	187
20%	not limited	-	190
50%	not limited	-	199
90%	not limited	-	227
End Point	300	-	248
Residue (vol % max)	1.5	-	1.0
Loss (%)	1.5	-	1.0
Flash Point (^{o}C min)	38.0	D56	59.
Density (API @ 15^{o}C min-max)	37.0-51.0	D287	44.7
Gravity Specific (kg/l at 15^{o}C min-max)	0.775-0.840	D1298	-
Fluidity			
Freeze Point (^{o}C max)	-50	D2386	-50
Viscosity (@ -20^{o}C cst. max)	-	D445	-32C,6.27; -40C,8.67; -45C, doesn't flow
Temperature (@ 12 cst ^{o}C)	-	-	-
Combustion			
Aniline-Gravity Product (min)	-	-	-
Net Heat of Combustion (BTU/lb min)	18400	D240	18557 (calc)
Smoke Point (mm min)	19	D1322	20.4 (calc)
Corrosion			
Copper Strip (2 hr @ 100^{o}C max)	1-b	D130	1-a
Stability			
JFTOT, Breakpoint Temp. ^{o}C	-	-	-
Contaminants			
Existent Gum (mg/100 ml max)	7.0	D381	1.2
Particulates (mg/liter max)	1.0	D2276	0.8 mg/gal
WSIM (min	70	D2550	9.0
Additives			
Anti-Icing (vol %)	0.1-0.15	-	0.05
Corrosion Inhibitor, (lb/1000 bbl)	-	-	-
Antioxidant, (lb/1000 bbl min-max)	6.0-8.4	-	-
Composition Data Available	No		

FUEL Jet A (83-POSF-709)
MILITARY SPECIFICATION

FUEL TYPE DESCRIPTION	SPEC RQMT	METHOD	RESULT
Composition			
Aromatics (vol % max)	25.0	D1319	-
Olefins (vol % max)	5.0	D1319	-
Sulfur, total (wt % max)	0.3	D1266	-
Acidity, total (mg KOH/g max)	0.015	D3242	-
Hydrogen Content (wt % min)	13.5	D1018	-
Volatility			
Distillation (^{o}C max)	-	D86	-
Initial BP	not limited	-	-
10%	205	-	-
20%	not limited	-	-
50%	not limited	-	-
90%	not limited	-	-
End Point	300	-	-
Residue (vol % max)	1.5	-	-
Loss (%)	1.5	-	-
Flash Point (^{o}C min)	38.0	D56	-
Density (API @ 15^{o}C min-max)	37.0-51.0	D287	-
Gravity Specific (kg/l at 15^{o}C min-max)	0.775-0.840	D1298	-
Fluidity			
Freeze Point (^{o}C max)	-50	D2386	-42
Viscosity (@ -20^{o}C cst. max)	-	D445	1.565
Temperature (@ 12 cst ^{o}C)	-	-	-40
Combustion			
Aniline-Gravity Product (min)	-	-	-
Net Heat of Combustion (BTU/lb min)	18400	D240	-
Smoke Point (mm min)	19	D1322	-
Corrosion			
Copper Strip (2 hr @ 100^{o}C max)	1-b	D130	-
Stability			
JFTOT, Breakpoint Temp. ^{o}C	-	-	-
Contaminants			
Existent Gum (mg/100 ml max)	7.0	D381	-
Particulates (mg/liter max)	1.0	D2276	-
WSIM (min	70	D2550	-
Additives			
Anti-Icing (vol %)	0.1-0.15	-	-
Corrosion Inhibitor, (lb/1000 bbl)	-	-	-
Antioxidant, (lb/1000 bbl min-max)	6.0-8.4	-	-
Composition Data Available	No		

FUEL JP-5, Modified (NAPC-1)
MILITARY SPECIFICATION MIL-T-5624L#1

FUEL TYPE DESCRIPTION	SPEC	METHOD	RESULT
Composition			
Aromatics (vol % max)	25.0	D1319	32.14
Olefins (vol % max)	5.0	D1319	1.79
Sulfur, total (wt % max)	0.4	D1266	0.002
Acidity, total (mg KOH/g max)	0.015	D3242	0.015
Hydrogen Content (wt % min)	13.5	D1018	13.36
Volatility			
Distillation (°C max)	-	D86	-
Initial BP	not limited	-	163
10%	205	-	190
20%	not limited	-	207
50%	not limited	-	242
90%	not limited	-	276
95%	-	-	-
End Point	290	-	297
Residue (vol % max)	1.5	-	2.0
Loss (vol % max)	1.5	-	0.9
Flash Point (°C min)	-	D93	57
Density (API @ 15°C min-max)	36-58	D1298	38.9
Gravity Specific (kg/l at 15°C min-max)	0.788-0.845	D1298	-
Fluidity			
Freeze Point, (°C max)	-46.0	D2386	-30
Viscosity (@ -20°C, cst max)	8.5	D445	1.78
Temperature (@ 12 cst, °C)	-	-	-30.6
Combustion			
Aniline-Gravity Product (min)	4500	D1405	5360
Net Heat of Combustion (BTU/lb min)	18300	D240	18480
Smoke Point (mm min)	19.0	D1322	17
Corrosion			
Copper Strip (2 hr @ 100°C max)	1-b	D130	1-a
Stability			
JFTOT, Breakpoint Temp. (°C)	-	-	282
Contaminants			
Existent Gum (mg/100 max)	7.0	D381	0.1
Particulates (mg/liter max)	1.0	D2276	1.4
WSIM (min)	85	D2550	26
Additives			
Anti-Icing (vol %)	0.1-0.15	-	0.14
Corrosion Inhibitor (lb/1000 bbl min-max)	7.5-16.0	-	13.0 (Hitec E-515)
Antioxidant (lb/1000 bbl min-max)	6.0-8.4	-	7.0 (Dupont AO-33)
Composition Data Available	Yes		

FUEL JP-5, Modified (NAPC-2)
MILITARY SPECIFICATION MIL-T-5624L#1

FUEL TYPE DESCRIPTION	SPEC	METHOD	RESULT
Composition			
Aromatics (vol % max)	25.0	D1319	25.0
Olefins (vol % max)	5.0	D1319	0.81
Sulfur, total (wt % max)	0.4	D1266	0.058
Acidity, total (mg KOH/g max)	0.015	D3242	0.027
Hydrogen Content (wt % min)	13.5	D1018	13.48
Volatility			
Distillation (°C max)	-	D86	-
Initial BP	205	-	168
10%	not limited	-	227
20%	not limited	-	242
50%	not limited	-	257
90%	not limited	-	272
95%	-	-	-
End Point	290	-	281
Residue (vol % max)	1.5	-	1.8
Loss (vol % max)	1.5	-	0.2
Flash Point (°C min)	-	D93	71
Density (API @ 15°C min-max)	36-58	D1298	37.8
Gravity Specific (kg/l at 15°C min-max)	0.788-0.845	D1298	-
Fluidity			
Freeze Point, (°C max)	-46.0	D2386	-24
Viscosity (@ -20°C, cst max)	8.5	D445	2.27
Temperature (@ 12 cst, °C)	-	-	-20.6
Combustion			
Aniline-Gravity Product (min)	4500	D1405	5557
Net Heat of Combustion (BTU/lb min)	18300	D240	18502
Smoke Point (mm min)	19.0	D1322	18.0
Corrosion			
Copper Strip (2 hr @ 100°C max)	1-b	D130	1-b
Stability			
JFTOT, Breakpoint Temp. (°C)	-	-	271
Contaminants			
Existent Gum (mg/100 max)	7.0	D381	0.0
Particulates (mg/liter max)	1.0	D2276	1.9
WSIM (min)	85	D2550	21
Additives			
Anti-Icing (vol %)	0.1-0.15	-	0.12 (Hitec E-515)
Corrosion Inhibitor (lb/1000 bbl min-max)	7.5-16.0	-	13.0 (Dupont AO-33)
Antioxidant (lb/1000 bbl min-max)	6.0-8.4	-	7.0
Composition Data Available	Yes		

FUEL JP-5, Modified (NAPC-3)
MILITARY SPECIFICATION MIL-T-5624L#1

FUEL TYPE DESCRIPTION	SPEC	METHOD	RESULT
Composition			
Aromatics (vol % max)	25.0	D1319	23.63
Olefins (vol % max)	5.0	D1319	0.75
Sulfur, total (wt % max)	0.4	D1266	0.018
Acidity, total (mg KOH/g max)	0.015	D3242	0.015
Hydrogen Content (wt % min)	13.5	D1018	13.66
Volatility			
Distillation (^{o}C max)	-	D86	-
Initial BP	not limited	-	171
10%	205	-	192
20%	not limited	-	203
50%	not limited	-	227
90%	not limited	-	261
95%	-	-	-
End Point	290	-	276
Residue (vol % max)	1.5	-	1.4
Loss (vol % max)	1.5	-	0.1
Flash Point (^{o}C min)	-	D93	59
Density (API @ 15^{o}C min-max)	36-58	D1298	41.3
Gravity Specific (kg/l at 15^{o}C min-max)	0.788-0.845	D1298	-
Fluidity			
Freeze Point, (^{o}C max)	-46.0	D2386	-34
Viscosity (@ -20^{o}C, cst max)	8.5	D445	1.62
Temperature (@ 12 cst, ^{o}C)	-	-	-35.6
Combustion			
Aniline-Gravity Product (min)	4500	D1405	5811
Net Heat of Combustion (BTU/lb min)	18300	D240	18527
Smoke Point (mm min)	19.0	D1322	20
Corrosion			
Copper Strip (2 hr @ 100^{o}C max)	1-b	D130	1-a
Stability			
JFTOT, Breakpoint Temp. (^{o}C)	-	-	288
Contaminants			
Existent Gum (mg/100 max)	7.0	D381	0.0
Particulates (mg/liter max)	1.0	D2276	1.84
WSIM (min)	85	D2550	50
Additives			
Anti-Icing (vol %)	0.1-0.15	-	0.19
Corrosion Inhibitor (lb/1000 bbl min-max)	3-8	-	13.0 (Hitec E-515)
Antioxidant (lb/1000 bbl min-max)	7.5-16.0	-	7.0 (Dupont AO-33
Composition Data Available	Yes		

FUEL JP-5 Modified (NAPC-4)
MILITARY SPECIFICATION MIL-T-5624L#1

FUEL TYPE DESCRIPTION	SPEC	METHOD	RESULT
Composition			
Aromatics (vol % max)	25.0	D1319	20.47
Olefins (vol % max)	5.0	D1319	0.79
Sulfur, total (wt % max)	0.4	D1266	0.008
Acidity, total (mg KOH/g max)	0.015	D3242	0.013
Hydrogen Content (wt % min)	13.5	D1018	13.82
Volatility			
Distillation (^{o}C max)	-	D86	-
Initial BP	not limited	-	180
10%	205	-	202
20%	not limited	-	210
50%	not limited	-	228
90%	not limited	-	264
95%	-	-	-
End Point	290	-	282
Residue (vol % max)	1.5	-	1.4
Loss (vol % max)	1.5	-	0.5
Flash Point (^{o}C min)	-	D93	69
Density (API @ 15^{o}C min-max)	36-58	D1298	41.6
Gravity Specific (kg/l at 15^{o}C min-max)	0.788-0.845	D1298	-
Fluidity			
Freeze Point, (^{o}C max)	-46.0	D2386	-34.5
Viscosity (@ -20^{o}C, cst max)	8.5	D445	1.74
Temperature (@ 12 cst, ^{o}C)	-	-	-31.7
Combustion			
Aniline-Gravity Product (min)	4500	D1405	6140
Net Heat of Combustion (BTU/lb min)	18300	D240	18562
Smoke Point (mm min)	19.0	D1322	21
Corrosion			
Copper Strip (2 hr @ 100^{o}C max)	1-b	D130	1-b
Stability			
JFTOT, Breakpoint Temp. (^{o}C)	-	-	282
Contaminants			
Existent Gum (mg/100 max)	7.0	D381	0.1
Particulates (mg/liter max)	1.0	D2276	0.75
WSIM (min)	85	D2550	38
Additives			
Anti-Icing (vol %)	0.1-0.15	-	0.16
Corrosion Inhibitor (lb/1000 bbl min-max)	7.5-16.0	-	13.0 (Hitec E-515)
Antioxidant (lb/1000 bbl min-max)	6.0-8.4	-	7.0 (Dupont AO-33)
Composition Data Available	Yes		

FUEL JP-5, Low Aromatic (NAPC-5)
MILITARY SPECIFICATION MIL-T-5624L#1

FUEL TYPE DESCRIPTION	SPEC	METHOD	RESULT
Composition			
Aromatics (vol % max)	25.0	D1319	14.99
Olefins (vol % max)	5.0	D1319	0.79
Sulfur, total (wt % max)	0.4	D1266	0.005
Acidity, total (mg KOH/g max)	0.015	D3242	0.004
Hydrogen Content (wt % min)	13.5	D1018	13.79
Volatility			
Distillation (^{o}C max)	-	D86	-
Initial BP	not limited	-	181
10%	205	-	191
20%	not limited	-	203
50%	not limited	-	217
90%	not limited	-	243
95%	-	-	-
End Point	290	-	261
Residue (vol % max)	1.5	-	1.2
Loss (vol % max)	1.5	-	0.2
Flash Point (^{o}C min)	-	D93	62
Density (API @ 15^{o}C min-max)	36-58	D1298	41.8
Gravity Specific (kg/l at 15^{o}C min-max)	0.788-0.845	D1298	-
Fluidity			
Freeze Point, (^{o}C max)	-46.0	D2386	-50
Viscosity (@ -20^{o}C, cst max)	8.5	D445	1.58
Temperature (@ 12 cst, ^{o}C)	-	-	-35.5
Combustion			
Aniline-Gravity Product (min)	4500	D1405	-
Net Heat of Combustion (BTU/lb min)	18300	D240	18516
Smoke Point (mm min)	19.0	D1322	21
Corrosion			
Copper Strip (2 hr @ 100^{o}C max)	1-b	D130	1-a
Stability			
JFTOT, Breakpoint Temp. (^{o}C)	-	-	271
Contaminants			
Existent Gum (mg/100 max)	7.0	D381	2.6
Particulates (mg/liter max)	1.0	D2276	1.0
WSIM (min)	85	D2550	85
Additives			
Anti-Icing (vol %)	0.1-0.15	-	0.10
Corrosion Inhibitor (lb/1000 bbl min-max)	3-8	-	Unknown (Hitec E-515)
Antioxidant (lb/1000 bbl min-max)	7.5-16.0	-	Unknown (Dupont AO-55)
Composition Data Available	Yes		

FUEL JP-5, High Aromatic (NAPC-6)
MILITARY SPECIFICATION MIL-T-5624L#1

FUEL TYPE DESCRIPTION	SPEC	METHOD	RESULT
Composition			
Aromatics (vol % max)	25.0	D1319	22.67
Olefins (vol % max)	5.0	D1319	1.62
Sulfur, total (wt % max)	0.4	D1266	0.006
Acidity, total (mg KOH/g max)	0.015	D3242	0.003
Hydrogen Content (wt % min)	13.5	D1018	13.49
Volatility			
Distillation (°C max)	-	D86	-
Initial BP	not limited	-	190
10%	205	-	204
20%	not limited	-	208
50%	not limited	-	218
90%	not limited	-	246
95%	-	-	-
End Point	290	-	264
Residue (vol % max)	1.5	-	1.0
Loss (vol % max)	1.5	-	0.5
Flash Point (°C min)	-	D93	70
Density (API @ 15°C min-max)	36-58	D1298	40.5
Gravity Specific (kg/l at 15°C min-max)	0.788-0.845	D1298	-
Fluidity			
Freeze Point, (°C max)	-46.0	D2386	-53
Viscosity (@ -20°C, cst max)	8.5	D445	1.5
Temperature (@ 12 cst, °C)	-	-	-35
Combustion			
Aniline-Gravity Product (min)	4500	D1405	5271
Net Heat of Combustion (BTU/lb min)	18300	D240	18491
Smoke Point (mm min)	19.0	D1322	21.0
Corrosion			
Copper Strip (2 hr @ 100°C max)	1-b	D130	1-a
Stability			
JFTOT, Breakpoint Temp. (°C)	-	-	271
Contaminants			
Existent Gum (mg/100 max)	7.0	D381	0.1
Particulates (mg/liter max)	1.0	D2276	0.11
WSIM (min)	85	D2550	60
Additives			
Anti-Icing (vol %)	0.1-0.15	-	0.11
Corrosion Inhibitor (lb/1000 bbl min-max)	7.5-16.0	-	Unknown (Hitec E-515)
Antioxidant (lb/1000 bbl min-max)	7.5-16.0	-	Unknown (Dupont AO-55)
Composition Data Available	Yes		

U.S.Government Printing Office: 1985 559 065/20696

END

FILMED

5-85

DTIC